ACCSCIENCE PUBLISHING

Microbes & Immunity

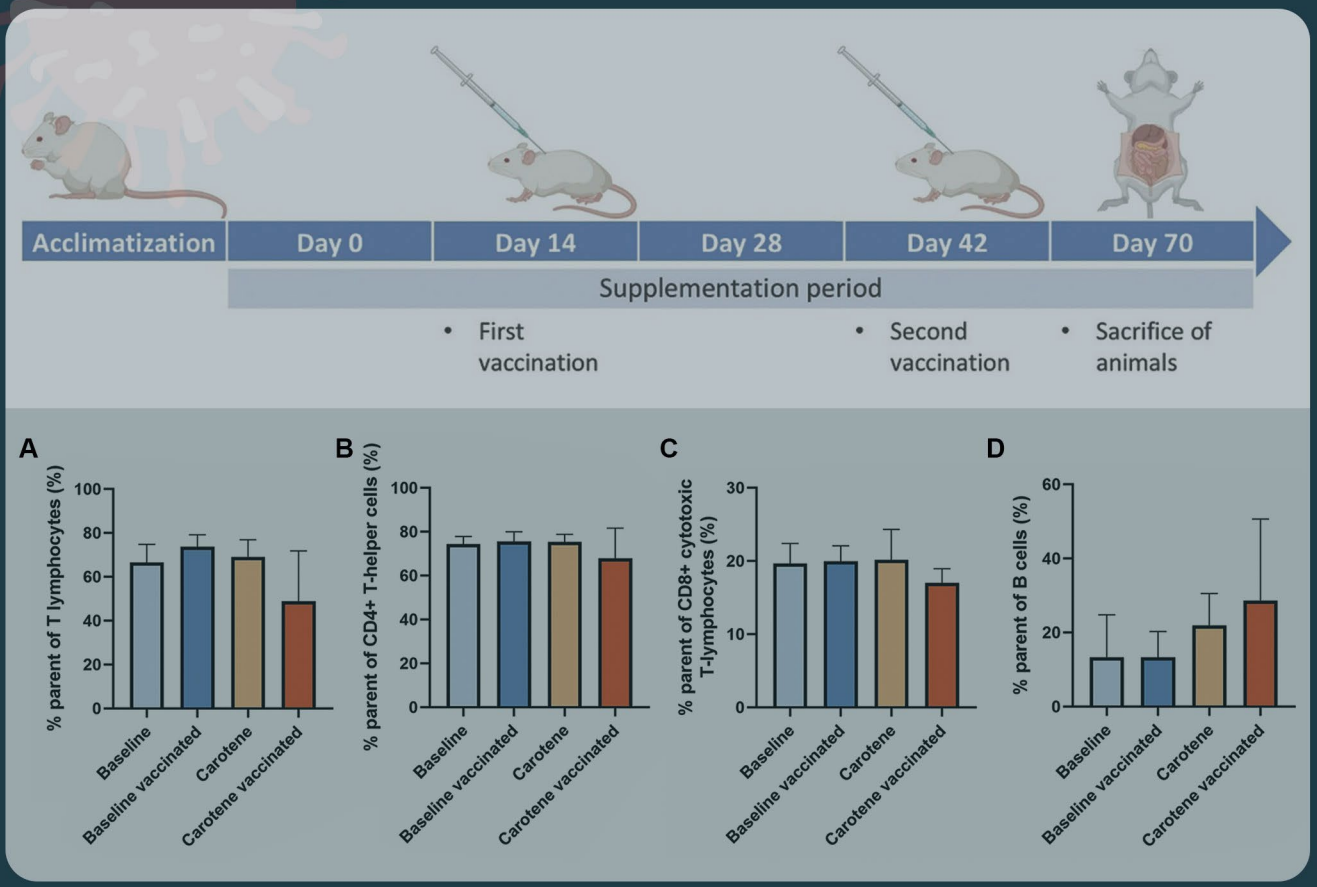

Modulation of host immune response by carotene supplementation in a COVID-19 vaccination mouse model

ISSN: 3041-0886 (Print)
ISSN: 3029-2883 (Online)
Volume 2 · Issue 3
July 2025

ACCSCIENCE PUBLISHING

Microbes & Immunity

Print ISSN: 3041-0886
Online ISSN: 3029-2883

Microbes & Immunity is a multidisciplinary peer-reviewed journal dedicated to advancing the understanding of the interactions between microbes and the immune system. The journal provides an open access publishing platform for researchers, clinicians, and scientists to disseminate their original research, reviews, and perspectives related to various aspects of microbes and immunity. The journal aims to foster collaboration and knowledge exchange in the fields of microbiology, immunology, infectious diseases, and related disciplines.

About the Publisher

AccScience Publishing is a publishing company based in Singapore. We publish a range of high-quality, open-access, peer-reviewed journals and books from a broad spectrum of disciplines.

Contact Us

Managing Editor
mi.office@accscience.sg

AccScience Publishing
9 Raffles Place, Republic Plaza 1 #06-00 Singapore 048619.

Volume 2 • Issue 3 • July 2025
ISSN 3041-0886 (print) ISSN 3029-2883 (online)

MICROBES & IMMUNITY

ACCSCIENCE PUBLISHING

Access Science Without Barriers

MICROBES & IMMUNITY

ISSN: 3041-0886 (print)
ISSN: 3029-2883 (online)

Editorial and Production Credits

Publisher: AccScience Publishing
Managing Editor: Jane Xu
Production Editor: Sharmila Velapasamy
Article Layout and Typeset: Sinjore Technologies (India)

For all advertising queries, contact mi.office@accscience.sg.

Supplementary file

Supplementary files of articles can be obtained at https://accscience.com/journal/MI/2/3.

Disclaimer

AccScience Publishing is not liable to the statements, perspectives, and opinions contained in the publications. The appearance of advertisements in the journal shall not be construed as a warranty, endorsement, or approval of the products or services advertised and/or the safety thereof. AccScience Publishing disclaims responsibility for any injury to persons or property resulting from any ideas or products referred to in the publications or advertisements. AccScience Publishing remains neutral with regard to jurisdictional claims in published maps and institutional affiliations.

Microbes & Immunity

Editorial Board

*Youth Editorial Board Members**

*Editorial Board Members as of July 23, 2025

ACCSCIENCE PUBLISHING

Volume 2 | Issue 3 | July 2025 | Page 1 – 177 |

Microbes & Immunity

https://accscience.com/journal/MI

CONTENTS

ACCSCIENCE PUBLISHING

Microbes & Immunity

REVIEW ARTICLE

Post-translational modifications in sepsis: Mechanistic insights and therapeutic opportunities

Wenyue Gao[1,2,3,4], Yue Zhang[1,2,3], and Liuluan Zhu[1,2,3]*

[1]Beijing Key Laboratory of Emerging Infectious Diseases, Institute of Infectious Diseases, Beijing Ditan Hospital, Capital Medical University, Beijing, China

[2]Beijing Institute of Infectious Diseases, Beijing, China

[3]National Center for Infectious Diseases, Beijing Ditan Hospital, Capital Medical University, Beijing, China

[4]Department of Infectious, The First Affiliated Hospital of Dalian Medical University, Dalian, Liaoning, China

Abstract

Sepsis, a life-threatening condition marked by systemic inflammation and multi-organ dysfunction, poses a persistent clinical challenge. Post-translational modifications (PTMs) dynamically regulated inflammatory signaling, immune responses, and cell death, positioning them as a pivotal focus in sepsis research. This review systematically explores the regulatory networks of five key PTMs – phosphorylation, ubiquitination, SUMOylation, acetylation, and lactylation – in sepsis. In this review, we highlight recent discoveries of genes and molecules that modulate these PTMs, influencing inflammation and organ dysfunction, and evaluate their potential as therapeutic targets or prognostic biomarkers. Furthermore, we discuss how PTMs offer novel therapeutic opportunities, providing novel insights to address the shortcomings of traditional anti-infective approaches.

Keywords: Sepsis; Post-translational modifications; Phosphorylation; Ubiquitination; SUMOylation; Acetylation; Lactylation; Inflammation

***Corresponding author:**
Liuluan Zhu
(zhuliuluan@ccmu.edu.cn)

Citation: Gao W, Zhang Y, Zhu L. Post-translational modifications in sepsis: Mechanistic insights and therapeutic opportunities. *Microbes & Immunity*. 2025;2(3):1-14. doi: 10.36922/MI025090016

Received: February 28, 2025

Revised: April 11, 2025

Accepted: April 14, 2025

Published online: April 24, 2025

1. Introduction

Sepsis arises from a dysregulated host response to infection, resulting in systemic inflammation and multiple organ dysfunctions.[1] Complications such as acute kidney injury (AKI), acute lung injury (ALI), and myocardial injury are frequent and severe, contributing to elevated morbidity and mortality rates.[2-4] Despite progress in anti-infective therapies and organ support, the intricate pathogenesis of sepsis continues to hinder effective clinical management.

In eukaryotes, protein function is diversified through post-translational modifications (PTMs), which dynamically regulate cellular processes.[5] Increasingly, PTMs have been recognized as central regulators of sepsis progression, modulating inflammatory signaling, immune cell polarization, and programmed cell death.[6] This review examines five major PTMs – phosphorylation, ubiquitination, SUMOylation, acetylation, and lactylation, an emerging form of modification – focusing on their roles in sepsis, and

explores their potential as biomarkers and therapeutic targets to enhance sepsis treatment enhance.

2. Host response dysregulation in sepsis

Sepsis arises from a dysregulated host immune response, characterized by a vicious cycle of hyperinflammation, immunosuppression, coagulation abnormalities, and metabolic dysregulation. This cascade disrupts immune homeostasis, driving complex molecular interactions that culminate in multi-organ dysfunction.

In the early phase of sepsis, pathogen-associated molecular patterns and damage-associated molecular patterns engage pattern recognition receptors, such as toll-like receptors (TLRs), on immune cells. This interaction activates signaling cascades, including nuclear factor-kappa B (NF-κB) and mitogen-activated protein kinase (MAPK) pathways, triggering a surge of pro-inflammatory cytokines, such as tumor necrosis factor alpha (TNF-α), interleukin 6 (IL-6), and interleukin 1 beta (IL-1β).[7] Concurrently, excessive activation of the complement system (*e.g.*, C3a, C5a) and the formation of neutrophil extracellular traps further amplify inflammation, damaging vascular endothelium, causing capillary leakage and tissue edema.[8,9] These processes exacerbate tissue injury and set the stage for systemic complications.

Following the initial inflammatory storm, the host immune system often transitions into a compensatory anti-inflammatory response syndrome. During this phase, pro-inflammatory cytokine production declines, while anti-inflammatory mediators (*e.g.*, IL-10, transforming growth factor beta) are overexpressed, suppressing immune cell function.[10] This shift is accompanied by widespread apoptosis of T cells and B cells, impaired antigen-presenting capacity of dendritic cells, and expansion of myeloid-derived suppressor cells. In addition, upregulation of immune checkpoint molecules (*e.g.*, programmed cell death protein 1 [PD-1], cytotoxic T-lymphocyte-associated protein 4 [CTLA-4]) on T cell surfaces induces T cell exhaustion.[11] This immunosuppressive state increases susceptibility to secondary infections, impairs pathogen clearance, and significantly increases mortality risk.

Dysregulated coagulation forms a positive feedback loop with inflammation, exacerbating sepsis pathology. Inflammatory cytokines inhibit the thrombomodulin-protein C system, impairing anticoagulation while upregulating tissue factor expression to activate the extrinsic coagulation pathway. Simultaneously, increased levels of plasminogen activator inhibitor-1 suppress fibrinolysis, promoting platelet activation and fibrin deposition.[12,13] These changes lead to microthrombi formation, compounded by complement activation products that further damage the endothelium and enhance platelet aggregation. The resulting disseminated intravascular coagulation disrupts organ microcirculation, causing ischemic injury and worsening multi-organ failure.[14]

Metabolic reprogramming is a hallmark of sepsis, driven by inflammatory signals that shift immune cell metabolism toward glycolysis, leading to lactate accumulation and metabolic acidosis.[15] Excessive reactive oxygen species (ROS) induces mitochondrial dysfunction, while lipid peroxidation promotes ferroptosis, a form of programmed cell death. These processes impair immune cell function and contribute to multi-organ metabolic failure.[16,17] Together, these metabolic disruptions exacerbate the systemic effects of sepsis and hinder recovery.

PTMs intricately regulate these dysregulated host responses, serving as critical molecular switches in sepsis pathogenesis. For instance, phosphorylation of NF-κB modulates excessive inflammation,[18] while phosphorylation of lymphocyte-specific protein-1 (Lsp1) triggers B cell apoptosis.[19] In addition, the E3 ubiquitin ligase TRIM47 promotes TNF-α-induced endothelial cell activation through ubiquitination,[20] and lactate-mediated lactylation of mitochondrial fission protein 1 (Fis1) drives mitochondrial dysfunction.[21] These PTM-mediated mechanisms, detailed in subsequent sections, highlight potential therapeutic targets for mitigating sepsis-induced organ damage.

3. Phosphorylation and sepsis

Protein phosphorylation, the earliest discovered PTM, is a well-studied mechanism in sepsis. It involves the kinase-mediated transfer of a phosphate group from ATP to specific amino acid residues,[6] regulating cellular signaling, metabolism, and inflammation.[22] In sepsis, phosphorylation modulates key pathways – such as NF-κB, MAPK, STAT3, and PI3K/ATK – affecting inflammation, immunity, and apoptosis, and thus influencing disease progression and outcomes.

3.1. NF-κB signaling pathway

NF-κB, a pivotal transcription factor in immune and inflammatory responses, comprises five subunits: p50, p52, RelA (p65), c-Rel, and RelB.[23] In resting cells, NF-κB is sequestered in the cytoplasm by its inhibitor, IκB.[24] Activation proceeds through two distinct pathways: classical and non-classical.[25]

The classical pathway, initiated by inflammatory cytokines, involves IKK complex-mediated phosphorylation and subsequent degradation of IκB, releasing NF-κB dimers (*e.g.*, p50/p65), which translocate

to the nucleus and drive pro-inflammatory gene transcription.[23] TNF-α-induced protein 8-like 2 (TIPE2) and echinatin (Ecn) inhibit p65 nuclear translocation, reducing inflammation and damage in sepsis.[26,27] In contrast, the microRNA-210 host gene (MIR210HG) enhances IκBα phosphorylation and p65 nuclear translocation, exacerbating sepsis-associated AKI.[18] In addition, p65 phosphorylation is a critical regulatory step; transcription factor Kruppel-like factor 13 (KLF13) and astragaloside IV (AST) suppress p65 phosphorylation, mitigating sepsis-related myocardial injury and inflammation,[28,29] whereas transcription coactivator PPARG coactivator 1 alpha (PGC-1α) promotes it, enhancing cytokine release and inhibiting cardiomyocyte apoptosis.[30] Parkinson's disease protein 7 (PARK7) protects against sepsis-induced AKI by simultaneously blocking p65 nuclear translocation and phosphorylation.[31]

The non-classical pathway is typically activated by specific stimuli, this pathway involves phosphorylation of p100, its processing to p52, and subsequently dimerization with RelB for nuclear translocation and target gene transcription.[23] SHP-1, a protein tyrosine phosphatase, inhibits this pathway by suppressing p52 phosphorylation and nuclear translocation, dampening hyperinflammation and ALI in sepsis. SHP-1 also negatively regulates the classical pathway by inhibiting the p50 phosphorylation and reducing p65 transcription and translation.[31]

Targeting dysregulated NF-κB signaling through molecules such as TIPE2, MIR210HG, KLF13, and SHP-1, alongside bioactive compounds such as Ecn and AST, offers promising anti-inflammatory strategies for sepsis management.

3.2. MAPK signaling pathway

MAPKs, a family of serine/threonine kinases, regulate proliferation, apoptosis, and inflammation, playing a pivotal role in sepsis pathogenesis through aberrant activation and subsequent overproduction of pro-inflammatory cytokines.[32] The MAPK signaling pathway encompasses four primary cascades: extracellular signal-regulated kinase (ERK) 1/2, c-Jun N-terminal kinase (JNK), p38, and ERK5. These cascades are phosphorylated and activated by upstream MAPK kinases to modulate downstream targets.[33] In sepsis, ERK1/2, JNK, and p38 are the most extensively studied subtypes, with their activation intricately linked to the inflammatory response and disease progression.

ERK1/2 is primarily activated by growth factors (*e.g.*, epidermal growth factor) and inflammatory signals (*e.g.*, TLR4) stimulation. Upon activation, ERK1/2 phosphorylates transcription factor c-Fos, promoting the expression of pro-inflammatory cytokines, including IL-1β and IL-6.[34] Beyond inflammation, ERK1/2 supports adaptive immunity by regulating cell proliferation and inhibiting apoptosis through the mitochondrial pathway. This sustains T and B cell survival, enhancing host defense against infection.[35,36] For instance, adrenomedullin 2 (ADM2) stimulates ERK1/2 phosphorylation, promoting T and B cell proliferation and bolstering anti-infective immunity.[37] Similarly, artesunate enhances ERK1/2 phosphorylation in $CD4^+$ and $CD8^+$ T cells, reducing apoptosis and mitigating sepsis-induced immunosuppression.[38]

JNK, activated by stress signals such as oxidative stress and pro-inflammatory cytokines, phosphorylates c-Jun and facilitates activating transcription factor 4 (ATF4) nuclear translocation. These events drive the transcription of inflammatory genes, amplifying the inflammatory response in sepsis.[39] JNK's role in exacerbating inflammation makes it a critical target for therapeutic intervention.

Several compounds have shown promise in modulating ERK1/2 and JNK activity to attenuate sepsis-induced inflammation. Tetrahydrocurcumin (THC) inhibits phosphorylation of both JNK and ERK1/2, reducing pro-inflammatory cytokine production and improving cardiac function in sepsis models.[40] Similarly, pinaverium bromide (PVB) suppresses ERK1/2 and JNK phosphorylation in neutrophils by decreasing ROS production. This attenuates inflammatory factor production and mitigates early-stage sepsis-induced inflammation. In addition, PVB inhibits phosphorylation of IκBα and p65, key components of NF-κB signaling pathway, further reducing pro-inflammatory responses in neutrophils.[41] These findings highlight the therapeutic potential of targeting MAPK pathways to balance inflammatory and immune responses in sepsis.

MAPK p38 drives inflammatory factor expression by phosphorylating transcription factors such as ATF2 and C/EBP homologous protein (CHOP).[42] It also directly regulates NLRP3 inflammasome assembly, promoting IL-1β/IL-18 maturation and release. Anti-inflammatory mediators such as maresin-1 (MaR1) and fisetin suppress p38 MAPK phosphorylation, decreasing pro-inflammatory factor expression and alleviating sepsis-induced organ damage.[43,44] Peptide-proline isomerase Pin1 enhances NLRP3 inflammasome transcription and activation through p38 MAPK phosphorylation, amplifying the inflammatory response and exacerbating organ damage in sepsis.[45] Furthermore, p38 MAPK enhances the activity of caspase-1, promoting gasdermin D cleavage and inducing pyroptosis.[46] In the pathogenesis of sepsis-associated AKI, the TLR4/MyD88 signaling pathway promotes p38 MAPK

phosphorylation, exacerbating renal tubular epithelial cell pyroptosis,[47] while the endogenous regulator Wild-type p53-induced phosphatase 1 (WIP1) exerts a negative regulatory effect by dephosphorylating p38 MAPK, alleviating pyroptosis-related kidney injury.[48]

Thus, targeting the MAPK pathway offers promising avenues for suppressing inflammation and balancing immune responses. Its interactions with NF-κB, the NLRP3 inflammasome, and cell death pathways demonstrate its potential in treating sepsis. Molecules such as ADM2, MaR1, peptidyl-prolyl cis/trans isomerase (Pin1), WIP1, and TLR4 provide opportunities for precise intervention by modulating MAPK phosphorylation. Natural products and synthetic compounds, including THC, PVB, artesunate, and fisetin, exhibit therapeutic potential by improving organ function and survival rates through multi-target effects.

3.3. Signal transducer and activator of transcription 3 (STAT3) signaling pathway

STAT3, a member of the STAT protein family, is a central transcription factor in immune and inflammatory signaling.[49] Following phosphorylation, STAT3 translocates to the nucleus, driving transcription of genes involved in inflammation, cell proliferation, differentiation, and apoptosis during the acute phase of sepsis, thereby modulating immune responses and multi-organ dysfunction.[50,51]

Colchicine inhibits NLRP3 inflammasome activation by suppressing STAT3 phosphorylation, reducing inflammation, pyroptosis, and oxidative stress in sepsis-induced ALI.[52] Conversely, phospholipase D2 (PLD2) enhances STAT3 phosphorylation through phospholipid acid, negatively regulating tight junction protein expression in pulmonary vascular endothelium and exacerbating ALI.[53] In sepsis-associated AKI, Lyn (a Src family kinase) and pectolinarigenin (a flavonoid) suppress STAT3 phosphorylation, inhibiting inflammatory factor release and reducing renal cell apoptosis, thus protecting against AKI.[54,55] In addition, 4-octyl itaconate, a multi-target itaconate derivative, suppresses STAT3 phosphorylation to mitigate renal inflammation and oxidative stress while promoting mitophagy and cell homeostasis.[56] Mesenchymal stem cells regulate inflammatory response by inhibiting both STAT1 and STAT3 phosphorylation, modulating T helper (Th) cell subset numbers and functions, reducing organ damage, and improving survival in septic models.[57]

The pivotal role of STAT3 in sepsis highlights the need to develop therapies that downregulate its signaling. Newly identified regulators such as PLD2 and Lyn offer novel therapeutic targets, while colchicine, pectolinarigenin, 4-octyl itaconate, and mesenchymal stem cells show promise as STAT3-targeting agents in sepsis management.

3.4. PI3K/AKT signaling pathway

The PI3K/AKT pathway is a vital intracellular signaling network wherein phosphatidylinositol 3-kinase (PI3K) activates AKT through phosphorylation.[58] Activated AKT regulates inflammation, oxidative stress, and apoptosis by influencing downstream effectors.[59]

Targeted modulation of the PI3K/AKT pathway can mitigate sepsis-induced organ damage by balancing inflammation and tissue repair. Blocking hepatocyte growth factor binding to c-Met inhibits PI3K/AKT phosphorylation, reducing oxidative stress, pro-inflammatory cytokine production (*e.g.*, IL-6), and cardiomyocyte apoptosis in early sepsis, though prolonged inhibition may impair tissue regeneration.[60,61] Alternatively, inhibiting sphingosine 1-phosphate lyase (S1P) and activating S1P receptor type 3 suppress AKT phosphorylation, preserving lung and kidney microvascular barriers and reducing systemic inflammation, offering potential for antibiotic-resistant cases.[62] AKT-driven NF-κB phosphorylation amplifies pro-inflammatory cascades, but compounds such as annexin A1 (Ac2-26) and hibifolin inhibit NF-κB, protecting against renal and lung injury.[63-65] In contrast, the traditional Chinese medicine compound Xuebijing (XBJ) activates AKT phosphorylation by increasing vascular endothelial growth factor A expression to improve intestinal microcirculation in sepsis.[66] Similarly, phenylpropylene (BNP) exerts anti-inflammatory effects by inducing AKT phosphorylation and reducing IL-6 expression.[67]

The dual role of the PI3K/AKT pathway in sepsis – both protective and detrimental – complicates its therapeutic application. Nevertheless, hibifolin, XBJ, and phenpropylline merit further exploration as potential sepsis treatments.

4. Ubiquitination and sepsis

Ubiquitination, mediated by E1-E2-E3 cascades, critically regulates immune responses and cell death in sepsis.[68] This process involves the attachment of ubiquitin, a 76-amino acid protein with seven lysine residues (K6, K11, K27, K29, K33, K48, K63), to substrate proteins, forming monomeric, branched and linear chains.[69] E3 ubiquitin ligases, categorized into RING, HECT, and RBR families, confer substrate specificity.[70] Ubiquitination modification plays a key role in modulating NLRP3 inflammasome activation and programmed cell death pathways, influencing sepsis pathogenesis.

4.1. NLRP3 inflammasome

The NLRP3 inflammasome, a multiprotein complex, is crucially regulated by ubiquitination in terms of its degradation or activation.[71,72] RING-type E3 ligases Cbl-b and RNF125 prevent sepsis by targeting NLRP3 for K63- and K48-linked polyubiquitination, inhibiting NLRP3 inflammasome activation.[73] β-TrCP1, another E3 ubiquitin ligase, promotes NLRP3 degradation through K27-linked ubiquitination, while the transcriptional coactivator yes-associated protein (YAP) stabilizes NLRP3 by blocking its interaction with β-TrCP1.[74] Conversely, the cullin-RING-type E3 ligase KBTBD7 promotes NLRP3 activation and pro-inflammatory factors release by ubiquitinating and degrading the transcription factor KLF15, exacerbating brain injury in sepsis.[75] Furthermore, heat shock protein family A member 8 (HSPA8) inhibition promotes the E3 ligase SKP2 degradation, attenuating NLRP3 ubiquitination, thereby exacerbating pyroptosis and sepsis-induced ALI.[76] Tissue inhibitor of metalloproteinase 2 (TIMP2) exerts a renoprotective role in sepsis-associated AKI by enhancing the E3 ligase MARCH7-mediated NLRP3 ubiquitination degradation and attenuating downstream pyroptosis.[77]

These findings highlight the therapeutic potential of targeting NLRP3 ubiquitination in sepsis. Newly identified regulators such as YAP, KLF15, HSPA8, and TIMP2 offer novel avenues for therapeutic intervention by modulating NLRP3 degradation and activation.

4.2. Programmed cell death

Sepsis induces programmed cell death, a process dynamically regulated by ubiquitination.[78] RING-type E3 ligase FBXW7 promotes alveolar epithelial cells ferroptosis and aggravates sepsis-induced ALI by mediating AUF1 ubiquitination and degradation.[79] Conversely, HECT-type E3 ligase WWP2 inhibits oxidative stress and ferroptosis in cardiomyocytes by promoting long-chain acyl CoA synthetase 4 (FACL4) ubiquitination, improving myocardial injury and cardiac function in sepsis.[80] In pyroptosis regulation, CHIP (a chaperone-dependent E3 ligase) inhibits NLRP3 activation and pyroptosis by promoting KPNA2 poly-ubiquitination, thus alleviating sepsis-induced cardiac dysfunction.[81] YL-109, a small molecule compound that upregulated CHIP expression, demonstrates therapeutic potential by inhibiting this pathway in various tissues, improving septic multi-organ damage.[82] Similarly, samotolisib, the PI3K/mTOR pathway inhibitor, activates HECT-type E3 ligase Nedd4, inducing caspase-11 ubiquitination, thereby specifically blocking hepatocyte pyroptosis and improving ALI in sepsis.[83] The TRIM family, a RING-type E3 ligases subfamily,[70] exhibits dual role of cell death regulation in sepsis. TRIM21 mediates OAS3 K48-linked polyubiquitination in lung epithelial cells, inhibiting apoptosis, thus attenuating sepsis-induced ALI.[84] It also promotes interferon regulatory factor 1 (IRF1) ubiquitination, reducing IRF1 enrichment, further improving sepsis-induced ALI.[85] However, TRIM31 activates the NF-κB pathway by binding to TAK1 and enhancing its ubiquitination, inducing cardiomyocyte apoptosis and a "pro-injury" phenotype in sepsis.[85]

These findings highlight the therapeutic potential of modulating E3 ligase networks – particularly through small-molecule compounds such as YL-109 and samotolisib – to reprogram programmed cell death pathways and improve sepsis outcomes.

5. SUMOylation and sepsis

Small ubiquitin-like modifier (SUMO), a protein containing ~100 amino acids, is covalently attached to lysine residues of target proteins through a three-step enzymatic cascade mediated by E1, E2 (UBC9), and E3 ligases.[86] This process, known as SUMOylation, participates in regulating diverse biological processes, including cell signaling, gene transcription, cell proliferation, and apoptosis.[87]

In sepsis, SUMOylation plays a critical role in modulating inflammation and immune homeostasis. Ubiquitin-conjugating enzyme 9 (UBC9), the sole E2 ligase for SUMOylation, its deficiency leads to dendritic cell hypermaturation, aberrant release of IL-18/IL-1β and enhances T cell activation, increasing mortality in septic mice by enhancing, which indicating a protective role for SUMOylation in suppressing excessive inflammation.[88] SUMO can competitively bind to the same site on IκBα as ubiquitin, inhibiting its ubiquitination and degradation, thus blocking NF-κB nuclear translocation and downstream pro-inflammatory factor transcription.[86] SUMOylation deficiency abolishes this inhibition, resulting in abnormal NF-κB-dependent inflammatory factors and type I interferon secretion, potentially by regulating interferon-β (Ifnb1) expression and suppressing unanticipated amplification of TLR signaling.[87] Macrophages are important immune cells, with a significant impact on immune homeostasis and inflammatory processes in sepsis.[89] SUMO-specific protease 1 (SENP1) regulates transcription factor KLF4 activity through deSUMOylation. As a key regulator of macrophage polarization, KLF4 upon SENP1-mediated deSUMOylation enhances NF-κB signaling, driving M1 macrophage polarization and exacerbating inflammation.[90] SENP1 also promotes Sp3 expression through deSUMOylation and interaction with NF-κB,

enhancing lipopolysaccharide-induced macrophage inflammation.[91] Conversely, ginkgolic acid inhibits SUMOyation, promoting NF-κB p65 phosphorylation and nuclear translocation, increasing the release of macrophage inflammatory factors and apoptosis, thereby exacerbating sepsis-induced organ damage.[92]

In summary, SUMOylation exerts an anti-inflammatory and protective role in sepsis by stabilizing IκBα to inhibit NF-κB signaling, regulating macrophage polarization, inflammatory responses, and cell apoptosis. The dynamic balance of the core regulatory nodes UBC9 and SENP1 profoundly impacts disease progression, suggesting that targeting UBC9 and SENP1 may offer novel sepsis treatments.

6. Acetylation and sepsis

Acetylation, a PTM catalyzed by acetyltransferase, modulates gene expression and participates in cellular processes, including gene transcription and signal transduction.[5] Aberrant acetylation within the TLR4 signaling complex is implicated in dysregulated immune responses, suggesting acetylation as a potential therapeutic target in sepsis.[93]

Table 1. Roles of regulatory factors involved in different PTMs and the corresponding targets in sepsis

Targets	Regulatory factors	Impact on sepsis	References
Phosphorylation			
NF-κB	MIR210HG, PGC-1α	Promote	18,30
	TIPE2, Ecn, KLF13, AST, PARK7, SHP-1, PVB	Inhibit	26-29,31,41
MAPK	Pin1, TLR4	Promote	45,47
	THC, PVB, ADM2, artesunate, MaR1, fisetin, WIP1	Inhibit	37,38,40,41,43,44,48
STAT3	PLD2	Promote	53
	Lyn, PEC, colchicine, 4-OI, MSCs	Inhibit	52,54-57
PI3K/ATK	HGF, S1P	Promote	60,62
	S1PR3, Ac2-26, Hibifolin, XBJ, BNP	Inhibit	62,64-67
Ubiquitination			
NLRP3	Cbl-b, RNF125, β-TrCP1, TIMP2	Promote	73,74,77
	YAP, KBTBD7, HSPA8	Inhibit	74-76
Other target	FBXW7	Promote	79
	WWP2, CHIP, YL-109, samotolisib	Inhibit	80-83
SUMOylation			
NF-κB	SENP1, GA	Promote	91,92
	UBC9, KLF4	Inhibit	88,90
Acetylation			
SIRTs	GITR	Promote	99
	GAS5, AVS, NMN, MK-4, Zn^{2+}	Inhibit	95-97,101,102
Lactylation			
Histone	METTL3, EGR1, RhoA	Promote	105-107
Non-histone	Fis1, HMGB1	Promote	21,109
	PDHA1	Inhibit	21

Abbreviations: Ac2-26: Annexin A1; ADM2: Adrenomedullin 2; AST: Astragaloside IV; AVS: Nicaraven; BNP: Phenpropylline; Cb1-b: Casitas B-lineage lymphoma proto-oncogene b; Ecn: Echinatin; EGR1: Early growth response protein 1; Fis1: Mitochondrial fission protein 1; GA: Ginkgolic acid; GAS5: Growth arrest-specific transcript 5; GITR: Glucocorticoid-induced TNFR-related protein; HGF: Hepatocyte growth factor; HMGB1: High mobility group box 1; HSPA8: Heat shock protein family A member 8; KLF: Kruppel-like factor; MaR1: Maresin-1; MIR210HG: MicroRNA-210 host gene; MK-4: Menadione 4; MSCs: Mesenchymal stem cells; NMN: Nicotinamide mononucleotide; 4-OI: 4-Octyl itaconate; PARK7: Parkinson's disease protein 7; PDHA1: Pyruvate dehydrogenase E1 component subunit α; PEC: Pectolinarigenin; PGC-1α: Peroxisome proliferator-activated receptor gamma coactivator 1-alpha; Pin1: Peptidyl-prolyl cis/trans isomerase; PLD2: Phospholipase D2; PVB: Pinaverium bromide; S1P: Sphingosine 1-phosphate lyase; S1PR3: S1P receptor type 3; SENP1: SUMO-specific peptidase 1; SHP-1: Src homology region 2 domain-containing phosphatase-1; THC: Tetrahydrocurcumin; TIMP2: Tissue inhibitor of metalloproteinase 2; TIPE2: TNF-α-induced protein 8-like 2; TLR4: Toll-like receptor 4; β-TrCP1: Beta-transducin repeats-containing protein 1; UBC9: Ubiquitin-conjugating enzyme 9; WIP1: Wild-type p53-induced phosphatase 1; XBJ: Xuebijing; YAP: Yes-associated protein.

Sirtuins (SIRTs), a family of nicotinamide adenine dinucleotide (NAD)-dependent deacetylases (SIRT1-7), exhibit antioxidant, anti-apoptotic, and anti-inflammatory properties, positioning them as key regulators in sepsis.[94] Specifically, SIRT1 activation, mediated by growth arrest-specific transcript 5 (GAS5), nicaraven (AVS), and nicotinamide mononucleotide (NMN), attenuates inflammation by inhibiting high mobility group box 1 (HMGB1) and NF-κB p65 acetylation, respectively, thereby improving survival and mitigating organ damage in sepsis models.[95-97] NMN also inhibits NF-κB p65 phosphorylation, thereby preventing sepsis-induced ALI.[97]

SIRT2 is a negative regulatory factor of autophagy. Its inhibition promotes autophagy and attenuates septic AKI through increasing FOXO1 acetylation.[98] Furthermore, the costimulatory molecule glucocorticoid-induced TNFR-related protein (GITR) induces SIRT2 degradation by recruiting E3 ligase MARCH7, reducing NLRP3 ubiquitination but increasing its acetylation, thereby exacerbating macrophage pyroptosis, and systemic inflammatory injury.[99] SIRT3, localized in the mitochondrial matrix,[100] mitigates oxidative stress and inflammation in sepsis-induced ALI by inhibiting p53 acetylation, an effect enhanced by menadione 4 (MK-4).[101] SIRT7 (the only sirtuin located in the nucleolus) is required for ribosomal DNA transcription.[100] SIRT7 inactivation by Zn^{2+} increases parkin acetylation, promoting parkin-mediated mitophagy and inhibiting NLRP3 activation, thus ameliorating AKI in sepsis.[102]

SIRTs and acetylation critically regulate inflammation and sepsis progression, making them promising therapeutic targets. Molecules such as GAS5, AVS, NMN, GITR, MK-4, and Zn^{2+} may offer avenues for targeted intervention.

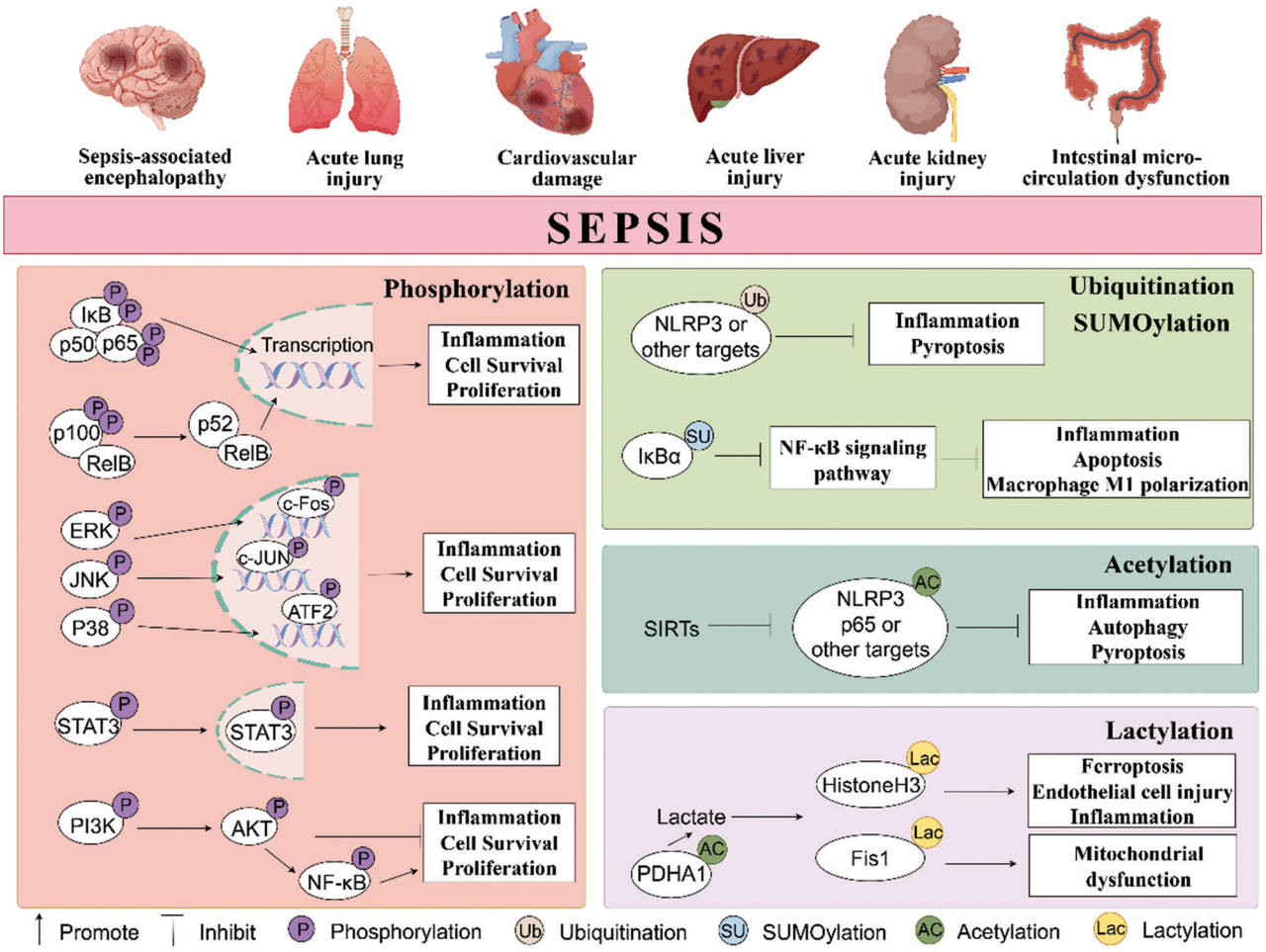

Figure 1. Overview of the regulatory mechanisms of post-translational modifications in sepsis. The main types of protein translation post-translational modifications involved in sepsis and multiple organ dysfunction syndrome are phosphorylation, ubiquitination, SUMOylation, acetylation, and lactylation. The schematic diagram was created on www.figdraw.com.

7. Lactylation and sepsis

Lactylation, the addition of lactyl groups to lysine residues, represents another PTM implicated in sepsis.[103] In sepsis, increased glycolysis leads to lactate accumulation, driving both histone and non-histone lactylation, thereby dynamically controlling gene expression and contributing to organ dysfunction.[104]

7.1. Histone lactylation

Histone H3 lysine 18 lactylation (H3K18la), a specific lactylation site, promotes METTL3 expression and transcription factor early growth response protein 1 (EGR1) enrichment, exacerbating ALI in sepsis.[105,106] Lactate-induced H3K18la activates RhoA protein and mediates downstream inflammation and apoptosis, leading to kidney injury. It also activates ezrin K263 lactylation, identifying ezrin as a lactate substrate for the 1st time.[107] Lactate also increases H3K14la levels, activating inflammation of endothelial cells and lung injury by promoting transcription of ferroptosis-related genes *TFRC* and *SLC40A1*.[108] These findings suggest histone lactylation as a regulator of sepsis-induced organ damage, with METTL3 and EGR1 represents promising therapeutic targets.

7.2. Non-histone lactylation

While initially identified on histones, non-histone lactylation is also a focus of current research. Lactate promotes HMGB1 lactylation and acetylation through a p300/CBP-dependent pathway, leading to its release and endothelial barrier dysfunction, promoting sepsis development.[109] In addition, lactate mediates mitochondrial fission 1 protein lysine 20 (Fis1 K20la) lactylation, promoting excessive mitochondrial fission and exacerbating sepsis-induced AKI. Notably, this process is driven by SIRT3 downregulation-mediated hyperacetylation and inactivation of pyruvate dehydrogenase E1 component subunit α (PDHA1), leading to lactate excess in endothelial cells of renal tubules.[21] The interplay between lactylation and acetylation, driven by lactate and acetyl-CoA, respectively, highlights the importance of metabolic homeostasis in sepsis.[110] Targeting HMGB1 and PDHA1 may offer novel therapeutic strategies by modulating the dynamic homeostasis between acetylation and lactylation.

8. Conclusion and perspectives

Sepsis pathogenesis involves an initial hyperinflammation phase driven by excessive inflammatory cytokines release, followed by immunosuppression characterized by anti-inflammatory cytokine production, immune cell death, and regulatory cell proliferation.[111] PTMs, critical regulators of protein function, are implicated in sepsis pathogenesis, offering potential therapeutic targets.[112]

This review summarizes the potential role of PTMs in sepsis and sepsis-induced multiple organ dysfunction identified in recent years (Figure 1 and Table 1). Phosphorylation, ubiquitination, and SUMOylation primarily contribute to the early inflammatory storm, with NF-κB, MAPK, and STAT3 phosphorylation driving pro-inflammatory cytokine release, and E3 ligase regulating NLRP3 inflammasome activation and cell death. The PI3K/AKT pathway exhibits dual role in sepsis. XBJ improves intestinal microcirculation by activating the PI3K/AKT pathway,[66] while hibifolin inhibits this pathway to alleviate lung injury,[65] highlighting the need for tissue-specific regulation. Acetylation and lactylation are dynamically regulated by metabolites (acetyl-CoA, lactate), forming a "metabolism–PTM-gene expression" cascade. SIRT3 downregulation-mediated PDHA1 acetylation induces Fis1 lactylation, suggesting that targeting metabolic enzymes may regulate multiple PTMs simultaneously.[21] Furthermore, NAD+ precursor NMN inhibits NF-κB by activating SIRT1, providing a strategy for combined metabolic and immune regulation.[97]

However, most studies are limited to single PTM or organ, lacking systematic analysis of multi-modification interactions like ubiquitination-acetylation competition, and systemic effects. Tissue-specific E3 ligase distribution, such as the opposing effects of TRIM21 in lung epithelium versus TRIM31 in myocardium, highlights the need for organ-targeted delivery systems, reducing off-target toxicity.[85,113] Future studies can focus on developing dual-function molecules such as inhibiting phosphorylation and activating deacetylation, synergistically regulating immune balance, or combining PTM inhibitors with drugs targeting various mechanisms to improve sepsis treatment efficacy.

In conclusion, exploring PTMs-related regulatory factors offers a novel strategy for developing sepsis therapeutics. However, translation to clinical application requires further investigation to shift sepsis treatment from "broad-spectrum anti-inflammation" to "precise modification and regulation."

Acknowledgments

None.

Funding

This work was supported by the Beijing Natural Science Foundation (grant number: L246039), the National Natural Science Foundation of China (grant numbers: 82372189, 81871586, and 82172128), and the Beijing High-

Level Public Health Technical Talent Training Program (Discipline Backbone Talent 02-32).

Conflict of interest

Liuluan Zhu is the Editorial Board Member of this journal but was not in any way involved in the editorial and peer-review process conducted for this paper, directly or indirectly. Separately, other authors declared that they have no known competing financial interests or personal relationships that could have influenced the work reported in this paper.

Author contributions

Conceptualization: Wenyue Gao
Visualization: Wenyue Gao
Writing – original draft: Wenyue Gao
Writing – review & editing: Liuluan Zhu, Yue Zhang

Ethics approval and consent to participate

Not applicable.

Consent for publication

Not applicable.

Availability of data

Not applicable.

References

1. Cecconi M, Evans L, Levy M, Rhodes A. Sepsis and septic shock. *Lancet*. 2018;392(10141):75-87.

   doi: 10.1016/S0140-6736(18)30696-2

2. White KC, Serpa-Neto A, Hurford R, *et al*. Sepsis-associated acute kidney injury in the intensive care unit: Incidence, patient characteristics, timing, trajectory, treatment, and associated outcomes. A multicenter, observational study. *Intensive Care Med*. 2023;49(9):1079-1089.

   doi: 10.1007/s00134-023-07138-0

3. Qiao X, Yin J, Zheng Z, Li L, Feng X. Endothelial cell dynamics in sepsis-induced acute lung injury and acute respiratory distress syndrome: Pathogenesis and therapeutic implications. *Cell Commun Signal*. 2024;22(1):241.

   doi: 10.1186/s12964-024-01620-y

4. Zhang K, Wang Y, Chen S, *et al*. TREM2^{hi} resident macrophages protect the septic heart by maintaining cardiomyocyte homeostasis. *Nat Metab*. 2023;5(1):129-146.

   doi: 10.1038/s42255-022-00715-5

5. Liu Y, Yang H, Liu X, Gu H, Li Y, Sun C. Protein acetylation: A novel modus of obesity regulation. *J Mol Med* (*Berl*). 2021;99(9):1221-1235.

   doi: 10.1007/s00109-021-02082-2

6. Song L, Jiang W, Lin H, Yu J, Liu K, Zheng R. Post-translational modifications in sepsis-induced organ dysfunction: Mechanisms and implications. *Front Immunol*. 2024;15:1461051.

   doi: 10.3389/fimmu.2024.1461051

7. Raymond SL, Holden DC, Mira JC, *et al*. Microbial recognition and danger signals in sepsis and trauma. *Biochim Biophys Acta Mol Basis Dis*. 2017;1863(10 Pt B):2564-2573.

   doi: 10.1016/j.bbadis.2017.01.013

8. Merle NS, Noe R, Halbwachs-Mecarelli L, Fremeaux-Bacchi V, Roumenina LT. Complement system part II: Role in immunity. *Front Immunol*. 2015;6:257.

   doi: 10.3389/fimmu.2015.00257

9. Sørensen OE, Borregaard N. Neutrophil extracellular traps - the dark side of neutrophils. *J Clin Invest*. 2016;126(5):1612-1620.

   doi: 10.1172/JCI84538

10. Venet F, Monneret G. Advances in the understanding and treatment of sepsis-induced immunosuppression. *Nat Rev Nephrol*. 2018;14(2):121-137.

    doi: 10.1038/nrneph.2017.165

11. Islam MM, Watanabe E, Salma U, *et al*. Immunoadjuvant therapy in the regulation of cell death in sepsis: Recent advances and future directions. *Front Immunol*. 2024;15:1493214.

    doi: 10.3389/fimmu.2024.1493214

12. Levi M, Poll T. Coagulation in patients with severe sepsis. *Semin Thromb Hemost*. 2015;41(1):9-15.

    doi: 10.1055/s-0034-1398376

13. Kappelmayer J, Debreceni IB, Fejes Z, Nagy B Jr. Inflammation, sepsis, and the coagulation system. *Hamostaseologie*. 2024;44(4):268-276.

    doi: 10.1055/a-2202-8544

14. Wei X, Tu Y, Bu S, Guo G, Wang H, Wang Z. Unraveling the intricate web: Complement activation shapes the pathogenesis of sepsis-induced coagulopathy. *J Innate Immun*. 2024;16(1):337-353.

    doi: 10.1159/000539502

15. Xiao M, Liu D, Xu Y, Mao W, Li W. Role of PFKFB3-driven glycolysis in sepsis. *Ann Med*. 2023;55(1):1278-1289.

    doi: 10.1080/07853890.2023.2191217

16. Singer M. The role of mitochondrial dysfunction in sepsis-induced multi-organ failure. *Virulence*. 2014;5(1):66-72.

    doi: 10.4161/viru.26907

17. Xl L, Gy Z, Guo R, Cui N. Ferroptosis in sepsis: The mechanism, the role and the therapeutic potential. *Front*

Immunol. 2022;13:956361.

doi: 10.3389/fimmu.2022.956361

18. Deng S, Gu B, Yu Z, Shen Z, Ren H. MIR210HG aggravates sepsis-induced inflammatory response of proximal tubular epithelial cell via the NF-κB Signaling pathway. *Yonsei Med J*. 2021;62(5):461-469.

doi: 10.3349/ymj.2021.62.5.461

19. Wu JL, Wu HY, Tsai DY, *et al*. Temporal regulation of Lsp1 O-GlcNAcylation and phosphorylation during apoptosis of activated B cells. *Nat Commun*. 2016;7:12526.

doi: 10.1038/ncomms12526

20. Qian Y, Wang Z, Lin H, *et al*. TRIM47 is a novel endothelial activation factor that aggravates lipopolysaccharide-induced acute lung injury in mice via K63-linked ubiquitination of TRAF2. *Signal Transduct Target Ther*. 2022;7(1):148.

doi: 10.1038/s41392-022-00953-9

21. An S, Yao Y, Hu H, *et al*. PDHA1 hyperacetylation-mediated lactate overproduction promotes sepsis-induced acute kidney injury via Fis1 lactylation. *Cell Death Dis*. 2023;14(7):457.

doi: 10.1038/s41419-023-05952-4

22. Singh V, Ram M, Kumar R, Prasad R, Roy BK, Singh KK. Phosphorylation: Implications in Cancer. *Protein J*. 2017;36(1):1-6.

doi: 10.1007/s10930-017-9696-z

23. Yu H, Lin L, Zhang Z, Zhang H, Hu H. Targeting NF-κB pathway for the therapy of diseases: Mechanism and clinical study. *Signal Transduct Target Ther*. 2020;5(1):209.

doi: 10.1038/s41392-020-00312-6

24. Lai JL, Liu YH, Liu C, *et al*. Indirubin inhibits LPS-induced inflammation via TLR4 abrogation mediated by the NF-kB and MAPK signaling pathways. *Inflammation*. 2017;40(1):1-12.

doi: 10.1007/s10753-016-0447-7

25. Zhou X, Zhang L, Lie L, *et al*. MxA suppresses TAK1-IKKα/β-NF-κB mediated inflammatory cytokine production to facilitate *Mycobacterium tuberculosis* infection. *J Infect*. 2020;81(2):231-241.

doi: 10.1016/j.jinf.2020.05.030

26. Yuan M, Jing G, Kong Q, *et al*. TIPE2 ameliorates neuroinflammation and cognitive impairment in sepsis-associated encephalopathy through regulating RhoA/ROCK2-NF-κB signaling pathway. *Biochem Pharmacol*. 2023;217:115816.

doi: 10.1016/j.bcp.2023.115816

27. Duan M, Jie J, Li C, *et al*. Echinatin alleviates sepsis severity through modulation of the NF-κB and MEK/ERK signaling pathways. *Biomed Pharmacother*. 2024;179:117359.

doi: 10.1016/j.biopha.2024.117359

28. Zeng N, Jian Z, Zhu W, Xu J, Fan Y, Xiao F. KLF13 overexpression protects sepsis-induced myocardial injury and LPS-induced inflammation and apoptosis. *Int J Exp Pathol*. 2023;104(1):23-32.

doi: 10.1111/iep.12459

29. Huang X, Zhang MZ, Liu B, Ma SY, Yin X, Guo LH. Astragaloside IV attenuates polymicrobial sepsis-induced cardiac dysfunction in rats via IKK/NF-κB pathway. *Chin J Integr Med*. 2021;27(11):825-831.

doi: 10.1007/s11655-021-2869-9

30. Huang Q, Liu DH, Chen CF, *et al*. Pgc-1α promotes phosphorylation, inflammation, and apoptosis in H9c2 cells during the early stage of lipopolysaccharide induction. *Inflammation*. 2021;44(5):1771-1781.

doi: 10.1007/s10753-021-01453-8

31. Li H, Liu Z, Wang Y, *et al*. PARK7 is induced to protect against endotoxic acute kidney injury by suppressing NF-κB. *Clin Sci* (*Lond*). 2022;136(24):1877-1891.

doi: 10.1042/CS20220493

32. Cargnello M, Roux PP. Activation and function of the MAPKs and their substrates, the MAPK-activated protein kinases. *Microbiol Mol Biol Rev*. 2011;75(1):50-83.

doi: 10.1128/MMBR.00031-10

33. Park HB, Baek KH. E3 ligases and deubiquitinating enzymes regulating the MAPK signaling pathway in cancers. *Biochim Biophys Acta Rev Cancer*. 2022;1877(3):188736.

doi: 10.1016/j.bbcan.2022.188736

34. Lucas RM, Luo L, Stow JL. ERK1/2 in immune signalling. *Biochem Soc Trans*. 2022;50(5):1341-1352.

doi: 10.1042/BST20220271

35. Crawford TQ, Hecht FM, Pilcher CD, Ndhlovu LC, Barbour JD. Activation associated ERK1/2 signaling impairments in $CD8^+$ T cells co-localize with blunted polyclonal and HIV-1 specific effector functions in early untreated HIV-1 infection. *PLoS One*. 2013;8(10):e77412.

doi: 10.1371/journal.pone.0077412

36. Liang D, Zeng Q, Xu Z, *et al*. BAFF activates Erk1/2 promoting cell proliferation and survival by $Ca2^+$-CaMKII-dependent inhibition of PP2A in normal and neoplastic B-lymphoid cells. *Biochem Pharmacol*. 2014;87(2):332-343.

doi: 10.1016/j.bcp.2013.11.006

37. Feng Z, Li M, Ma A, *et al*. Intermedin (adrenomedullin 2) plays a protective role in sepsis by regulating T- and B-cell proliferation and activity. *Int Immunopharmacol*. 2023;121:110488.

doi: 10.1016/j.intimp.2023.110488

38. Yuan Y, Hua L, Zhou J, *et al*. The effect of artesunate to reverse CLP-induced sepsis immunosuppression mice

with secondary infection is tightly related to reducing the apoptosis of T cells via decreasing the inhibiting receptors and activating MAPK/ERK pathway. *Int Immunopharmacol*. 2023;124(Pt A):110917.

doi: 10.1016/j.intimp.2023.110917

39. Hammouda MB, Ford AE, Liu Y, Zhang JY. The JNK signaling pathway in inflammatory skin disorders and cancer. *Cells*. 2020;9(4):857.

doi: 10.3390/cells9040857

40. Zhu H, Zhang L, Jia H, *et al*. Tetrahydrocurcumin improves lipopolysaccharide-induced myocardial dysfunction by inhibiting oxidative stress and inflammation via JNK/ERK signaling pathway regulation. *Phytomedicine*. 2022;104:154283.

doi: 10.1016/j.phymed.2022.154283

41. Ouyang J, Hong Y, Wan Y, *et al*. PVB exerts anti-inflammatory effects by inhibiting the activation of MAPK and NF-κB signaling pathways and ROS generation in neutrophils. *Int Immunopharmacol*. 2024;126:111271.

doi: 10.1016/j.intimp.2023.111271

42. Coulthard LR, White DE, Jones DL, McDermott MF, Burchill SA. p38(MAPK): Stress responses from molecular mechanisms to therapeutics. *Trends Mol Med*. 2009;15(8):369-379.

doi: 10.1016/j.molmed.2009.06.005

43. Dai M, Sun S, Dai Y, *et al*. Maresin-1 ameliorates sepsis-induced microglial activation through modulation of the P38 MAPK pathway. *Neurochem Res*. 2024;50(1):26.

doi: 10.1007/s11064-024-04280-z

44. Zhang HF, Zhang HB, Wu XP, Guo YL, Cheng WD, Qian F. Fisetin alleviates sepsis-induced multiple organ dysfunction in mice via inhibiting p38 MAPK/MK2 signaling. *Acta Pharmacol Sin*. 2020;41(10):1348-1356.

doi: 10.1038/s41401-020-0462-y

45. Dong R, Xue Z, Fan G, *et al*. Pin1 promotes NLRP3 inflammasome activation by phosphorylation of p38 MAPK pathway in septic shock. *Front Immunol*. 2021;12:620238.

doi: 10.3389/fimmu.2021.620238

46. Li D, Ren W, Jiang Z, Zhu L. Regulation of the NLRP3 inflammasome and macrophage pyroptosis by the p38 MAPK signaling pathway in a mouse model of acute lung injury. *Mol Med Rep*. 2018;18(5):4399-4409.

doi: 10.3892/mmr.2018.9427

47. Yue L, Liu X, Wu C, *et al*. Toll-like receptor 4 promotes the inflammatory response in septic acute kidney injury by promoting p38 mitogen-activated protein kinase phosphorylation. *J Bioenerg Biomembr*. 2023;55(5):353-363.

doi: 10.1007/s10863-023-09972-9

48. Wang Y, Cui C, Zhao W, *et al*. WIP1-mediated regulation of p38 MAPK signaling attenuates pyroptosis in sepsis-associated acute kidney injury. *Immunobiology*. 2024;229(5):152832.

doi: 10.1016/j.imbio.2024.152832

49. Hillmer EJ, Zhang H, Li HS, Watowich SS. STAT3 signaling in immunity. *Cytokine Growth Factor Rev*. 2016;31:1-15.

doi: 10.1016/j.cytogfr.2016.05.001

50. Lei W, Liu D, Sun M, *et al*. Targeting STAT3: A crucial modulator of sepsis. *J Cell Physiol*. 2021;236(11):7814-7831.

doi: 10.1002/jcp.30394

51. Paul WE, Zhu J. How are T(H)2-type immune responses initiated and amplified? *Nat Rev Immunol*. 2010;10(4):225-235.

doi: 10.1038/nri2735

52. Liu Y, Yang H, Zhu F, Ouyang Y, Pan P. Inhibition of STAT3 phosphorylation by colchicine regulates NLRP3 activation to alleviate sepsis-induced acute lung injury. *Inflammopharmacology*. 2023;31(4):2007-2021.

doi: 10.1007/s10787-023-01199-9

53. Qian T, Qi B, Fei Y, *et al*. PLD2 deletion alleviates disruption of tight junctions in sepsis-induced ALI by regulating PA/STAT3 phosphorylation pathway. *Int Immunopharmacol*. 2023;114:109561.

doi: 10.1016/j.intimp.2022.109561

54. Li N, Lin G, Zhang H, *et al*. Lyn attenuates sepsis-associated acute kidney injury by inhibition of phospho-STAT3 and apoptosis. *Biochem Pharmacol*. 2023;211:115523.

doi: 10.1016/j.bcp.2023.115523

55. Tan Z, Liu Q, Chen H, *et al*. Pectolinarigenin alleviated septic acute kidney injury via inhibiting Jak2/Stat3 signaling and mitochondria dysfunction. *Biomed Pharmacother*. 2023;159:114286.

doi: 10.1016/j.biopha.2023.114286

56. Xu L, Cai J, Li C, *et al*. 4-Octyl itaconate attenuates LPS-induced acute kidney injury by activating Nrf2 and inhibiting STAT3 signaling. *Mol Med*. 2023;29(1):58.

doi: 10.1186/s10020-023-00631-8

57. Wang L, Deng Z, Sun Y, *et al*. The study on the regulation of Th cells by mesenchymal stem cells through the JAK-STAT signaling pathway to protect naturally aged sepsis model rats. *Front Immunol*. 2022;13:820685.

doi: 10.3389/fimmu.2022.820685

58. Ersahin T, Tuncbag N, Cetin-Atalay R. The PI3K/AKT/mTOR interactive pathway. *Mol Biosyst*. 2015;11(7):1946-1954.

doi: 10.1039/c5mb00101c

59. Liu H, Weng XJ, Yao JY, *et al*. Neuregulin-1 β protects the rat diaphragm during sepsis against oxidative stress and

inflammation by activating the PI3K/Akt pathway. *Oxid Med Cell Longev*. 2020;2020:1720961.

doi: 10.1155/2020/1720961

60. Liang LD, Peng HX, Huang MJ, *et al*. HGF ameliorates cardiomyocyte apoptosis and inflammatory response in sepsis via the phosphatidylinositol 3-kinase (PI3K)/protein kinase B (AKT) pathway. *Gene*. 2024;928:148763.

doi: 10.1016/j.gene.2024.148763

61. Zhao Y, Ye W, Wang YD, Chen WD. HGF/c-met: A key promoter in liver regeneration. *Front Pharmacol*. 2022;13:808855.

doi: 10.3389/fphar.2022.808855

62. Ziegler AC, Haider RS, Hoffmann C, Gräler MH. S1PR3 agonism and S1P lyase inhibition rescue mice in the severe state of experimental sepsis. *Biomed Pharmacother*. 2024;174:116575.

doi: 10.1016/j.biopha.2024.116575

63. Wang L, Jiang S, Li X, Lin T, Qin T. Astringin protects LPS-induced toxicity by suppressing oxidative stress and inflammation via suppression of PI3K/AKT/NF-κB pathway for pediatric acute lung injury. *Naunyn Schmiedebergs Arch Pharmacol*. 2023;396(10):2369-2377.

doi: 10.1007/s00210-023-02439-z

64. Zheng Y, Li Y, Li S, Hu R, Zhang L. Annexin A1 (Ac2-26)-dependent Fpr2 receptor alleviates sepsis-induced acute kidney injury by inhibiting inflammation and apoptosis *in vivo* and *in vitro*. *Inflamm Res*. 2023;72(2):347-362.

doi: 10.1007/s00011-022-01640-9

65. Ng YY, Ho YC, Yen CH, *et al*. Protective Effect of hibifolin on lipopolysaccharide-induced acute lung injury through akt phosphorylation and NFκB pathway. *Environ Toxicol*. 2024;40:524-531.

doi: 10.1002/tox.24383

66. Tang AL, Li Y, Sun LC, *et al*. Xuebijing improves intestinal microcirculation dysfunction in septic rats by regulating the VEGF-A/PI3K/Akt signaling pathway. *World J Emerg Med*. 2024;15(3):206-213.

doi: 10.5847/wjem.j.1920-8642.2024.035

67. Kawamura A, Ito A, Takahashi A, Sawamoto A, Okuyama S, Nakajima M. Benproperine reduces IL-6 levels via Akt signaling in monocyte/macrophage-lineage cells and reduces the mortality of mouse sepsis model induced by lipopolysaccharide. *J Pharmacol Sci*. 2024;156(2):125-133.

doi: 10.1016/j.jphs.2024.08.001

68. Popovic D, Vucic D, Dikic I. Ubiquitination in disease pathogenesis and treatment. *Nat Med*. 2014;20(11):1242-1253.

doi: 10.1038/nm.3739

69. Swatek KN, Komander D. Ubiquitin modifications. *Cell Res*. 2016;26(4):399-422.

doi: 10.1038/cr.2016.39

70. Shao S, Zhou D, Feng J, *et al*. Regulation of inflammation and immunity in sepsis by E3 ligases. *Front Endocrinol* (*Lausanne*). 2023;14:1124334.

doi: 10.3389/fendo.2023.1124334

71. Shim DW, Lee KH. Posttranslational regulation of the NLR family pyrin domain-containing 3 inflammasome. *Front Immunol*. 2018;9:1054.

doi: 10.3389/fimmu.2018.01054

72. Toldo S, Mezzaroma E, Buckley LF, *et al*. Targeting the NLRP3 inflammasome in cardiovascular diseases. *Pharmacol Ther*. 2022;236:108053.

doi: 10.1016/j.pharmthera.2021.108053

73. Tang J, Tu S, Lin G, *et al*. Sequential ubiquitination of NLRP3 by RNF125 and Cbl-b limits inflammasome activation and endotoxemia. *J Exp Med*. 2020;217(4):133674.

doi: 10.1084/jem.20182091

74. Wang D, Zhang Y, Xu X, *et al*. YAP promotes the activation of NLRP3 inflammasome via blocking K27-linked polyubiquitination of NLRP3. *Nat Commun*. 2021;12(1):2674.

doi: 10.1038/s41467-021-22987-3

75. Shen W, Zhang X, Tang M, Chen W, Wang Y, Zhou H. Targeting of ubiquitination and degradation of KLF15 by E3 ubiquitin ligase KBTBD7 regulates LPS-induced septic brain injury in microglia. *Exp Cell Res*. 2024;443(1):114317.

doi: 10.1016/j.yexcr.2024.114317

76. Liu J, Song K, Lin B, *et al*. The suppression of HSPA8 attenuates NLRP3 ubiquitination through SKP2 to promote pyroptosis in sepsis-induced lung injury. *Cell Biosci*. 2024;14(1):56

doi: 10.1186/s13578-024-01239-z

77. Xu D, Jiang J, Liu Y, et al. TIMP2 protects against sepsis-associated acute kidney injury by cAMP/NLRP3 axis-mediated pyroptosis. *Am J Physiol Cell Physiol*. 2024;326(5):C1353-C1366.

doi: 10.1152/ajpcell.00577.2023

78. Cockram PE, Kist M, Prakash S, Chen SH, Wertz IE, Vucic D. Ubiquitination in the regulation of inflammatory cell death and cancer. *Cell Death Differ*. 2021;28(2):591-605.

doi: 10.1038/s41418-020-00708-5

79. Wang Y, Chen D, Xie H, *et al*. AUF1 protects against ferroptosis to alleviate sepsis-induced acute lung injury by regulating NRF2 and ATF3. *Cell Mol Life Sci*. 2022;79(5):228.

doi: 10.1007/s00018-022-04248-8

80. Li Z, Wu B, Chen J, *et al*. WWP2 protects against sepsis-

induced cardiac injury through inhibiting cardiomyocyte ferroptosis. *J Transl Int Med*. 2024;12(1):35-50.

doi: 10.2478/jtim-2024-0004

81. Liao J, Su X, Wang M, *et al*. The E3 ubiquitin ligase CHIP protects against sepsis-induced myocardial dysfunction by inhibiting NF-κB-mediated inflammation via promoting ubiquitination and degradation of karyopherin-α 2. *Transl Res*. 2023;255:50-65.

doi: 10.1016/j.trsl.2022.11.006

82. Wang M, Liao J, Lin W, *et al*. YL-109 attenuates sepsis-associated multiple organ injury through inhibiting the ERK/AP-1 axis and pyroptosis by upregulating CHIP. *Biomed Pharmacother*. 2024;175:116633.

doi: 10.1016/j.biopha.2024.116633

83. Zhao YY, Wu DM, He M, *et al*. Samotolisib attenuates acute liver injury through inhibiting caspase-11-mediated pyroptosis via regulating E3 ubiquitin ligase Nedd4. *Front Pharmacol*. 2021;12:726198.

doi: 10.3389/fphar.2021.726198

84. Chen Z, Lin B, Yao X, *et al*. OAS3 deubiquitination due to E3 ligase TRIM21 downregulation promotes epithelial cell apoptosis and drives sepsis-induced acute lung injury. *Int J Biol Sci*. 2024;20(14):5594-5607.

doi: 10.7150/ijbs.96089

85. Ma W, Zheng J, Wu B, Wang M, Kang Z. Regulatory mechanism of TRIM21 in sepsis-induced acute lung injury by promoting IRF1 ubiquitination. *Clin Exp Pharmacol Physiol*. 2024;51(11):e13911.

doi: 10.1111/1440-1681.13911

86. Li O, Ma Q, Li F, Cai GY, Chen XM, Hong Q. Progress of small ubiquitin-related modifiers in kidney diseases. *Chin Med J* (*Engl*). 2019;132(4):466-473.

doi: 10.1097/CM9.0000000000000094

87. Decque A, Joffre O, Magalhaes JG, *et al*. Sumoylation coordinates the repression of inflammatory and anti-viral gene-expression programs during innate sensing. *Nat Immunol*. 2016;17(2):140-149.

doi: 10.1038/ni.3342

88. Wang G, Yang F, Gao T, Wu D, Huang J, Li J. Effect of deletion of SUMOylation on dendritic cell function in septic mice and its role in sepsis. *Zhong Nan Da Xue Xue Bao Yi Xue Ban*. 2020;45(3):314-321.

doi: 10.11817/j.issn.1672-7347.2020.190684

89. Qiu P, Liu Y, Zhang J. Review: The role and mechanisms of macrophage autophagy in sepsis. *Inflammation*. 2019;42(1):6-19.

doi: 10.1007/s10753-018-0890-8

90. Wang K, Xiong J, Lu Y, Wang L, Tian T. SENP1-KLF4 signalling regulates LPS-induced macrophage M1 polarization. *FEBS J*. 2023;290(1):209-224.

doi: 10.1111/febs.16589

91. Zheng C, Li D, Zhan W, He K, Yang H. Downregulation of SENP1 suppresses LPS-induced macrophage inflammation by elevating Sp3 SUMOylation and disturbing Sp3-NF-κB interaction. *Am J Transl Res*. 2020;12(11):7439-7448.

92. Liu X, Chen L, Zhang C, *et al*. Ginkgolic acid promotes inflammation and macrophage apoptosis via SUMOylation and NF-κB pathways in sepsis. *Front Med* (*Lausanne*). 2022;9:1108882.

doi: 10.3389/fmed.2022.1108882

93. Li X, Li X, Huang P, *et al*. Acetylation of TIR domains in the TLR4-Mal-MyD88 complex regulates immune responses in sepsis. *EMBO J*. 2024;43(21):4954-4983.

doi: 10.1038/s44318-024-00237-8

94. Covarrubias AJ, Perrone R, Grozio A, Verdin E. NAD^+ metabolism and its roles in cellular processes during ageing. *Nat Rev Mol Cell Biol*. 2021;22(2):119-141.

doi: 10.1038/s41580-020-00313-x

95. Zeng Z, Lan Y, Chen Y, *et al*. LncRNA GAS5 suppresses inflammatory responses by inhibiting HMGB1 release via miR-155-5p/SIRT1 axis in sepsis. *Eur J Pharmacol*. 2023;942:175520.

doi: 10.1016/j.ejphar.2023.175520

96. Zha D, Yang Y, Huang X, *et al*. Nicaraven protects against endotoxemia-induced inflammation and organ injury through modulation of AMPK/Sirt1 signaling in macrophages. *Eur J Pharmacol*. 2023;946:175666.

doi: 10.1016/j.ejphar.2023.175666

97. He S, Jiang X, Yang J, *et al*. Nicotinamide mononucleotide alleviates endotoxin-induced acute lung injury by modulating macrophage polarization via the SIRT1/NF-κB pathway. *Pharm Biol*. 2024;62(1):22-32.

doi: 10.1080/13880209.2023.2292256

98. Yu B, Weng L, Li J, *et al*. Inhibiting SIRT2 Attenuates sepsis-induced acute kidney injury via FOXO1 acetylation-mediated autophagy activation. *Shock*. 2025;63(2):255-266.

doi: 10.1097/SHK.0000000000002505

99. Liang S, Zhou J, Cao C, *et al*. GITR exacerbates lysophosphatidylcholine-induced macrophage pyroptosis in sepsis via posttranslational regulation of NLRP3. *Cell Mol Immunol*. 2024;21(7):674-688.

doi: 10.1038/s41423-024-01170-w

100. Morigi M, Perico L, Benigni A. Sirtuins in renal health and disease. *J Am Soc Nephrol*. 2018;29(7):1799-1809.

doi: 10.1681/ASN.2017111218

101. Gao N, Liu XY, Chen J, Hu TP, Wang Y, Zhang GQ.

Menaquinone-4 alleviates sepsis-associated acute lung injury via activating SIRT3-p53/SLC7A11 pathway. *J Inflamm Res*. 2024;17:7675-7685.

doi: 10.2147/JIR.S486984

102. Guo J, Yuan Z, Wang R. Zn^{2+} improves sepsis-induced acute kidney injury by upregulating SIRT7-mediated parkin acetylation. *Am J Physiol Renal Physiol*. 2024;327(1):F184-F197.

doi: 10.1152/ajprenal.00337.2023

103. Zhang D, Tang Z, Huang H, *et al*. Metabolic regulation of gene expression by histone lactylation. *Nature*. 2019;574(7779):575-580.

doi: 10.1038/s41586-019-1678-1

104. Liu S, Yang T, Jiang Q, *et al*. Lactate and lactylation in sepsis: A comprehensive review. *J Inflamm Res*. 2024;17:4405-4417.

doi: 10.2147/JIR.S459185

105. Wu D, Spencer CB, Ortoga L, Zhang H, Miao C. Histone lactylation-regulated METTL3 promotes ferroptosis via m6A-modification on ACSL4 in sepsis-associated lung injury. *Redox Biol*. 2024;74:103194.

doi: 10.1016/j.redox.2024.103194

106. Lu Z, Fang P, Li S, *et al*. Lactylation of histone H3k18 and Egr1 promotes endothelial glycocalyx degradation in sepsis-induced acute lung injury. *Adv Sci* (*Weinh*). 2024;12:e2407064.

doi: 10.1002/advs.202407064

107. Qiao J, Tan Y, Liu H, *et al*. Histone H3K18 and ezrin lactylation promote renal dysfunction in sepsis-associated acute kidney injury. *Adv Sci* (*Weinh*). 2024;11(28):e2307216.

doi: 10.1002/advs.202307216

108. Gong F, Zheng X, Xu W, *et al*. H3K14la drives endothelial dysfunction in sepsis-induced ARDS by promoting SLC40A1/transferrin-mediated ferroptosis. *MedComm* (*2020*). 2025;6(2):e70049.

doi: 10.1002/mco2.70049

109. Yang K, Fan M, Wang X, *et al*. Lactate promotes macrophage HMGB1 lactylation, acetylation, and exosomal release in polymicrobial sepsis. *Cell Death Differ*. 2022;29(1):133-146.

doi: 10.1038/s41418-021-00841-9

110. Sun Z, Song Y, Li J, Li Y, Yu Y, Wang X. Potential biomarker for diagnosis and therapy of sepsis: Lactylation. *Immun Inflamm Dis*. 2023;11(10):e1042.

doi: 10.1002/iid3.1042

111. Liu Z, Ting Y, Li M, Li Y, Tan Y, Long Y. From immune dysregulation to organ dysfunction: Understanding the enigma of Sepsis. *Front Microbiol*. 2024;15:1415274.

doi: 10.3389/fmicb.2024.1415274

112. Wu X, Xu M, Geng M, *et al*. Targeting protein modifications in metabolic diseases: Molecular mechanisms and targeted therapies. *Signal Transduct Target Ther*. 2023;8(1):220.

doi: 10.1038/s41392-023-01439-y

113. Yang X, Sun J, Sun F, *et al*. TRIM31 promotes apoptosis via TAK1-mediated activation of NF-κB signaling in sepsis-induced myocardial dysfunction. *Cell Cycle*. 2020;19(20):2685-2700.

doi: 10.1080/15384101.2020.1826235

ACCSCIENCE PUBLISHING

Microbes & Immunity

REVIEW ARTICLE

Correlation between varicella-zoster virus infection and cancer development: A comprehensive analysis

Fernando Cisneros IV, Blake Martin, and Shizue Mito*

Department of Medical Education, School of Medicine, The University of Texas Rio Grande Valley, Edinburg, Texas, United States of America

Abstract

Varicella-zoster virus (VZV) is a highly prevalent pathogen primarily recognized for causing chickenpox during primary infection, and herpes zoster (HZ), also known as shingles, upon reactivation. While post-infectious complications of VZV, such as encephalitis, pneumonia, and post-herpetic neuralgia, are well-established, recent large population-based studies suggest that HZ may increase the risk of occult cancers. This has sparked discussions on the need for cancer screening in patients with HZ to improve early diagnosis and prognosis. However, the specific types of cancers most strongly associated with VZV reactivation have not been systematically identified, and the subsequent cancer risk remains inconclusive. Emerging evidence suggests that VZV may also modulate key oncogenic pathways, such as the inhibition of apoptosis, alteration of cell cycle regulatory enzymes, and interference with immunosurveillance, which could potentially promote cancer development. These findings indicate that VZV's role in cancer biology extends beyond merely increasing cancer risk and may involve direct cellular manipulation that facilitates oncogenesis. Understanding the interplay between VZV and cancer is critical for public health. Further exploration of the mechanisms of viral oncogenesis could provide valuable insights into how VZV contributes to cancer development and open avenues for targeted preventive and therapeutic strategies.

Keywords: Varicella-zoster virus; Herpes zoster; Post-herpetic neuralgia; Cancer; Apoptosis; Cell cycle regulatory enzymes; Immunosurveillance; Oncogenesis

***Corresponding author:**
Shizue Mito
(shizue.mito@utrgv.edu)

Citation: Cisneros IV F, Martin B, Mito S. Correlation between varicella-zoster virus infection and cancer development: A comprehensive analysis. *Microbes & Immunity*. 2025;2(3):15-30. doi: 10.36922/mi.8320

Received: December 31, 2024

Revised: April 9, 2025

Accepted: April 9, 2025

Published online: May 2, 2025

1. Introduction

Varicella-zoster virus (VZV), a member of the DNA virus family *Herpesviridae*, is a highly prevalent pathogen primarily recognized for causing chickenpox during primary infection and shingles, also known as herpes zoster (HZ) upon reactivation.[1] Chickenpox is a common, self-limiting childhood disease characterized by a vesicular rash and fever, whereas HZ occurs later in life when the virus reactivates, often following periods of immunosuppression.[2] Beyond these well-known presentations, VZV is associated with a range of post-infectious complications. Neurological conditions such as encephalitis and cerebellar ataxia, respiratory issues such as varicella pneumonia, and chronic pain syndromes, including post-herpetic neuralgia (PHN), are well-documented in the medical literature. These complications not only contribute significantly to the disease

burden but also underscore the systemic impact of VZV beyond its primary manifestations.

Following primary infection, viral latency occurs in neurons, where it resides until reactivation, either spontaneously or due to an immunocompromised state in the host.[3] Although there are not typically any clinical symptoms that occur during the latency period, VZV may reactivate from ganglia in the entire neuraxis, causing a multitude of clinical pathology.[4] The most common clinical manifestation of VZV reactivation is a pruritic dermatomal rash; however, there are other infrequent and more serious complications that can occur if it is reactivated in the cranial nerves or if cerebral vasculature is affected.[5] At the molecular and cellular level, it is the interaction of VZV's genome with the host's immune cells, which are of particular importance in the link between VZV infection and cancer development.[6]

The link between chickenpox and VZV was first described in 1888; however, conclusive evidence proving this connection was not established until the 1950s.[7] Although chickenpox and HZ have been clinically characterized from the 16th and 17th centuries, respectively, the pathophysiology involving viral latency, reactivation triggers, and the role of the immune response in controlling VZV remains poorly understood. This is partly because VZV is a human-specific virus, limiting the use of most animal and animal-derived neuron models.[8]

Interestingly, emerging evidence suggests that VZV may have oncogenic potential. Previous studies have investigated potential links between VZV infection and the development of certain neoplasms, such as glioblastomas and other malignancies, though the mechanisms underlying this association remain unclear.[9] It is hypothesized that chronic inflammation, immune evasion strategies, or viral genome integration may play a role in promoting tumorigenesis associated with VZV infection.[10] Others have suggested that cancer diagnosis could result from immune system insufficiency, hypothesizing that a weakened immune system may allow HZ to occur, which could serve as an early sign of hidden cancer. The virus may also reduce immune surveillance, enabling tumors to escape detection.[11] However, other studies have strongly suggested that VZV infection is not associated with occult malignancy.[12]

This review evaluates the existing literature on the association between VZV and various cancer types, examining potential correlations with oncogenesis, addressing discrepancies and inconsistencies in the findings, and discussing the suggested mechanisms responsible for VZV's potential oncogenic effects.

2. Epidemiology of VZV

VZV is highly contagious, primarily spreading through respiratory droplets and direct contact with vesicular fluid from skin lesions.[13] The contagious period for varicella starts 1 – 2 days before the rash appears and continues until all lesions have crusted over, usually 5 days after rash onset in immunocompetent individuals.[14] VZV infection has been noted to follow a seasonal pattern, peaking during the winter and spring months, with many environmental factors influencing its transmission. These factors include elements such as ultraviolet radiation, which can reduce the rupture of vesicles.[15] In addition, population density increases contact rates, allowing for more infectivity. Both of these factors taken together may explain why there is a higher chance of VZV infection in temperate regions than in urban regions.[16]

The Centers for Disease Control and Prevention (CDC) estimated that from 1980 to 1990, there were 4 million annual cases of varicella, with 77% of cases in children under 9 and over 90% in those under 15. Seroprevalence data from 1988 to 1994 showed that the majority of adults (95.5% of those aged 20 – 29, 98.9% of those aged 30 – 39, and 99.6% of those 40 and older) were immune to varicella.[17] The varicella vaccination program, introduced in the United States in 1996, has had a profound impact on the incidence and complications of varicella infections over the past 25 years by significantly decreasing the number of VZV infections per year and reducing complications due to infection.[18] Varicella-related hospitalizations and deaths have been reduced by 94% and 97%, respectively, among those aged <50 years. Moreover, more than 91 million cases of varicella, 238,000 hospitalizations, and close to 2,000 deaths were prevented during the period between 1996 and 2020.[19]

During primary infection, VZV enters sensory nerve endings and establishes latency in the dorsal root ganglion. This latency period can last from 5 to 40 years or even longer. During this time, the virus resides in a non-replicative state within the neurons of the dorsal root ganglia, cranial nerve ganglia, and autonomic ganglia.[20] Although VZV latency is highly prevalent, only approximately 10 – 30% of individuals experience symptomatic reactivation. This reactivation is known as HZ and presents as a vesiculopapular rash along a single dermatome, which classically does not cross the midline.[21] Like primary VZV infection, HZ is typically a self-limiting condition and usually resolves within 2 – 4 weeks. However, HZ is most associated with the development of PHN, which is defined as pain that persists for at least 90 days after the resolution of the acute rash and can be debilitating, occurring in approximately 10 – 20% of HZ cases.[22,23] There are several

less common but significant complications associated with HZ, such as HZ ophthalmicus, disseminated zoster, meningitis, encephalitis, cranial nerve palsies, and more.[24] However, one complication that has yet to reach a consensus is the development of cancer secondary to HZ infection.

3. VZV's effects on the immune system

The reactivation of latent VZV in the dorsal root ganglia remains poorly understood. Immunodeficient states caused by coinfections, medications, or other diseases strongly correlate with reactivation.[25] Age is another key factor, with 68% of HZ cases occurring in individuals over 50.[26] Further clarification is needed to determine if HZ effects on the immune system make the body prone to cancer manifestation or if cancer diagnosis after HZ infection is a result of undetected cancer-suppressing the immune system allowing for VZV reactivation. In addition, understanding how VZV manipulates the immune system to establish latency could provide insights into its reactivation mechanisms and potential oncogenic properties.[3]

After exposure to infected respiratory droplets, VZV initially infects epithelial cells and resident dendritic cells in the upper respiratory tract. It then reaches local lymphoid tissues and transfers to mature T-lymphocytes.[27] Early theories suggested VZV preferentially infected T cells with specific phenotypes, but newer evidence indicates that VZV activates T cell signaling and remodels surface proteins, impairing immune function.[28] RNA sequencing of T cells from the lungs of simian varicella virus (SVV)-infected rhesus macaques showed that genes involved in gene regulation, cell cycle progression, and antiviral immune responses were activated, whereas genes related to antigen presentation and cellular metabolism were suppressed.[29] In addition, VZV disrupts immune responses by altering apoptotic signaling, interferon (IFN) signaling, and immune-related genes such as *CXCL10* and *IRF1*.[30,31] The infection progresses through dissemination into the bloodstream to internal organs before undergoing a 2-week incubation period. The infection progresses by disseminating through the bloodstream to internal organs during a 2-week incubation period. It then moves from the respiratory mucosa to the skin, infecting keratinocytes and causing vesiculopustular exanthema, which manifests as highly contagious lesions across the body and mucous membranes, including the oral cavity.

In immunocompetent individuals, primary VZV infection is typically self-limiting and resolves within 2 weeks. However, immunocompromised individuals may experience more extensive dissemination and complications. Regardless of immune status, VZV establishes lifelong latency in sensory ganglia through retrograde axonal transport and potentially through hematogenous spread.[32] Hematogenous dissemination may lead to less common but serious infections associated with VZV. Complications include VZV encephalitis,[33] cerebellar ataxia,[34] demyelinating neuropathy,[35] myelitis,[36] pneumonia,[37] meningitis,[38] and vasculopathy.[39]

Foreign DNA detection is necessary to amount an innate immune response during VZV infection. VZV can evade DNA sensing through antagonism of the cytosolic DNA sensor cyclic GMP-AMP synthase (cGAS) using VZV tegument protein ORF9.[40] The cGAS pathway ultimately leads to the production of type I IFN; however, inhibition of this pathway allows for viral persistence and chronic inflammation, which are known risk factors for oncogenesis.[41] Inhibition of the cGAS is especially important in this discussion as interruption of this pathway has been shown to have significant implications in cancer biology. In a normal physiological state, cGAS interferes with homologous recombination-mediated DNA repair, thus promoting tumor growth.[42] In addition, cGAS localization in the mitochondria helps maintain mitochondrial function, reduces reactive oxygen species accumulation, and prevents ferroptosis which facilitates tumor growth.[43] Alternatively, tumorigenesis may be promoted by a decrease in type I IFN, as discussed later in this review, making cancer manifestation through cGAS modulation a multifaceted subject.

Controlled process of programmed cell death that helps maintain the balance of cell life and death in the body with key roles in the elimination of damaged or abnormal cells, removal of infected cells during an immune response, and prevention of autoimmune responses by eliminating cells with autophagy potential. The usual viral infection immune response is accompanied by induction of programmed cell death.[44] Literature suggests VZV plays a role in the modulation of apoptotic processes in neuronal cells through Bcl-2 upregulation.[45] In immune cells, VZV has been shown to induce apoptosis; however, Steain *et al.*[46] observed increased apoptosis in human fetal fibroblasts compared to human fetal sensory neurons. This anti-apoptotic tropism in neuronal cells has been identified in other studies observing the genes associated with the inhibition of apoptosis (Trail-R4, BIRC5 [SURVIVIN], and BAG3) in human embryonic stem cell-derived neurons. It was found that genes protective of apoptosis were increased in neuronal cells as opposed to non-neuronal cells. In addition, non-neuronal cells were found have increased expression of pro-apoptotic genes, such as caspase-3; proteins, such as Fas-associated death domain,

BH3 interacting domain death agonist, cytochrome C, and apoptotic protease activating factor-1; and ligands and receptors associated with apoptosis, such as tumor necrosis factor-alpha (TNF-α), TNFR1, TRAIL-R, and interleukin-1 (IL-1). The authors conclude that neurons infected with VZV do not undergo apoptosis, whereas other cells do.[47]

3.1. Survivin's effect on the immune system

Inhibition of apoptosis is one of the many biological mechanisms in cancer manifestation and has been linked to multiple cancers.[48] Survivin, one of the genes associated with the inhibition of apoptosis, plays a key role in the intrinsic pathway of apoptosis, serving as an inhibitor of caspase-9, effector caspase-3, and effector caspase-7.[49] The interaction interrupts the caspase cascade and cleavage process, leading to reduced apoptosis.[50] Another mediator affected by survivin and that plays a role in apoptosis is the mitochondrial protein apoptosis-inducing factor (AIF). Survivin prevents the release of AIF from the mitochondrial intermembrane space and its movement to the nucleus, thereby blocking caspase-independent apoptosis.[51] Furthermore, survivin overexpression in human lung cancer cells inhibits p53-dependent apoptosis, suggesting it regulates the p53-dependent apoptotic pathway.[52] Similar findings between altered expression of p53 and survivin in oral squamous cell carcinoma were noted by Aggarwal *et al.*[53] where there was a significantly higher level of both p53 and survivin in the experimental group versus the control group. Altering survivin's function has provided strong evidence of its role in apoptosis, as a mutation in survivin (T34A) triggers the release of cytochrome c from the mitochondria, thereby promoting apoptosis.[54] It is through these mechanisms that survivin plays a critical role in inhibiting apoptosis by blocking key pro-apoptotic events and promoting cell survival under stressful conditions, contributing to its involvement in oncogenesis. Further investigations into the mechanism of VZV's ability to induce oncogenesis in non-neuronal cells through survivin-manipulating pathways need to be conducted, especially considering that it is only neuronal cells that experience anti-apoptotic effects, but these cells have not been reported to show a significant increase in cancer development compared to non-neuronal cells.

Investigations into the effects VZV has on the cell cycle of human foreskin fibroblasts determined the dysregulation of multiple key regulatory proteins.[55] In VZV-infected confluent fibroblasts, there was an unusual increase in the levels of CDK1, CDK2, cyclin B1, cyclin D3, and cyclin A proteins, along with significant activation of CDK2, CDK4, and cyclin B1 kinase activities.[56] Further, CD1d transcription is targeted by VZV, causing downregulation of the expression of the antigen presentation molecule, disrupting the cytokine response responsible for the connection between the innate and adaptive immune responses.[57] Reports have shown that CD1d downregulation and disappearance are seen in late-stage cancer progression.[58] An increase in these key cell cycle regulators has been detected in many types of cancers, including many cancers discussed in this discussion.[59] Reports of epidermal hyperplasia found on skin biopsies support the possibility of increased cell proliferation caused by the cell cycle dysregulation caused by VZV.[60]

3.2. ORF's effects on the immune system

3.2.1. Downregulation of IFN-β

VZV's genome contains over 70 distinct open reading frames (ORFs), each of which encodes proteins that contribute to various aspects of viral pathogenesis.[61] These include structural proteins that form the viral particle, enzymes that aid in viral DNA replication,[62] and regulatory proteins that help the virus evade the host immune system[63] or facilitate the transition to latency.[64] ORF66 phosphorylates the IE62 protein, the gene product of ORF12, preventing the nuclear import of IE62, causing it to accumulate in the cytoplasm.[65] The cytoplasmic accumulation of IE62 has significant implications by causing the inhibition of IFN regulatory factor 3 (IRF3) phosphorylation by TANK-binding kinase 1 (TBK1), which is crucial for IRF3 activation. This inhibition prevents IRF3 from undergoing the necessary conformational changes required for its dimerization and nuclear translocation. Without phosphorylation, IRF3 cannot bind to the IFN-β promoter or activate the transcription of IFN-β[66] (Figure 1). IFN-β plays a crucial role in the host's immune response, serving as a key mediator in the defense against viral infections and malignant cells; therefore, inhibition of IFN-β production through TBK1-mediated processes leaves the host susceptible to cancer manifestation.[67]

3.2.2. ORF66's role in preventing apoptosis

VZV gene products, including ORF66, are involved in inhibiting apoptosis. Specifically, ORF66 prevents apoptosis in T cells, as T cells infected with a virus lacking functional ORF66 protein are more prone to undergoing apoptosis through unspecified mechanisms.[68] In addition, ORF66 also modulates caspase 8 and IFN-γ antiviral effects.[2] Finally, previous studies have shown that ORF66 sequesters major histocompatibility complex (MHC) class I molecules in the Golgi of infected MeWo cells and fibroblasts; however, the viral gene product(s) and molecular mechanisms involved in modulation of cell-surface immune molecule expression

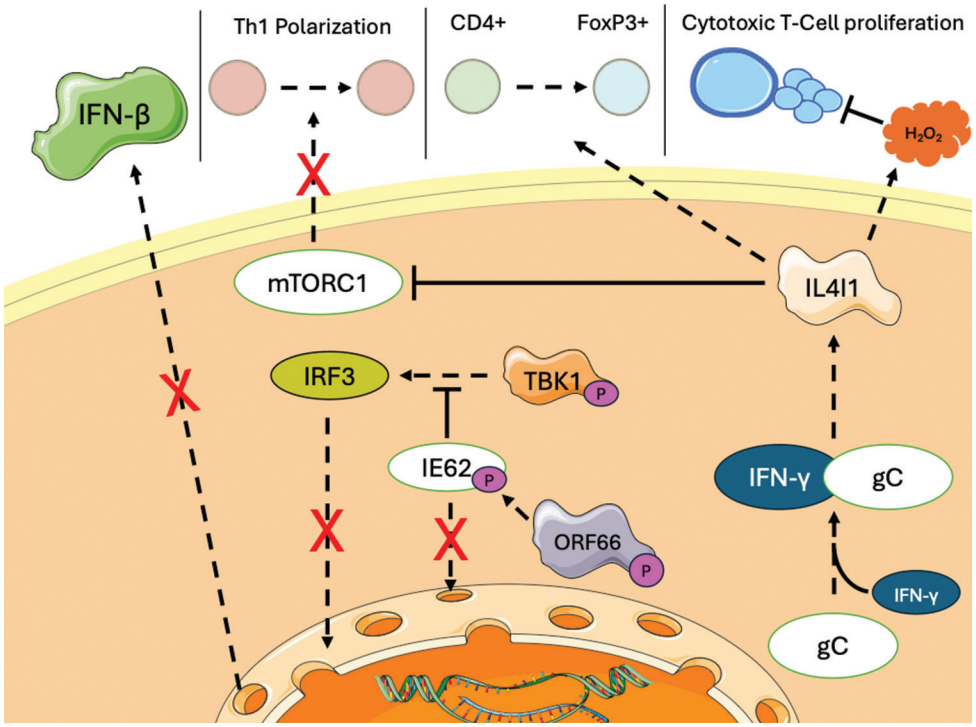

Figure 1. ORF's modulation of the immune system and its components. VZV's genome encodes multiple proteins that help it evade the immune response, including IE62 and STPK, which manipulate host cell processes such as IRF3 activation, inhibiting IFN-β production and weakening immune defenses. In addition, VZV's gC induces IL4I1, which suppresses anti-tumor immune responses by inhibiting T cell proliferation, inhibiting Th1 polarization, and promoting the differentiation of naive $CD4^+$ T cells into $FoxP3^+$ Tregs, thereby contributing to a tumor-friendly microenvironment. Schematic created by the authors.

Abbreviations: $CD4^+$: Cluster of differentiation 4; $FoxP3^+$: Forkhead box P3; gC: Glycoprotein C; IE62: Immediate early 62; IFN-β: Interferon beta; IFN-γ: Interferon gamma; IL4I1: Interleukin-4-induced-1; IRF3: Interferon regulatory factor 3; MTORC1: Mammalian target of rapamycin complex 1; ORF: Open reading frame; TBK1: TANK-binding kinase 1; Th1: Type 1 T helper; VZV: Varicella-zoster virus.

on mature monocyte-derived dendritic cells are not well defined[68] (Figure 2).

3.2.3. Immunomodulatory effects of glycoprotein C

The gene product of VZV, glycoprotein C (gC), is involved in immunomodulation and has been shown to bind IFN-γ,[69] inducing multiple chemokines and adhesion molecule intercellular adhesion molecule 1 (ICAM1), and, most importantly in oncogenesis.[70] IL4I1-producing cells in the tumor microenvironment suppress the anti-tumor immune response by inhibiting cytotoxic T cell proliferation and T helper 1 (Th1) cells while promoting T regulatory cell (Treg) accumulation through several mechanisms.[70] IL4I1 produces hydrogen peroxide as a byproduct of its enzymatic activity, which is toxic to effector/memory T cells, thereby inhibiting their proliferation. Furthermore, IL4I1 limits Th1 polarization by inhibiting the mammalian target of the rapamycin complex 1 (mTORC1) signaling pathway, which is crucial for T-cell activation and differentiation.[71] The effects on Tregs are due to IL4I1 promoting the differentiation of naive $CD4^+$ T cells into $FoxP3^+$ Tregs through inhibition of mTORC1[72] (Figure 1). These mechanisms collectively contribute to the immunosuppressive tumor microenvironment, facilitating tumor growth and immune evasion.

3.3. VZV's effects on major histocompatibility complexes

3.3.1. VZV's effects on MHC class I molecules

MHC molecules are cell-surface proteins that present peptides to T cells, enabling the immune system to recognize and respond to pathogens and tumorigenic cells.[73] Therefore, MHC molecules are key factors in tumor immunosurveillance and maintaining a robust immune system to prevent immune evasion.[74] VZV infection has been shown to prevent the expression of MHC class I molecules on the surface of cells by keeping them in the Golgi compartment. This immune evasion is facilitated by the viral protein VZV IE4, which sequesters the MHC class I molecules in the Golgi, reducing their surface expression.[75] VZV also inhibits the nuclear factor kappa B (NF-κB) pathway, which is crucial for the expression of various immune molecules, including MHC class I. The

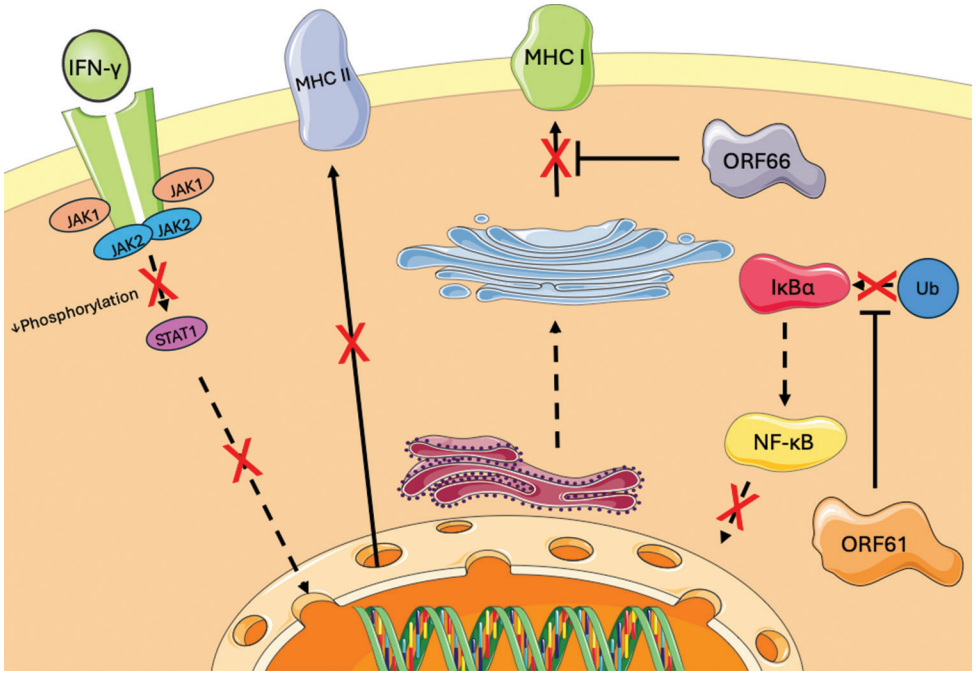

Figure 2. VZV's effects on major histocompatibility protein expression. VZV infection disrupts the JAK-STAT pathway by decreasing the levels of JAK1, JAK2, and STAT1 proteins, preventing the phosphorylation and nuclear translocation of STAT1, which is essential for the transcriptional activation of IFN-γ-inducible genes, including those encoding MHC class II molecules. Furthermore, VZV modulates NF-κB activity by preventing the ubiquitination of IκBα through the action of the ORF61 protein, leading to the cytoplasmic retention of NF-κB subunits and inhibition of NF-κB-dependent gene transcription. Finally, ORF66 disrupts the transport of MHC class I molecules from the Golgi apparatus to the cell surface, leading to their retention in the Golgi compartment. Schematic created by the authors.
Abbreviations: IFN-γ: Interferon-gamma; IκBα: Nuclear factor of kappa light polypeptide gene enhancer in B-cells inhibitor alpha; JAK: Janus kinase; MHC: Major histocompatibility complex; NF-κB: Nuclear factor-kappa B; ORF: Open reading frame; STAT: Signal transducer and activator of transcription; Ub: Ubiquinone; VZV: Varicella-zoster virus.

VZV ORF61 protein has been identified as an inhibitor of NF-κB activity by interfering with the degradation of IκBα, the inhibitor of NF-κB. Normally, IκBα is phosphorylated, ubiquitinated, and subsequently degraded, allowing NF-κB subunits (p50 and p65) to translocate to the nucleus and activate transcription of target genes. However, VZV ORF61 prevents the ubiquitination of IκBα, thereby stabilizing it and preventing its degradation. ORF61 retains NF-κB subunits in the cytoplasm, preventing their nuclear translocation and subsequent activation of NF-κB-dependent genes[76] (Figure 2).

3.3.2. VZV's effects on MHC class II molecules

In addition, VZV infection impairs IFN-γ-induced MHC class II expression by the disruption of the Janus kinase transducer and activator of the JAK-STAT signal transduction pathway. It causes infected cells to be less responsive to cytokine signals. This disruption specifically inhibits the expression of JAK1, JAK2, and STAT1 proteins, which are critical components of the IFN-γ signaling pathway. Reduction in protein levels prevents the phosphorylation and subsequent nuclear translocation of STAT1, which is essential for the transcriptional activation of IFN-γ-inducible genes, including those encoding MHC class II molecules[30] (Figure 2). MHC class II molecule downregulation is further supported by Abendroth *et al.*[77] who showed that during natural skin infection, VZV-infected dermal and epidermal cells did not express MHC class II transcripts, while nearby uninfected bystander cells did show MHC class II expression. With that said, not all cells experience the downregulatory effects of VZV. For example, while mature MDDCs showed no significant change in MHC class II expression but exhibited reduced levels of other immune molecules, including MHC class I, CD80, CD83, and CD86, opposite effects were noted with monocytes.[78] MHC class I and II proteins have been proven to play an important role in cancer immunosurveillance with a reported MHC class I downregulation in 40 – 90% of human tumors and be associated with a worse prognosis in disease.[79]

4. Reactivation of VZV

VZV reactivates from latency in sensory, enteric, and other autonomic neurons, leading to HZ. While many

correlations for VZV reactivation have been observed, such as immunosuppression due to age, medication, concurrent infection, and disease, the specific mechanistic cause has yet to be determined. A notable factor is decreased T-cell immunity, particularly in aging individuals or those undergoing immune-suppressive treatments, which can trigger VZV reactivation and lead to HZ. This suggests that $CD4^+$ and $CD8^+$ T cells play a critical role in maintaining VZV latency and preventing reactivation.[80]

Evidence for this postulation comes from research by Arnold and Messaoudi[29] on primate models studied, where animals with higher viral loads in their nerve clusters (ganglia) were more likely to experience mild, asymptomatic reactivation compared to those with lower viral levels. Subclinical reactivation was associated with higher viral levels in the ganglia.[29] In SVV-infected BSC-1 cells, significant reductions in key proteins such as STAT1, JAK1, and JAK2 were observed. In addition, the activation and nuclear movement of STAT1 were blocked, though this was not due to cellular or viral enzymes.[81] Furthermore, VZV reactivation has been linked to co-infections, such as mycobacterial infections and reactivated herpes simplex virus 1 (HSV-1). However, it remains uncertain whether specific antigens are directly associated with VZV reactivation or these occurrences simply reflect a weakened immune response.[82]

Investigations into the severity of disease progression following reactivation and viral load provided valuable insight into anticipation of VZV pathogenesis. Real-time quantitative polymerase chain reaction (qPCR) is used to quantify the genome copies of pathogens in samples.[83] Using qPCR, it was found that in patients with PHN, higher viral loads persisting over time are linked to a longer recovery period. Viral loads measured in patients with neurologic symptoms; however, showed significantly lower viral loads compared to patients with HZ without neurological symptoms. In addition, less than half of the patients experiencing neurological symptoms in one study had detectable serum levels of VZV DNA.[84] Viral load detection may be valuable in patient prognosis; unfortunately, there are limited studies investigating viral load and cancer manifestation.

4.1. Nerve growth factor's (NGF) effects in VZV latency and reactivation

NGF is crucial for the survival and maintenance of sensory neurons and plays a significant role in the reactivation of VZV from latency. Because both HSV and VZV establish latency in neurons, HSV animal models have been used to study the intricate mechanism of latency and reactivation.[85] Animal studies on neuronal cultures from embryonic rats demonstrated that latent HSV-1 was reactivated in response to NGF deprivation.[86] The study by Thellman *et al.*[87] utilized an immortalized human dorsal root ganglion cell line (HD10.6) to model HSV-1 latency and reactivation. They found that HSV-1 infection in these human neurons resulted in a quiescent state resembling latency, and reactivation could be induced by depletion of NGF, indicating that NGF is crucial for maintaining latency in human neurons as well. Furthermore, Cohrs *et al.*[88] found that interruption of NGF signaling in human trigeminal ganglia led to an increase in VZV DNA, although full viral replication was not noted. Sadaoka *et al.*[89] further demonstrated that treatment of latently infected human neurons with antibodies to NGF resulted in the production of infectious VZV in about 25% of the cultures, indicating that NGF deprivation can trigger reactivation. HSV, in the same *Herpesviridae* family as VZV, on the other hand, is able to reactivate fully *in vitro* in cadaver ganglia.[90] These findings highlight the importance of NGF in maintaining VZV latency and suggest that its interruption can lead to viral reactivation, although additional factors or conditions are likely required for complete viral replication and reactivation.[89]

4.2. PI3-Kinase/Akt pathway in VZV latency and reactivation

The PI3-kinase/Akt pathway is involved in regulating several cellular functions, including cell survival, growth, and metabolism, which are essential for maintaining viral latency and facilitating reactivation. Studies have shown that the PI3-kinase/Akt pathway is activated during VZV infection and is necessary for efficient viral replication. Inhibition of this pathway can lead to a decline in viral replication and an increase in apoptosis.[91] Specifically, the VZV ORF12 protein activates the PI3K/Akt pathway to regulate cell cycle progression, which is crucial for viral replication in both dividing and non-dividing cells.[92] In human stem cell-derived neurons, VZV can establish a persistent non-productive infection that can be reactivated by inhibiting the PI3-kinase pathway.[93] This suggests that the PI3-kinase/Akt pathway is involved in maintaining latency and that its disruption can trigger reactivation.

4.3. c-Jun N-terminal kinase (JNK) pathway in VZV latency and reactivation

The JNK pathway is a critical component of the mitogen-activated protein kinase (MAPK) signaling pathways. It is primarily involved in regulating cellular processes such as apoptosis, inflammation, and stress responses. Activation of the JNK pathway leads to the phosphorylation of c-Jun, a transcription factor that forms part of the activator protein-1 (AP-1) complex, which then transactivates

various genes involved in these cellular processes.[94] In the context of VZV latency and reactivation, studies have shown that VZV infection activates the JNK pathway, which is essential for efficient viral protein expression and replication. Specifically, the activation of JNK following VZV infection leads to the phosphorylation of c-Jun, which is crucial for the transactivation of viral genes necessary for lytic infection and reactivation. Interestingly, inhibition of the JNK pathway in melanoma cells led to an increase in VZV replication[94] but resulted in a decrease in replication in fibroblasts, suggesting that the role of JNK in VZV pathogenesis depends upon the type of cell infected.[95] Furthermore, inhibition of the JNK pathway has been shown to block viral replication and significantly reduce reactivation in human neuronal models. Zapata *et al.*[95] found that the competitive inhibitor SP600125 effectively reduced VZV yield in human fibroblast cells by eliminating phosphorylated c-Jun, thereby confirming the specificity and efficacy of the inhibitor. Further studies with SP600125 resulted in a marked reduction in VZV reactivation, indicating that the JNK pathway is critical for the reactivation process.[96] These findings underscore the critical role of the JNK pathway in VZV replication and reactivation, highlighting SP600125 as a potential therapeutic agent for controlling VZV reactivation and related diseases.

5. VZV in cancer

5.1. VZV in cancer overview

VZV's ability to manipulate host cell functions, evade immune surveillance, and remain dormant in a latent state raises questions about its potential role in the onset and progression of certain cancers. While VZV is not traditionally classified as an oncogenic virus such as human papillomavirus or Epstein-Barr virus (EBV), emerging research has suggested its involvement in tumor development. Specifically, VZV's ability to trigger chronic inflammation[97] and interact with cancer-associated pathways may contribute to the formation of malignant lesions.[98] Cotton *et al.*[11] outline some of the earliest publications linking VZV infection to cancer diagnosis, noting that while early studies failed to establish a clear association, recent evidence indicates otherwise, but due to differences in methods, demographics, and cancer types reported by various articles on this topic, it is still difficult to determine if there is a clear association between VZV infection and cancer diagnosis.

One critical observation is the increased relative risk (RR) of certain cancers, particularly hematologic malignancies such as lymphoma and leukemia, in the 1st year following HZ infection.[99] This heightened risk may be linked to immune suppression, such as through the upregulation of immune checkpoint receptors and ligands such as programmed cell death protein 1 (PD-1) and programmed death-ligand 1 (PD-L1),[6] and subsequent VZV reactivation, which could facilitate tumor development.[100] In addition, the inflammatory response triggered by HZ infection through the release of pro-inflammatory cytokines, along with the virus's effects on cellular pathways associated with cancer, such as JAK-STAT, NFκB, and TNF-α, likely plays a role in this increased risk.[101] Research has shown that the 1st year following HZ infection is a crucial period for cancer risk. For example, a population-based study conducted by Sorensen *et al.*[102] reported an RR of 4.0 in the first 3 months of hospitalization due to HZ, which decreased over time but remained elevated at 2.1 between 9 and 12 months. The RR further declined to 1.9 between 1 and 5 years, and 1.3 between 5 and 10 years with a higher prevalence of distant metastases within 1 year of follow-up compared to control groups when considering multiple cancer types. Of note, because the population used in this study is hospitalized individuals, the results in this report may be subject to selection bias, reverse causality, or confounding by comorbidity. Cotton *et al.*[11] accounted for this in their retrospective cohort study of a primary care population, where they also found an increased risk of cancer diagnosis within the first 90 days when controlling for patients using immunosuppressive agents. Mahale *et al.*[103] state similar findings reporting that HZ was significantly associated with several cancers when diagnosed 13 – 35 months before cancer diagnosis or control selection. A meta-analysis published by Schmidt *et al.*[104] reviewed 46 studies investigating an association between HZ and cancer, reporting an overall RR of 1.42 for any type of cancer and 1.83 for the risk of cancer following 1 year after an HZ diagnosis. These findings highlight the importance of the 1st year after HZ infection as a critical window for cancer risk, though further studies are needed to better understand the underlying mechanisms that contribute to this elevated risk.[105]

A case–control study done on the U.S. elderly population ages ≥65 reported similar results of an increased cancer diagnosis with HZ infection in 2016 when investigating the link of VZV infection to 48 different cancer types. Hematologic malignancies had a higher association with cancer diagnosis versus solid tumor malignancy in HZ patients. Stages of solid tumors of the cancers diagnosed in this study were also reported which most papers on this topic fail to report. HZ was most strongly associated with solid cancers diagnosed at regional or distant stages. Significant associations were found for regional stage colon cancer (OR: 1.13), non-melanoma skin cancer (OR: 1.97), and distant stage oral cavity/pharyngeal cancer

(OR: 1.74) and lung cancer (OR: 1.17) after adjustment for risk factors. No significant associations were observed for localized-stage cancers.[103] These findings require further investigation as data on cancer stage diagnosis in VZV patients is limited, and this paper serves as one of the only papers investigating this topic.[103]

5.2. VZV and oropharyngeal cancer

Just as other viruses of the *Herpesviridae* family that are able to affect the oropharynx, such as EBV's association with nasopharyngeal carcinoma or HSV-1's association with esophagitis, VZV has shown some association with oropharyngeal cancer (OPC). A nationwide case–control study utilizing Taiwan's Longitudinal Health Insurance Database 2010 found a significantly higher odds ratio (OR) for HZ of OPC patients versus controls. The study reported an odds ratio of 2.198 (95% confidence interval [CI]: 2.001 – 2.415) for head and neck cancers, including these specific subtypes, after adjusting for comorbidities and risk factors. Specific OPCs found to have an elevated OR were oral cavity cancer, oropharynx, larynx, hypopharynx, nasopharynx, and salivary gland cancers.[106] Furthermore, a case–control study by Mahale *et al.*[103] found a significant association between HZ and an increased risk of oral cavity/pharyngeal cancers, with an adjusted odds ratio (aOR) of 1.21. Schmidt *et al.*[104] further supported these findings, reporting an RR of 1.76 (95% CI: 1.13 – 2.50). With that said, population-based studies and meta-analysis which included investigations into OPC and HZ infection found no significant association or even a lower risk of these cancers.[11,102,104,107,108]

5.3. VZV and hematological cancer

Given the established links between viral diseases and hematological cancers, such as EBV's role in Hodgkin's lymphoma, Burkitt lymphoma, and non-Hodgkin's lymphoma, there has been growing interest in investigating the potential association between VZV and hematological cancers. Of all the meta-analysis and population-based studies investigating the risk of multiple cancers after HZ infection used for this review, all of them showed a significant increase in one or multiple hematologic malignancies.[11,102,104,107,108] A longitudinal follow-up study in the Korean population by Choi *et al.*[109] reported an increased risk of lymphoid neoplasms in patients with HZ, with an adjusted HR of 1.58 (95% CI: 1.23 – 2.02). This study also found that the risks of Hodgkin's disease and multiple myeloma/malignant plasma cell neoplasms were significantly elevated in patients with HZ. In addition, a case–control study in the U.S. elderly population by Mahale *et al.*[103] identified significant associations between HZ and various hematologic malignancies, including myeloma (aOR = 1.38), diffuse large B-cell lymphoma (aOR = 1.30), lymphoplasmacytic lymphoma (aOR = 1.99), and chronic lymphocytic leukemia/small lymphocytic lymphoma (aOR = 1.55). A nationwide population-based matched-control study in the Taiwan region by Liu *et al.*[110] found that patients with HZ had a significantly higher risk of developing lymphoid malignancies, with an adjusted hazard ratio (HR) of 1.68 (95% CI: 1.35 – 2.42). The most common lymphoid malignancies observed were non-Hodgkin's lymphoma and multiple myeloma. Buntinx *et al.*[111] found a significantly increased risk of developing lymphoid malignancies, particularly Hodgkin's disease and multiple myeloma, in the Korean population in a retrospective cohort study reporting an adjusted hazard ratio (HR) of 1.58 (95% CI: 1.23 – 2.02) for lymphoid malignancies in patients with HZ.

5.4. VZV and pulmonary cancer

As stated before, VZV can spread through respiratory droplets when an infected person coughs, sneezes, or talks, possibly linking to lung cancer development following VZV infection. Sim *et al.*[108] investigated this in a nationwide population-based matched control study in South Korea, reporting that the diagnosis is most evident in PHN patients, with a hazard ratio (HR) of 1.65 compared to non-PHN patients. A population-based study by Chiu *et al.*[105] found that the hazard ratio (HR) for subsequent cancer, particularly lung cancer, was significantly higher during the first 2 years after an initial diagnosis of HZ. Specifically, the HR for lung cancer was elevated within the 1st year (HR = 1.58, 95% CI: 1.38 – 1.80) and remained significant between 1 and 2 years (HR = 1.30, 95% CI: 1.15 – 1.46). Mahale *et al.*[103] also reported a modestly increased risk of lung cancer associated with HZ, with an aOR of 1.11. Cotton *et al.*[11] also reported a significantly elevated hazard ratio for developing lung cancer with a reported HR of 2.90 (95% CI: 2.23 – 3.76). Just as with OPC, other population-based studies and meta-analyses which included investigations into pulmonary cancers and HZ infection found no significant association or even a lower risk of these cancers.[102,107,108]

5.5. VZV and gastrointestinal (GI) cancer

The enteric nervous system (ENS) plays a crucial role in regulating GI function, and growing evidence suggests that VZV can infect and establish latency in enteric neurons, similar to its behavior in sensory neurons.[112] One of the earliest population-based cohort studies investigating the link between VZV and an increased risk of cancer was conducted in 1982.[113] Although limited by sample size, the study reported a modestly elevated RR of 1.1 for colon and bladder tumors in women. Schmidt *et al.*[104] also

reported a positive significant RR of 1.27 (95% CI: 1.05 – 1.53) in colorectal cancer development after HZ diagnosis. Cotton *et al.*[11] also reported a significantly positive HR of 1.87 27 (95% CI: 1.45 – 2.40) in colorectal cancer but no association in stomach cancer with an HR of 1.04 27 (95% CI: 0.40 – 2.72). Interestingly, Sim *et al.*[108] reported a decreased risk of GI cancers in HZ patients without PHN, with a hazard ratio (HR) of 0.86 (95% CI: 0.81 – 0.91). However, an increased risk of GI cancer diagnosis was evident in PHN patients, with an HR of 1.33 (95% CI: 1.20 – 1.47), compared to non-PHN patients. Contrary to the positive associations found in the previous studies, a large retrospective cohort study by Leyh *et al.*[113] analyzed data from over 200,000 outpatients in Germany and found no significant association between HZ infection and the subsequent development of GI cancer. The study included 103,123 patients with a first diagnosis of HZ and a matched cohort of 103,123 patients without HZ. Over a follow-up period of up to 10 years, the incidence of GI cancer did not differ significantly between the two cohorts (HZ cohort: 2.26 cases/1000 patient-years vs. non-HZ cohort: 2.37 cases/1000 patient-years, p=0.548). The hazard ratio (HR) for developing GI cancer in the HZ cohort was 0.97 (95% CI: 0.89 – 1.05).[114] Further, population-based studies and meta-analysis publications investigating associations between HZ infection with GI cancer diagnosis also refute any significant associations.[102,107]

6. Studies in cancers potentially associated with VZV

While several studies have explored the potential link between VZV and cancer, not all research has found a clear association. Some studies have failed to establish any significant connection between VZV infection or reactivation and cancer diagnosis, suggesting that the virus may not play a major role in tumor development. Meanwhile, studies that determine a clear association of VZV with some cancers fail to replicate the association with cancers as shown in different papers. For example, Chiu *et al.*[105] offer suggestions for the discrepancy detected in their results to four other studies, stating that the lack of statistically significant associations may suggest either insufficient statistical power or a weak or non-existent relationship when comparing results to populations of men and women in the other papers. Leyh *et al.*[114] concurs with this hypothesis of insufficient statistical power when their comparison yielded no association of HZ infection with subsequent GI cancer as determined in another study that suggests a statistically significant increase in cancer rates after HZ infection. It is plausible to speculate that a cancer diagnosis made shortly after the onset of HZ could suggest the existence of an undiagnosed, latent tumor at the time the individual developed HZ. In this context, the occurrence of HZ may serve as a clinical manifestation of tumor-associated immunodeficiency, where the immune system is weakened by the presence of the tumor, facilitating the reactivation of VZV.[115] Sim *et al.*[108] provides an explanation to their findings when noting an inconsistency with previous publications after determining a lower risk of cancers in the oropharynx, GI, and respiratory systems in a South Korean population-based matched control study. They claimed that their inconsistent results could be attributed to controls matching by age, gender, and health status, or to a trend specific to the Korean population. Preferential incidence of cancers caused by *Herpesviridae* family viruses would not be unique to VZV as EBV has also shown significantly higher rates of nasopharyngeal cancer in Asian and Pacific islander populations.[116] Choi *et al.*[109] offer another explanation for conflicting results determined by Liu *et al.*[110] and Wang *et al.*[107] in lymphoid neoplasms, stating that the conflicting data may be due to differences in ethnicity (Han vs. Korean) or variations in study methods, such as differing criteria for subject inclusion. These studies often point to the complexities of cancer etiology, where multiple factors – genetic, environmental, and viral – may influence disease onset. While VZV's role in cancer remains a topic of debate, these findings underscore the need for further research to clarify whether VZV has any direct or indirect influence on cancer risk.[9]

7. Conclusion

In recent years, there has been growing evidence linking VZV infection, particularly in individuals with a history of HZ, to certain types of cancers, such as hematologic, pulmonary, and GI cancers. Studies have consistently shown higher cancer incidence rates in patients diagnosed with VZV-related conditions and the risk of cancer seems to be highest in the 1st year after HZ infection, with the risk decreasing in the following months which may be through its modulation of immune checkpoint proteins, cell-surface proteins, chemokines, apoptotic enzymes, and cell cycle regulatory enzymes. This raises the question of whether VZV infection triggers the manifestation of a pre-existing, subclinical malignancy, or wheher VZV's impact on the immune system enables opportunistic cancer development. While some even suggest enhancing post-HZ infection cancer detection efforts, which others never attempted.[113,117,118] Nonetheless, despite numerous studies suggesting a link between certain cancers and VZV infection, many others contradict these findings, and the results remain conflicting, with no consensus having been reached. Further investigation into how VZV interacts with cellular pathways, particularly those related to apoptosis

and cell survival, may help clarify potential connections between the virus and tumorigenesis. Understanding how VZV manipulates host cell functions – such as inhibiting apoptosis or altering cell cycle regulation – could shed light on how normal cells might transform into cancerous ones. These insights are crucial in determining whether VZV is merely a viral pathogen or if it could also act as an oncogenic factor, contributing to cancer development in certain cells or conditions, similar to other viruses in the *Herpesviridae* family.

Acknowledgments

None.

Funding

None.

Conflict of interest

Shizue Mito is the Youth Editorial Board Member of this journal but was not in any way involved in the editorial and peer-review process conducted for this paper, directly or indirectly. Separately, other authors declared that they have no known competing financial interests or personal relationships that could have influenced the work reported in this paper.

Author contributions

Conceptualization: Fernando Cisneros IV, Blake Martin
Supervision: Shizue Mito
Visualization: Fernando Cisneros IV
Writing – original draft: Fernando Cisneros IV, Blake Martin
Writing – review & editing: Fernando Cisneros IV, Shizue Mito

Ethics approval and consent to participate

Not applicable.

Consent for publication

Not applicable.

Availability of data

Not applicable.

References

1. Gershon AA, Gershon MD, Breuer J, Levin MJ, Oaklander AL, Griffiths PD. Advances in the understanding of the pathogenesis and epidemiology of herpes zoster. *J Clin Virol*. 2010;48 Suppl 1(Suppl 1):S2-S7.

   doi: 10.1016/S1386-6532(10)70002-0

2. Arvin AM. Creating the "dew drop on a rose petal": The molecular pathogenesis of varicella-zoster virus skin lesions. *Microbiol Mol Biol Rev*. 2023;87(3):e0011622.

   doi: 10.1128/mmbr.00116-22

3. Kennedy PG, Mogensen TH. Determinants of neurological syndromes caused by varicella zoster virus (VZV). *J Neurovirol*. 2020;26(4):482-495.

   doi: 10.1007/s13365-020-00857-w

4. Eshleman E, Shahzad A, Cohrs RJ. Varicella zoster virus latency. *Future Virol*. 2011;6(3):341-355.

   doi: 10.2217/fvl.10.90

5. Kennedy PGE, Gershon AA. Clinical features of varicella-zoster virus infection. *Viruses*. 2018;10(11):609.

   doi: 10.3390/v10110609

6. Jones D, Como CN, Jing L, *et al*. Varicella zoster virus productively infects human peripheral blood mononuclear cells to modulate expression of immunoinhibitory proteins and blocking PD-L1 enhances virus-specific CD8+ T cell effector function. *PLoS Pathog*. 2019;15(3):e1007650.

   doi: 10.1371/journal.ppat.1007650

7. Wyburn-Mason R. Malignant change arising in tissues affected by herpes. *Br Med J*. 1955;2(4948):1106-1109.

   doi: 10.1136/bmj.2.4948.1106

8. Sorel O, Messaoudi I. Insights into the pathogenesis of varicella viruses. *Curr Clin Microbiol Rep*. 2019;6(3):156-165.

   doi: 10.1007/s40588-019-00119-2

9. Wrensch M, Weinberg A, Wiencke J, *et al*. History of chickenpox and shingles and prevalence of antibodies to varicella-zoster virus and three other herpesviruses among adults with glioma and controls. *Am J Epidemiol*. 2005;161(10):929-938.

   doi: 10.1093/aje/kwi119

10. Multhoff G, Molls M, Radons J. Chronic inflammation in cancer development. *Front Immunol*. 2011;2:98.

    doi: 10.3389/fimmu.2011.00098

11. Cotton SJ, Belcher J, Rose P, Jagadeesan SK, Neal RD. The risk of a subsequent cancer diagnosis after herpes zoster infection: Primary care database study. *Br J Cancer*. 2013;108(3):721-726.

    doi: 10.1038/bjc.2013.13

12. Fueyo MA, Lookingbill DP. Herpes zoster and occult malignancy. *J Am Acad Dermatol*. 1984;11(3):480-482.

    doi: 10.1016/s0190-9622(84)70195-2

13. Utpat S, Utpat N, Nookala V, Podakula L, Utpat K. Case report: Hospital-acquired chickenpox in a healthcare setting. *Epidemiol Infect*. 2023;152:e3.

    doi: 10.1017/S0950268823001917

14. Newman AM, Jhaveri R. Myths and misconceptions: Varicella-zoster virus exposure, infection risks, complications, and treatments. *Clin Ther*. 2019;41(9): 1816-1822.

doi: 10.1016/j.clinthera.2019.06.009

15. Zhang Z, Liu N, Zhang J, *et al*. Epidemiological characteristics of varicella under different immunisation strategies in Suzhou prefecture, Jiangsu province. *Vaccines (Basel)*. 2022;10(10):1745.

doi: 10.3390/vaccines10101745

16. Rice PS. Ultra-violet radiation is responsible for the differences in global epidemiology of chickenpox and the evolution of varicella-zoster virus as man migrated out of Africa. *Virol J*. 2011;8:189.

doi: 10.1186/1743-422X-8-189

17. Institute of Medicine (U.S.). Committee to review adverse effects of vaccines. In: Stratton KR, editor. *Adverse Effects of Vaccines: Evidence and Causality*. United States: National Academies Press; 2012. p. 865.

18. Marin M, Lopez AS, Melgar M, Dooling K, Curns AT, Leung J. Decline in severe varicella disease during the United States varicella vaccination program: Hospitalizations and deaths, 1990-2019. *J Infect Dis*. 2022;226(Suppl 4):S407-S415.

doi: 10.1093/infdis/jiac242

19. Zhou F, Leung J, Marin M, Dooling KL, Anderson TC, Ortega-Sanchez IR. Health and economic impact of the United States varicella vaccination program, 1996-2020. *J Infect Dis*. 2022;226(Suppl 4):S463-S469.

doi: 10.1093/infdis/jiac271

20. Depledge DP, Sadaoka T, Ouwendijk WJD. Molecular aspects of varicella-zoster virus latency. *Viruses*. 2018;10(7):349.

doi: 10.3390/v10070349

21. Doan HQ, Ung B, Ramirez-Fort MK, Khan F, Tyring SK. Zostavax: A subcutaneous vaccine for the prevention of herpes zoster. *Expert Opin Biol Ther*. 2013;13(10): 1467-1477.

doi: 10.1517/14712598.2013.830101

22. Serpell M, Gater A, Carroll S, Abetz-Webb L, Mannan A, Johnson R. Burden of post-herpetic neuralgia in a sample of UK residents aged 50 years or older: Findings from the Zoster Quality of Life (ZQOL) study. *Health Qual Life Outcomes*. 2014;12:92.

doi: 10.1186/1477-7525-12-92

23. Saguil A, Kane S, Mercado M, Lauters R. Herpes zoster and postherpetic neuralgia: Prevention and management. *Am Fam Physician*. 2017;96(10):656-663.

24. Forbes HJ, Bhaskaran K, Grint D, *et al.* Incidence of acute complications of herpes zoster among immunocompetent adults in England: A matched cohort study using routine health data. *Br J Dermatol*. 2021;184(6):1077-1084.

doi: 10.1111/bjd.19687

25. Dhillon RS, Smith PD. Diskogenic reactivation of herpes zoster. *World Neurosurg*. 2018;109:138-139.

doi: 10.1016/j.wneu.2017.09.132

26. Patil A, Goldust M, Wollina U. Herpes zoster: A review of clinical manifestations and management. *Viruses*. 2022;14(2):192.

doi: 10.3390/v14020192

27. Purohit SK, Corbett AJ, Slobedman B, Abendroth A. Varicella Zoster Virus infects mucosal associated invariant T cells. *Front Immunol*. 2023;14:1121714.

doi: 10.3389/fimmu.2023.1121714

28. Sen N, Mukherjee G, Arvin AM. The use of single cell mass cytometry to define the molecular mechanisms of varicella-zoster virus lymphotropism. *Front Microbiol*. 2020;11:1224.

doi: 10.3389/fmicb.2020.01224

29. Arnold N, Messaoudi I. Simian varicella virus causes robust transcriptional changes in T cells that support viral replication. *Virus Res*. 2017;238:226-235.

doi: 10.1016/j.virusres.2017.07.004

30. Ouwendijk WJD, van Veen S, Mahalingam R, Verjans G. Simian varicella virus inhibits the interferon gamma signalling pathway. *J Gen Virol*. 2017;98(10):2582-2588.

doi: 10.1099/jgv.0.000925

31. Zerboni L, Sen N, Oliver SL, Arvin AM. Molecular mechanisms of varicella zoster virus pathogenesis. *Nat Rev Microbiol*. 014;12(3):197-210.

doi: 10.1038/nrmicro3215

32. Sorel O, Messaoudi I. Varicella virus-host interactions during latency and reactivation: Lessons from simian varicella virus. *Front Microbiol*. 2018;9:3170.

doi: 10.3389/fmicb.2018.03170

33. Lizzi J, Hill T, Jakubowski J. Varicella zoster virus encephalitis. *Clin Pract Cases Emerg Med*. 2019;3(4):380-382.

doi: 10.5811/cpcem.2019.8.43010

34. Cross C, English S, Krause M, Zalewski N. A 59-year-old immunocompetent man with rapid onset of truncal ataxia: A case of acute cerebellitis secondary to varicella zoster virus. (P4.9-035). *Neurology*. 2019;92(15 Suppl):P4.9-035.

doi: 10.1212/WNL.92.15_supplement.P4.9-035

35. Shoji H, Matsuo K, Matsushita T, *et al*. Herpes zoster peripheral nerve complications: Their pathophysiology in spinal ganglia and nerve roots. *Intractable Rare Dis Res*. 2023;12(4):246-250.

doi: 10.5582/irdr.2023.01090

36. Sebastian AP, Basu A, Mitta N, Benjamin D. Transverse myelitis caused by varicella-zoster. *BMJ Case Rep.* 2021;14(8):e243217.

doi: 10.1136/bcr-2020-238078

37. Mirouse A, Vignon P, Piron P, *et al.* Severe varicella-zoster virus pneumonia: A multicenter cohort study. *Crit Care*. 2017;21(1):137.

doi: 10.1186/s13054-017-1731-0

38. Cao LJ, Zheng YM, Li F, Hao HJ, Gao F. Varicella-zoster virus meningitis with hypoglycorrhachia: A case report. *World J Clin Cases*. 2023;11(29):7101-7106.

doi: 10.12998/wjcc.v11.i29.7101

39. Eleftheriou D, Moraitis E, Hong Y, *et al*. Microparticle-mediated VZV propagation and endothelial activation: Mechanism of VZV vasculopathy. *Neurology*. 2020;94(5):e474-e480.

doi: 10.1212/WNL.0000000000008885

40. Hertzog J, Zhou W, Fowler G, *et al.* Varicella-Zoster virus ORF9 is an antagonist of the DNA sensor cGAS. *EMBO J*. 2022;41(14):e109217.

doi: 10.15252/embj.2021109217

41. Zahid A, Ismail H, Li B, Jin T. Molecular and structural basis of DNA sensors in antiviral innate immunity. *Front Immunol*. 2020;11:613039.

doi: 10.3389/fimmu.2020.613039

42. Liu H, Zhang H, Wu X, *et al.* Nuclear cGAS suppresses DNA repair and promotes tumorigenesis. *Nature*. 2018;563(7729):131-136.

doi: 10.1038/s41586-018-0629-6

43. Du JM, Qian MJ, Yuan T, *et al*. cGAS and cancer therapy: A double-edged sword. *Acta Pharmacol Sin*. 2022;43(9): 2202-2211.

doi: 10.1038/s41401-021-00839-6

44. Nguyen LN, Kanneganti TD. PANoptosis in viral infection: The missing puzzle piece in the cell death field. *J Mol Biol*. 2022;434(4):167249.

doi: 10.1016/j.jmb.2021.167249

45. Kennedy PG, Graner MW, Gunaydin D, Bowlin J, Pointon T, Yu X. Varicella-Zoster Virus infected human neurons are resistant to apoptosis. *J Neurovirol*. 2020;26(3):330-337.

doi: 10.1007/s13365-020-00831-6

46. Steain M, Slobedman B, Abendroth A. Modulation of apoptosis and cell death pathways by varicella-zoster virus. *Curr Top Microbiol Immunol*. 2023;438:59-73.

doi: 10.1007/82_2021_249

47. Markus A, Waldman Ben-Asher H, Kinchington PR, Goldstein RS. Cellular transcriptome analysis reveals differential expression of pro- and antiapoptosis genes by varicella-zoster virus-infected neurons and fibroblasts. *J Virol*. 2014;88(13):7674-7677.

doi: 10.1128/JVI.00500-14

48. Wong RS. Apoptosis in cancer: From pathogenesis to treatment. *J Exp Clin Cancer Res*. 2011;30(1):87.

doi: 10.1186/1756-9966-30-87

49. Chen X, Duan N, Zhang C, Zhang W. Survivin and tumorigenesis: Molecular mechanisms and therapeutic strategies. *J Cancer*. 2016;7(3):314-323.

doi: 10.7150/jca.13332

50. Ge J, Wang Y, Li X, *et al.* Phosphorylation of caspases by a bacterial kinase inhibits host programmed cell death. *Nat Commun*. 2024;15(1):8464.

doi: 10.1038/s41467-024-52817-1

51. Albadari N, Li W. Survivin small molecules inhibitors: Recent advances and challenges. *Molecules*. 2023;28(3):1376.

doi: 10.3390/molecules28031376

52. Warrier NM, Agarwal P, Kumar P. Emerging importance of survivin in stem cells and cancer: The development of new cancer therapeutics. *Stem Cell Rev Rep.* 2020;16(5):828-852.

doi: 10.1007/s12015-020-09995-4

53. Aggarwal D, Shetty DC, Jain A, Gulati N, Juneja S. Pathogenetic model of survivin-dependent molecular signalling pathways in tumorigenesis of oral cancer and precursor lesions. *J Oral Maxillofac Pathol*. 2023;27(2): 287-294.

doi: 10.4103/jomfp.jomfp_5_23

54. Liu T, Brouha B, Grossman D. Rapid induction of mitochondrial events and caspase-independent apoptosis in Survivin-targeted melanoma cells. *Oncogene*. 2004;23(1): 39-48.

doi: 10.1038/sj.onc.1206978

55. Moffat JF, Greenblatt RJ. Effects of varicella-zoster virus on cell cycle regulatory pathways. *Curr Top Microbiol Immunol*. 2010;342:67-77.

doi: 10.1007/82_2010_28

56. Kovalishyn V, Severin O, Kachaeva M, *et al*. *In silico* design and experimental validation of novel oxazole derivatives against varicella zoster virus. *Mol Biotechnol*. 2024;66(4): 707-717.

doi: 10.1007/s12033-023-00670-w

57. Traves R, Opadchy T, Slobedman B, Abendroth A. Varicella zoster virus downregulates expression of the nonclassical antigen presentation molecule CD1d. *J Infect Dis*. 2024;230(2):e416-e426.

doi: 10.1093/infdis/jiad512

58. Radhakrishnan V, Golla U, Kudva AK. Role of immune cells and immunotherapy in multiple myeloma. *Life (Basel)*. 2024;14(4):461.

doi: 10.3390/life14040461

59. Advani D, Kumar P. Uncovering cell cycle dysregulations and associated mechanisms in cancer and neurodegenerative disorders: A glimpse of hope for repurposed drugs. *Mol Neurobiol*. 2024;61(11):8600-8630.

doi: 10.1007/s12035-024-04130-7

60. Zerboni L, Sung P, Lee G, Arvin A. Age-associated differences in infection of human skin in the SCID mouse model of varicella-zoster virus pathogenesis. *J Virol*. 2018;92(11):e00002-18.

doi: 10.1128/JVI.00002-18

61. Oliver SL. The structures and functions of VZV glycoproteins. *Curr Top Microbiol Immunol*. 2023;438:25-58.

doi: 10.1007/82_2021_243

62. Kaufer BB, Smejkal B, Osterrieder N. The varicella-zoster virus ORFS/L (ORF0) gene is required for efficient viral replication and contains an element involved in DNA cleavage. *J Virol*. 2010;84(22):11661-11669.

doi: 10.1128/JVI.00878-10

63. Rossi L, Tiecco G, Venturini M, Castelli F, Quiros-Roldan E. Human orf with immune-mediated reactions: A systematic review. *Microorganisms*. 2023;11(5):1138.

doi: 10.3390/microorganisms11051138

64. Ouwendijk WJD, Depledge DP, Rajbhandari L, *et al.* Varicella-zoster virus VLT-ORF63 fusion transcript induces broad viral gene expression during reactivation from neuronal latency. *Nat Commun*. 2020;11(1):6324.

doi: 10.1038/s41467-020-20031-4

65. Eisfeld AJ, Turse SE, Jackson SA, Lerner EC, Kinchington PR. Phosphorylation of the varicella-zoster virus (VZV) major transcriptional regulatory protein IE62 by the VZV open reading frame 66 protein kinase. *J Virol*. 2006;80(4): 1710-1723.

doi: 10.1128/JVI.80.4.1710-1723.2006

66. Sen N, Sommer M, Che X, White K, Ruyechan WT, Arvin AM. Varicella-zoster virus immediate-early protein 62 blocks interferon regulatory factor 3 (IRF3) phosphorylation at key serine residues: a novel mechanism of IRF3 inhibition among herpesviruses. *J Virol*. 2010;84(18):9240-9253.

doi: 10.1128/JVI.01147-10

67. Borden EC. Interferons alpha and beta in cancer: Therapeutic opportunities from new insights. *Nat Rev Drug Discov*. 2019;18(3):219-234.

doi: 10.1038/s41573-018-0011-2

68. Gerada C, Campbell TM, Kennedy JJ, *et al.* Manipulation of the innate immune response by varicella zoster virus. *Front Immunol*. 2020;11:1.

doi: 10.3389/fimmu.2020.00001

69. Jacobsen C, Pluckebaum N, Ssebyatika G, *et al.* Viral modulation of type II interferon increases T cell adhesion and virus spread. *Nat Commun*. 2024;15(1):5318.

doi: 10.1038/s41467-024-49657-4

70. Molinier-Frenkel V, Prevost-Blondel A, Castellano F. The IL4I1 enzyme: A new player in the immunosuppressive tumor microenvironment. *Cells*. 2019;8(7):757.

doi: 10.3390/cells8070757

71. Cousin C, Aubatin A, Le Gouvello S, Apetoh L, Castellano F, Molinier-Frenkel V. The immunosuppressive enzyme IL4I1 promotes FoxP3(+) regulatory T lymphocyte differentiation. *Eur J Immunol*. 2015;45(6):1772-1782.

doi: 10.1002/eji.201445000

72. Romagnani S. IL4I1: Key immunoregulator at a crossroads of divergent T-cell functions. *Eur J Immunol*. 2016;46(10): 2302-2305.

doi: 10.1002/eji.201646617

73. Jiang J, Natarajan K, Margulies DH. MHC molecules, T cell receptors, natural killer cell receptors, and viral immunoevasins-key elements of adaptive and innate immunity. *Adv Exp Med Biol*. 2019;1172:21-62.

doi: 10.1007/978-981-13-9367-9_2

74. Wu Y, Zhang N, Hashimoto K, Xia C, Dijkstra JM. Structural comparison between MHC classes I and II; in evolution, a class-II-like molecule probably came first. *Front Immunol*. 2021;12:621153.

doi: 10.3389/fimmu.2021.621153

75. Ye Y, Li S, Yan X, *et al.* VZV IE4 downregulates cellular surface MHC-I via sequestering it to the Golgi complex. *Cell Mol Life Sci*. 2024;82(1):23.

doi: 10.1007/s00018-024-05477-9

76. Whitmer T, Malouli D, Uebelhoer LS, DeFilippis VR, Fruh K, Verweij MC. The ORF61 protein encoded by simian varicella virus and varicella-zoster virus inhibits NF-kappaB signaling by interfering with Ikappabalpha degradation. *J Virol*. 2015;89(17):8687-8700.

doi: 10.1128/JVI.01149-15

77. Abendroth A, Kinchington PR, Slobedman B. Varicella zoster virus immune evasion strategies. *Curr Top Microbiol Immunol*. 2010;342:155-171.

doi: 10.1007/82_2010_41

78. Abendroth A, Slobedman B. Modulation of MHC and MHC-like molecules by varicella zoster virus. *Curr Top Microbiol Immunol*. 2023;438:85-102.

doi: 10.1007/82_2022_254

79. Cornel AM, Mimpen IL, Nierkens S. MHC class I downregulation in cancer: Underlying mechanisms and potential targets for cancer immunotherapy. *Cancers (Basel)*. 2020;12(7):1760.

doi: 10.3390/cancers12071760

80. Horiuchi Y. Th1 regulatory events by infectious pathogens, herpes zoster and herpes simplex viruses: Prospects for therapeutic options for atopic eczema. *Postepy Dermatol Alergol*. 2022;39(4):662-667.

doi: 10.5114/ada.2022.118920

81. Jankeel A, Coimbra-Ibraim I, Messaoudi I. Simian varicella virus: Molecular virology and mechanisms of pathogenesis. *Curr Top Microbiol Immunol*. 2023;438:163-188.

doi: 10.1007/82_2021_241

82. Grose C, Shaban A, Fullerton HJ. Common features between stroke following varicella in children and stroke following herpes zoster in adults: Varicella-zoster virus in trigeminal Ganglion. *Curr Top Microbiol Immunol*. 2023;438:247-272.

doi: 10.1007/82_2021_236

83. Lei B, Wang Z, Shu Q, *et al*. Observation of varicella zoster virus-induced acute retinal necrosis: Viral load detection and visual outcome. *Eye (Lond)*. 2022;36(6):1209-1216.

doi: 10.1038/s41433-021-01609-8

84. Grahn A, Bergstrom T, Runesson J, Studahl M. Varicella-zoster virus (VZV) DNA in serum of patients with VZV central nervous system infections. *J Infect*. 2016;73(3): 254-260.

doi: 10.1016/j.jinf.2016.04.035

85. Richter ER, Dias JK, Gilbert JE 2nd, Atherton SS. Distribution of herpes simplex virus type 1 and varicella zoster virus in ganglia of the human head and neck. *J Infect Dis*. 2009;200(12):1901-1906.

doi: 10.1086/648474

86. Smith RL, Pizer LI, Johnson EM Jr., Wilcox CL. Activation of second-messenger pathways reactivates latent herpes simplex virus in neuronal cultures. *Virology*. 1992;188(1):311-318.

doi: 10.1016/0042-6822(92)90760-m

87. Thellman NM, Botting C, Madaj Z, Triezenberg SJ. An immortalized human dorsal root ganglion cell line provides a novel context to study herpes simplex virus 1 latency and reactivation. *J Virol*. 2017;91(12):e00080-17.

doi: 10.1128/JVI.00080-17

88. Cohrs RJ, Badani H, Baird NL, White TM, Sanford B, Gilden D. Induction of varicella zoster virus DNA replication in dissociated human trigeminal ganglia. *J Neurovirol*. 2017;23(1):152-157.

doi: 10.1007/s13365-016-0480-1

89. Sadaoka T, Depledge DP, Rajbhandari L, Venkatesan A, Breuer J, Cohen JI. *In vitro* system using human neurons demonstrates that varicella-zoster vaccine virus is impaired for reactivation, but not latency. *Proc Natl Acad Sci U S A*. 2016;113(17):E2403-E2412.

doi: 10.1073/pnas.1522575113

90. Saitoh H, Momma Y, Inoue H, Yajima D, Iwase H. Viable herpes simplex virus type 1 and varicella-zoster virus in the trigeminal ganglia of human cadavers. *J Med Virol*. 2013;85(5):833-838.

doi: 10.1002/jmv.23527

91. Rahaus M, Desloges N, Wolff MH. Varicella-zoster virus requires a functional PI3K/Akt/GSK-3alpha/beta signaling cascade for efficient replication. *Cell Signal*. 2007;19(2): 312-320.

doi: 10.1016/j.cellsig.2006.07.003

92. Liu X, Cohen JI. Varicella-zoster virus ORF12 protein activates the phosphatidylinositol 3-kinase/Akt pathway to regulate cell cycle progression. *J Virol*. 2013;87(3): 1842-1848.

doi: 10.1128/JVI.02395-12

93. Markus A, Lebenthal-Loinger I, Yang IH, Kinchington PR, Goldstein RS. An *in vitro* model of latency and reactivation of varicella zoster virus in human stem cell-derived neurons. *PLoS Pathog*. 2015;11(6):e1004885.

doi: 10.1371/journal.ppat.1004885

94. Karin M, Gallagher E. From JNK to pay dirt: Jun kinases, their biochemistry, physiology and clinical importance. *IUBMB Life*. 2005;57(4-5):283-295.

doi: 10.1080/15216540500097111

95. Zapata HJ, Nakatsugawa M, Moffat JF. Varicella-zoster virus infection of human fibroblast cells activates the c-Jun N-terminal kinase pathway. *J Virol*. 2007;81(2):977-990.

doi: 10.1128/JVI.01470-06

96. Kurapati S, Sadaoka T, Rajbhandari L, *et al*. Role of the JNK pathway in varicella-zoster virus lytic infection and reactivation. *J Virol*. 2017;91(17):e00640-17.

doi: 10.1128/JVI.00640-17

97. Kuper H, Adami HO, Trichopoulos D. Infections as a major preventable cause of human cancer. *J Intern Med*. 2000;248(3):171-183.

doi: 10.1046/j.1365-2796.2000.00742.x

98. Sen N, Che X, Rajamani J, *et al*. Signal transducer and activator of transcription 3 (STAT3) and survivin induction by varicella-zoster virus promote replication and skin pathogenesis. *Proc Natl Acad Sci U S A*. 2012;109(2): 600-605.

doi: 10.1073/pnas.1114232109

99. Ho JD, Xirasagar S, Lin HC. Increased risk of a cancer

diagnosis after herpes zoster ophthalmicus: A nationwide population-based study. *Ophthalmology*. 2011;118(6): 1076-1081.

doi: 10.1016/j.ophtha.2010.10.008

100. Han Y, Liu D, Li L. PD-1/PD-L1 pathway: Current researches in cancer. *Am J Cancer Res*. 2020;10(3):727-742.

101. Zhou H, Ye Z, Gao Z, *et al*. Construction of a pathological model of skin lesions in acute herpes zoster virus infection and its molecular mechanism. *Mamm Genome*. 2024;35(2):296-307.

doi: 10.1007/s00335-024-10039-2

102. Sorensen HT, Olsen JH, Jepsen P, Johnsen SP, Schonheyder HC, Mellemkjaer L. The risk and prognosis of cancer after hospitalisation for herpes zoster: A population-based follow-up study. *Br J Cancer*. 2004;91(7):1275-1279.

doi: 10.1038/sj.bjc.6602120

103. Mahale P, Yanik EL, Engels EA. Herpes zoster and risk of cancer in the elderly U.S. population. *Cancer Epidemiol Biomarkers Prev*. 2016;25(1):28-35.

doi: 10.1158/1055-9965.EPI-15-1033

104. Schmidt SA, Mor A, Schonheyder HC, Sorensen HT, Dekkers OM, Cronin-Fenton D. Herpes zoster as a marker of occult cancer: A systematic review and meta-analysis. *J Infect*. 2017;74(3):215-235.

doi: 10.1016/j.jinf.2016.11.005

105. Chiu HF, Chen BK, Yang CY. Herpes zoster and subsequent risk of cancer: A population-based study. *J Epidemiol*. 2013;23(3):205-210.

doi: 10.2188/jea.je20120155

106. Chen CH, Xirasagar S, Hung SH, Lin HC, Chen CS. Associations of head and neck cancers with herpes zoster in the preceding five years. *Sci Rep.* 2024;14(1):21541.

doi: 10.1038/s41598-024-72893-z

107. Wang YP, Liu CJ, Hu YW, Chen TJ, Lin YT, Fung CP. Risk of cancer among patients with herpes zoster infection: A population-based study. *CMAJ*. 2012;184(15):E804-E809.

doi: 10.1503/cmaj.120518

108. Sim JH, Cho HS, Kim YD, *et al*. The association between herpes zoster and increased cancer risk: A nationwide population-based matched control study. *Curr Oncol*. 2021;28(4):2720-2730.

doi: 10.3390/curroncol28040237

109. Choi HG, Zehnder JL, Lee YK, Lim H, Kim M. Increased risk of lymphoid malignancy in patients with herpes zoster: A longitudinal follow-up study using a national cohort. *BMC Cancer*. 2019;19(1):1148.

doi: 10.1186/s12885-019-6349-y

110. Liu YC, Yang YH, Hsiao HH, *et al*. Herpes zoster is associated with an increased risk of subsequent lymphoid malignancies - a nationwide population-based matched-control study in Taiwan. *BMC Cancer*. 2012;12:503.

doi: 10.1186/1471-2407-12-503

111. Buntinx F, Bartholomeeusen S, Belmans A, *et al*. Association between recent herpes zoster but not herpes simplex infection and subsequent risk of malignancy in women: A retrospective cohort study. *Epidemiol Infect*. 2014;142(5):1008-1017.

doi: 10.1017/S0950268813001702

112. Gershon M, Gershon A. Varicella-Zoster virus and the enteric nervous system. *J Infect Dis*. 2018;218(Suppl 2):S113-S119.

doi: 10.1093/infdis/jiy407

113. Ragozzino MW, Melton LJ 3rd, Kurland LT, Chu CP, Perry HO. Risk of cancer after herpes zoster: A population-based study. *N Engl J Med*. 1982;307(7):393-397.

doi: 10.1056/NEJM198208123070701

114. Leyh C, Roderburg C, Luedde T, Loosen SH, Kostev K. Herpes zoster is not associated with subsequent gastrointestinal cancer: Data from over 200,000 outpatients in Germany. *J Cancer Res Clin Oncol*. 2023;149(19): 17115-17121.

doi: 10.1007/s00432-023-05432-4

115. Kim M, Han K, Yoo SA, Lee JH. Herpes zoster and subsequent cancer risk: A nationwide population-based cohort study in Korea. *Dermatology*. 2021;237(1):73-78.

doi: 10.1159/000505911

116. Lee AW, Sou A, Patel M, Guzman S, Liu L. Early onset of nasopharyngeal cancer in Asian/Pacific Islander Americans revealed by age-specific analysis. *Ann Epidemiol*. 2023;80: 25-29.

doi: 10.1016/j.annepidem.2023.02.006

117. Zaha M, Hayashi I, Odashiro M, *et al*. Herpes zoster and malignancy. *Masui*. 1993;42(9):1343-1346.

118. Yamamoto M, Mine H, Akazawa K, Maehara Y, Sugimachi K. Gastrointestinal cancer and herpes zoster in adults. *Hepatogastroenterology*. 2003;50(52):1043-1046.

ACCSCIENCE PUBLISHING

Microbes & Immunity

REVIEW ARTICLE

Modulating the microbial landscape: A probiotic odyssey from ancient wisdom to modern medicine

Edward Brell*

Independent Researcher, Brisbane, Queensland, Australia

Abstract

The historical journey of probiotics is fascinating, from their ancient roots in fermented foods to their potential as personalized medicine. This paper honors the pioneers who paved the path to current advancements. Significant progress has been made in understanding probiotics, including their mechanisms of action, such as competitive exclusion and immune modulation. For example, *Lactobacillus plantarum* has been shown to improve eczema and the common cold, whereas *Bifidobacterium longum* aids in nutrient absorption and fights off harmful organisms. In addition, *Saccharomyces boulardii* has been demonstrated to be effective in preventing antibiotic-associated diarrhea. Probiotics are applied in various fields, including digestive health, immunity enhancement, and chronic condition management. This review discusses the applications of probiotics and addresses challenges such as strain specificity, safety considerations, and regulatory oversights. The future of probiotics lies in precision medicine, with personalized interventions combined with prebiotics (food for probiotics) to unlock their full potential for enhancing human health and well-being. The paper serves as a valuable resource and a gateway for further research.

Keywords: Gut health; Microbiome; Microbiota; Flora; Digestion; Yoghurt; Sauerkraut; Kimchi

***Corresponding author:**
Edward Brell
(drbrell@gmail.com)

Citation: Brell E. Modulating the microbial landscape: A probiotic odyssey from ancient wisdom to modern medicine. *Microbes & Immunity*. 2025;2(3):31-46. doi: 10.36922/mi.6424

Received: November 21, 2024

Revised: February 18, 2025

Accepted: March 7, 2025

Published online: May 21, 2025

1. Introduction

The growing understanding of the human microbiome and its profound impact on human health has led to a surge of interest in probiotics – live microorganisms that can confer health benefits when administered in adequate amounts, according to the International Scientific Association for Probiotics and Prebiotics.[1] The degree of interest can be gauged by the number of publications. Figure 1 illustrates the trend in the number of publications, based on a 5-year moving average of articles with "probiotic" in the title, retrieved from PubMed (pubmed.ncbi.nlm.nih.gov). The number of publications nearly doubled in the last 5 years, highlighting the growing prominence and relevance of probiotic research.

Fermented foods have been a staple in human diets for millennia, with evidence of their consumption dating back to ancient civilizations.[2-4] These foods are a source of essential nutrients and are believed to possess health benefits. The scientific basis for

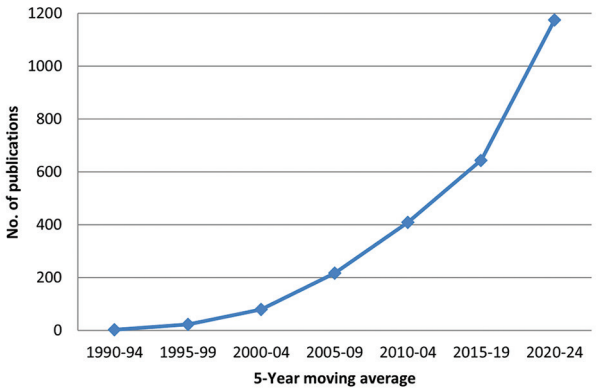

Figure 1. Number of articles published with "probiotic" in the title. Graph created by the author using Microsoft Excel. Data source: PubMed.

these traditional practices is now being elucidated through the study of probiotics, live microorganisms that confer health benefits on the host.[1] The field of probiotics is growing rapidly, as indicated by Figure 1.

This review aims to explore the origins of probiotics and summarize their mechanisms of action. Their diverse applications will be discussed, and the challenges in current probiotic research and future directions will be evaluated. While this is not a meta-analysis, it aims to provide a comprehensive overview of the field and identify areas for future research.

1.1. Impact on human endeavors

The global microbiome is a vast and diverse community of microorganisms, including bacteria, archaea, fungi, viruses, and bacteriophages (viruses that infect bacteria). The microbiome lives in symbiosis with humans and has a profound impact on human health. These microorganisms are found everywhere – from the soil, water, and air to every part of the human body, including the brain, skin, and gut. Their habitat is so pervasive that it can be considered a distinct community.[5] The association of this pervasive nature with humans is succinctly summarized as follows:[6]

- Health implications: Dysbiosis, a deviation from normal microbial composition, can lead to adverse health effects. The microbiome affects health in various ways, influencing areas such as mental health, reproductive health, and immune response.
- Agricultural applications: Beneficial bacteria play crucial roles in agriculture, including decomposing organic matter, enhancing soil fertility, and acting as biopesticides and biofertilizers. These applications are critical for sustainable farming practices.
- Environmental remediation: Certain bacteria are involved in the remediation of environmental pollutants in water, air, and soil, helping in the degradation of pollutants, such as hydrocarbons, heavy metals, and synthetic dyes.
- Food industry: Microorganisms are used in the production of fermented foods and beverages, which offer various health benefits. They are involved in the fermentation of dairy and non-dairy products, enhancing flavor, texture, and nutritional value.
- Probiotics and health: Probiotics, which are beneficial microorganisms, play a significant role in maintaining gut health and overall well-being. They can help in restoring healthy microbiome communities and preventing infections.
- Pharmaceutical and nutraceutical applications: Microbial products are used in the pharmaceutical industry for their antimicrobial, antioxidant, and immunomodulatory properties. They also have applications in nutraceuticals and cosmeceuticals.

Furthermore, recent findings demonstrated that skin-associated bacterial communities may serve as more distinctive personal identifiers than the human genome.[7]

2. Modulation of gut microbiome

Shifting the focus from the broader ecosystem of microbes to the human gut, the gut microbiome is a complex community of trillions of microorganisms, including (unsurprisingly) bacteria, archaea, fungi, and viruses.[8] The gut microbial community plays a critical role in human health, affecting digestion, nutrient absorption, immune function, and even mental well-being.[9] Probiotics are thought to modulate the gut microbiome by promoting the growth of beneficial bacteria and suppressing the growth of harmful ones.[10] *Lactobacillus plantarum* and *Bifidobacterium longum* are two of the most commonly studied probiotic strains. These strains have been shown to exert their beneficial effects through a variety of mechanisms. To better understand their morphology and how they interact with the environment, the relevant micrographs and details are provided in Figure 2.

The scanning electron micrographs (Figure 2) provide a visual representation of *L. plantarum* and *B. longum,* highlighting their distinctive morphological features, such as cell shape, size, and arrangement (Table 1).

2.1. WebMD overview of *L. plantarum*

WebMD (https://www.webmd.com/), a comprehensive online resource providing health information and tools, suggests *L. plantarum* is potentially effective for:

- Eczema (atopic dermatitis): Oral intake of *L. plantarum* has been associated with improvements in eczema symptoms in children and adults.

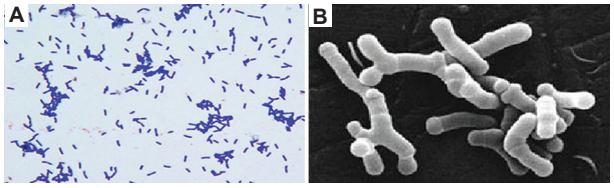

Figure 2. Micrographs and details of the most commonly studied probiotic strains, (A) *Lactobacillus plantarum*[11] and (B) *Bifidobacterium longum*[12]

Table 1. Typical morphological and microscopic characteristics of *Lactobacillus plantarum* and *Bifidobacterium longum*

Probiotic strains	*L. plantarum*	*B. longum*
Magnification	Typically×1,000	Typically ×~5000
Staining method	Gram staining	Nil staining
Cell shape	Rod-shaped	Rod-shaped with a characteristic Y-shape or bifurcation
Cell size	0.7 – 1.1 µm in diameter, 2 – 4 µm in length	0.5 – 1.2 µm in diameter, 2 – 5 µm in length
Arrangement	Single cells or short chains	Single cells or short chains

- Common cold: Oral intake of *L. plantarum* with another probiotic, *Lactobacillus paracasei*, has been associated with improvements in common cold symptoms.
- High cholesterol: Oral intake of *L. plantarum* has been associated with modest reductions in cholesterol levels.
- Irritable bowel syndrome, a long-term disorder of the large intestine that causes stomach pain: Oral intake of *L. plantarum* alone or with other probiotics has been associated with improvements in irritable bowel syndrome.
- Infection of the airways: Oral intake of *L. plantarum* alone or with other probiotics has been associated with preventing airway infections in adults.
- Ulcerative colitis, a type of inflammatory bowel disease: Oral intake of *L. plantarum,* together with standard treatment, has been associated with increased remission and prevention of relapse in people with ulcerative colitis.

2.2. WebMD overview of *B. longum*

According to WebMD, *B. longum* resides in the intestines and produces lactic and acetic acids, which aid in food digestion, nutrient absorption, and defense against potentially harmful microorganisms.

2.3. Mechanisms of probiotic action

As with many scientific endeavors, understanding is deepened when considered in conjunction with the mechanisms of action.[13,14] *B. longum* and *L. plantarum* exert their health benefits through several mechanisms,[15,16] including:

- Competition with pathogens: Both probiotics compete with harmful bacteria for nutrients and adhesion sites, preventing the harmful bacteria from colonizing the intestinal epithelium (gut wall). This is shown graphically in Figure 3, where a slug of lumen is traced as it passes through the intestine. The clock faces depicted here merely mark the passage of time (and not the time of day).
- Inactivation of pathogenic toxins: Some strains can neutralize toxins produced by pathogenic bacteria.
- Production of beneficial substances: These probiotics produce substances, such as lactic acid, that inhibit the growth of harmful bacteria.
- Enhancement of mucosal barrier: They interact with epithelial cells to strengthen the mucosal barrier, protecting against infections.
- Modulation of immune responses: These probiotics can interact with immune cells, enhancing the body's immune response by stimulating the production of immune mediators, such as cytokines and secretory immunoglobulin A. These help to protect the host against infection.[17]
- Metabolic modulation: Some strains can influence metabolic processes, such as insulin resistance and cholesterol metabolism. They can ferment carbohydrates in the gut, resulting in the production of short-chain fatty acids that promote gut health, including butyrate, which has anti-inflammatory properties.[18]
- Neurological effects: Emerging research suggests these probiotics may impact neurological signaling pathways.[19]
- Protection: These probiotics can exert their effects through the production of antimicrobial substances, such as bacteriocins, which inhibit the growth of pathogenic bacteria. "Friendly" gut bacteria may eliminate pathogens by competing for energy resources.[20,21] In addition, these probiotic strains can modulate gut motility, further contributing to a healthy gut environment.

Figure 4 graphically illustrates how probiotics occupy the gut mucus lining, preventing harmful bacteria and their toxins from gaining access. By competitively inhabiting the mucosal area, a beneficial climate is created for other beneficial bacteria to grow.

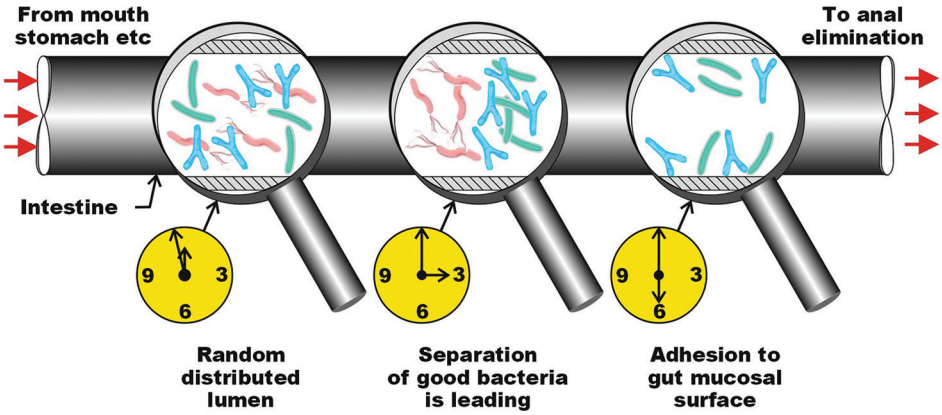

Figure 3. Timeline idealization of *Bifidobacterium longum* and *Lactobacillus plantarum,* protecting the intestinal wall from harmful bacteria (shown pink with flagella). By author uses Corel Graphics Suite 2017.

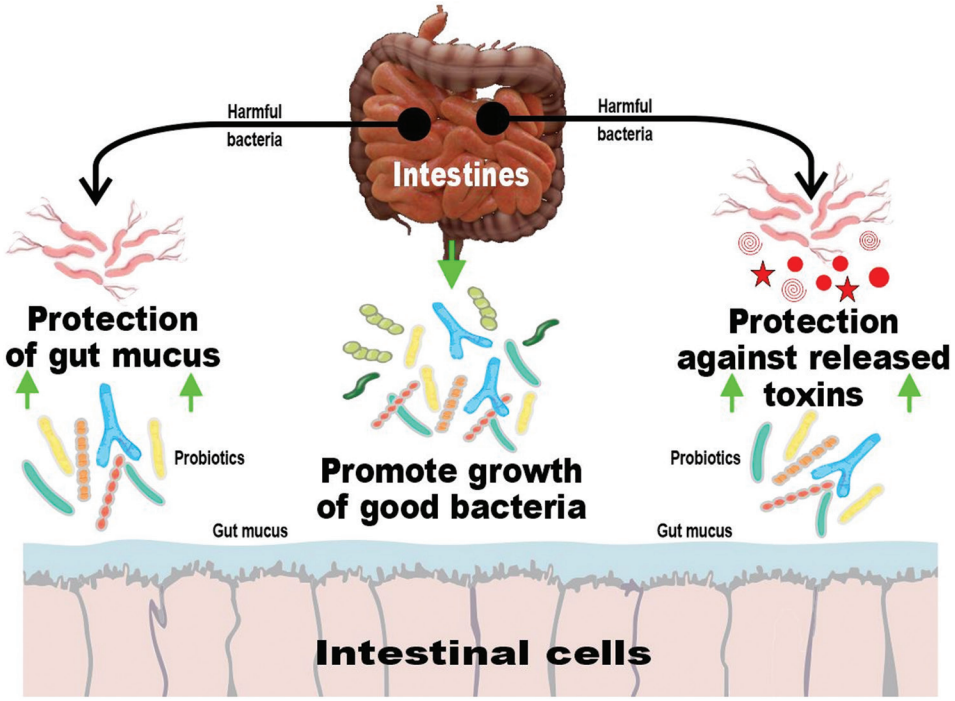

Figure 4. Schematic cross-section of the intestine shows the protective mechanisms of gut mucus against harmful bacteria (shown pink with flagella) invasion and toxin release. Image created by author using Corel Graphics Suite 2017. Information is attributed to WebMD.

2.4. Shelf life of probiotic products

A 2017 nationally representative survey of 1,006 American adults found that about one-third had not cleaned out their medicine cabinet in the past year, and nearly one-fifth had not done so in the past 3 years.[22] Consequently, many households store pharmaceuticals past their use-by dates. This poses a concern, as manufacturers are legally required to guarantee product safety only up to the indicated use-by date; any use beyond that point cannot be assumed to be safe.

To assess the implications of product expiration, one study investigated the viability of microorganisms in expired probiotic products and how packaging and storage conditions impact their efficacy.[23] Of the 33 expired products evaluated, 22 still had viable contents despite being expired, on average, for more than 11 years. However, only five met or exceeded their original cell count claims. Microbial viability was significantly influenced by factors such as packaging type, storage conditions, and time since expiry.

While some expired probiotics retained viability, the total counts in this research were mostly below the recommended effective dose, suggesting that consuming expired probiotics may not provide the intended health benefits. Therefore, it is crucial to follow storage guidelines and use probiotics before their expiration dates to ensure their effectiveness.

2.5. Disposal of unused medication

Improper disposal of unused medication poses several significant risks:

- Environmental contamination: Flushing medications down the toilet or discarding them in the rubbish can contaminate water supplies and soil. Wastewater treatment plants are often not designed to remove pharmaceutical chemicals, resulting in their release into the environment, where they may harm aquatic life, disrupt ecosystems, and pose risks to human health through contaminated drinking water.
- Accidental poisoning: Unsecured and improperly disposed medications can be easily accessed by children and pets, resulting in accidental poisoning with serious health consequences, including hospitalization and even death. Even seemingly harmless over-the-counter medications can be dangerous in the wrong hands or when overdosed.
- Antibiotic resistance: Improper disposal contributes to the growing problem of antibiotic resistance. When antibiotics are released into the environment, they can promote the development of antibiotic-resistant bacteria, making infections harder to treat and posing a serious threat to public health.
- Drug abuse: Unused medications left unsecured in homes can be a source of drug abuse, particularly among teenagers and young adults, potentially leading to addiction, overdose, and other serious health problems.
- Ineffective medication: Improper storage, such as in humid or hot environments, can degrade medications, making them less effective or even harmful, even if they are still within their use-by dates. The improper disposal of such degraded medications still carries the risks mentioned above.
- Financial waste: Unused and expired medications represent a financial waste for individuals and health-care systems. This waste can be reduced through better medication management and adherence to prescribed regimens.

A study assessed the accumulation of waste around the world caused by poor pharmaceutical disposal practices.[24] Their data tables categorize disposal habits across various countries, distinguishing between discarding medications in the rubbish, flushing them into the sewer system, or returning them to pharmacies. Aggregating the data for Germany, Sweden, and the Netherlands under "Europe," and for the United States of America (USA) and England under "English" for comparison, the average rates of disposal by rubbish and return to the pharmacy – approximated from the chart data in the study – are as follows:

- Disposal by rubbish by "English" was 43% against "Europe" at 6%
- Disposal by return to pharmacy by "Europe" was 56% against "English" at 27%.

While the "English" group heavily favors disposing of rubbish, the "Europe" group prefers returning it to pharmacies. This reflects a significant cultural difference in disposal practices, suggesting that the "English" group may lack convenient pharmacy return programs or that people are not aware of them. In contrast, pharmacy-based disposal appears to be the dominant method in the "Europe" group. This difference could have implications for environmental concerns (e.g., landfill issues and public health), as improperly disposed medications pose a risk. It highlights a potential area for improvement in England and the USA.

3. History of probiotics

The use of fermented foods for health purposes dates back to ancient civilizations. For example, Egyptians consumed fermented milk products, such as yogurt, whereas Chinese people consumed fermented soybean.[25,26] These practices were likely driven by empirical observations of the health benefits associated with consuming fermented foods. The term "probiotic" was first introduced by Elie Metchnikoff, who hypothesized that consuming bacteria from yogurt could promote longevity.[27]

The discovery of antibiotics during and after World War I and World War II led to a temporary shift away from the focus on probiotics, with some exceptions. Over the decades, the term "probiotics" was redefined by various scientists to refer specifically to beneficial live microbial supplements.[28]

The contribution of Elie Metchnikoff cannot be understated, as we recall his Messina story: While his family was at the circus, Metchnikoff, being alone with his microscope, observed motile cells in a starfish larva. He theorized that these cells could defend against invaders, such as a splinter in a finger. He immediately tested this by inserting rose thorns into the larva. The next morning, he excitedly found that the motile cells had surrounded the thorns, proving his hypothesis. This Messina experiment became the foundation for his theory of *phagocytosis*

(from the Greek words "to eat," a process where cells engulf large particles), which he explored for the next 25 years.[29]

The historical progression of probiotics traces its origins to age-old fermentation traditions. Along this journey, we recognize the trailblazing contributions of scientists, such as Louis Pasteur (Figure 5), to the cutting-edge field of precision medicine. In this context, probiotics are harnessed as microscopic allies for personalized health. Figure 5 presents a pictorial timeline of these key milestones, with the photo collage highlighting the pioneers whose contributions have shaped the field.

The discoveries do not end with the pioneers in Figure 5. There is a long list of masters in the field, among whom are:

(a) Gregor Reid:[36]

- 1980s: Started his research on probiotics, focusing on their role in women's health and gut health
- 2001 – 2002: Chaired the United Nations/World Health Organization expert panel that defined the modern term "probiotics"
- Ongoing: Continues to advocate for the use of probiotics in health care and develop novel probiotic therapies.

(b) Mary Ellen Sanders:[37]

- 1990s – present: A leading figure in the field, focusing on the scientific substantiation of probiotic benefits and their safe use
- Ongoing: Actively involved in research, education, and advocacy related to probiotics.

(c) Francisco Guarner:[38]

- 1990s – present: Has extensively studied the mechanisms of action of probiotics and their impact on gut health.
- Ongoing: Continues to contribute to the understanding of probiotics and their potential therapeutic applications.

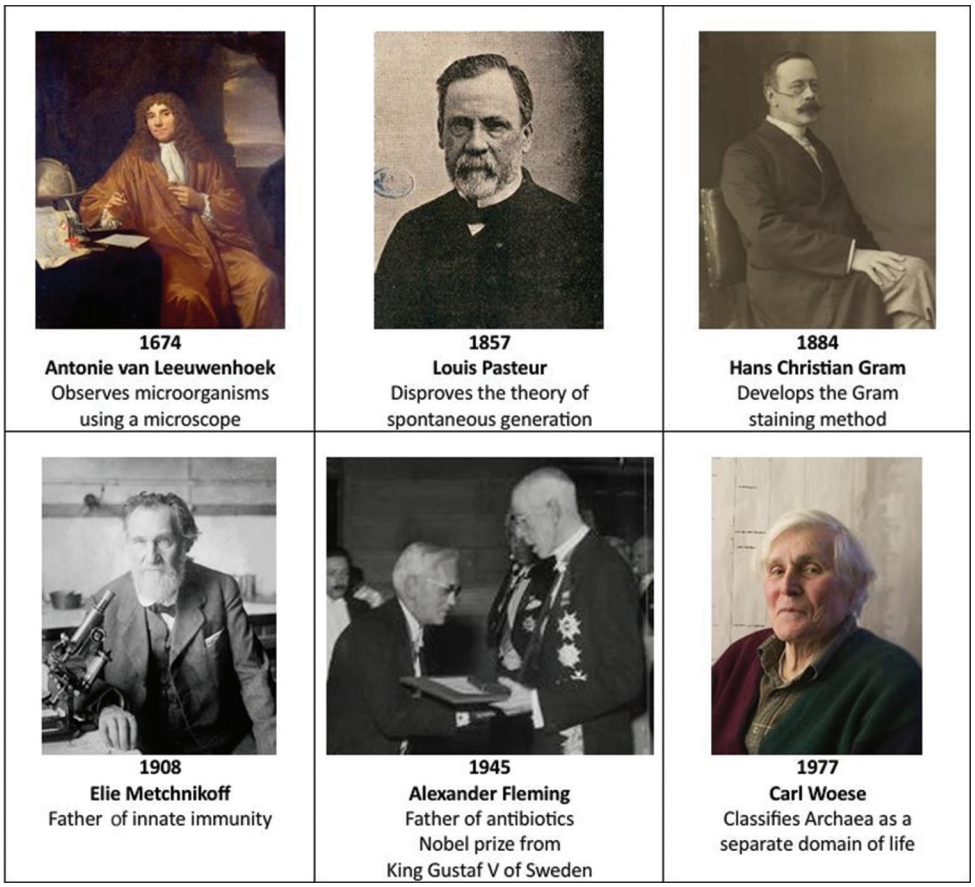

Figure 5. The faces of probiotics: Pioneers in microbial health. Years indicate years of main contribution to science. The public domain image of Antonie van Leeuwenhoek was reprinted from commons.wikimedia.org.[30] The public domain image of Louis Pasteur was reprinted from nlm.nih.[31] The public domain image of Hans Christian Gram was reprinted from commons.wikimedia.org.[32] The public domain image of Elie Metchnikoff was reprinted from loc.gov.[33] The public domain image of Alexander Fleming was reprinted from nobelprize.org.[34] Image of Carl Woese was reprinted from en.wikipedia.org.[35] CC3.0 Don Hamerman – Hansen and Weller.

(d) Lorenzo Morelli:[39]

- 1980s – present: Specializes in the characterization and application of probiotic strains, particularly in infant health
- Ongoing: Continues to research and develop new probiotic products for various health needs.

(e) Danisco:

- 1990s – present: A global bioscience company with a strong focus on probiotic research and development
- Ongoing: Danisco is now part of DuPont and continues to invest in research and innovation in the field of probiotics, contributing to new product development and scientific advancements.

4. Human microbiome project (HMP)

The HMP was a groundbreaking research initiative launched by the USA National Institutes of Health in 2007.[40] Its primary goal was to characterize the microbial communities inhabiting the human body, including bacteria, viruses, fungi, and archaea. Through comprehensive sampling and analysis of microbial DNA, the HMP generated a wealth of data on the composition and function of the human microbiome across various body sites, including the gut, skin, oral cavity, and respiratory tract. This project significantly advanced our understanding of the complex interplay between human health and the microbial world, providing a crucial foundation for the field of microbiome research. The mention of HMP here is relevant to underscore the profound impact of the human microbiome on human health and disease.

5. The influence of genetics on the gut microbiome: Insights from the United Kingdom Twins study

The United Kingdom Twins Study provides invaluable insights into the interplay between genetics and the gut microbiome.[41] By examining the microbiome of monozygotic (identical) and dizygotic (fraternal) twins, this study offers a unique opportunity to disentangle the relative contributions of genetic and environmental factors to the composition and function of the gut microbiota. The findings of this study are highly relevant to this review, as they emphasize the importance of considering individual genetic variations and their influence on the gut microbiome when developing personalized probiotic interventions.

This study analyzed the gut microbiomes of 2,731 individuals, including monozygotic and dizygotic twins. It aimed to quantify the heritability of various gut microbiota components and investigate the association between microbial abundances and host genetic variations. The expanded dataset enabled researchers to refine heritability estimates for previously identified microbial taxa. In addition, it uncovered novel associations between heritable microbes and host genes involved in diet, immunity, and other key biological processes. Notably, the study demonstrated that host genetics can influence the gut microbiome through shaping dietary preferences, which are heritable traits. These findings emphasize the crucial role of host genetics in shaping the gut microbial landscape. In addition, they highlight the importance of considering individual genetic variations when developing personalized probiotic interventions.

6. Potential applications of probiotics

The contribution of WebMD referred to only two of the most common probiotics. Probiotics have been investigated for a much wider range of potential applications in human health, including (but not limited to):

- Gastrointestinal disorders: Probiotics have been shown to be effective in preventing and treating diarrhea, including antibiotic-associated diarrhea and traveler's diarrhea.[42-44]
- Inflammatory bowel disease (IBD): Probiotics may be beneficial in managing IBD, such as ulcerative colitis and Crohn's disease.[45]
- Allergic diseases: Probiotics may help to prevent and treat allergies, such as eczema and asthma.[46]
- Metabolic disorders: Probiotics are being investigated for their potential role in managing obesity, diabetes, and non-alcoholic fatty liver disease.[47,48]

The practice of matching a strain of probiotics for a particular disorder condition is vast and well beyond the scope of this article. Nevertheless, we present a table of reported successes for given maladies with selected probiotics in Table 2. It should be noted that other combinations of probiotics may also work successfully for the particular condition.

Table 2. Successful matches of probiotics and maladies – gastrointestinal disorders

Condition	Probiotics
Antibiotic-associated diarrhea[44]	*Saccharomyces boulardii*
General digestive discomfort[49]	*Lactobacillus plantarum* 299v
Irritable bowel syndrome+diarrhea[50]	*S. boulardii*
Irritable bowel syndrome+constipation[51]	*Bifidobacterium lactis*
Leaky gut[52]	*Lactobacillus rhamnosus* GG

7. Personalized medicine and probiotics

The concept of personalized medicine or precision medicine is transforming health care by tailoring treatments to individual patients based on their unique genetic and microbial profiles. This approach holds great promise for the field of probiotics, as the composition of the gut microbiome varies significantly between individuals.[53] By analyzing an individual's gut microbiome, researchers can identify specific probiotic strains that may be most beneficial for that individual. This personalized approach can help to maximize the efficacy and safety of probiotic interventions.

Practitioners will need to understand both the pathology of a patient's dysbiosis and the specific strain of probiotics that has the propensity to address the problem – an essential foundation for effective treatment. Strategies for developing personalized probiotic therapies can then include comprehensive microbiome profiling, strain-specific testing, and potentially the use of artificial intelligence (AI) to predict individual responses to different probiotic strains.

Some companies(e.g Zoe.com)[53] now offer at-home microbiome tests. Typically, stool samples are taken at home and sent in for analysis. One consumer advocacy group.[54] Evaluated three such companies and offered some caution:

- If you are curious about your gut health, a gut microbiome test can be interesting
- However, if you have gastrointestinal symptoms, it is best to see your health-care provider for routine clinical testing to detect common pathogens
- Companies offering these services caution against making major dietary changes based on home gut microbiome test results
- They recommend seeking further advice from qualified health-care professionals before making significant changes to your diet
- Remember, these tests are fascinating but are not yet diagnostic tools.

As an aside, this trend presents a great opportunity for gathering vast amounts of microbiome data, though it also raises important privacy and ethical considerations.

7.1. Strain specificity

The effects of probiotics are highly strain-specific. Not all probiotic strains are equally effective or safe for all individuals.[55] This further supports the need to account for both the particular strain of probiotics as well as the target disease.

Lactobacillus rhamnosus GG (LGG) is a well-researched probiotic strain, first isolated by scientists Sherwood Gorbach and Barry Goldwin, hence the "GG" designation. This strain is known for its ability to survive stomach acid and bile, allowing it to reach the gut alive and provide health benefits. A study analyzed 100 different strains of *L. rhamnosus*.[56] Out of the 100 strains considered identified strain A and strain B, which were different strains of *L. rhamnosus*. Both strains could be found in the intestines, but strain B could be characterized similarly to the well-known GG strain. Strain A and strain B can be distinguished by the following:

- Lack of pili: Strain A does not have the hair-like pili, which are crucial for adhesion to the mucus gut lining
- Carbohydrate metabolism: Strain A metabolizes different carbohydrates, including *D*-lactose and *D*-maltose. This is indicative of its adaptation to a dairy-like environment (making cheese).

On the other hand, strain B has traits that make it well-suited for the intestinal tract, such as bile resistance, the production of pili, and the ability to utilize *L*-fucose, a type of sugar. Thus, strain B survives stomach gastric juices better and lasts longer in the intestines, adhering to the mucus lining. It is therefore not surprising that strain B performs better in fixing the illness above. Whatever number of strain A survives the hostile environment of the stomach, it just passes through, not having pili to anchor. All of which is to illustrate the importance of getting the type of strain right to suit the intended disease application.

7.2. Limitations of probiotics

To illustrate this section, we offer an excerpt from a Social Media post,[57] as follows:

Taking certain strains of probiotics years ago gave me severe health problems, when before I was perfectly healthy. My body initially reacted to them as if I (had) caught a severe stomach bug. After taking them, I got diarrhea, nausea, swollen lymph nodes, fatigue, nerve pain, severe chronic belching, chronic mal-digestion of foods, constant sore throat, etc. It continued to progress to the point of panic attacks, having zero appetite, and having severe flu-like symptoms all the time. I did an antibiotic regiment and recovered in less than a week, being able to eat anything and everything without any problems besides feeling completely amazing. I then took a different probiotic with different strains, and my body got just as sick from it. I was never able to truly recover after that point. Antibiotics helped again temporarily but stopped working. Without severe intervention on my part, my body slips quickly into misery, and I basically go insane. Medical tests are inconclusive, and my gastroenterologist thinks it's my immune system overreacting and I agree.

I think I am a one in a million case where taking certain probiotics shifted the bacteria in my gut to a point

where my immune/nervous system is in a constant state of reaction. I do not think it's that the bacteria are bad necessarily, it's how my immunity reacts to whatever is going on in my microbiome. The only things that provide me relief are antibiotics (which eventually stop working completely) and osmotic laxatives.

Not all probiotics are without side effects. Here are some things to watch out for:

- Digestive symptoms: Some people may experience temporary digestive issues, such as gas, bloating, constipation, or increased thirst, when first introducing probiotics. To minimize discomfort, it is generally recommended to begin with a low dose and gradually increase as tolerated.
- Allergic reactions: Probiotics can occasionally trigger allergic reactions in sensitive individuals. Some people may also experience intolerance due to increased histamine levels, which can trigger symptoms such as itching, watery eyes, runny noses, or difficulty breathing. Particular caution may be warranted with strains such as *Lactobacillus buchneri*, *Lactobacillus helveticus*, *Lactobacillus hilgardii*, and *Streptococcus thermophilus*.
- Infections: People with weakened immune systems or serious health conditions may be at a higher risk of infections from probiotics. People with venous catheters, recent surgery, acute pancreatitis, or prolonged hospitalizations should avoid taking probiotics.
- Headaches: Certain probiotic-rich foods contain biogenic amines, which can trigger headaches in sensitive individuals.
- Regulation and quality: Probiotics are not regulated by the USA Federal Drug Authority (FDA), which can lead to inconsistencies in the quality and contents of probiotic products. To reduce the risk of ineffective or contaminated products, it is advisable to avoid off-brand options and purchase from reputable, well-established suppliers.

8. Delivery methods

The focus so far has been on the ingestion of probiotics, with benefits attributed largely to their occupation and proliferation in the intestines. However, emerging research is beginning to explore applications beyond the gut – an area still in its early stages of development. The delivery methods are listed in the following sections.

8.1. Topical applications (creams, ointments, and lotions)

- Mechanism: Topical probiotics aim to deliver beneficial bacteria directly to the skin, where they can interact with the skin microbiome and potentially influence skin health.
- Applications:
  - Eczema (atopic dermatitis): Some studies suggest that topical probiotics may help reduce inflammation and improve skin barrier function in eczema.[58]
  - Acne: Topical probiotics may help control acne by reducing inflammation and the growth of *Cutibacterium acnes* (formerly *Propionibacterium acnes*), the bacteria implicated in acne development.[59]
  - Rosacea: Probiotics may help manage rosacea by reducing inflammation and restoring the balance of the skin microbiome.[60]
  - Wound healing: Preliminary research suggests topical probiotics might promote wound healing.[61]
  - Anti-aging: Some cosmetic products incorporate probiotics, claiming they can improve skin hydration, reduce wrinkles, and enhance skin radiance. However, more robust scientific evidence is needed to support these claims.[62]

8.2. Vaginal suppositories/capsules

- Mechanism: These methods deliver probiotics directly to the vaginal area to restore and maintain a healthy vaginal microbiome.
- Applications:
  - Bacterial vaginosis: Vaginal probiotics can be an effective treatment for bacterial vaginosis, helping to restore the balance of beneficial bacteria such as *Lactobacillus*.[63]
  - Yeast infections: Probiotics may help prevent recurrent yeast infections by competing with *Candida* and restoring a healthy vaginal flora.[64]

8.3. Oral rinses/toothpastes

- Mechanism: These products deliver probiotics to the oral cavity to promote oral health.
- Applications:
  - Periodontal disease: Probiotics may help reduce inflammation and improve gum health in people with periodontal disease[65]
  - Dental caries (cavities): Some studies suggest that probiotics may help reduce the levels of bacteria that contribute to cavities[66]
  - Halitosis (bad breath): Probiotics may help reduce bad breath by targeting the bacteria that produce odor-causing compounds.[67]

8.4. Injections and intravenous delivery

- Prevalence:[68] The practice of probiotic delivery through injection or intravenous methods has little

support in the literature, given that introducing a live culture to enter the bloodstream may have unpredictable consequences.

- An example is found in a case report of a 25-year-old who was accidentally injected intravenously with 2 billion spores of *Bacillus clausii*. It took 5 months of various antibiotic treatments before blood tests finally confirmed clearance of the infection[69]
- A study showed that extracellular vesicles (EVs) secreted by *B. longum* and *L. plantarum* could be used for intravenous and subcutaneous administration in mice, with the subcutaneous pathway showing particular promise[70]

- Mechanism: EVs[71] offer a promising avenue for circumventing the risks associated with the direct administration of live probiotics.
  - EVs are nanosized particles released by cells, composed of a cellular membrane and associated proteins, enclosing an aqueous core containing soluble molecules, such as proteins and nucleic acids. Figure 6 is an artist's impression of EVs being transferred from a donor cell to a recipient cell.
  - EVs play a crucial role in various physiological and pathological processes by facilitating the transfer of biological molecules between cells.[72]
  - In the study conducted using a pre-clinical myocardial infarction animal model, intravenous intervention led to a significant improvement in cardiac function.[73] The authors concluded: "Our results suggest the cell-derived, genetically engineered EVs may be used therapeutically for the delivery of miRNAs for the rescue of myocardial infarction and may benefit patients in the future."

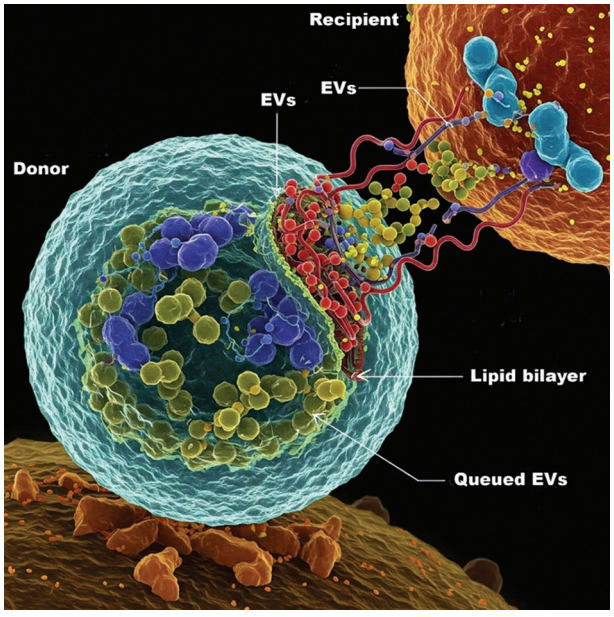

Figure 6. Schematic illustration of extracellular vesicles being transferred from a donor cell to a recipient cell. Image created by the author using Gemini artificial intelligence (CorelDraw Graphics Suite 2017).

8.5. Other delivery methods

- Nasal sprays: Probiotics are being explored for their potential to improve sinus health and prevent respiratory infections. In a pioneering effort, one study developed a probiotic nasal spray that showed success in treating upper respiratory issues.[74]
- Inhalable probiotics: Research into the use of inhaled probiotics delivered for lung health is ongoing, though it remains in the early stages. Nonetheless, the development of a dry powder inhaler formulation offers a promising avenue for targeting the lower respiratory tract.[75]

9. Challenges and considerations

Despite their potential benefits, the use of probiotics also presents some challenges:

- Strain specificity: The effects of probiotics are highly strain-specific. Not all probiotic strains are equally effective or safe for all individuals. McFarland *et al.*[55] concluded from their work: "Strong evidence was found supporting the hypothesis that the efficacy of probiotics is both strain-specific and disease-specific." This further supports the need to account for both the particular strain of probiotics and the target disease.
- Variability in clinical outcomes: The results of clinical trials with probiotics have been inconsistent, highlighting the need for further research to identify the most effective strains and dosages for specific conditions.[76] Achieving reliable, credible, and repeatable results remains a significant challenge in the field.
- Safety concerns: While generally considered safe, some probiotic strains may pose risks for immunocompromised individuals, such as those with acquired immunodeficiency syndrome or undergoing chemotherapy.[77]
- Regulatory issues: The regulatory landscape for probiotics varies across different countries, which can create challenges for the development and marketing of new probiotic products. For example, the European Food Safety Authority takes a stringent approach to regulating the probiotic landscape as "must do good" rather than "does no harm." This becomes particularly challenging as many diseases have long incubation

periods, complicating compliance.[78] In contrast, the US FDA approves probiotics as "generally recognized as safe" (GRAS). However, this designation does not equate to "tested safe." While the FDA does not specifically "approve" probiotics, it regulates them based on their intended use. GRAS status is a common designation for probiotics in food and supplements, but it differs from the "tested safe" standard applied to drugs.

- Labeling: Recognizing that consumers are increasingly making informed choices about probiotic products, a goal of improved labeling has emerged in the industry.[79] Organizations, such as the International Probiotics Association and the Council for Responsible Nutrition, have developed guidelines for probiotic labeling to promote transparency and consistency.
- Limitations of current probiotic research include inconsistent study designs, short-term follow-up periods, and a lack of standardization in probiotic formulations. This makes it difficult to draw definitive conclusions about their efficacy and safety.

10. Future directions

Future probiotics will likely be personalized, targeting specific health needs and leveraging advanced technologies, such as gene editing, to enhance their efficacy and delivery.

10.1. AI

The global conversation around AI is intensifying. Although AI-driven systems have demonstrated superior performance over humans in some analytical tasks in the health-care sector, the persistent issue of "explainability" remains a source of criticism. The so-called "black box" decisions often lead to user apprehension. Explainability, in essence, refers to opening the system to scrutiny – an area of active research that lies beyond the scope of this paper. While explainability can engender trust, trust may also be cultivated in other ways, such as consistent, successful application, independent validation, and cross-verification. One such approach includes comparing outputs across different large language models (LLMs), as illustrated below. Here is an example of cross-checking a simple question posed to four LLMs:

"I have been taking Yakult for the last few weeks and feel no different."

- Reply from GPT-4o Mini: "It is not uncommon to feel no immediate changes after taking probiotics such as Yakult, as their effects can vary from person to person. Probiotics work gradually to support gut health and may not produce noticeable results right away. Factors such as your overall diet, lifestyle, and individual gut microbiome can influence how you respond. It is also important to give your body some time to adjust; some people may experience benefits after several weeks or even months of consistent use. If you have specific health concerns or conditions, consulting a health-care professional may provide more personalized insights."
- Reply from Poe: "While many people report positive effects from taking Yakult, such as improved digestion and gut health due to its probiotic content, individual experiences can vary widely. Factors such as diet, overall health, and personal microbiome composition can influence how you feel after consuming probiotics. It may take time for some individuals to notice significant changes, or they might not experience any noticeable effects at all. If you are not feeling any difference, it is worth considering other aspects of your lifestyle or consulting with a health-care professional for personalized advice."
- Reply from Gemini: "Yakult is a probiotic drink that contains live bacteria. Probiotics are believed to be beneficial for gut health. However, it is important to note that the research on the benefits of probiotics is still ongoing. Some studies have shown that probiotics can help with digestive issues, such as constipation and diarrhea. However, other studies have shown no benefit. It is also important to note that not all probiotics are created equal. Different strains of bacteria have different effects on the body. Yakult contains a strain of bacteria called *Lactobacillus casei* Shirota. This strain has been shown in some studies to be beneficial for gut health. However, more research is needed to confirm these findings."
- Reply from CoPilot: "It is understandable to feel a bit disappointed if you have not noticed any difference after a few weeks of taking Yakult. It is a popular probiotic drink, and while some people experience positive changes quickly, others might not notice any immediate effects. Probiotics work by promoting the growth of beneficial bacteria in the gut, but this process can vary from person to person depending on individual microbiomes and other factors such as diet and lifestyle. It might take more time, or you might benefit from consulting with a health-care professional to explore other options or adjustments that could work better for you. Keep in mind that patience and consistency are key when it comes to probiotics."

The four responses were analyzed for consistent threads throughout. Rather than evaluating each response as a whole, the analysis focused on individual steps – assessing whether each step was logical and followed coherently from the previous one.

- All four LLM responses acknowledge that the effects of Yakult (or probiotics in general) can vary significantly from person to person.
- They all mention factors such as individual gut microbiome, diet, lifestyle, and existing health conditions as potential influences on whether or not someone experiences noticeable benefits.
- They also point out that it may take time to see results.
- All four suggest consulting a health-care professional for personalized advice if concerns persist.

While it is entirely possible that all four LLMs might each be misguided, their reliance on distinct underlying data sources helps mitigate the risk of shared errors or hallucinations. In essence, cross-referencing multiple models reduces the likelihood of misinformation. Taken together, this reflects a broader trend toward AI adoption, which will undoubtedly influence the trajectory of probiotic research.

10.2. Directions of future research

Continued research is crucial to address the current limitations in probiotic research, develop robust clinical trial methodologies, and establish clear regulatory guidelines for the production and marketing of probiotic products. Future research in the field of probiotics should focus on:

- Identifying new probiotic strains: Continued exploration of the human microbiome will lead to the discovery of novel probiotic strains with unique health benefits.
- Developing personalized probiotic therapies: Advances in genomics and metagenomics will enable the development of personalized probiotic therapies tailored to individual needs.
- Investigating the role of probiotics in preventing and treating chronic diseases: Further research is needed to investigate the potential of probiotics in preventing and treating chronic diseases, such as obesity, diabetes, and cardiovascular disease.
- Improving the quality and safety of probiotic products: Ensuring the quality and safety of probiotic products is crucial for consumer confidence and public health.
- Expanding probiotic applications beyond the gut: Potential applications of probiotics include their use in skincare products to improve skin health, reduce inflammation, and promote wound healing. In addition, research is exploring the potential of probiotics as antimicrobial agents, leveraging their ability to inhibit the growth of harmful bacteria and fungi.
- Engineered probiotic strains: Lactic acid bacteria are considered appropriate chassis organisms that can be genetically engineered for therapeutic and industrial applications.[80]

Educating the public about the appropriate use of probiotics and raising consumer awareness of the importance of selecting high-quality products are essential for ensuring the safe and effective use of these beneficial microorganisms.

11. Conclusion

Probiotics have a rich history rooted in traditional medicine and offer diverse health benefits by modulating the gut microbiome. They enhance digestive health, boost immunity, and reduce disease risks. The development of personalized probiotic therapies tailored to individual needs and microbial profiles represents the future of this field. Continued research is crucial to fully harnessing the potential of probiotics in improving human health. Amply illustrated, the paper offers the following:

- Historical significance: It acknowledges the long history of probiotic use in traditional medicine. It also acknowledges those credited with advances in science along the way.
- Mechanisms of action: It emphasizes the ability of probiotics to modulate the gut microbiome through various mechanisms, such as competitive exclusion and immune modulation. An example is provided of different strains of the same probiotic causing different results, highlighting the importance of strain specificity.
- Health benefits: Showcasing the diverse health benefits of probiotics, including improved digestive health, enhanced immunity, and good potential for reducing the risk of certain diseases.
- Personalized medicine: It underscores the importance of personalized probiotic therapies tailored to individual needs and microbial profiles, with examples illustrating when it all went wrong.
- Future directions: It emphasizes the need for future research to fully explore the potential of probiotics for improving human health, both for internal use and applied topically. The future of probiotics is also discussed in terms of regulation and standardization.

Acknowledgments

None.

Funding

None.

Conflict of interest

The author declares no conflicts of interest.

Author contributions

This is a single-authored article.

Ethics approval and consent to participate

Not applicable.

Consent for publication

Not applicable.

Availability of data

Not applicable.

Further disclosure

The paper has been uploaded to a preprint server (ScienceOpen Preprints DOI: 10.14293/PR2199.000709.v1; SO-VID: 429d7842-b571-4059-aee9-c26608c561c2)

References

1. Stahl U. Traditional fermented foods. *J Appl Bacteriol*. 1987;63(6):465-75.
2. Hill C, Guarner F, Reid G, *et al*. Expert consensus document. The international scientific association for probiotics and prebiotics consensus statement on the scope and appropriate use of the term probiotic. *Nat Rev Gastroenterol Hepatol*. 2014;11(8):506-514.

   doi: 10.1038/nrgastro.2014.66
3. Gasbarrini G, Bonvicini F, Gramenzi A. Probiotics history. *J Clin Gastroenterol*. 2016;50(Suppl 1):S116-S119.

   doi: 10.1097/MCG.0000000000000697
4. Ozen M, Dinleyici EC. The history of probiotics: The untold story. *Benef Microbes*. 2015;6(2):159-166.

   doi: 10.3920/BM2014.0103
5. Shade A, Peter H, Allison SD, *et al*. Fundamentals of microbial community resistance and resilience. *Front Microbiol*. 2012;3:417.

   doi: 10.3389/fmicb.2012.00417
6. Kamble NS, Bera S, Bhedase SA, Gaur V, Chowdhury D. Review on applied applications of microbiome on human lives. *Bacteria*. 2024;3(3):141-159.

   doi: 10.3390/bacteria3030010
7. Fierer N, Lauber CL, Zhou N, McDonald D, Costello EK, Knight R. Forensic identification using skin bacterial communities. *Proc Natl Acad Sci U S A*. 2010;107(14):6477-6481.

   doi: 10.1073/pnas.1000162107
8. Sender R, Fuchs S, Milo R. Revised estimates for the number of human and bacteria cells in the body. *PLoS Biol*. 2016;14(7):e1002533.

   doi: 10.1371/journal.pbio.1002533
9. Cryan JF, O'Riordan KJ, Cowan CSM, *et al*. The microbiota-gut-brain axis. *Physiol Rev*. 2019;99(4):1877-2013.

   doi: 10.1152/physrev.00018.2018
10. Fuller R. Probiotics in man and animals. *J Appl Bacteriol*. 1989;66(5):365-378.
11. Royal Society of Chemistry. *Lactobacillus plantarum Gram Stained CC 3.0 BYNC*. United Kingdom: Royal Society of Chemistry.

    doi: 10.1039/C9RA10446A
12. Julie6301. *Lactobacillus plantarum*. *CC 3.0 BYSA Wikimedia Commons*. Available from: https://commons.wikimedia.org/w/index.php?curid=15311964 [Last accessed on 2025 May 08].
13. Craver C, Tabery J, Illari P. *Mechanisms in Science*. United Kingdom: Cambridge University Press; 2015.
14. *Mechanisms of Probiotics. Biology Notes Online*. Available from: https://biologynotesonline.com/probiotics/?form=mg0av3#mechanisms_of_probiotics [Last accessed on 2025 May 08].
15. Hemaiswarya S, Raja R, Ravikumar R, Carvalho IS. Mechanism of action of probiotics. *Braz Arch Biol Technol*. 2013;56:113-119.

    doi: 10.1590/S1516-89132013000100015
16. Slykerman RF, Davies N, Vlckova K, *et al*. Precision psychobiotics for gut-brain axis health: Advancing the discovery pipelines to deliver mechanistic pathways and proven health efficacy. *Microb Biotechnol*. 2025;18(1):e70079.

    doi: 10.1111/1751-7915.70079
17. Perdigón G, Fuller R, Raya R. Lactic acid bacteria and their effect on the immune system. *Curr Issues Intest Microbiol*. 2001;2(1):27-42.
18. Den Besten G, Van Eunen K, Groen AK, *et al*. Short-chain fatty acids and their role in human health. *Adv Nutr*. 2014;5(1):5-17.

    doi: 10.1194/jlr.R036012
19. Petrut SM, Bragaru AM, Munteanu AE, Moldovan AD, Moldovan CA, Rusu E. Gut over mind: Exploring the powerful gut-brain Axis. *Nutrients*. 2025;17(5):842.

    doi: 10.3390/nu17050842
20. Liou MJ, Miller BM, Litvak Y, *et al*. Host cells subdivide nutrient niches into discrete biogeographical microhabitats for gut microbes. *Cell Host Microbe*. 2022;30(6):836-847.e6.

    doi: 10.1016/j.chom.2022.04.012
21. Aghamohammad S, Hafezi A, Rohani M. Probiotics as functional foods: How probiotics can alleviate the symptoms of neurological disabilities. *Biomed Pharmacother*. 2023;163:114816.

    doi: 10.1016/j.biopha.2023.114816
22. *Consumer Reports*. *The Problem with Expired Medication*. Available from: https://www.consumerreports.org/drug-

safety/the-problem-with-expired-medication [Last accessed on 2025 May 08].

23. Wilcox H, Carr C, Seney S, Reid G, Burton JP. Expired probiotics: What is really in your cabinet? *FEMS Microbes*. 2020;1(1):xtaa007.

doi: 10.1093/femsmc/xtaa007

24. Alnahas F, Yeboah P, Fliedel L, Abdin AY, Alhareth K. Expired medication: Societal, regulatory and ethical aspects of a wasted opportunity. *Int J Environ Res Public Health*. 2020;17(3):787.

doi: 10.3390/ijerph17030787

25. Han BZ, Rombouts FM, Nout MJ. A Chinese fermented soybean food. *Int J Food Microbiol*. 2001;65(1-2):1-10.

doi: 10.1016/s0168-1605(00)00523-7

26. Steinkraus K. *Handbook of Indigenous Fermented Foods, Revised and Expanded*. United States: CRC Press; 2018.

27. Metchnikoff E. *Immunity in Infective Diseases*. Oxford: University Press; 1907.

28. Anukam KC, Reid G. Probiotics: 100 years (1907-007) after Elie Metchnikoff's observation. In: *Communicating Current Research and Educational Topics and Trends in Applied Microbiology*. Vol. 1. Mumbai: Formatex; 2007. p. 466-474.

29. Gordon S. Elie Metchnikoff, the man and the myth. *J Innate Immun*. 2016;8(3):223-227.

doi: 10.1159/000443331

30. Leeuwenhoek. Available from: https://commons.wikimedia.org/wiki/File:Anthonie_van_Leeuwenhoek_(1632-1723)._Natuurkundige_te_Delft_Rijksmuseum_SK-A-957.jpeg [Last accessed on 2025 May 21].

31. Pasteur. Available from: http://resource.nlm.nih.gov/101425953 [Last accessed on 2025 May 21].

32. Gram. Available from: https://commons.wikimedia.org/wiki/File:hans_christian_gram_portrait_by_hansen_weller.jpg [Last accessed on 2025 May 21].

33. Metchnikoff. Available from: https://www.loc.gov/pictures/item/2014694764 [Last accessed on 2025 May 21].

34. Fleming. Available from: https://www.nobelprize.org/prizes/medicine/1945/fleming/photo-gallery [Last accessed on 2025 May 21].

35. Woese. Available from: https://en.wikipedia.org/wiki/ file: carl_woese.jpg [Last accessed on 2025 May 21].

36. Reid G. *Probiotics: A Story About Hope*. Available from: https://www.amazon.com.au [Last accessed on 2025 May 21].

37. Sanders ME, Merenstein DJ, Reid G, Gibson GR, Rastall RA. Probiotics and prebiotics in intestinal health and disease: From biology to the clinic. *Nat Rev Gastroenterol Hepatol*. 2019;16(10):605-616.

doi: 10.1038/s41575-019-0173-3

38. Guarner F. *The Enteric Microbiota*. San Rafael: Morgan and Claypool Publishers; 2012.

39. Morelli L. Probiotics: Definition and Taxonomy 10 Years after the FAO/WHO Guidelines. In: *Probiotic Bacteria and Their Effect on Human Health and Well-Being*. Basel: Karger Medical and Scientific Publishers; 2013. p. 1-8.

40. Human Microbiome Project Consortium. Structure, function and diversity of the healthy human microbiome. *Nature*. 2012;486(7402):207-214.

doi: 10.1038/nature11234

41. Goodrich JK, Davenport ER, Beaumont M, *et al*. Genetic determinants of the gut microbiome in UK twins. *Cell Host Microbe*. 2016;19(5):731-743.

doi: 10.1016/j.chom.2016.04.017

42. Sazawal S, Hiremath G, Dhingra U, Malik P, Deb S, Black RE. Efficacy of probiotics in prevention of acute diarrhoea: A meta-analysis of masked, randomised, placebo-controlled trials. *Lancet Infect Dis*. 2006;6(6):374-382.

doi: 10.1016/S1473-3099(06)70495-9

43. Allen SJ, Wareham K, Wang D, *et al*. Lactobacilli and bifidobacteria in the prevention of antibiotic-associated diarrhoea and *Clostridium difficile* diarrhoea in older inpatients (PLACIDE): A randomised, double-blind, placebo-controlled, multicentre trial. Lancet. 2013;382(9900):1249-1257.

44. Szajewska H, Konarska Z, Kołodziej M. Probiotic bacterial and fungal strains: Claims with evidence. *Dig Dis*. 2016;34(3):251-259.

doi: 10.1159/000443359

45. Loftus EV Jr., Sandborn WJ. Epidemiology of inflammatory bowel disease. *Gastroenterol Clin North Am*. 2002;31(1):1-20.

doi: 10.1016/s0889-8553(01)00002-4

46. Gupta V, Garg R. Probiotics. *Indian J Med Microbiol*. 2009;27(3):202-209.

doi: 10.4103/0255-0857.53201

47. Collado MC, Isolauri E, Laitinen K, Salminen S. Distinct composition of gut microbiota during pregnancy in overweight and normal-weight women. *Am J Clin Nutr*. 2008;88(4):894-899.

doi: 10.1093/ajcn/88.4.894

48. Shen YL, Zhang LQ, Yang Y, Yin BC, Ye BC, Zhou Y. Advances in the role and mechanism of lactic acid bacteria in treating obesity. *Food Bioeng*. 2022;1(1):101-115.

doi: 10.1002/fbe2.12002

49. Ducrotté P, Sawant P, Jayanthi V. Clinical trial: *Lactobacillus plantarum* 299v (DSM 9843) improves symptoms of irritable bowel syndrome. *World J Gastroenterol*. 2012;18(30):4012-4018.

50. Im E, Pothoulakis C. Recent advances in *Saccharomyces*

boulardii research. *Gastroenterol Clin Biol*. 2010;34(Suppl 1):S62-S70.

doi: 10.1016/S0399-8320(10)70023-3

51. Horvat IB, Gobin I, Kresović A, Hauser G. How can probiotic improve irritable bowel syndrome symptoms? *World J Gastrointest Surg*. 2021;13(9):923-931.

doi: 10.4240/wjgs.v13.i9.923

52. Khailova L, Baird CH, Rush AA, Barnes C, Wischmeyer PE. *Lactobacillus rhamnosus* GG treatment improves intestinal permeability and modulates inflammatory response and homeostasis of spleen and colon in experimental model of *Pseudomonas aeruginosa* pneumonia. *Clin Nutr*. 2017;36(6):1549-1557.

doi: 10.1016/j.clnu.2016.09.025

53. Available from: https://www.medicalnewstoday.com/articles/microbiome-testing#considerations [Last accessed on 2025 May 21].

54. Available from: https://www.choice.com.au/health-and-body/conditions/general-health/articles/diy-gut-flora-testing-kits [Last accessed on 2025 May 21].

55. McFarland LV, Evans CT, Goldstein EJ. Strain-specificity and disease-specificity of probiotic efficacy: A systematic review and meta-analysis. *Front Med* (*Lausanne*). 2018;5:124.

doi: 10.3389/fmed.2018.00124

56. Douillard FP, Ribbera A, Kant R, *et al*. Comparative genomic and functional analysis of 100 *Lactobacillus rhamnosus* strains and their comparison with strain GG. *PLoS Genet*. 2013;9(8):e1003683.

doi: 10.1371/journal.pgen.1003683

57. LastMojojomo. *How Probiotics Destroyed My Health (Long STORY/Rant)*; 2020. Available https://www.reddit.com/r/ibs/comments/jpkol3/how_probiotics_destroyed_my_health_long_storyrant [Last accessed on 2025 May 21].

58. Gueniche A, Philippe D, Bastien P, *et al*. Randomised double-blind placebo-controlled study of the effect of *Lactobacillus paracasei* NCC 2461 on skin reactivity. *Benef Microbes*. 2014;5(2):137-145.

doi: 10.3920/BM2013.0001

59. Sutema IAMP, Latarissa IR, Widowati IGAR, Sartika CR. Topical probiotics in acne vulgaris treatment: A systematic review and meta-analysis. *J Dermatol Treat*. 2023;34(1):2208123.

60. Levin J, Momin A. How robust is the evidence for probiotics in the management of rosacea? *Dermatol Ther*. 2010;23(6):680-689.

61. Valdez JC, Ramos AN, Fernández D, *et al*. Probiotics and their potential use in wound treatment. In: *Probiotics: Immunobiotics and Immunogenics*. United States: CRC Press; 2013:298-335.

62. Nobile V, Hajat C, Cestone E, Cascella F, Santus G. Skin Antiaging and Skin Health Benefits of Probiotics Intake Combined with Topical Ectoin and Sodium Hyaluronate: A Randomized, Double-Blind, Placebo-Controlled Trial. Available from: https://www.mdpi.com/2079-9284/12/2/34 [Last accessed on 2025 May 21].

63. Falagas ME, Betsi GI, Athanasiou S. Probiotics for the treatment of women with bacterial vaginosis. *Clin Microbiol Infect*. 2007;13(7):657-664.

doi: 10.1111/j.1469-0691.2007.01688.x

64. Pendharkar S, Brandsborg E, Hammarström L, Marcotte H, Larsson PG. Vaginal colonisation by probiotic lactobacilli and clinical outcome in women conventionally treated for bacterial vaginosis and yeast infection. *BMC Infect Dis*. 2015;15:255.

doi: 10.1186/s12879-015-0971-3

65. Chatterjee A, Bhattacharya H, Kandwal A. Probiotics in periodontal health and disease. *J Indian Soc Periodontol*. 2011;15(1):23-28.

doi: 10.4103/0972-124X.82260

66. Chinnappa A, Konde H, Konde S, Raj S, Beena JP. Probiotics for future caries control: A short-term clinical study. *Indian J Dent Res*. 2013;24(5):547-549.

doi: 10.4103/0970-9290.123363

67. Karbalaei M, Keikha M, Kobyliak NM, *et al*. Alleviation of halitosis by use of probiotics and their protective mechanisms in the oral cavity. *New Microbes New Infect*. 2021;42:100887.

doi: 10.1016/j.nmni.2021.100887

68. *CN103520216A - Probiotic Human Injection*. Available from: https://patents.google.com/patent/CN103520216A/en [Last accessed on 2025 May 08].

69. Monnerat N, Lambert AC, Genné D. What happens after an accidental intravenous probiotic injection? *Clin Microbiol Infect*. 2020;26(4):517-518.

doi: 10.1016/j.cmi.2019.11.027

70. Morishita M, Kida M, Motomura T, *et al*. Elucidation of the tissue distribution and host immunostimulatory activity of exogenously administered probiotic-derived extracellular vesicles for immunoadjuvant. *Mol Pharm*. 2023;20(12):6104-6113.

doi: 10.1021/acs.molpharmaceut.3c00460

71. *Extracellular Vesicles: An Introduction*. Abcam. Available from: https://www.abcam.cn/primary-antibodies/extracellular-vesicles-an-introduction [Last accessed on 2025 May 08].

72. Yáñez-Mó M, Siljander PR, Andreu Z, *et al*. Biological properties of extracellular vesicles and their physiological functions. *J Extracell Vesicles*. 2015;4(1):27066.

doi: 10.3402/jev.v4.27066

73. Song Y, Zhang C, Zhang J, *et al*. Localized injection of miRNA-21-enriched extracellular vesicles effectively restores cardiac function after myocardial infarction. *Theranostics*. 2019;9(8):2346-2360.

doi: 10.7150/thno.29945

74. Jokicevic K, Kiekens S, Byl E, *et al*. Probiotic nasal spray development by spray drying. *Eur J Pharm Biopharm*. 2021;159:211-220.

doi: 10.1016/j.ejpb.2020.11.008

75. Tran TT, Cheow WS, Pu S, Park JW, Hadinoto K. Dry powder inhaler formulation of *Lactobacillus rhamnosus* GG targeting *Pseudomonas aeruginosa* infection in bronchiectasis maintenance therapy. *Pharmaceutics*. 2024;16(8):980.

doi: 10.3390/pharmaceutics16080980

76. Gazerani P, Papetti L, Dalkara T, *et al*. The brain, the eating plate, and the gut microbiome: Partners in migraine pathogenesis. *Nutrients*. 2024;16(14):2222.

doi: 10.3390/nu16142222

77. Snydman DR. The safety of probiotics. *Clin Infect Dis*. 2008;46(Suppl 2):S104-S111, discussion S144-S151.

78. Vogel L, Van den Abeele E. *Better Regulation: A Critical Assessment*. Belgium: ETUI; 2010.

79. Wong CB, Odamaki T, Xiao JZ. Beneficial effects of *Bifidobacterium longum* subsp. longum BB536 on human health: Modulation of gut microbiome as the principal action. *J Funct Foods*. 2019;54:506-519.

doi: 10.1016/j.jff.2019.02.002

80. Mugwanda K, Hamese S, Van Zyl WF, *et al*. Recent advances in genetic tools for engineering probiotic lactic acid bacteria. *Biosci Rep*. 2023;43(1):BSR202112.

doi: 10.1042/BSR20211299

ACCSCIENCE PUBLISHING

Microbes & Immunity

REVIEW ARTICLE

Lung development, health, and diseases

Feranmi Emmanuel Obe[1]*, Isaac Olamide Babalola[2], Victor Abiodun Adebiyi[2], Ayomide Oreoluwa Adetoro[3], Florence Inioluwa Omotoso[2], and Oluwafemi Rachel Alamu[2]

[1]Department of Biology, College of Arts and Sciences, University of Texas at Tyler, Tyler, Texas, United States of America

[2]Department of Medical Laboratory Science, Faculty of Basic Medical Sciences, Ladoke Akintola University of Technology, Ogbomoso, Nigeria

[3]Department of Nursing Science, Faculty of Nursing, Ladoke Akintola University of Technology, Ogbomoso, Nigeria

(This article belongs to the *Special Issue: Immune Responses to Pulmonary Infections*)

Abstract

The lungs emerge from the foregut during the embryonic stage, and as they mature, they go through additional morphological and functional changes that extend into the postnatal stage of development. Each developmental stage of the lung is tightly regulated by specific signaling pathways. Nkx2.1 signaling, which is essential for lung specification, is improved by Wnt/β-catenin signaling but necessitates active bone morphogenic protein signaling. Branching morphogenesis of the lungs requires fibroblast growth factor, while vascular endothelial growth factor signaling promotes endothelial cell survival and capillary development. Disruption at any of these developmental stages can result in congenital lung disorders. Although the lungs are quiescent in adulthood, they retain the capacity for regeneration in response to injury caused by infectious and non-infectious agents. Essentially, the lung's microbiota plays a role in maintaining lung health and disease. Treatment with probiotics has been established in many infectious lung diseases; however, further research is necessary to fully establish their therapeutic potential in treating these conditions.

Keywords: Development; Embryogenesis; Lungs; Regeneration; Signaling

***Corresponding authors:**
Feranmi Emmanuel Obe
(obeferanmi1@gmail.com)

Citation: Obe FE, Babalola IO, Adebiyi VA, Adetoro AO, Omotoso FI, Alamu OR. Lung development, health, and diseases. *Microbes & Immunity*. 2025;2(3):47-59.
doi: 10.36922/mi.7719

Received: December 16, 2024

1st revised: March 18, 2025

2nd revised: April 10, 2025

3rd revised: April 21, 2025

Accepted: May 6, 2025

Published online: June 12, 2025

1. Introduction

The development of the lungs is a complex and coordinated process that spans from embryogenesis to postnatal maturation. The process involves cellular differentiation and tissue morphogenesis. Lung development begins at approximately 3 – 4 weeks of gestation and evolves through six major developmental stages characterized by structural and functional changes necessary for effective gas exchange. These stages include the embryonic stage, pseudoglandular stage, canalicular stage, saccular stage, alveolar stage, which begins just before birth and continues into the first few years of life, and the microvascular stage.[1] Each developmental stage is regulated by signaling that drives the functional and structural changes from embryogenesis to postnatal maturation.

According to the prevailing historical theory, the lung originated as an aquatic organ that resembles a swim bladder.[2] Due to the presence of epithelial cells lining the swim bladder that contains surfactant proteins, lipids, and lamellar bodies – organelles that transport surfactant to the cell surface – sonic hedgehog expression in the endoderm is essential for swim bladder development in zebrafish. It is also known that the development of the heart's inflow and outflow tracts is regulated by signals from the pulmonary and pharyngeal endoderm. This implies that the cardiovascular system and lungs may have coevolved.[3]

The developmental stages are regulated by signaling pathways that drive the functional and structural changes from embryogenesis to postnatal maturation. The formation of a localized expression of Nkx2-1 (also known as Titf1) in the ventral wall of the anterior foregut marks the initiation of lung development. SRY-box transcription factor 2 (Sox2), wingless-type MMTC integration site family member 2 (Wnt2), and Wnt2b are all involved in this process, which lasts until the lungs reach full maturity.[4]

This review aims to provide clear insights into the interplay of molecular mechanisms involved in lung maturation and respiratory adaptation both *in utero* and after birth. In addition, it captures the genetic and epigenetic influences on lung development, as well as the lung's regenerative potential following injury caused by infectious and non-infectious agents.

2. Stages of lung development in human

Lung development spans three major periods of life, namely the embryonic, fetal, and postnatal stages. Lung organogenesis begins during the embryonic stage, followed by the fetal period, which encompasses the pseudoglandular, canalicular, and saccular stages. The postnatal period includes alveolarization and microvascular maturation. Figure 1 highlights these developmental stages, which overlap as growth advances from proximal to peripheral regions.[5] A comprehensive summary of the lung developmental process is shown in Table 1.

2.1. Key signaling pathways involved in lung development

The developmental stages of the lung are tightly regulated. This section of the review explores central signaling pathways eliciting the initiation of lung specification from the ventral foregut through to lung vascularization. summary of the signaling pathways active at each stage of lung development is shown in Table 2.

The earliest known stage in respiratory system development, encompassing the trachea and lungs, is marked by the localized expression of Nkx2-1 in the ventral wall of the anterior foregut. Sox2 expression is most prominent dorsally in the prospective esophagus, whereas Nkx2-1 expression, which designates the prospective trachea, is most prominent ventrally.[16] This spatial patterning is regulated by signals from the surrounding mesenchyme, such as fibroblast growth factors, Wnts, bone morphogenetic proteins, and their antagonist, noggin. Deficiencies in any of these genes can result in foregut separation failure and aberrant mesenchymal and epithelial differentiation.[17] Wnt signaling, in particular, plays an important role at this stage. The loss of Nkx2-1 expression, expansion of Sox2 expression, and failure of foregut separation occur when Wnt2 and Wnt2b, expressed in the mesoderm surrounding the anterior foregut, are coupled with beta-catenin in the endoderm.[18]

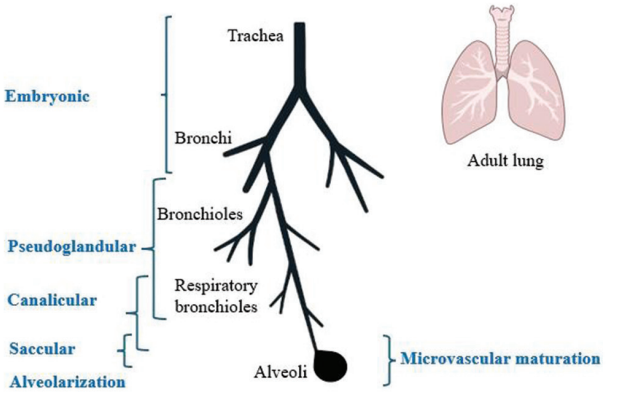

Figure 1. Stages of lung development. This diagram illustrates how the airway tree develops step-by-step from the trachea to the alveoli during the important developmental phases of embryonic, pseudoglandular, canalicular, saccular, and alveolarization. To ensure complete respiratory function in the adult lung, microvascular maturation continues after birth. Copyright © The Author(s) 2017.[5]

2.2. Transition from embryonic to postnatal development: First breath and respiratory adaptations

Surfactants are a mixture of lipids and proteins that are released during labor. Alveolar stretch caused by the onset of breathing further increases the release of surfactants.[19] The release of surfactants into the fetal airways at the initiation of labor induces significant physiological changes in the lungs. Concurrent secretion increases surfactant content in the fetal lung fluid.[20] This secretion is primarily mediated by increased catecholamine levels, which activate beta-adrenergic receptors. In addition, purinergic agonists such as ATP may influence this pre-delivery secretion. After birth, the initiation of ventilation causes type II alveolar cells to stretch and deform within the alveoli, which results in more secretion.[21] Type II

Table 1. Summary of human lung development from the embryonic stage to adulthood

Stage	Duration	Characteristics
Embryonic	4 – 7 weeks of gestation	Organogenesis begins with the formation of the lung anlage, main airways, and pleura.
Pseudoglandular	5 – 17 weeks of gestation	Formation of large respiratory parenchyma, development of bronchial trees, formation of early acinar structures.
Canalicular	16 – 26 weeks of gestation	Airway branching is completed, surfactant production begins, and the initial appearance of the air-blood barrier.
Saccular (terminal sac)	4 – 38 weeks of gestation	Characterized by the expansion of future airspaces, followed by differentiation and preparation for postnatal breathing.
Alveolarization (first phase)	36 weeks of gestation – 3 years	Immature alveoli emerge, and the septa contain double-layered capillary networks.
Continued alveolarization	2 years–17 – 21 years	Alveolar maturation and the formation of single-layered capillary networks in the alveolar septa.
Microvascular maturation	Term–3 – 21 years	Septa remodeling: the capillary beds are transformed into single-layered structures.

Note: Adapted from Schittny[5]

Table 2. Development stages and associated signaling

Development stage	Key signal and factors	References
Lung specification	Nkx2.1 expression in the ventral foregut endoderm triggers this process. Wnt/β-catenin signaling enhances Nkx2.1, but requires active BMP signaling.	4,6
Lung bud initiation	Retinoic acid signaling is critical to lung budding. Deficiency of this leads to hypoplasia. RAR-γ mutations affect alveolar development.	7,8
Airway branching	Epithelial branching is important for airway branching, and it is induced by peripheral lung mesenchyme.	9
Branching morphogenesis	FGF signaling (FGF10, FGFR2b) regulates branching morphogenesis; FGF10 mutations or FGFR2b inactivation prevents branching completely. FGF10 deficiency or increased Sprouty 2 expression causes tiny, poorly branching lungs.	10-12
Histone modifications	The balance between HAT and HDAC is essential for proximal cell growth and branching.	13
Vascular development	VEGF signaling supports endothelial survival and capillary formation, critical for alveolar development. Inhibiting VEGF signaling impairs pulmonary endothelial survival and inhibits postnatal alveolarization.	11,14,15

Abbreviations: BMP: Bone morphogenetic protein; FGF: Fibroblast growth factor; HAT: Histone acetyltransferases; HDAC: Histone deacetylase; SOX2: SRY-box transcription factor 2; RAR: Retinoic acid receptor; VEGF; Vascular endothelial growth factor.

alveolar cells, also referred to as type II pneumocytes, play an essential role in maintaining lung function. They are responsible for producing and releasing surfactant to lower surface tension within the alveoli, thereby preventing collapse. Moreover, these cells also act as progenitors for alveolar epithelial regeneration following injury.[3] As adult tissue stem cells, type II alveolar cells also contribute to the maintenance, repair, and regeneration of lung tissue to support pulmonary homeostasis.[22]

Alveolar type II cells play a crucial role in maintaining the unique microenvironment of the alveoli. They secrete pulmonary surfactants and collections such as surfactant protein A and surfactant protein D, along with a range of substances that possess anti-inflammatory and anti-microbial properties, including lysozyme, β-defensin 2, secretory leukocyte proteinase inhibitor, and lipocalin 2.[20] These polar molecules help reduce alveolar surface tension, thereby lowering pressure within the lungs[23] and promoting gas exchange.

Also, the clearance of fetal lung fluid commences before birth and is accelerated by labor, typically completed within 2 h following delivery.[24] Following birth, newborns establish respiratory patterns that are more regular than *in utero*. Both term and preterm babies will initiate spontaneous breathing unless affected by severe hypoxemia, which suppresses breathing.[25] Gas exchange stabilizes in most babies within 2 min after vaginal delivery, with an improved heart rate serving as the strongest clinical indicator of effective breathing.[26] However, preterm babies may experience delays and often require assistance through mechanical ventilation.

2.3. Epigenetic regulation of lung development from early lung development to advanced age

Epigenetic mechanisms such as DNA methylation, histone modifications, and non-coding RNA activity regulate extracellular processes that are essential for lung development and remodeling. These processes are important in chronic remodeling disorders, including

idiopathic pulmonary fibrosis (IPF), chronic obstructive pulmonary disease (COPD), bronchopulmonary dysplasia (BPD), and pulmonary hypertension. They are impacted by environmental factors like oxidative stress, infections, and aging.[27]

Lung myofibroblast differentiation has been demonstrated to be altered by histone deacetylases (HDACs).[28] A study involving profibrotic fibroblast phenotypes, derived from IPF patient fibroblasts and a murine model of lung fibrosis, showed that epigenetic modification of the Fas promoter through histone acetylation is associated with altered expression of HDAC2 and HDAC4. Moreover, profibrotic fibroblasts treated with HDAC inhibitors had higher expression of Fas and were more susceptible to Fas-mediated apoptosis.[29] HDACs are members of a broad family of multiprotein complexes that regulate various biological processes.[30] The Fas promoter modification indicates a potential way to identify or modify the regulatory elements that govern Fas gene expression, which produces a cell surface protein involved in apoptotic signaling.[31] In addition, oxidative stress induced by factors such as cigarette smoke, environmental pollutants, and aging can alter chromatin folding and gene expression. The disruption which involves HDACs and histone acetyltransferases (HATs) contributes to inflammation, impaired autophagy, and cellular senescence, especially in COPD.[32]

The acetylation of lysine residues, especially those located in the N-terminal of core histones, is controlled by two opposing enzyme families, such as HDACs and HATs.[33] HDACs are essential for host defense by promoting pro-inflammatory responses. However, certain HDACs can also reprogram macrophages and monocytes to exhibit immunosuppressive characteristics.[33] Histone acetylation affects chromatin structure and, consequently, gene expression. In addition to histones, certain lysine residues in non-histone proteins can also undergo acetylation, which affects the stability and biological roles of these proteins.[34] Monocytes must maintain a proper balance in acetylation dynamics to respond to numerous physiological and pathological stimuli. Notably, aberrant expression or activity of specific HDACs has been associated with various chronic inflammatory illnesses, including autoimmune disorders, infections, and cancer.[30]

3. Lung developmental disorders

Congenital lung disorders are the outcome of aberrant embryonic development, often caused by disturbed signaling pathways or genetic factors. These deformities include a variety of anatomical abnormalities affecting the lungs and respiratory tract.[35] Common congenital lung disorders include congenital pulmonary airway malformation (CPAM), bronchopulmonary sequestration (BPS), bronchogenic cysts, bronchial atresia, congenital lobar emphysema (CLE), and congenital tracheal obstruction.

3.1. CPAM

CPAM is a developmental anomaly of the lower respiratory tract.[36] Formerly known as congenital cystic adenomatoid malformation, CPAM is a benign lung disorder marked by the presence of cystic lesions. It is the most prevalent cystic lung lesion detected prenatally, typically between 18 and 20 weeks of gestation. It accounts for about 95% of congenital cystic lung diseases. Since the advent of prenatal ultrasound, previously unidentified lesions are now more frequently identified. Hence, it is likely that the actual prevalence has been underestimated.[37] The treatment of asymptomatic CPAMs remains under discussion, whereas the management of symptomatic CPAMs is generally well-established.[36]

3.2. BPS

BPS is an uncommon condition characterized by non-functioning lung tissue that is detached from the main bronchial tree and may obtain blood supply from the systemic circulation. Such aberrant tissue frequently leads to recurrent respiratory infections and typically requires surgical removal.[38,39] The intralobar type is defined and distinguished by the aberrant lung tissue located within the normal lung and sharing its visceral pleura, whereas the extralobar type possesses its own distinct pleural covering.[40] Several percutaneous prenatal intervention procedures have been found to improve perinatal outcomes for large lesions linked to hydrops. These consist of intratumor sclerosant injections, thoracocentesis, thoraco-amniotic shunt insertion, and combined therapeutic approaches. Although hydropic fetuses are rare and evidence of the condition remains limited, it is evident that intrusive therapy can provide significant benefits.[41]

3.3. Bronchogenic cysts

Bronchogenic cysts are congenital abnormalities originating from the tracheobronchial tree and foregut, best known as intrapulmonary bronchogenic cysts. These rare cystic anomalies of the respiratory system typically develop early in gestation within the mediastinum, while later in gestation, they are more likely to arise in the thoracic cavity. Nevertheless, they may originate anywhere along the foregut.[42] The identification of these cysts can be difficult due to their diverse clinical and radiologic characteristics, especially in areas where hydatid disease is prevalent. Despite complications like infection may occur, endoscopic drainage has been investigated as

both a diagnostic and potentially therapeutic technique. Nonetheless, surgical excision remains the established treatment, offering symptomatic relief and enabling conclusive diagnosis through pathological testing.[43]

3.4. CLE

CLE is a rare developmental lung disorder marked by hyperinflation of one or more lung lobes. This compresses the surrounding lung tissue, potentially causing respiratory complications. In severe conditions, surgical removal of the hyperinflated lobe may be required.[44] CLE develops during lung development, with parenchymal deformities possibly resulting from abnormalities occurring as early as the 3rd week of gestation when the respiratory system starts to mature. Alternative terms for CLE include congenital lobar overinflation, congenital big hyperlucent lobe, and congenital alveolar overdistension.[45] Approximately half of affected patients experience symptoms within the first 6 months of life, with nearly 50% exhibiting symptoms at birth. Overinflation of the affected lobe results in compromised perfusion and ventilation. As overinflation worsens, compression of adjacent organs and lung tissue further impairs ventilation and perfusion in these regions, potentially leading to progressive respiratory failure. Clinical symptoms include wheezing, feeding difficulties, cyanosis, and chest retractions. In infancy, frequent respiratory tract infections, wheezing, and a persistent cough are also commonly observed.[44]

3.5. Congenital tracheal obstruction

Congenital tracheal lesions are rare but important causes of morbidity in newborns and children. Their management is therefore not centralized, and clinical experience remains limited.[46] The juvenile diameter of the pediatric trachea makes it vulnerable to occlusion, whether from congenital anomalies or surgical interventions. It takes a high degree of suspicion to diagnose a congenital tracheal obstructive abnormality, particularly in newborns and toddlers presenting with respiratory distress and retractions.[47]

4. Mechanism of lung regeneration

Tissues exhibit varying capacities for regeneration in response to injury. Some, such as the skin and gut, undergo continuous turnover, while others, including the heart and brain, possess low regenerative capacity. Positioned between these extremes are tissues, such as the lung, liver, and pancreas, that are quiescent in adults but can undergo regeneration following injury.[48] There are several studies that have documented the regenerative potential of the lung using experimental models. An overview of available models used in lung regeneration research is shown in Figure 2.

Human-induced pluripotent stem cells (iPSCs) can be differentiated into key lung epithelial cell types such as alveolar type I and II cells, basal cells, and airway secretory cells, which are required for lung function and barrier integrity. Figure 3 depicts a proposed pathway for the differentiation of proximal and distal epithelial lineages in the lung after activation of human iPSC-derived airway epithelium through Wnt signaling.

4.1. Infectious injury

The COVID-19 pandemic has emphasized the negative impact of infectious injuries on the respiratory system.[50] Infectious diseases that affect the lungs can cause cellular damage, resulting in increased permeability and susceptibility to secondary infections. While the lungs remain quiescent during homeostasis, infections such as

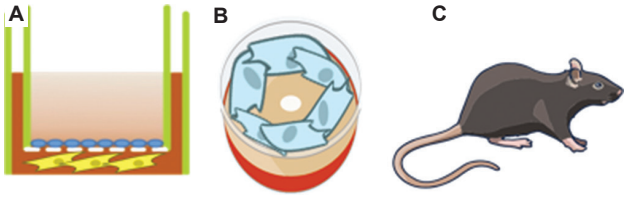

Figure 2. Available models for lung regeneration. Image created with NIH BioArt. (A) Two-dimensional model, (B) Three-dimensional model, (C) Animal model.

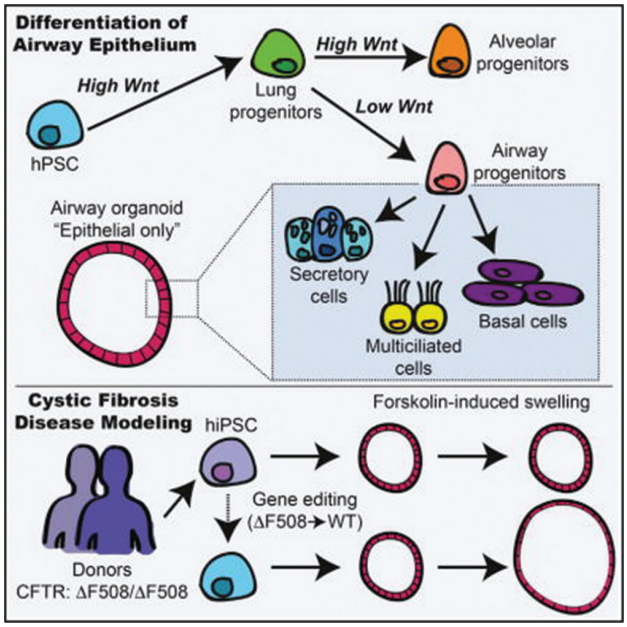

Figure 3. Wnt signaling directs human induced pluripotent stem cell (hiPSC) differentiation into proximal (airway) and distal (alveolar) lung lineages. The lower panel models cystic fibrosis using gene-edited hiPSCs to restore cystic fibrosis transmembrane conductance regulator (CFTR) function. This holds great promise for precision medicine, drug screening, disease modeling, and the treatment of cystic fibrosis.[49]
Abbreviations: hPSC: Human pluripotent stem cell; WT: Wild-type.

influenza result in the loss of epithelial cells. This infection triggers the activation of many progenitor cells related to a particular compartment of the lung. In particular, alveolar type 2 cells respond to Wnt signaling and begin to grow rapidly during the first 2 – 3 weeks following infection,[3,51] contributing to the restoration of alveolar function.

4.2. Non-infectious injury

Lung injury can also be caused by chemicals such as naphthalene and polidocanol, as well as gases like sulfur dioxide. Special pollution-resistant Clara-like epithelial (CE) stem cells have been demonstrated to survive in the terminal bronchioles following naphthalene-induced damage that impairs the normal progenitor (Clara) cells. The study concluded that due to their resilience to pollutants and their role in regenerating and renewing the terminal bronchiolar epithelium, CE cells constitute a crucial stem cell population for lung repair.[52]

5. Placenta-gut-lung triad

The placenta-gut-lung triad highlights the overlapping developmental and functional relationships among these organs. Lung morphogenesis is directly impacted by the placenta through its regulation of immunological and hormonal signals, as well as its provision of oxygen and nutrients.

The foregut is the common embryonic organ that gives rise to both the lung and the gut. To generate the two initial lung buds, the foregut endoderm specifically evaginates and extends into the surrounding mesenchyme.[53] As the interface between mother and fetus, the placenta facilitates the exchange of nutrients and is necessary to preserve a healthy intrauterine environment. Through the lung-gut axis, the gut, which houses diverse microbiota, plays a modulatory role in lung immunity. Figure 4 provides a schematic description of the placenta-gut-lung triad.

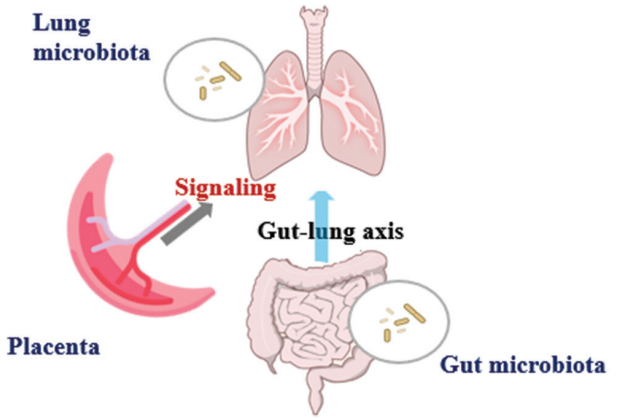

Figure 4. Placenta-gut-lung triad. This illustration represents the hypothetical interplay among the placenta, gut, and lung. Placental signaling promotes early lung development and initiates microbial priming. Postnatally, the gut–lung axis facilitates bidirectional immune and microbial communication. Together, this triad supports the coordinated maturation of mucosal immunity. Image created with NIH BioArt.

6. Lung microbiota in health and diseases

The term microbiota first appeared in the early 1900s, when it was discovered that a vast number of microorganisms, such as bacteria, yeasts, and viruses, cohabit in diverse parts of the human body. In addition, the human microbiota, popularly known as "the hidden organ," contributes about 150 times more genetic information than the entire human genome.[54] The United States National Institutes of Health launched the Human Microbiome Project (HMP) in 2007, which catalyzed a surge in research on the human microbiome. The primary purpose of the HMP was to discover and characterize microbiomes at critical locations across the human body.[55] This review focuses specifically on the lungs.

According to a 16S rRNA sequencing study, the healthy lung microbiota at the family level is dominated by Firmicutes, Bacteroidetes, Proteobacteria, Fusobacteria, and Actinobacteria, while at the Operational Taxonomic Unit level, *Prevotella*, *Veillonella*, and *Streptococcus* species are most prominent.[56]

Changes in lung microbiota have been implicated in chronic lung diseases, such as asthma and COPD. In fact, the beneficial lung bacteria may also enhance the efficacy of radiotherapy by reducing radiation-induced damage.

The organs in the respiratory system are in charge of absorbing oxygen and releasing carbon dioxide. The upper and lower respiratory tracts make up the two functioning sections of the respiratory system. The lungs facilitate the transport of oxygen from inhaled air into the bloodstream and the removal of carbon dioxide from the blood into the air.[57] Given the lung's extensive surface area and continuous exposure to the external environment through breathing, they are constantly exposed to foreign substances. However, it is surprising that despite this exposure and the volume of air inhaled daily, inflammatory responses within the lungs are relatively rare.

6.1. Lung microbiota in maintaining homeostasis

A state of immunological tolerance is established and maintained by the lung microbiota, which stops superfluous and damages inflammatory responses to minor stimuli.

Microbial compounds derived from the lung microbiota are detected by pattern recognition receptors in the lung, which promote the differentiation of naive T

cells. The differentiation of T helper (Th) cells into two subsets, Th1 and Th2, each producing unique cytokines and triggering unique immune responses, is referred to as polarization. Th2 cells predominate in the immune system before birth. Following birth, naive T lymphocytes in the lungs undergo a polarization shift from a Th2 to a Th1 phenotype, which helps prevent allergic disorders and newborn asthma.[58]

The polarization of T cells is largely determined by cytokines. The presence of interleukin (IL)-12 and/or interferon γ (IFN-γ) promotes polarization toward Th1 cytokine production, whereas IL-4 promotes polarization toward Th2 cytokine secretion.

Throughout the first 2 weeks of life, the bacterial phyla Gammaproteobacteria and Firmicutes give way to Bacteroidetes in the lungs. These microbiome alterations are associated with programmed death ligand 1 (PD-L1)-dependent growth of Helios-negative regulatory T cells (Tregs) in the lungs. Inhibition of PD-L1 or loss of microbiota leads to a heightened inflammatory response to allergens persisting into adulthood.[59]

For instance, amphiregulin produced by Tregs protects lung tissue after inflammation caused by viruses.[54] Loss of C-C motif chemokine receptor 7 affects Treg homeostasis and trafficking within the lungs, which further impacts wound healing in pulmonary fibrosis.[55] Furthermore, CD73-dependent adenosine synthesis by Tregs contributes to the recovery from acute lung injury.[56] Tregs also aid in limiting damage by lowering allergic airway inflammation and disrupting the epithelial barrier in house dust mite-derived protease-induced allergy diseases.

6.2. Lung microbiota in diseases

Certain illnesses may feature disturbances in the balance of lung microbiota. This includes, but is not limited to, asthmatic conditions, COPD, IPF, cystic fibrosis (CF), COVID-19, and influenza.

6.2.1. Asthma

Asthma is a chronic, complex condition impacted by environmental factors such as allergens and air pollution, as well as hereditary factors. It is more prevalent in industrialized nations, where the diversity and composition of the lung microbiota are influenced by living conditions, which in turn greatly influences the disease onset. Studies have demonstrated that asthma patients exhibit different lung microbiota than healthy individuals, with a lower prevalence of Bacteroidetes and a higher prevalence of Proteobacteria.[60,61] As a result, the development and course of asthma are heavily dependent on the composition of the lung microbiota and its interaction with the host.

In recent years, probiotics have shown promise in the treatment of asthma. Studies employing organisms from the genera *Bifidobacterium* and *Lactobacillus* have shown promising anti-inflammatory properties, along with reductions in mucus production and airway hyperresponsiveness.[62]

6.2.2. COPD

COPD is an obstructive lung condition characterized by inadequate airflow. Research has shown that, in contrast to asthma patients who exhibit notable alterations in their lung microbiota even in the early stages of the illness, patients with mild-to-moderate COPD possess lung microbiota very similar to that of healthy individuals.[63] Alterations in lung microbiota become evident only in advanced stages of COPD, whereas *Actinomycetes* species are more common in mild-to-moderate COPD. In more severe cases, the microbial shift found in asthma patients is characterized by a decrease in Bacteroidetes and an increase in Proteobacteria or Firmicutes.[63,64] However, given that asthma and COPD are distinct illnesses, this suggests that factors other than the microbiota composition may play a more important role in disease development.[64]

Furthermore, it has been demonstrated that cigarette smoke extract stimulates the release of chemokines and pro-inflammatory cytokines in both human and animal epithelial cells. Probiotics may reduce the inflammatory response in COPD by strengthening the tolerance of epithelial cells to the harmful effects of cigarette smoke extract.[65]

6.2.3. CF

CF is a prevalent autosomal recessive genetic disorder that primarily impacts the lungs, leading to thickened secretions, altered microbiota diversity, and increased susceptibility to infections due to progressive airway colonization.[66] There is ongoing debate regarding the relationship between CF pathophysiology and the lung microbiome, particularly concerning respiratory pathogens such as *Staphylococcus aureus* and *Pseudomonas aeruginosa*. In addition, alterations in the gut microbiome have also been observed in CF patients.[67]

However, some studies have shown that antibiotic treatment does not significantly impact disease progression. Clinical investigations have explored the effectiveness and safety of probiotics in improving health outcomes for CF patients.[68] Common probiotic strains used in these studies include *Lactobacillus spp.*, *Bifidobacterium* spp., *Saccharomyces* spp., and *Streptococcus* spp., typically administered as single or multi-strain formulations.[66] These studies found that probiotics can reduce fecal calprotectin

levels, a marker of intestinal inflammation, in both children and adults with CF. However, probiotics did not appear to influence the rate of pulmonary exacerbations and were sometimes associated with side effects such as vomiting, diarrhea, or allergic reactions. The researchers conclude that while probiotics may offer potential benefits for CF patients, further research and validation are necessary to confirm these findings.[69]

6.2.4. IPF

The development and progression of IPF have been linked to changes in lung microbiota and bacterial infections. Patients with IPF have a higher bacterial load in their bronchoalveolar lavage fluid (BALF) compared to healthy controls, with an increased prevalence of *Streptococcus*, *Pneumococcus*, and *Staphylococcus* species. IPF is a rapidly progressing chronic lung disease characterized by a progressive decline in lung function and an unknown etiology.[70,71]

Studies have found that bacteria present in the BALF of newly diagnosed IPF patients, with a loss of lung microbiome diversity, correlates with the progression of the disease. This decline in diversity is linked to a decrease in Proteobacteria and an increase in Firmicutes and Bacteroidetes, including families such as Streptococcaceae, Veillonellaceae, and Prevotellaceae. Moreover, these microbial changes are linked to important indicators of IPF, including decreased 6-min walk distance, decreased forced vital capacity, and elevated serum levels of lactate dehydrogenase and surfactant protein D. Although this study did not include healthy controls, prior research has suggested a decrease in microbiome diversity in IPF patients compared to healthy individuals.[72]

6.2.5. COVID-19

Healthy gut microbiota can increase the number of $CD8^+$ T cells and enhance the antiviral response in the lungs, potentially affecting the severity and clinical symptoms of the virus. Studies on COVID-19 patients have revealed significant changes in gut microbiota composition, including a decrease in beneficial bacteria and an increase in opportunistic pathogens. Moreover, oral administration of *Lactobacillus* has been found to increase serum vitamin D levels, which may mitigate the severity of COVID-19 through immunomodulatory effects and inhibition of cytokine storms.[73]

Probiotics may also interfere with SARS-CoV-2 by blocking its major receptor, angiotensin-converting enzyme 2, through the release of peptides with high binding affinity. This relationship is crucial for the progression of the illness. Therefore, probiotics may help lower COVID-19 morbidity and death rates. The lung microbiota, as well as the gut microbiota, play a crucial role in the infection process.[74] The lung microbiomes of COVID-19 patients differ markedly from those of healthy individuals. Elevated levels of *Acinetobacter, Chryseobacterium*, *Burkholderia*, *Brevundimonas*, *Sphingobium*, and members of the Enterobacteriaceae family have been observed in the lungs of affected patients. In addition, microbial species can be identified through the 16S rRNA sequencing to analyze BALF samples from COVID-19 patients. Missing microorganisms can be injected into the lungs to promote local immunity and boost the immune response.[75]

6.2.6. Influenza

Influenza is a viral illness that remains a major concern for public health officials worldwide. Although vaccination is used to prevent the disease, its efficacy is restricted due to rapid viral mutagenesis. As a result, boosting natural defenses by stimulating cellular immunity may serve as an effective method to combat influenza. *Lactobacilli* strains, such as *Lactobacillus casei* Shirota, have been demonstrated to activate lung natural killer cells, resulting in greater cytotoxic activity and higher levels of IL-1β, tumor necrosis factor (TNF), and MCP-1 mRNA in lung cells from probiotic-treated mice.[76]

In a different study, mice infected with influenza viruses (PR8 and H1N1) had a substantially lower viral titter in their nasal wash fluid than those not receiving probiotics. After intranasal probiotic administration, mediastinal lymph nodes were removed, and the node cells were cultivated with and without PR8 exposure. Interestingly, these cells produced cytokines such as IL-12, IFN-γ, and TNF-α, similar to what was observed during *in vivo* viral infection. Notably, *Lactobacillus casei* Shirota, a bacterium used in fermented milk production, has demonstrated both safety and efficacy in combating respiratory tract infections when applied as an aerosol or spray.[77,78]

The onset and course of chronic lung illnesses are influenced by the lung microbiome. However, several questions remain unresolved, such as the reasons behind microbiota variation in chronic lung disorders and whether these alterations are a result of or a cause of the illness.

7. Discussion

Lung development is a highly regulated process that involves six major stages such as embryonic, pseudoglandular, canalicular, saccular, alveolar, and microvascular, with each stage governed by intricate signaling pathways. These pathways drive cellular differentiation and tissue morphogenesis, ensuring the lungs' structural and functional maturation.[5] Understanding these mechanisms

is vital for improving neonatal care, especially for preterm infants at risk of respiratory distress due to incomplete lung development.

The transition from fetal to neonatal life requires key respiratory adaptations, including fetal lung fluid clearance and surfactant production for efficient gas exchange. Disruptions in these processes can lead to neonatal respiratory complications.[19,21] While interventions such as surfactant therapy and mechanical ventilation have enhanced survival rates in preterm infants, further research is needed to optimize these treatments and reduce long-term pulmonary complications.

Epigenetic regulation significantly influences lung development and disease, modifying gene expression through DNA methylation, histone modifications, and non-coding RNA activity.[79] These mechanisms contribute to chronic lung diseases such as IPF, COPD, and BPD.[80] Environmental factors such as oxidative stress, infections, and pollutants further impact epigenetic patterns, potentially leading to long-term lung dysfunction.[81] Future research should focus on therapeutic interventions that can modulate epigenetic changes and prevent disease progression.

Congenital lung disorders, including CPAM, BPS, and CLE, result from developmental abnormalities.[82] Some cases remain asymptomatic, while others require surgical intervention. Advances in prenatal imaging have improved early detection, yet optimal management strategies remain uncertain. More studies are needed to evaluate the long-term outcomes of surgical and non-surgical approaches.[21]

Lung regeneration is another critical aspect of pulmonary biology. While the lungs generally remain quiescent, they activate progenitor cells for repair following injury. The COVID-19 pandemic underscored the importance of lung regeneration in recovering pulmonary function post-infection. However, chronic exposures to pollutants and smoking can impair these regenerative mechanisms, contributing to progressive lung diseases.[83]

The placenta-gut-lung triad highlights the interconnectedness of organ systems, particularly in immune regulation. Although lung microbiota is less studied compared to the gut microbiota, it influences respiratory health, with dysbiosis linked to asthma and COPD.[21,67] Probiotic interventions show promise, but further research is necessary to clarify their role in lung function modulation.[84]

8. Conclusion

The normal development of the lungs is a multistage process involving structural and functional changes that are tightly controlled by signaling pathways. Alterations of this process result in congenital lung disorders. The lungs possess regenerative potential, which suggests the possibility of healing and functional restoration following injury caused by infectious and non-infectious agents. Future research endeavors should be directed toward bridging the gaps in the understanding of molecular and epigenetic mechanisms that influence postnatal lung disorders such as COPD. Continued investigation using *in vivo* models and organoid systems to evaluate therapeutic strategies for the management of both congenital and acquired lung illnesses holds significant promise. In particular, advancements may emerge by harnessing the lung's regenerative capacity and integrating probiotics into standardized treatment protocols.

Acknowledgments

None.

Funding

None.

Conflict of interest

The authors declare no conflict of interest.

Author contributions

Conceptualization: Feranmi Obe, Isaac Babalola
Visualization: Isaac Babalola, Oluwafemi Alamu
Writing – original draft: Feranmi Obe, Isaac Babalola, Victor Adebiyi, Ayomide Adetoro, Florence Omotoso
Writing – review & editing: Feranmi Obe, Isaac Babalola, Oluwafemi Alamu

Ethics approval and consent to participate

Not applicable.

Consent for publication

Not applicable.

Availability of data

Not applicable.

References

1. Correia-Pinto J, Gonzaga S, Huang Y, Rottier R. Congenital lung lesions--underlying molecular mechanisms. Semin Pediatr Surg. 2010;19:171-179.

   doi: 10.1053/j.sempedsurg.2010.03.003

2. Funk EC, Birol EB, McCune AR. Does the bowfin gas bladder represent an intermediate stage during the lung-to-gas bladder evolutionary transition? *J Morphol.*

2021;282(4):600-611.

doi: 10.1002/jmor.21330

3. Zacharias WJ, Frank DB, Zepp JA, *et al*. Regeneration of the lung alveolus by an evolutionarily conserved epithelial progenitor. *Nature*. 2018;555:251-255.

doi: 10.1038/nature25786

4. Domyan ET, Ferretti E, Throckmorton K, Mishina Y, Nicolis SK, Sun X. Signaling through BMP receptors promotes respiratory identity in the foregut via repression of Sox2. *Development*. 2011;138(5):971-981.

doi: 10.1242/dev.0594694

5. Schittny JC. Development of the lung. Cell Tissue Res. 2017;367:427-444.

doi: 10.1007/s00441-016-2545-0

6. Goss AM, Tian Y, Tsukiyama T, *et al*. Wnt2/2b and beta-catenin signaling are necessary and sufficient to specify lung progenitors in the foregut. Dev Cell. 2009;17:290-298.

doi: 10.1016/j.devcel.2009.06.005

7. Chytil F. Retinoids in lung development. *FASEB J.* 1996;10:986-992.

doi: 10.1096/fasebj.10.9.8801181

8. McGowan S, Jackson SK, Jenkins-Moore M, Dai HH, Chambon P, Snyder JM. Mice bearing deletions of retinoic acid receptors demonstrate reduced lung elastin and alveolar numbers. *Am J Respir Cell Mol Biol.* 2000;23:162-167.

doi: 10.1165/ajrcmb.23.2.3904

9. Alescio T, Cassini A. Induction *in vitro* of tracheal buds by pulmonary mesenchyme grafted on tracheal epithelium. *J Exp Zool*. 1962;150:83-94.

doi: 10.1002/jez.1401500202

10. Fox E, Shojaie S, Wang J, *et al*. Three-dimensional culture and FGF signaling drive differentiation of murine pluripotent cells to distal lung epithelial cells. *Stem Cells Dev*. 2015;24:21-35.

doi: 10.1089/scd.2014.0227

11. Mullassery D, Smith NP. Lung development. Semin Pediatr Surg. 2015;24:152-155.

doi: 10.1053/j.sempedsurg.2015.01.011

12. Yin Y, Wang F, Ornitz DM. Mesothelial-and epithelial-derived FGF9 have distinct functions in the regulation of lung development. *Development*. 2011;138:3169-3177.

doi: 10.1242/dev.065110

13. Wang Y, Tian Y, Morley MP, *et al*. Development and regeneration of Sox2^{+} endoderm progenitors are regulated by a Hdac1/2-Bmp4/Rb1 regulatory pathway. *Dev Cell*. 2013;24:345-358.

doi: 10.1016/j.devcel.2013.01.012

14. Chinoy MR, Graybill MM, Miller SA, Lang CM, Kauffman GL. Angiopoietin-1 and VEGF in vascular development and angiogenesis in hypoplastic lungs. *Am J Physiol Lung Cell Mol Physiol*. 2002;283:L60-L66.

doi: 10.1152/ajplung.00317.2001

15. Pauling MH, Vu TH. Mechanisms and regulation of lung vascular development. *Curr Top Dev Biol.* 2004;64:73-99.

doi: 10.1016/S0070-2153(04)64005-1

16. Kadzik RS, Morrisey EE. Directing lung endoderm differentiation in pluripotent stem cells. *Cell Stem Cell*. 2012;10(4):355-361.

doi: 10.1016/j.stem.2012.03.013

17. Han L, Chaturvedi P, Kishimoto K, *et al*. Single cell transcriptomics identifies a signaling network coordinating endoderm and mesoderm diversification during foregut organogenesis. *Nat Commun*. 2020;11(1):4158.

doi: 10.1038/s41467-020-17968-x

18. Rankin SA, Han L, McCracken KW, *et al*. A retinoic acid-hedgehog cascade coordinates mesoderm-inducing signals and endoderm competence during lung specification. *Cell Rep*. 2016;16(1):66-78.

doi: 10.1016/j.celrep.2016.05.060

19. Nikolić M, Sun D, Rawlins E. Human lung development: Recent progress and new challenges. *Development*. 2018;145:dev163485.

doi: 10.1242/dev.163485

20. Desai TJ, Brownfield DG, Krasnow MA. Alveolar progenitor and stem cells in lung development, renewal and cancer. *Nature*. 2014;507(7491):190-194.

doi: 10.1038/nature12930

21. David M, Lamas-Pinheiro R, Henriques-Coelho T. Prenatal and postnatal management of congenital pulmonary airway malformation. *Neonatology*. 2016;110(2):101-115.

doi: 10.1159/000440894

22. Nabhan AN, Brownfield DG, Harbury PB, *et al*. Single-cell Wnt signaling niches maintain stemness of alveolar type 2 cells. *Science*. 2018;359(6380):1118-1123.

doi: 10.1126/science.aam6603

23. Morton SU, Brodsky D. Fetal physiology and the transition to extrauterine life. *Clin Perinatol*. 2016;43:395-407.

doi: 10.1016/j.clp.2016.04.001

24. Elias N, O'Brodovich H. Clearance of fluid from airspaces of newborns and infants. *Neoreviews*. 2006;7:88-94.

doi: 10.1542/neo.7-2-e88

25. O'Donnell CP, Kamlin CO, Davis PG. Crying and breathing by extremely preterm infants immediately after birth. J Pediatr. 2010;156:846-847.

doi: 10.1016/j.jpeds.2010.01.007

26. Vento M, Saugstad OD. Resuscitation of the term and preterm infant. *Semin Fetal Neonatal Med*. 2010;15:216-222.

doi: 10.1016/j.siny

27. Hagood JS. Beyond the genome: Epigenetic mechanisms in lung remodelling. *Physiology* (*Bethesda*). 2014;29:177-185.

doi: 10.1152/physiol.00048.2013

28. Guo W, Shan B, Klingsberg RC, Qin X, Lasky JA. Abrogation of TGF-beta1-induced fibroblast-myofibroblast differentiation by histone deacetylase inhibition. *Am J Physiol Lung Cell Mol Physiol.* 2009;297:L864-L870.

doi: 10.1152/ajplung.00128.2009

29. Huang SK, Scruggs AM, Donaghy J, *et al.* Histone modifications are responsible for decreased Fas expression and apoptosis resistance in fibrotic lung fibroblasts. *Cell Death Dis.* 2013;4:e621.

doi: 10.1038/cddis.2013.146

30. Witt O, Deubzer HE, Milde T, Oehme I. HDAC family: What are the cancer relevant targets? *Cancer Lett.* 2009;277(1):8-21.

doi: 10.1016/j.canlet.2008.08.016

31. Yosef N., Shalek AK, Gaublomme, JT, *et al*. Dynamic regulatory network controlling TH17 cell differentiation. *Nature*. 2013;496(7446):461-468.

doi: 10.1038/nature11981

32. Sundar IK, Yao H, Rahman I. Oxidative stress and chromatin remodeling in chronic obstructive pulmonary disease and smoking-related diseases. *Antioxid Redox Signal.* 2013;18:1956-1971.

doi: 10.1089/ars.2012.4863

33. De Ruijter AJ, van Gennip AH, Caron HN, Kemp S, van Kuilenburg AB. Histone deacetylases (HDACs): Characterization of the classical HDAC family. *Biochem J.* 2003;370(3):737-749.

doi: 10.1042/bj20021321

34. Bertrand P. Inside HDAC with HDAC inhibitors. *Eur J Med Chem*. 2010;45(6):2095-2116.

doi: 10.1016/j.ejmech.2010.02.030

35. Caldeira I, Fernandes-Silva H, Machado-Costa D, Correia-Pinto J, Moura RS. Developmental pathways underlying lung development and congenital lung disorders. *Cells*. 2021;10:2987.

doi: 10.3390/cells10112987

36. Ursini WP, Ponce CC. Congenital pulmonary airway malformation. *Autopsy case Rep.* 2018;2:e2018022.

doi: 10.4322/acr.2018.022

37. Yaremenko AV, Pechnikova NA, Porpodis K, *et al*. Association of fetal lung development disorders with adult diseases: A comprehensive review. *J Pers Med.* 2024;14:368.

doi: 10.3390/jpm14040368

38. Belcher E, Lawson MH, Nicholson AG, Davison A, Goldstraw P. Congenital cystic adenomatoid malformation presenting as in-flight systemic air embolisation. *Eur Respir J*. 2007;30:801-804.

doi: 10.1183/09031936.00153906

39. Ou J, Lei X, Fu Z, et al. Pulmonary sequestration in children: A clinical analysis of 48 cases. Int J Clin Exp Med. 2014;7:1355-1365.

40. Bolca N, Topal U, Bayram S. Bronchopulmonary sequestration: Radiologic findings. *Eur J Radiol.* 2004;52:185-191.

doi: 10.1016/j.ejrad.2004.03.005

41. Litwinska M, Litwinska E, Szaflik K, *et al*. Management options for fetal bronchopulmonary sequestration. *J Clin Med*. 2022;11:1724.

doi: 10.3390/jcm11061724

42. Ribet ME, Copin MC, Gosselin BH. Bronchogenic cysts of the lung. *Ann Thorac Surg.* 1996;61:1636-1640.

doi: 10.1016/0003-4975(96)00172-5

43. Ortiz RJ, Reusmann A, Boglione MM, *et al*. Bronchogenic cyst: Lessons learned in 20 years of experience at a tertiary pediatric center. *J Pediatr Surg.* 2023;58:2516-2159.

doi: 10.1016/j.jpedsurg.2023.06.010

44. Demir OF, Hangul M, Kose M. Congenital lobar emphysema: Diagnosis and treatment options. *Int J Chron Obstruct Pulmon Dis.* 2019;14:921-928.

doi: 10.2147/COPD.S170581

45. Ranke FM, Freitas HM, Dinoá V, Miraldi F, Marchiori E. Congenital lobar emphysema. *Radiol Bras.* 2018;51:205-206.

doi: 10.1590/0100-3984.2016.0224

46. Vaikunth SS, Morris LM, Polzin W, *et al*. Congenital high airway obstruction syndrome due to complete tracheal agenesis: An accident of nature with clues for tracheal development and lessons in management. *Fetal Diagn Ther*. 2009;26:93-97.

doi: 10.1159/000242454

47. Sandu K, Monnier P. Congenital tracheal anomalies. *Otolaryngol Clin North Am*. 2007;40:193-217.

doi: 10.1016/j.otc.2006.10.001

48. Herriges M, Morrisey EE. Lung development: Orchestrating the generation and regeneration of a complex organ. *Development.* 2014;141:502-513.

doi: 10.1242/dev.098186

49. McCauley KB, Hawkins F, Serra M, Thomas DC, Jacob A, Kotton DN. Efficient derivation of functional human airway epithelium from pluripotent stem cells via temporal

regulation of Wnt signaling. *Cell Stem Cell*. 2017;20:844-857.

doi: 10.1016/j.stem.2017.03.001

50. Basil MC, Alysandratos KD, Kotton DN, Morrisey EE. Lung repair and regeneration: Advanced models and insights into human disease. *Cell Stem Cell.* 2024;31:439-454.

doi: 10.1016/j.stem.2024.02.009

51. Xi Y, Kim T, Brumwell AN, *et al*. Local lung hypoxia determines epithelial fate decisions during alveolar regeneration. *Nat Cell Biol.* 2017;19:904-914.

doi: 10.1038/ncb3580

52. Giangreco A, Reynolds SD, Stripp BR. Terminal bronchioles harbor a unique airway stem cell population that localizes to the bronchoalveolar duct junction. *Am J Pathol.* 2002;161:173-182.

doi: 10.1016/S0002-9440(10)64169-7

53. Faure S, de Santa Barbara P. Molecular embryology of the foregut. *J Pediatr Gastroenterol Nutr.* 2011;52:S2-S3.

doi: 10.1097/MPG.0b013e3182105a1a

54. Hou K, Wu ZX, Chen XY, *et al*. Microbiota in health and diseases. *Signal Transduct Target Ther*. 2022;23:135.

doi: 10.1038/s41392-022-00974-4

55. Moffatt MF, Cookson WO. The lung microbiome in health and disease. *Clin Med*. (*Lond*). 2017;17:525-529.

doi: 10.7861/clinmedicine.17-6-525

56. Man MA, Ungur RA, Motoc NS, Pop LA, Berindan-Neagoe I, Ruta VM. Lung microbiota in idiopathic pulmonary fibrosis, hypersensitivity pneumonitis, and unclassified interstitial lung diseases: A preliminary pilot study. *Diagnostics* (*Basel*). 2023;13:3157.

doi: 10.3390/diagnostics13193157

57. Aung HH, Sivakumar A, Gholami SK, Venkateswaran SP, Gorain B, Shadab Md. An overview of the anatomy and physiology of the lung. In: *Nanotechnology-based Targeted Drug Delivery Systems for Lung Cancer*. United States: Academic Press; 2019. p. 1-20.

doi: 10.1016/B978-0-12-815720-6.00001-0

58. Lloyd CM, Hessel EM. Functions of T cells in asthma: More than just $T(H)_{2\ cells}$. *Nat Rev Immunol*. 2010;10:838-848.

doi: 10.1038/nri2870

59. Gollwitzer ES, Saglani S, Trompette A, *et al*. Lung microbiota promotes tolerance to allergens in neonates via PD-L1. *Nat Med*. 2014;20:642-647.

doi: 10.1038/nm.3568

60. Hilty M, Burke C, Pedro H, *et al*. Disordered microbial communities in asthmatic airways. *PLoS One*. 2010;5:e8578.

doi: 10.1371/journal.pone.0008578

61. Marri PR, Stern DA, Wright AL, Billheimer D, Martinez FD. Asthma-associated differences in microbial composition of induced sputum. *J Allergy Clin Immunol*. 2013;131:346-352.

doi: 10.1016/j.jaci.2012.11.013

62. Kleniewska P, Pawliczak R. Can probiotics be used in the prevention and treatment of bronchial asthma? *Pharmacol Rep.* 2024;76:740-753.

doi: 10.1007/s43440-024-00618-0

63. Garcia-Nuñez M, Millares L, Pomares X, *et al*. Severity-related changes of bronchial microbiome in chronic obstructive pulmonary disease. *J Clin Microbiol.* 2014;52:4217-4223.

doi: 10.1128/JCM.01967-14

64. Wu D, Hou C, Li Y, *et al*. Analysis of the bacterial community in chronic obstructive pulmonary disease sputum samples by denaturing gradient gel electrophoresis and real-time PCR. *BMC Pulm Med*. 2014;14:179.

doi: 10.1186/1471-2466-14-179

65. Carvalho JL, Miranda M, Fialho AK, *et al.* Oral feeding with probiotic *Lactobacillus rhamnosus* attenuates cigarette smoke-induced COPD in C57Bl/6 mice: Relevance to inflammatory markers in human bronchial epithelial cells. *PLoS One.* 2020;15:e0225560.

doi: 10.1371/journal.pone.0225560

66. Hurley MN, Ariff AH, Bertenshaw C, Bhatt J, Smyth AR. Results of antibiotic susceptibility testing do not influence clinical outcome in children with cystic fibrosis. *J Cyst Fibros*. 2012;11:288-292.

doi: 10.1016/j.jcf.2012.02.006

67. Wu BG, Segal LN. Lung microbiota and its impact on the mucosal immune phenotype. *Microbiol Spectr*. 2017;5(3).

doi: 10.1128/microbiolspec.BAD-0005-2016

68. Smith AL, Fiel SB, Mayer-Hamblett N, Ramsey B, Burns JL. Susceptibility testing of *Pseudomonas aeruginosa* isolates and clinical response to parenteral antibiotic administration: Lack of association in cystic fibrosis. *Chest*. 2003;123:1495-1502.

doi: 10.1378/chest.123.5.1495

69. Coffey MJ, Garg M, Homaira N, Jaffe A, Ooi CY. Probiotics for people with cystic fibrosis. *Cochrane Database Syst Rev.* 2020;22:CD012949.

doi: 10.1002/14651858.CD012949.pub2

70. Collard HR, Moore BB, Flaherty KR, *et al.* Acute exacerbation of idiopathic pulmonary fibrosis. An international working group report. *Am J Respir Crit Care Med*. 2007;194:636-643.

doi: 10.1164/rccm.201604-0801CI

71. Han ML, Zhou Y, Murray S. Lung microbiome and disease progression in idiopathic pulmonary fibrosis: An analysis of the COMET study. *Lancet Respir Med.* 2014;2:548-556.

doi: 10.1016/S2213-2600(14)70069-4

72. Takahashi Y, Saito A, Chiba H, *et al*. Impaired diversity of the lung microbiome predicts progression of idiopathic pulmonary fibrosis. *Respir Res*. 2018;19:34.

doi: 10.1186/s12931-018-0736-9

73. Tiwari SK, Dicks LM, Popov IV, *et al*. Probiotics at war against viruses: What is missing from the picture? *Front Microbiol*. 2020;11:1877.

doi: 10.3389/fmicb.2020.01877

74. Kurian SJ, Unnikrishnan MK, Miraj SS, *et al*. Probiotics in prevention and treatment of COVID-19: Current perspective and future prospects. *Arch Med Res*. 2021;52:582-594.

doi: 10.1016/j.arcmed.2021.03.002

75. Khatiwada S, Subedi A. Lung microbiome and coronavirus disease 2019 (COVID-19): Possible link and implications. *Hum Microb J*. 2020;17:100073.

doi: 10.1016/j.humic.2020.100073

76. Harata G, He F, Hiruta N, Kawase M, Kubota A, Hiramatsu M, Yausi H. Intranasal administration of *Lactobacillus rhamnosus* GG protects mice from H1N1 influenza virus infection by regulating respiratory immune responses. *Lett Appl Microbiol*. 2010;50:597-602.

doi: 10.1111/j.1472-765X.2010.02844.x

77. Jung YJ, Lee YT, Ngo VL, *et al*. Heat-killed *Lactobacillus casei* confers broad protection against influenza a virus primary infection and develops heterosubtypic immunity against future secondary infection. *Sci Rep*. 2017;7:17360.

doi: 10.1038/s41598-017-17487-8

78. Hori T, Kiyoshima J, Shida K, Yasui H. Effect of intranasal administration of *Lactobacillus casei* shirota on influenza virus infection of upper respiratory tract in mice. *Clin Diagn Lab Immunol*. 2001;8:593-597.

doi: 10.1128/CDLI.8.3.593-597.2001

79. Okwor VC, Okwor CJ, Musayayi SA, *et al*. Immune modulation and epigenetic therapies for enhanced outcome of treatment in triple-negative breast cancer. *Tumor Discov*. 2024;3(3):3383.

doi: 10.36922/td.3383

80. Allis C, Jenuwein T. The molecular hallmarks of epigenetic control. *Nat Rev Genet*. 2016;17(8):487-500.

doi: 10.1038/nrg.2016.59

81. Angrish MM, Allard P, McCullough, SD, *et al*. Epigenetic applications in adverse outcome pathways and environmental risk evaluation. *Environ Health Perspect*. 2018;126(4):045001.

doi: 10.1289/EHP2322

82. Leblanc C, Baron M, Desselas E, *et al*. Congenital pulmonary airway malformations: State-of-the-art review for pediatrician's use. *Eur J Pediatr*. 2017;176(12):1559-1571.

doi: 10.1007/s00431-017-3032-7

83. Beers M, Morrisey E. The three R's of lung health and disease: Repair, remodeling, and regeneration. *J Clin Invest*. 2011;121:2065-2073.

doi: 10.1172/JCI45961

84. Schmidt TSB, Raes J, Bork P. The human gut microbiome: From association to modulation. *Cell*. 2018;172(6):1198-1215.

doi: 10.1016/j.cell.2018.02.044

ACCSCIENCE PUBLISHING

Microbes & Immunity

PERSPECTIVE ARTICLE

The patentability of natural phages as therapeutics in the United States

Qimao Yang[1], Shiyi Zeng[1], Biao Zhu[1], Tongyu Zhu[2]*, and Nannan Wu[1,2,3]*

[1]CreatiPhage Biotechnology Co., Ltd., Shanghai, China

[2]Fudan University Phage Institute, Zhongshan Hospital, Shanghai Medical College, Fudan University, Shanghai, China

[3]Shanghai Public Health Clinical Center, Shanghai Institute of Phage, Fudan University, Shanghai, China

Abstract

The resurgence of phage therapy as a potent countermeasure against antimicrobial resistance has been accompanied by significant challenges in patent protection. This perspective paper examines the patentability of natural phages as therapeutics, focusing on the United States and extending to the European Union and Australia – jurisdictions at the forefront of this biotechnological innovation. We dissect the legal frameworks and identify the patent claims that have successfully navigated the complex intellectual property landscape. Our analysis reveals a dichotomy between the natural origin of therapeutic phages and the inventive steps required for patent eligibility. Despite hurdles, we highlight strategic innovations and specific patent claims that have been granted, suggesting a path forward for the commercialization and protection of phage therapy. We conclude with a call for a more adaptive legal framework to foster innovation and recognize the transformative potential of phage therapy in modern medicine.

Keywords: Phage therapy; Patentability; Natural phage; Biological invention; Legal regulation

***Corresponding authors:**
Nannan Wu
(wunannan@shphc.org.cn)
Tongyu Zhu
(tyzhu@fudan.edu.cn)

Citation: Yang Q, Zeng S, Zhu B, Zhu, T, Wu, N. The patentability of natural phages as therapeutics in the United States. *Microbes & Immunity.* 2025;2(3):60-71. doi: 10.36922/mi.4758

Received: September 4, 2024

Revised: October 19, 2024

Accepted: November 10, 2024

Published online: December 2, 2024

1. Introduction

The advent of antimicrobial resistance has propelled phage therapy back into the spotlight, offering a biological solution to the crisis. As the field advances, so does the complexity of securing intellectual property (IP) rights. Upon a thorough examination of the IP landscape within the realm of burgeoning biotechnologies, the topic of phage therapy patentability emerges as a particularly intriguing one. The natural origin of therapeutic phages poses significant hurdles in securing patent protection for related products and inventions.[1] This lack of robust IP safeguards acts as a deterrent for commercial enterprises, hindering their investment in promoting and advancing phage therapy.

This perspective paper provides an in-depth analysis of the patentability of natural phages as therapeutics, with a focus on the United States (US), then extending to the European Union (EU) and Australia. We explore legal challenges and identify strategies that have led to successful patent grants and draw parallels between the patentability challenges faced by natural phages, oncolytic viruses, and other microbes, offering

a roadmap for future research and commercialization efforts.

2. Patentability in the US

In the US, the patentability of natural phages has been fraught with debate. Traditionally, a discovery must fulfill the criteria of "any new and useful process, machine, manufacture, or composition of matter, or any new and useful improvement thereof" (35 U.S.C. 101) to be eligible for being granted a patent. Concurrently, the discovery must not encompass laws of nature, natural phenomena, and abstract ideas.[2] Given these parameters, obtaining patents for natural phages has historically been inherently challenging due to the debatable nature of whether their use in killing bacteria constitutes a creative invention or merely a manifestation of natural laws, and whether it falls under the category of an abstract idea. As discussed by Todd,[2] three significant cases have further complicated the patentability of phages.

First, in the landmark case of *Mayo Collaborative Services v. Prometheus Laboratories, Inc., 566 U.S. 66 (2012)*, the Supreme Court of the US ruled that a patent claiming a method of determining the proper dosage of a drug was invalid. The court deemed that the patent merely recited a natural law that a high dosage of the drug may be dangerous while a low dosage may be ineffective.[3] Relating this to phage therapy, courts may similarly conclude that phage therapy merely involves applying a natural principle, whereby a phage is utilized to kill its host bacteria. Second, in the case of *Assoc. For Molecular Pathology v. Myriad Genetics, Inc., 569 U.S. 576 (2013)*, the Supreme Court ruled that the DNA sequences patented by Myriad were invalid because one cannot patent something naturally occurring. Conversely, the court upheld the patentability of cDNA derived from those DNA sequences, as the cDNA was artificially created.[4] This ruling casts again doubt on the patentability of natural phages and their DNA, simultaneously offering hope for genetically or chemically modified phages that are out of the scope of natural occurrence and endow the patented therapy with an inventive step. More details regarding the patentability of novel technologies, including phage therapy, are illuminated in the third case, *Alice Corp. v. CLS Bank Int'l, 573 U.S. 208 (2014)*, which led to the establishment of the Mayo/Alice test. The ruling in this case invalidated a patent pertaining to a computerized trading platform, deeming it as an abstract idea.[5] Subsequently, this case gave rise to the Mayo/Alice test, which employs a two-step process to evaluate the eligibility of a patent. Initially, it examines whether the patent merely delineates a natural law. If affirmative, the subsequent step involves assessing whether the patent incorporates an inventive concept sufficient to transform the ineligible abstract idea into a patent-eligible subject matter. This test outlines a framework for assessing patent eligibility in cases involving controversial subject matters.

3. Patentability in the EU and Australia

In the EU, the European Patent Convention (EPC) serves as the cornerstone legislation outlining the criteria for patentability, and it is complemented by the European Biotech Directive, which provides additional clarity for biological inventions. Specifically, Rule 27 (a) and Rule 29 (2) of the EPC allow the patentability of biological isolates and products derived from technical processes, even if they naturally exist.[6] While European patents cannot be granted to plant or animal varieties and their production processes, Article 53 (b) offers exceptions for microbiological processes and related products.[7] Furthermore, Article 54(4) enables the patentability of inventions claiming novel substances or compositions for therapeutic purposes that were previously unknown.[7] These provisions open abundant spaces for patenting inventions related to phage therapy, encompassing claims based on genetic identity, phage cocktail compositions, phage-derived products, and numerous other aspects.

However, Article 53(c) of the EPC excludes "methods for treatment of the human or animal body by surgery or therapy and diagnostic methods practiced on the human or animal body," with the exception of products such as substances or compositions used in those processes.[7] This provision raises queries regarding the extent of its limitation and introduces a degree of uncertainty surrounding the patentability of therapeutic biological inventions, including those related to phage therapy.

In Australia, the legal framework governing the patentability of inventions pertaining to phage therapy falls under the umbrella of biological inventions, and IP Australia stipulates that biological materials are patentable only if they have been isolated from their natural state or synthetically/recombinantly produced.[8] Beyond directly patenting biological materials, Australia recognizes the patentability of methods and processes that involve the application of these materials. IP Australia provides a comprehensive array of examples showcasing the breadth of biological inventions that can be patented,[8] offering insights into the potential for granting patents related to phage therapy. This includes but is not limited to, inventions claiming genetic modifications, cocktail compositions, methods utilizing these compositions, phage delivery techniques, and phage-derived products. However, it is crucial to note that patents asserting claims related to the genetic identity of naturally occurring DNA and gene sequences are not permissible, regardless of the

production method employed. Nevertheless, one leeway in this restriction is that if a claim pertains to a specific utilization of a gene, a patent encapsulating the specific method of employing that gene may be eligible for a grant.

4. Overview of representative granted patents in phage therapy

Despite the legal complexities, dozens of patents related to natural phage therapy have been granted. These achievements underscore an intriguing interplay between biological ingenuity and legal constraints, demonstrating the resilience and perseverance of researchers and stakeholders in this domain despite stringent barriers. To illustrate this point, Table 1 presents a curated list of natural therapeutic phage-related patents granted to several representative companies in the industry in the US and the patents' corresponding registrations in the EU and Australia if exist. This compilation was meticulously made by screening the granted patents of these companies through the US Patent and Trademark Office's (USPTO) website. The "Basic Search" option was used to sort for the keyword "phage" and the phage-based companies' names. Once potential patents were found, a closer examination of them was done by reading their abstracts and claims. Further refinement was applied to ensure that only patents pertaining to therapeutic phage applications and with successful grant status were included, resulting in a total of 21 patents. Patents regarding bioengineering modification methods and manufacturing processes are not included for their more obvious patentability and less relevance to the biological nature of phage therapy. Following the selection process on USPTO, another sorting process was performed on Espacenet to link the selected patents from the US to their corresponding applications in the EU and Australia if exist. Note that there may be repeated corresponding patents for a single patent from the US in other regions. This is caused by various legal reasons that are not of concern here. While A1 and A2 patents are recorded for the ones in the EU and Australia, focus should be emphasized on B-patents because A-patents represent published patent applications, but only B-patents are granted.

Overall, these 21 patents were exclusively held by four companies: Armata Pharmaceuticals, Intralytix, Locus Bioscience, and Pherecydes Pharma. It is worth mentioning that although other organizations including SNIPR Biome, Adaptive Phage Therapeutics, Eligo Biosciences, BiomX, Fixed Phage, and PhageLux possess a considerable number of patents in bacterial infection treatment, such patents are not directly related to natural therapeutic phages or are not yet granted. As such, they were excluded from this analysis. The selected patents can be categorized based on their respective claims that encompass three categories: Single phage, phage combination, and phage combination and method pertaining to its use. This taxonomy highlights the diversity and depth of innovations within the natural phage therapy landscape.

It might seem counterintuitive that many patents, particularly those concerning single phages or straightforward phage combinations, have been granted within the current framework of biological product patentability. To delve deeper into this phenomenon, a two-pronged analysis was conducted. First, the temporal shifts in the prevalence of various phage patent categories were examined. It was found that patents for single, naturally occurring phages surfaced only once, in 2009. Meanwhile, patents for phage combinations were predominantly granted in and before 2010, with a solitary exception granted in 2023. In contrast, the frequency of patents for phage combinations and their associated usage methods has remained consistent from 2008 to 2023. Another trend among more recently granted patents is an increased likelihood of including claims that specify sequence similarity thresholds. Before 2014, no patents featured claims with such thresholds. However, in 2014, Intralytix received two patents (10517908-B2; 11253557-B2) that incorporated Restriction Fragment Length Polymorphism (RFLP) DNA profiles, albeit with a vague threshold described as "substantially equivalent." A pivotal shift occurred in 2018 when Pherecydes secured a patent (10077431-B2) with a defined 97% DNA sequence similarity threshold, marking the first instance of a precise quantitative threshold. Following this precedence, more subsequent patents established this standard in their claims, all setting thresholds at over 90% (Table 1).

Second, we conducted a comparative analysis between the claims in the granted patents and their original applications to identify any rejected claims. Our analysis revealed that there was no blanket rejection of any specific type of claim. Instead, the granted patents typically exhibited a higher degree of specificity compared to their initial applications, often achieved by introducing additional limitations within the scope of the claims. For example, in some instances, the sequence similarity thresholds were raised (*e.g.*, from 90% in 20210228659-A1 to 99% in 11779617-B2). In others, the patented compositions were amended to necessitate a minimum of two phages instead of just one (*e.g.*, from 20200171108-A1 to 11253557-B2) (Table A1 in Appendix). These adjustments underscore the importance of precision and clarity in patent claims to enhance their chances of approval.

Table 1. Representative granted patents in phage therapy in the US

US Patent number	Issue date (month/day/year)	Assignee	Title	Target	Main claim (s)	Sequence similarity threshold	Certain phage (s)	EP Record	AU Record
7635584-B2	December 22, 2009	Intralytix	O157: H7 bacteriophage and uses thereof	*E. coli*	A natural phage	NA	ATCC No. PTA-7948		
7507571-B2	March 24, 2009	Intralytix	*Listeria monocytogenes* bacteriophages and uses thereof	*Listeria*	Natural phage compositions	NA	ATCC No. PTA-5372, PTA-5373, PTA-5374, PTA-5375, PTA-5376, and PTA-5377		
7622293-B2	November 24, 2009	Intralytix	*P. aeruginosa*: bacteriophage and uses thereof	*P. aeruginosa*	Natural phage compositions	NA	ATCC No. PTA-8358, PTA-8359, PTA-8360, PTA-8361, PTA-8362, PTA-8363, and PTA-8364		
7625739-B2	December 1, 2009	Intralytix	*C. perfringens* bacteriophage and uses thereof	*C. perfringens*	Natural phage compositions	NA	ATCC No. PTA-9479, PTA-8479, and PTA-8480		
7625740-B2	December 1, 2009	Intralytix	*C. perfringens* bacteriophage and uses thereof	*C. perfringens*	Natural phage compositions	NA	ATCC No. PTA-8481, and PTA-8483		
7674467-B2	March 9, 2010	Intralytix	*Salmonella* bacteriophage and uses thereof	*Salmonella*	Natural phage compositions	NA	ATCC No. PTA-5280, PTA-5281, PTA-5282, PTA-5283, PTA-5284, and PTA-5285	EP1663302B1	
7625556-B2	December 1, 2009	Intralytix	*E. coli* bacteriophage and uses thereof	*E. coli*	Natural phage compositions and a method of its use in food	NA	ATCC No. PTA-8347, PTA-8348, PTA-8351, and PTA-8352		
7625741-B2	December 1, 2009	Intralytix	*E. coli* O157: H7 bacteriophage and uses thereof	*E. coli*	Natural phage compositions and a method of its use in food	NA	ATCC No. PTA-7950, and PTA-7949		

(*Cont'd...*)

doi: 10.36922/mi.4758

Table 1. (*Continued*)

US Patent number	Issue date (month/day/year)	Assignee	Title	Target	Main claim (s)	Sequence similarity threshold	Certain phage (s)	EP Record	AU Record
8685697-B1	April 1, 2014	Intralytix	*Listeria monocytogenes* bacteriophages and uses thereof	*Listeria*	Natural phage compositions and a method of its use in food	Same RFLP profile	ATCC No. PTA-8353, PTA-8354, PTA-8355, PTA-8356, and PTA-8357		
8685696-B2	April 1, 2014	Intralytix	*Salmonella* bacteriophage and uses thereof	*Salmonella*	Natural phage compositions and a method of its use in food	Same RFLP profile	ATCC No. PTA-12381, PTA-12382, PTA-12379, PTA-8365, PTA-12380, PTA-8366, and PTA-8367		
10711252-B2	July 14, 2020	Intralytix	*Shigella* bacteriophages and uses thereof	*Shigella*	Natural phage compositions, dosage, and its use in mammals	Same RFLP profile	ATCC No. PTA-121236, PTA-121234, PTA-121238, PTA-121241, PTA-121239, PTA-121240, PTA-121242, PTA-121237, and PTA-121235	EP3253215B1; EP3253215C0	AU2016209252B2
10517908-B2	December 31, 2019	Armata Pharmaceuticals	Therapeutic bacteriophage compositions	*S. aureus*	A method of using natural phage compositions (at least one phage) in mammals, surface, or food	NA	Sa87, J-Sa36, and Sa83		
11253557-B2	Feburary 22, 2022	Armata Pharmaceuticals	Therapeutic bacteriophage compositions (continuation of U.S. Pat. No. 10517908)	*S. aureus*	Natural phage compositions, quality, dosage, and delivery for pulmonary infection	NA	Sa87, J-Sa36, and Sa83		

(*Cont'd...*)

doi: 10.36922/mi.4758

Table 1. (*Continued*)

US Patent number	Issue date (month/day/year)	Assignee	Title	Target	Main claim (s)	Sequence similarity threshold	Certain phage (s)	EP Record	AU Record
11654166-B2	May 23, 2023	Armata Pharmaceuticals	Therapeutic bacteriophage compositions for treating infection	*S. aureus*	Natural phage compositions, quality, dosage, and formulation	90% (fragment)	Sa87, J-Sa36, and Sa83	EP3735275A1	AU2019205242A1
10077431-B2	September 18, 2018	Pherecydes Pharma	Phage therapy for *Pseudomonas* infections	*P. aeruginosa*	A method of using natural phage compositions (at least two phages and their dosage, and formulation) in mammals	97% (fragment)	BP1384, BP1429, BP1430, BP1433, BP1450, BP1644, BP1647, BP1648, BP1649, BP1650, BP1658, BP1661, and BP1662	EP3060226B1	AU2014338859B2
10260051-B2	April 16, 2019	Pherecydes Pharma	Phage therapy of *Pseudomonas* infections (continuation of U.S. Pat. No. 10077431)	*P. aeruginosa*	A method of using natural phage compositions (at least one phage and its dosage, and formulation) in mammals	97% (fragment)	BP1384, BP1429, BP1430, BP1433, BP1450, BP1644, BP1647, BP1648, BP1649, BP1650, BP1658, BP1661, and BP1662	EP3060226B1	AU2014338859B2
10898530-B2	January 26, 2021	Pherecydes Pharma	Phage therapy	*P. aeruginosa*	A method of using natural phage compositions (at least two phages and their dosage, and formulation) in mammals	99% (fragment)	BP1384, BP1777, BP1792, BP1797, BP1800, BP1902, and BP1940	EP3215607B1	AU2015341683B2
11779617-B2	October 10, 2023	Pherecydes Pharma	Phage therapy (continuation of U.S. Pat. No. 10898530)	*P. aeruginosa*	A method of using natural phage compositions (at least one phage and its dosage, and formulation) in mammals	99% (fragment)	BP1777, BP1792, BP1797, BP1800, BP1902, and BP1940	EP3215607B1	AU2015341683B2

(*Cont'd...*)

doi: 10.36922/mi.4758

Table 1. (*Continued*)

US Patent number	Issue date (month/day/year)	Assignee	Title	Target	Main claim (s)	Sequence similarity threshold	Certain phage (s)	EP Record	AU Record
10918680-B2	February 16, 2021	Pherecydes Pharma	Phage therapy for *E. coli* infections	*E. coli*	A method of using natural phage compositions (at least two phages and their dosage, and formulation) in mammals	99% (fragment)	BP539, BP700, BP753, BP814, BP953, BP954, BP970, BP1002, BP1151, BP1155, BP1176, BP1197, BP1226, and BP1229	EP3091992B1	AU2015205512B2
11690885-B2	July 4, 2023	Pherecydes Pharma	Anti-bacterial compositions and uses thereof	*S. aureus*	A method of using natural phage compositions (at least one phage and its dosage, and formulation) in human, animal, or decontamination	95% (fragment)	PN1137, PN1493, PN1815 and PN1957	EP3372085A1; EP3592150A1	AU2018231408B2
11311582-B2	April 26, 2022	Locus Biosciences	Bacteriophage compositions and methods of use thereof	*E. coli*	A method of using natural phage compositions (at least two phages) for treating or preventing a bacterial infection in an individual	95% (fragment)	p0031, p0032, p0033, and p0034		

Notes:
(i) NA (not applicable) for sequence similarity threshold: normally the same phenotypic characteristics and the same lytic activity against certain bacteria Restriction Fragment Length Polymorphism (RFLP) profile
(ii) Pherecydes Pharma has been merged with Erytech to Phaxiam.
(iii) The table was updated until May 2024.
Abbreviation: *E. coli: Escherichia coli; P. aeruginosa: Pseudomonas aeruginosa; C. perfringens: Clostridium perfringens; S. aureus: Staphylococcus aureus.*

doi: 10.36922/mi.4758

5. Comparative analysis of patentability in oncolytic viruses and microbial therapies

Phage products, oncolytic viruses, and other microbial therapies exhibit similar biological characteristics, which subject them to analogous legal complexities in the realm of patentability. Consequently, advancements in patentability within these related fields can provide significant insights and value for the progression of phage therapy patentability. Preliminary patent searches reveal the presence of several oncolytic virotherapy-related patents in the US and EU, primarily falling into two categories: methods of treatment using oncolytic virotherapy and patents for recombinant oncolytic viruses with distinct characteristics. Notable examples of granted patents include US10238698B2, which is associated with EP2806883B1 and relates to treatment methodologies, and US9862932B2, which is associated with EP3473708B1 and concerns genetic recombination. These granted patents bolster the prospects for achieving patentability in phage therapy through claims involving genetic modifications and innovative methodologies, as previously discussed. In the past decade, there has been a notable increase in the prevalence of patents related to phages with biochemical modifications or conjugations such as encapsulating phage compositions in polymer microcapsules for delivery and binding phages to a plurality of particles to enhance performance, reflecting a strategic shift in patent applications to address the legal challenges.

While comprehensive reviews on the patentability in therapeutic phages and oncolytic viruses are scarce, FitzGerald and Spek provide an exhaustive analysis of patent protection in microbial therapies, specifically concerned with various bacterial therapies including therapeutics based on fecal microbiota transplantation, defined bacterial consortia, single commensal bacterial strains, and single engineered bacterial strains.[9] The review echoes similar concerns about the challenges posed by the current US legal framework but also outlines potential future trajectories. These include the ongoing evolution of legal patent guidelines and the development of innovative approaches that are in harmony with regulatory principles. The analysis further highlights the progress made by key companies in their respective therapeutic areas, underscoring the dynamic nature of the field and the potential for further advancements in patentability.

6. Conclusion

The legal complexities surrounding phage therapy patentability, stemming from its reliance on natural elements, have not extinguished innovation within the field. Despite some challenges, examples of granted patents showcase how targeting aspects such as phage combinations and methods pertaining to their usages may be useful. The perspective here reaffirms the critical need to protect IP while nurturing innovation. Resolving the patentability issues regarding phage therapy also has immense economic implications. Stronger IP protections are positively correlated with pharmaceutical investments and R&D expenses in general.[10] This is expected to hold in phage therapy, encouraging its market dynamics and promoting its sources of funding for advancements. Furthermore, the patentability issues resonate with current regulatory hurdles revolving around phage therapy. For instance, as the FDA classifies phage therapy as a biological product, patenting it must align with the relevant regulatory framework to facilitate broader market access and clinical application.[11] Only by carefully analyzing existing patents, adhering to the principles of specificity and innovation established by precedent cases, and learning from the progress made in similar therapeutic areas such as oncolytic virotherapy and other microbial therapies can the full potential of phage therapy to revolutionize global health be unlocked, transforming this century-old therapy into a cornerstone of modern medicine.

Looking into the times ahead, it can be argued that the future of phage therapy patentability lies in fostering a more dynamic and adaptive legal framework. Countries with more flexibility can serve as examples for others, potentially leading to a more uniform and encouraging global patent environment for phage therapy. With more upcoming innovations and biological discoveries, the field of phage therapy will eventually welcome more diverse and mind-altering technologies.

Acknowledgments

We thank members of the Shanghai Institute of Phage and CreatiPhage Biotechnology for thoughtful discussions.

Funding

This work is supported by a grant from the National Key Research and Development Program of China (2021YFA0911200).

Conflict of interest

Qimao Yang and Shiyi Zeng were interns at CreatiPhage Biotechnology. Biao Zhu is an employee of CreatiPhage and Nannan Wu is a cofounder of CreatiPhage Biotechnology. In addition, Nannan Wu is an Editorial Board Member of this journal but was not in any way involved in the editorial and peer-review process conducted for this paper, directly or indirectly. All authors declare that the research was conducted in the absence of any commercial or financial

relationships that could be construed as a potential conflict of interest.

Author contributions

Conceptualization: Nannan Wu, Tongyu Zhu, Qimao Yang
Writing – original draft: Qimao Yang, Shiyi Zeng
Writing – review & editing: Nannan Wu, Tongyu Zhu, Biao Zhu

Ethics approval and consent to participate

Not applicable.

Consent for publication

Not applicable.

Availability of data

Not applicable.

References

1. Sacher J. *Breaking down Phage Patentability. Capsid and Tail*. Vol. 13; 2019. Available from: https://phage.directory/capsid/phage-patentability [Last accessed on 2024 Oct 18].
2. Todd K. The promising viral threat to bacterial resistance: The uncertain patentability of phage therapeutics and the necessity of alternative incentives. *Duke Law J.* 2019;68:767-805.
3. Justia US Supreme Court Center. *Mayo Collaborative Services v. Prometheus Laboratories, Inc., 566 U.S. 66*; 2012. Available from: https://supreme.justia.com/cases/federal/us/566/66 [Last accessed on 2024 Oct 18].
4. Justia US Supreme Court Center. *Association for Molecular Pathology v. Myriad Genetics, Inc., 569 U.S.* 576; 2013. Available from: https://supreme.justia.com/cases/federal/us/569/576 [Last accessed on 2024 Oct 18].
5. Justia US Supreme Court Center. *Alice Corp. v. CLS Bank Int'l, 573 U.S. 208*; 2014. Available from: https://supreme.justia.com/cases/federal/us/573/208 [Last accessed on 2024 Oct 18].
6. European Patent Office. *Biotechnological Inventions*; Ch. 5. Available from: https://www.epo.org/en/legal/epc/2020/rcii_v.html [Last accessed on 2024 Oct 18].
7. European Patent Office. *Patentability*. Ch. 1. Available from: https://www.epo.org/en/legal/epc/2020/acii_i.html [Last accessed on 2024 Oct 18].
8. IP Australia. *What Biological Inventions can be Patented*. Available from: https://www.ipaustralia.gov.au/patents/what-are-patents/what-biological-inventions-can-be-patented [Last accessed on 2024 Oct 18].
9. FitzGerald MJ, Spek EJ. Microbiome therapeutics and patent protection. *Nat Biotechnol*. 2020;38(7):806-810.
   doi: 10.1038/s41587-020-0579-z
10. Grabowski H. Patents, innovation and access to new pharmaceuticals. *J Int Econ Law*. 2002;5(4):849-860.
    doi: 10.1093/jiel/5.4.849
11. Yang Q, Le S, Zhu T, Wu N. Regulations of phage therapy across the world. *Front Microbiol*. 2023;14:1250848.
    doi: 10.3389/fmicb.2023.1250848

Appendix

Table A1. Comparison of claims in the application and granted form of two patents

Patent	Application form (20210228659-A1)	Granted form (11779617-B2)	Note
Patent 1	1. An antibacterial composition comprising at least one bacteriophage having lytic activity against a *P. aeruginosa* strain, said at least one bacteriophage selected from the bacteriophages having a genome comprising a nucleotide sequence of any one of SEQ ID NOs: 1 – 7 or a sequence having at least 90% identity thereto. 2 – 4. (canceled)	1. An antibacterial composition comprising at least one bacteriophage having lytic activity against a *P. aeruginosa* strain and a pharmaceutically acceptable excipient or carrier, said at least one bacteriophage being selected from the bacteriophages having a genome comprising a nucleotide sequence of any one of SEQ ID NOs: 2 – 7 or a sequence having at least 99% identity thereto, and said pharmaceutically acceptable excipient or carrier comprising a preservative in an amount effective to preserve the activity of the bacteriophage.	Canceled SEQ ID NO1; sequence identity requirement changed from 90% to 99%
	5. The composition of claim 1, comprising at least one bacteriophage of Table 1. 6. (canceled)	2. The composition of claim 1, comprising at least one bacteriophage selected from the group consisting of BP1777, BP1792, BP1797, BP1800, BP1902, and BP1940, said bacteriophage having a genome comprising the nucleotide sequence of SEQ ID NOs: 2 – 7, respectively.	The phage names and sequences were specified
	7. The composition of claim 1, which is lytic against antibiotic-resistant *P. aeruginosa* strains.	3. The composition of claim 1, which is lytic against antibiotic-resistant *P. aeruginosa* strains.	Unchanged
	8. The composition of claim 1, which is lytic against more than 90% of all bacterial strains of the LMG collection.	4. The composition of claim 1, which is lytic against more than 90% of all bacterial strains of the LMG collection.	Unchanged
	9. The composition of claim 1, which further comprises a pharmaceutically acceptable excipient or carrier.	5. The composition of claim 1, wherein the pharmaceutically acceptable excipient or carrier comprises buffered physiological saline.	Pharmaceutically acceptable excipients or carriers were specified
	10. The composition of claim 1, in the form of a liquid, semi-liquid, solid, or lyophilized formulation.	6. The composition of claim 1, in the form of a liquid, semi-liquid, solid, or lyophilized formulation.	/
	11. The composition of claim 10, which comprises between 10e4 and 10e12 PFU of each bacteriophage.	7. The composition of claim 6, which comprises between 10e4 and 10e12 PFU of each bacteriophage.	/
	12. A method of treatment of an infection in a mammal in need thereof comprising contacting the mammal with a composition of claim 1.	8. A method of treatment of an infection in a mammal in need thereof comprising contacting the mammal with an effective amount of an antibacterial composition, wherein said composition comprises at least one bacteriophage having lytic activity against a *P. aeruginosa* strain, said at least one bacteriophage being selected from the bacteriophages having a genome comprising any one of SEQ ID NOs: 2 – 7 or a sequence having at least 99% identity thereto.	The phage composition amount and sequence identity were specified
	13. The method of claim 12, wherein the infection is an infection of the respiratory tract.	9. The method of claim 8, wherein the infection is an infection of the respiratory tract.	Unchanged
	14. A method for improving the condition of a mammal by modifying the microbial flora in said mammal comprising contacting the mammal with a composition of claim 1.	10. A method for improving the condition of a mammal by modifying the microbial flora in said mammal comprising contacting the mammal with an effective amount of an antibacterial composition, wherein said composition comprises at least one bacteriophage having lytic activity against a *P. aeruginosa* strain, said at least one bacteriophage being selected from the bacteriophages having a genome comprising any one of SEQ ID NOs: 2 – 7 or a sequence having at least 99% identity thereto.	The phage composition amount and sequence identity were specified

(*Cont'd...*)

Table A1. (*Continued*)

Patent	Application form (20210228659-A1)	Granted form (11779617-B2)	Note
	15. A method for decontaminating a material, comprising exposing the material to a composition of claim 1.	11. A method for decontaminating a material, comprising exposing the material to an effective amount of an antibacterial composition, wherein said composition comprises at least one bacteriophage having lytic activity against a *P. aeruginosa* strain, said at least one bacteriophage being selected from the bacteriophages having a genome comprising any one of SEQ ID NOs: 2 – 7 or a sequence having at least 99% identity thereto.	The phage composition amount and sequence identity were specified
	16 – 17. (canceled)	12. The method of claim 8, wherein the composition comprises at least one of the bacteriophages selected from the group consisting of BP1777, BP1792, BP1797, BP1800, BP1902, and BP1940, said bacteriophage having a genome comprising the nucleotide sequence of SEQ ID NOs: 2 – 7, respectively.	The phage names and sequences were specified
		13. The method of claim 10, wherein the composition comprises at least one of the bacteriophages selected from the group consisting of BP1777, BP1792, BP1797, BP1800, BP1902, and BP1940, said bacteriophage having a genome comprising the nucleotide sequence of SEQ ID NOs: 2 – 7, respectively.	The phage names and sequences were specified
		14. The method of claim 11, wherein the composition comprises at least one of the bacteriophages selected from the group consisting of BP1777, BP1792, BP1797, BP1800, BP1902, and BP1940, said bacteriophage having a genome comprising the nucleotide sequence of SEQ ID NOs: 2 – 7, respectively.	The phage names and sequences were specified
Patent	**Application form (20200171108-A1)**	**Granted form (11253557-B2)**	**Note**
Patent 2	1. A bacteriophage composition comprising one or more bacteriophages selected from Sa87, J-Sa36, and Sa83.	1. A bacteriophage composition comprising at least two bacteriophages selected from Sa87, J-Sa36, and Sa83.	A minimum of two phages instead of just one for a composition
	2. The bacteriophage composition of claim 1, comprising at least two bacteriophages selected from Sa87, J-Sa36, and Sa83.		
	3. The bacteriophage composition of claim 1, comprising purified bacteriophages Sa87, J-Sa36, and Sa83.	2. The bacteriophage composition of claim 1, comprising purified bacteriophages Sa87, J-Sa36, and Sa83.	Unchanged
	4. A bacteriophage composition consisting essentially of Sa87, J-Sa36, and Sa83.	3. A bacteriophage composition consisting essentially of Sa87, J-Sa36, and Sa83.	Unchanged
	5. The bacteriophage composition of claim 1, further comprising an antibiotic.	4. The bacteriophage composition of claim 1, further comprising an antibiotic.	Unchanged
	6. The bacteriophage composition of claim 1, further comprising a pharmaceutically acceptable carrier, diluent, excipient, or combinations thereof.	5. The bacteriophage composition of claim 1, further comprising a pharmaceutically acceptable carrier, diluent, excipient, or combinations thereof.	Unchanged
	7. The bacteriophage composition of claim 3, wherein the composition comprises 1×10^{11} PFU/mL per phage.	6. The bacteriophage composition of claim 2, wherein the composition comprises 1×10^{11} PFU/mL per phage.	Unchanged
	8. The bacteriophage composition of claim 7, wherein the composition has a final endotoxin level <1000 EU/mL.	7. The bacteriophage composition of claim 6, wherein the composition has a final endotoxin level <1000 EU/mL.	Unchanged
	9. The composition of claim 8, wherein the composition is diluted 1:10.	8. The composition of claim 7, wherein the composition is diluted 1:10.	Unchanged
	10. The composition of claim 8, wherein the composition is diluted 1:100.	9. The composition of claim 7, wherein the composition is diluted 1:100.	Unchanged

(*Cont'd...*)

Table A1. (*Continued*)

Patent	Application form (20210228659-A1)	Granted form (11779617-B2)	Note
	11. The composition of claim 1, wherein the composition is administered to a mammal in a dosage range between about 1×10^{7} to about 1×10^{11} PFU of each phage at least once daily.	10. The composition of claim 1, wherein the composition is administered to a mammal in a dosage range between about 1×10^{7} to about 1×10^{11} PFU of each phage at least once daily.	Unchanged
	12. A bacteriophage composition comprising two or more purified bacteriophage populations selected from Sa87, J-Sa36, and Sa83.	11. A bacteriophage composition comprising two or more purified bacteriophage populations selected from Sa87, J-Sa36, and Sa83.	Unchanged
	13. The bacteriophage composition of claim 12, further comprising an antibiotic.	12. The bacteriophage composition of claim 11, further comprising an antibiotic.	Unchanged
	14. The bacteriophage composition of claim 12, further comprising a pharmaceutically acceptable carrier, diluent, excipient, or combination thereof.	13. The bacteriophage composition of claim 11, further comprising a pharmaceutically acceptable carrier, diluent, excipient, or combination thereof.	Unchanged
	15. The bacteriophage composition of claim 12, wherein the composition comprises 1×10^{11} PFU/mL per phage.	14. The bacteriophage composition of claim 11, wherein the composition comprises 1×10^{11} PFU/mL per phage.	Unchanged
	16. The bacteriophage composition of claim 15, wherein the composition has a final endotoxin level <1000 EU/mL.	15. The bacteriophage composition of claim 14, wherein the composition has a final endotoxin level <1000 EU/mL.	Unchanged
	17. The composition of claim 16, wherein the composition is diluted 1:10.	16. The composition of claim 15, wherein the composition is diluted 1:10.	Unchanged
	18. The composition of claim 16, wherein the composition is diluted 1:100.	17. The composition of claim 15, wherein the composition is diluted 1:100.	Unchanged
	19. The composition of claim 16, wherein the composition is administered to a mammal in a dosage range between about 1×10^{7} to about 1×10^{11} PFU of each phage at least once daily.	18. The composition of claim 15, wherein the composition is administered to a mammal in a dosage range between about 1×10^{7} to about 1×1011 PFU of each phage at least once daily.	Unchanged
	20. A kit comprising: a. bacteriophage composition according to claim 1; and b. instructions for use of the same.	19. A kit comprising: a. bacteriophage composition according to claim 1; and b. instructions for use of the same.	Unchanged
	21. The kit of claim 20, further comprising an antibiotic and instructions for the use of the same in combination with the bacteriophage composition.	20. The kit of claim 19, further comprising an antibiotic and instructions for the use of the same in combination with the bacteriophage composition.	Unchanged
	22. The kit of claim 21, wherein said instructions are for use of the same in treating a *S. aureus* infection, preferably a *S. aureus* pulmonary infection.	21. The kit of claim 20, wherein said instructions are for use of the same in treating a *S. aureus* infection.	Unchanged
		22. The kit of claim 21, wherein the *S. aureus* infection is a pulmonary infection.	Unchanged

Abbreviations: PFU: Plaque-forming unit; LMG: Laboratory of Microbiology, Ghent University; *P. aeruginosa: Pseudomonas aeruginosa; S. aureus: Staphylococcus aureus.*

ACCSCIENCE PUBLISHING

Microbes & Immunity

ORIGINAL RESEARCH ARTICLE

Modulation of host immune response by carotene supplementation in a COVID-19 vaccination mouse model

Kang Wei Tan, Saatheeyavaane Bhuvanendran, Kar Wai Hong, Uma Devi Palanisamy, and Ammu Kutty Radhakrishnan*

Food as Medicine Research Strength, Jeffrey Cheah School of Medicine and Health Sciences, Monash University Malaysia, Selangor, Malaysia

Abstract

Carotenoids, known for their immunomodulatory and gut microbiota-modulating effects, have drawn attention as potential dietary adjuvants to enhance vaccine efficacy and maintain gut health. This study aimed to evaluate the effect of carotene supplementation on immune response with insight into gut microbiome using an *in vivo* animal model. The BALB/c mice were fed daily with CaroGaia (50 mg/kg of body weight), a carotene supplement that contained 33.3% α-carotene and 66.6% β-carotene, by oral gavage for 70 days. Mice fed with the vehicle served as controls. The mice in the vaccinated groups received two doses of the CoronaVac inactivated virus vaccine on days 14 and 42. Flow cytometry revealed no significant modulation of lymphocyte subsets (total T lymphocytes, T-helper cells, cytotoxic T lymphocytes, and B cells) with carotene supplementation. In addition, there were no significant differences in the levels of SARS-CoV-2 immunoglobulin G and interferon-gamma in plasma between treatment and control groups. In contrast, the vaccinated carotene group showed an increased SARS-CoV-2 antigen-specific splenocyte proliferation. In the gut microbiome, carotene supplementation appeared to alter the gut microbiota composition. However, no significant changes were observed in the short-chain fatty acids (SCFA) levels, such as acetic acid, butyric acid, and propionic acid. Furthermore, the differential abundance analysis showed that carotene supplementation reduced the levels of SCFA producers (*Odoribacter* and *Monoglobus* genera) in unvaccinated mice compared to the control group, while it enriched the level of SCFA producers (Ruminococcaceae family) and reduced pathobiont levels, commensal bacteria that have pathogenic potential (*Mucispirillum* genus), in the vaccinated group.

Keywords: COVID-19; SARS-CoV-2; Vaccination; Carotenoid; Carotene; Immune-modulation; Gut microbiota; Short-chain fatty acid

***Corresponding author:**
Ammu Kutty Radhakrishnan (ammu.radhakrishnan@monash.edu)

Citation: Tan KW, Bhuvanendran S, Hong KW, Palanisamy UD, Radhakrishnan AK. Modulation of host immune response by carotene supplementation in a COVID-19 vaccination mouse model. *Microbes & Immunity*. 2025;2(3):72-86. doi: 10.36922/MI025110021

Received: March 10, 2025

Revised: April 8, 2025

Accepted: April 21, 2025

Published online: May 15, 2025

1. Introduction

The coronavirus disease 2019 (COVID-19), caused by the severe acute respiratory syndrome coronavirus 2 (SARS-CoV-2), emerged in China in late 2019.[1] By March 2020, the World Health Organization had declared it a pandemic. The virus rapidly spread worldwide, causing severe disruptions to societies, economies, and politics. The pandemic had led to millions of infections and deaths without signs of abating. Given

the ability of vaccines to expose the immune system to antigens and activate targeted immune responses, there was an urgent need to roll out vaccination programs to reduce the morbidity and mortality associated with COVID-19. Therefore, mass vaccination against SARS-CoV-2 has been widely implemented to curb the spread of the disease.

Vaccination offers substantial protection by generating immunological memory against the virus, enabling the rapid production of neutralizing antibodies upon subsequent exposure. Among the COVID-19 vaccines, the mRNA platform has garnered significant attention as it represents the first widespread application of mRNA vaccination in humans. Despite this advancement, the seemingly traditional inactivated virus vaccines continue to be administered due to factors including public hesitancy toward mRNA vaccines and the logistical challenges posed by the stringent storage and delivery requirements.[2] However, inactivated virus vaccines have generally demonstrated lower efficacy against COVID-19 than their mRNA counterparts.[3] Two to three doses of inactivated COVID-19 vaccines were reported to provide 90.15% protection against severe and critical COVID-19 cases, even in the most vulnerable elderly population (≥60 years old).[4] However, the immune response specific to SARS-CoV-2 elicited by two doses of CoronaVac, an inactivated virus vaccine, was reported to wane significantly after 6 months.[5] Consequently, a booster or third dose of the vaccine was highly recommended.[5] Hence, there is a need to improve and maintain the immune response to the vaccine. Various factors affect the normal functioning of the immune system, including nutrition, lifestyle habits, stress levels, and sleep quality.

The immune system comprises a repertoire of cells, tissues, and molecules that work together to mediate resistance against infections.[6] It is well established that B cells, cluster of differentiation 4-positive ($CD4^+$) regulatory T (Treg) cells, and $CD8^+$ cytotoxic T lymphocytes (CTLs) are the three essential components of the adaptive immune system responsible for controlling SARS-CoV-2 infection.[7] Clinical trials reported that inactivated SARS-CoV-2 vaccination activates both innate and adaptive immunity, resulting in the upregulation of immune cells, such as $CD16^+$ monocytes, $CD4^+$ Treg cells, and $CD8^+$ CTLs, along with increased levels of neutralizing antibodies.[8] B cells play a pivotal role in antibody-mediated (humoral) immunity.[9] Upon activation, the activated antigen-specific B cells differentiate into plasma cells, which produce antigen-specific antibodies, and memory B cells, which enable a swift response upon reinfection.[9] The T-helper (Th) cells secrete cytokines that can regulate B cell activation and CTLs,[7] while the CTLs kill virus-infected or abnormal cells.[10] A well-balanced diet is widely recognized as crucial for optimal cellular functioning, including those in the immune system.[11] When the immune system is activated during an infection, it requires abundant energy for clonal expansion and the production of new proteins and structures. Therefore, optimal nutrition is essential for immune cells to respond to pathogens rapidly and effectively. Micronutrients, such as vitamins and trace elements, are essential to support both the innate and adaptive immune systems.[11] Research suggests that deficiencies or low levels of these micronutrients can weaken immune function and reduce resistance to infections.[11]

Nutritional interventions have potent effects on the activation of host immune systems. Carotenoid supplements are nutritional interventions that exhibit diverse bioactivities, including antioxidant, anti-inflammatory, and anticancer properties.[12] The main carotenoids in crude palm oil are α- and β-carotenes, which comprise 41.3% and 41.0% of the total carotenoids in commercial red palm oil, respectively.[13] Carotenes are fat-soluble Vitamin A pre-cursors metabolized in the gut or liver to produce retinol, commonly known as Vitamin A. Vitamin A deficiency is the most common micronutrient deficiency globally, especially in developing countries with low meat and protein intake.[14] In addition, Vitamin A deficiency in infants and children has been associated with reduced immune response and is a risk factor for several diseases, particularly vision impairment.[15] Besides animal products, Vitamin A can be obtained from Vitamin A pre-cursors, such as α- and β-carotenes.[14] Carotenoids have been reported to have immunomodulatory effects by increasing the activity of natural killer (NK) cells and plasma interferon-gamma (IFN-γ) levels in a xenograft model of human breast cancer.[16] In this model, carotene supplementation upregulated anti-inflammatory markers (interleukin 4 [IL-4] and IL-13) while downregulating pro-inflammatory markers (IL-β, IL-6, and tumor necrosis factor-α) in nude mice.[17] In addition, carotene supplementation enhanced the production of peripheral blood NK cells and B cells, thus supporting the immunomodulatory effects of carotenes.[17] Numerous cellular models concluded that β-carotene and its metabolites display antioxidant activity through the inhibition of reactive nitrogen ($ONOO^-$) and oxygen species (H_2O_2), respectively, reducing lipid peroxidation activity.[15] In addition, Vitamin A supplementation in porcine circovirus type 2-vaccinated pre-pubertal gilts has been reported to significantly increase circovirus antibody titers compared to the control group.[18] Although numerous studies have demonstrated the immunomodulatory potential of Vitamin A and its pre-cursors as dietary supplements, their mechanism of action remains poorly understood.

The gastrointestinal tract (GIT) is the home to the gut-associated lymphoid tissue (GALT), the largest immune organ in the human body.[19] GALT forms part of the mucosa-associated lymphoid tissue and comprises many immune cells. Hence, GIT is a primary site for immune activities. At the same time, the GIT, particularly the colon, serves as an invaluable repository for gut microbiota, such as bacteria, viruses, and fungi.[19] The comprehensive collection of gut microbiomes can contribute to a vast palette of metabolic enzymes and pose a greater metabolic potential than their host.[19] Due to the proximity between gut microbiota and GALT, they inevitably affect one another as these gastrointestinal inhabitants can interact with nutrition and selectively promote or inhibit specific bacteria, thereby modulating gut microbiota populations.[20] In addition, the gut microbiome plays crucial roles in nutrition metabolism, energy metabolism, and immunomodulation.[20] Studies reported that short-chain fatty acids (SCFAs), metabolites produced by the gut microbiota, can enhance B-cell metabolism to support the production of the energy required to generate antibodies and cytokines.[21] These metabolites also upregulate genes responsible for plasma cell differentiation and class switching, vital for immune responses to pathogens or vaccines. The present literature suggests that carotene supplementation can modulate host gut microbiota and SCFA production.

The SCFAs are key metabolites produced by gut microbiota, which can modulate immune response and regulate the activity of innate cells, such as macrophages, neutrophils, and dendritic cells.[22] For example, SCFAs were reported to limit SARS-CoV-2 infection by downregulating the level of angiotensin-converting enzyme 2, the main receptor responsible for viral infections, while improving antiviral immunity.[23] In addition, SCFAs can also control SARS-CoV-2 infection by downregulating transcription of genes responsible for modulation of viral entry and replication, such as IFN, transmembrane protease serine 2, and retinoic acid-inducible gene 1 receptors, while maintaining the permeability of intestinal cells.[19] Moreover, SCFAs can modulate the differentiation of T lymphocytes and B cells, which are responsible for the adaptive immune response.[22]

This study used a mouse model to investigate how daily carotene supplementation modulates the immune response to COVID-19 vaccination. This research aimed to unveil the mechanism of action of carotene supplementation in immune response post-vaccination and provide evidence of its health benefits. In addition, this study also explored how carotene influences gut microbiota and SCFA production, offering insights into the overall action of carotene supplementation.

2. Materials and methods

2.1. Materials

CaroGaia (30% oil suspension) used for dietary intervention was a gift from PhytoGaia Sdn Bhd, Malaysia. The vehicle used was palm oil (Buruh Cooking Oil, Lam Soon, Malaysia). The inactivated SARS-CoV-2 vaccine (CoronaVac, Sinovac Biotech Ltd, China) was a kind gift from Pharmaniaga Lifescience Sdn Bhd, Malaysia.

2.2. Ethical approval

The ethical approval for this study was obtained from the Monash University Animal Ethics Committee (AEC Project ID: 29899).

2.3. Animal study design

Ten-week-old male BALB/c mice were obtained and housed individually at the animal holding facility of Monash University Malaysia. A total of 32 mice were used in this study. The mice were acclimated to the housing conditions for 1 week before the study began. During the study, the mice were subjected to a 12-h light/12-h dark cycle with *ad libitum* access to food and water. A standard mouse pellet chow was provided throughout the study. The experimental design is illustrated in Figure 1. Briefly, 32 male BALB/c mice were evenly divided into two dietary intervention groups, that is, (i) control (fed with the vehicle – palm oil) and (ii) carotene-fed group. The mice were fed daily with 100 µL of carotene (50 mg/kg body weight) or palm oil (vehicle) through gavage. On day 14, the mice in each dietary group were split into two sub-groups, that is, (i) non-vaccinated (phosphate-buffered saline [PBS]) and (ii) vaccinated (CoronaVac) (Table 1). Vaccination was administered by an intramuscular injection into the hind leg of the mice using a 30G needle, with 0.1 mL of CoronaVac (0.6 µg) as vaccine intervention for the vaccinated subgroup and 0.1 mL of PBS as control for the non-vaccinated subgroup. On day 42, plasma samples were collected from the mice and were given a second dose of CoronaVac or PBS. At the study's endpoint (day 70), the mice were humanely euthanized, and samples of plasma, feces, and spleens were collected for analysis.

2.4. Mice euthanasia

On day 70, the mice were weighed to calculate and prepare the dosage for a ketamine and xylazine cocktail, at concentrations of 100 mg/kg and 10 mg/kg, respectively. The concoction was administered through intraperitoneal injection. Once the mice were determined to be fully anesthetized, euthanasia was performed by cardiac puncture.

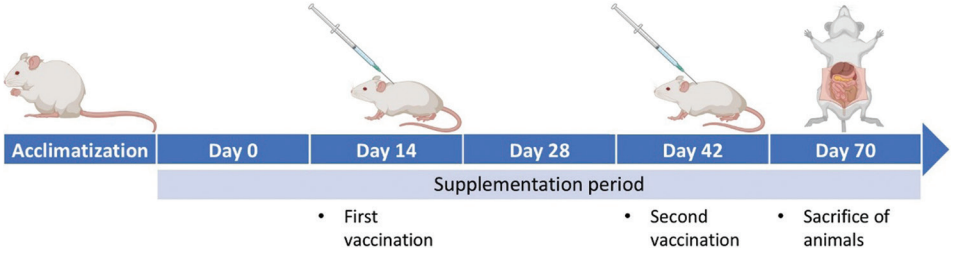

Figure 1. The animal study design. In the supplementation period, half the mice were fed daily with 100 µL vehicle (palm oil), while the other half were fed with 100 µL carotene (50 mg/kg body weight) by oral gavage for 70 days. For vaccination, half the mice in each supplementation arm received intramuscular injections of 100 µL (0.6 µg) of the CoronaVac or 100 µL PBS (control) on days 14 and 42.

Table 1. Animal grouping

Dietary intervention	Vaccine intervention	Number of mice
Vehicle (palm oil)	PBS	8
	C19V	8
Carotene (50 mg/kg body weight)	PBS	8
	C19V	8
Total		32

Abbreviations: C19V: CoronaVac vaccine; PBS: Phosphate-buffered saline.

2.5. Isolation of splenocyte

During the autopsy, the spleen was aseptically collected and transferred to a petri dish containing 6 mL of RPMI 1640 culture medium (11875-093, Gibco, USA) supplemented with 5% fetal bovine serum (FBS; A5256701, Gibco, USA), 1% penicillin-streptomycin (15140122, Gibco, USA), and 1% glutamine. The splenic capsules were carefully snipped to release the splenocytes into the medium. The resulting splenocyte suspension was transferred into 15 mL Falcon tubes and kept on ice. Splenocytes were isolated through centrifugation (1,200 rpm for 10 min at 4°C).

2.6. Splenocyte proliferation assay

This assay was carried out to determine the proliferation of splenocytes in response to stimulation with CoronaVac. The supernatant was discarded, and the splenocytes were resuspended in 1 mL of complete culture medium (RPMI 1640 medium supplemented with 10% FBS and penicillin-streptomycin). The cell density was adjusted to 5×10^4 splenocytes/mL in complete medium containing 10 µg/mL of COVID-19 vaccine. The cells were seeded into a 96-well culture plate at 200 µL per well (5×10^3 cells/well), and the plate was incubated for 72 h at 37°C in a humidified incubator with 5% CO_2. Splenocyte proliferation was assessed using the Cell Counting Kit-8 (CK04-01, Dojindo, Japan). The culture supernatants were harvested and stored at -80°C for subsequent cytokine analysis.

2.7. Immunophenotyping using flow cytometry

The peripheral blood lymphocytes collected in heparinized tubes were analyzed using fluorochrome-labeled antibodies to $CD3^+$ T lymphocytes, $CD4^+$ Th cells, $CD8^+$ CTLs, and B cells, and a flow cytometer (FACSVerse cell analyzer, BD, USA). The immunostaining was carried out according to the manufacturer's protocol.

2.8. IFN-γ production

The amount of IFN-γ, a cytokine crucial for macrophage activation and antigen presentation, in the supernatant of splenocyte cultures, was quantified using a commercial mouse IFN-γ enzyme-linked immunosorbent assay (ELISA) kit (#88-7314-88, Invitrogen, USA) using the manufacturer-recommended protocol.

2.9. Plasma SARS-CoV-2 recombinant receptor-binding-domain antibody levels

The plasma SARS-CoV-2 recombinant receptor-binding-domain (RBD) antibody level was quantified using the SARS-CoV-2 RBD mouse immunoglobulin G (IgG) ELISA kit (CoV2-RBD mIgG, Novatein Biosciences, USA) as per the manufacturer-recommended protocol. A mouse SARS-CoV-2 spike-neutralizing antibody (#40592-MM57, Sino Biological, China) was used as a positive control. The assay was carried out according to the recommended protocol.

2.10. Characterization of gut microbiota

2.10.1. DNA purification and sequencing

To evaluate the impact of carotene supplementation on gut microbiota, 16S amplicon sequencing was performed on fecal samples collected at the endpoint, day 70. The bacterial genomic DNA (gDNA) was extracted using the QIAamp® PowerFecal® Pro kit (QIAGEN, Germany) according to the manufacturer's instructions. The quality and concentration of the gDNA were determined using a nano-spectrophotometer. The V3–V4 region was targeted for sequencing, using forward primer

5'-CCTAYGGGRBGCASCAG and reverse primer 5'-GGACTACNNGGGTATCTAAT. The DNA samples were sent to an accredited laboratory (NovogeneAIT Genomics, Singapore) for library preparation, sequencing, and bioinformatics analysis.

2.10.2. Bioinformatics analysis pipeline

The raw FASTQ files from sequencing were analyzed using the bioinformatics methods outlined in Table 2.

2.11. Determination of SCFA levels in fecal samples

The levels of SCFAs in fecal samples were identified and determined using gas chromatography-mass spectrometry (GC-MS) (Agilent 7890A Gas Chromatograph, Agilent, USA). The water-methanol (80:20, v/v, pH 1.5 – 2.5) diluent, standard stock, and internal standards were prepared according to Gray *et al.*[24] with slight modifications. Stock solutions of acetic acid (30.0 µL), propionic acid (30.3 µL), isobutyric acid (39.0 µL), and butyric acid (32.7 µL) were prepared in acidified diluent to achieve the final concentrations of 52.60 mM, 39.43 mM, 42.05 mM, and 36.80 mM, respectively. The internal standard (4-methyl valeric acid) was spiked into all calibration standards at a concentration of 7.9 mM. The calibration curves of all SCFA standards were then established to allow quantification of SCFA levels in fecal samples.

The fecal samples were withdrawn from −80°C storage, thawed, and homogenized in 1,993 µL of the water-methanol diluent with 7 µL of phosphoric acid (85% w/w) and mixed thoroughly for 10 min using a vortex (Vortex-Genie 2, Scientific Industries, USA). The fecal suspensions were centrifuged (12,000 rpm for 10 min), and 1,800 µL of the supernatant was transferred to 2 mL GC vials. The 46.7 µL of internal standard (7.9 mM) was added to each vial before analysis.

SCFAs were quantified using an Agilent 8890 gas chromatograph (G3542A, Agilent Technologies, USA) paired with a 5977C mass selective detector (G7077C, Agilent Technologies, USA), and a 7693A automatic liquid sampler (G4513A, Agilent Technologies, USA). Hydroguard FS water-resistant guard column (5 m length, 0.25 mm ID, 10079, Restek, USA) was used in combination with a high polarity, DB-FATWAX Ultra Inert PEG column (30 m length, 0.25 mm ID, 0.25 film thickness, G3903-63008, Agilent Technologies, USA). Data were analyzed using the Enhanced ChemStation software (version E.02.02.1431, Agilent, USA).

2.12. Statistical analysis

All statistical analyses were performed using Prism 10.3.1 (GraphPad, USA). Comparisons between two groups were evaluated with a two-tailed unpaired *t*-test with Welch's correction, while multiple group comparisons were conducted using analysis of variance (ANOVA) with Tukey *post hoc* test. A $p<0.05$ was considered statistically significant.

3. Results

This section outlines the results of the study.

3.1. Modulation of immune responses by carotene supplementation

The effect of carotene supplementation under various conditions is outlined in the following subsections.

3.1.1. Effect of carotene supplementation on lymphocyte subsets

The data from the flow cytometry analysis revealed no significant differences in $CD3^+$ T lymphocytes, $CD4^+$ Th cells, $CD8^+$ CTLs, and B cells between the baseline groups and carotene supplementation groups (Figure 2 and Table A1).

3.1.2. Effect of carotene supplementation on SARS-CoV-2-specific antibody production

The plasma samples collected on days 42 and 70 of the intervention were used to determine the SARS-CoV-2-specific

Table 2. Methods used for bioinformatics analysis

Data processing	Description	Methods/packages
Sequence assembly	Merge paired-end reads	BBMap
Data split	Trimming primer sequences	QIIME
Amplicon sequence variant (ASV) denoise	Reconstruct ASVs from noisy amplicon sequencing reads	DADA2 in QIIME
Taxonomy classification	Classify pre-processed reads to the respective taxonomy	QIIME using silva138 AB V3–V4 classifier
Generation of phyloseq object	Export QIIME artifact into phyloseq	QIIME2R
Heatmap	Visualization of microbiome compositions	pheatmap in R
Alpha diversity	Estimation of alpha diversity	Tidyverse in R
Beta diversity	Estimation of beta diversity	mia and miaViZ in R
Differential abundance analysis	Identify differentially abundant microbes	LEfSe, DESeq2, and corncob in R

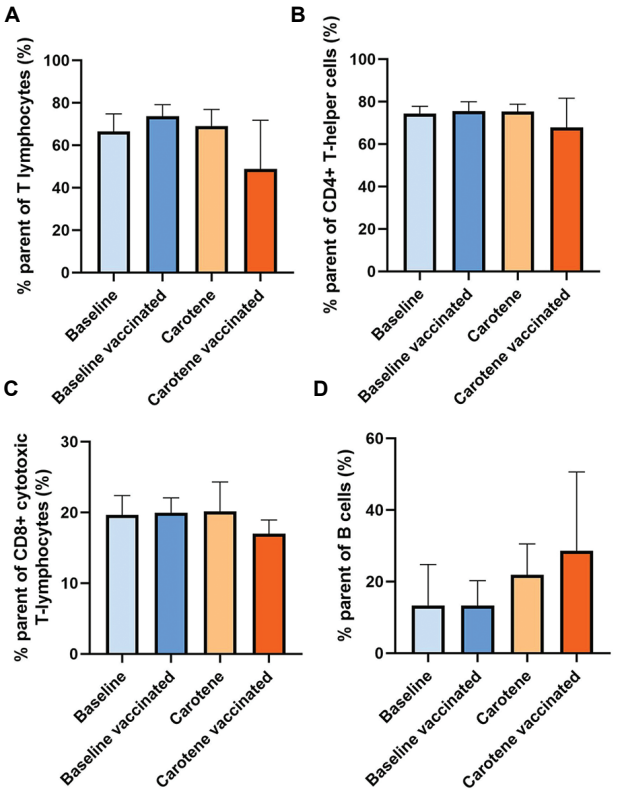

Figure 2. Quantification of (A) cluster of differentiation 3-positive ($CD3^+$) T lymphocytes, (B) $CD4^+$ T-helper cells, (C) $CD8^+$ cytotoxic T lymphocytes, and (D) B cells in the peripheral blood of mice from the four study groups: (i) baseline (control mice fed daily with the vehicle palm oil), (ii) baseline vaccinated (control mice fed daily with the vehicle and injected with CoronaVac), (iii) carotene (mice fed daily with carotene), and (iv) carotene vaccinated (mice fed daily with the carotene and injected with CoronaVac). Multiple comparisons using ordinary one-way ANOVA revealed no significant differences in the percentage of lymphocytes between these groups ($p>0.05$). Data are presented as mean ± SD, derived from three mice ($n=3$) per group.

IgG antibody level (Figure 3). There were no significant differences in the plasma SARS-CoV-2 levels between the carotene supplementation group and the vehicle group.

3.1.3. Effect of carotene supplementation on SARS-CoV-2 antigen-induced splenocyte proliferation

Splenocytes from carotene-fed mice cultured in the presence of the SARS-CoV-2 antigen showed significantly higher proliferation than splenocytes from the vehicle-vaccinated animals ($p<0.05$, Figure 4 and Table A2).

3.1.4. Effect of carotene supplementation on IFN-γ production

The supernatant of splenocyte cultures from the carotene-vaccinated group showed higher levels of IFN-γ production (Figure 5). However, the difference was not statistically significant ($p>0.05$).

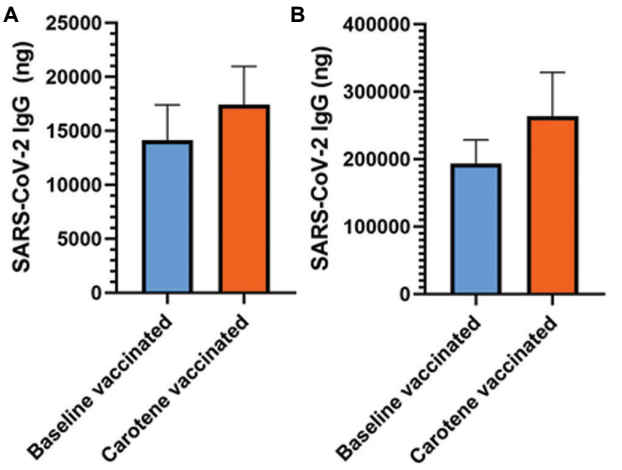

Figure 3. Quantification of plasma SARS-CoV-2 immunoglobulin G (IgG) levels from mice in the baseline vaccinated (control mice fed daily with the vehicle and injected with CoronaVac) and carotene vaccinated (mice fed daily with the carotene and injected with CoronaVac) groups on days (A) 42 and (B) 70. Data are presented as mean ± SD, derived from three mice ($n=3$) per group.

3.2. Modulation of gut microbiota by carotene supplementation

3.2.1. Alpha diversity

Alpha diversity determines the structure of single microbial communities based on richness and evenness.[25] Richness represents the total number of species present in a community, whereas evenness represents the uniformity of relative species abundances within a community.[25] Several alpha diversity indices, such as Chao1, Inverse Simpson, Pielou, and Shannon, are applied to determine alpha diversity. The Chao1 index is a diversity estimator of species richness, highlighting rare species. The inverse Simpson index measures both richness and evenness.[25] Pielou's index indicates the evenness of species distribution. The Shannon index also measures species richness and evenness, emphasizing rare species more than the Simpson index.[25] Carotene supplementation did not significantly affect the alpha diversity in vaccinated and unvaccinated subjects compared across all groups (Figure 6), suggesting that carotene supplementation did not substantially impact the overall microbial diversity in terms of richness and evenness.

3.2.2. Beta diversity

Beta diversity is a comparative analysis of the composition of different microbial communities. It measures how distinct one microbial community is from another, illustrating the variability of microbial composition between samples.[25] No significant differences were observed across the groups in the principal coordinate analysis scatter plot based on multidimensional scaling of Aitchison distance (Figure 7).

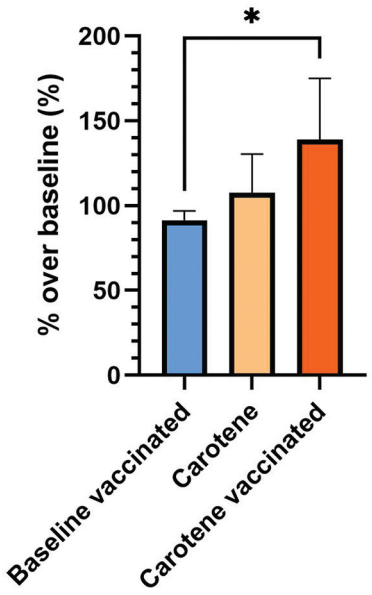

Figure 4. Splenocyte proliferation rate across baseline (fed daily with the vehicle), baseline vaccinated (fed daily with the vehicle and injected with CoronaVac), carotene (fed daily with carotene), and carotene vaccinated (fed daily with carotene and injected with CoronaVac) groups at day 70. The splenocytes were cultured in the presence of CoronaVac (10 μg/mL) for 72 h. Splenocyte proliferation was determined using the Cell Counting Kit-8. Data are presented as the percentage of cell culture compared to proliferation observed in the splenocyte cultured from mice in the baseline group, expressed as mean ± SD, derived from six mice (n=6) per group.
Note: *p<0.05.

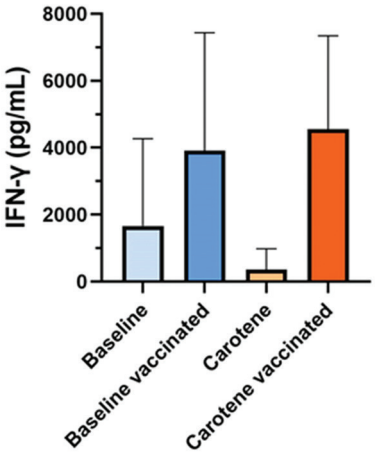

Figure 5. Quantification of interferon-gamma (IFN-γ) across baseline (fed daily with the vehicle), baseline vaccinated (fed daily with the vehicle and injected with CoronaVac), carotene (fed daily with carotene), and carotene vaccinated (fed daily with the carotene and injected with CoronaVac) groups at day 70. The splenocytes were cultured in the presence of CoronaVac (10 μg/mL) for 72 h. The IFN-γ concentration in each group's culture supernatant was determined using a commercial IFN-γ enzyme-linked immunosorbent assay kit. Data are presented as mean ± SD, derived from three mice (n=3) per group.

3.2.3. Taxonomic abundance cluster heatmap

The composition of the microbial community was visualized with a composition heatmap (Figure 8). The Y-axis represents the bacterial taxa, and the X-axis represents samples. The colour of each intersection depicts the taxon abundance in the sample.

3.2.4. Differential abundance analysis

Differential abundance analysis is carried out to determine the differences between microbial communities. In this project, multiple differential abundance analysis methods (e.g., DESeq2, LEfSe, and Corncob) were utilized to cross-validate results as different methods varied in statistical assumptions regarding data distribution, sparsity, and the handling of zero inflation.[26] Applying multiple methods yielded overlapping and distinct sets of differentially abundant taxa. The differences can be attributed to the varying statistical assumptions. Overlapping taxa suggest a high level of confidence in the biological relevance of these taxa, as they are robustly detected across methods that handle data differently. This combined approach allows for a comprehensive assessment of microbial changes, and taxa that were consistently identified across methods were prioritized for interpretation in this study.

(a) Modulation of gut microbiome by carotene in unvaccinated groups

Carotene supplementation in the unvaccinated group displayed a reduction in *Odoribacter*, as identified by both LEfSe and DESeq2 analyses, and a reduction of *Monoglobus*, as indicated by DESeq2 and corncob methods (Figure 9).

(b) Modulation of gut microbiome by carotene in vaccinated groups

The DESeq2 and corncob analyses reported enrichment of the Ruminococcaceae family and reduction of the *Mucispirillum* genus in the vaccinated carotene supplementation group (Figure 10).

3.3. Effect of carotene supplementation on SCFA production

SCFAs are crucial metabolites produced by intestinal microbiota that contribute to intestinal and immune homeostasis. Targeted metabolomics was carried out to quantify the levels of SCFAs in fecal samples using GC-MS (Figure 11). There were no significant differences observed in the fecal acetic acid, butyric acid, or propionic acid across the four groups.

4. Discussion

In this study, the effects of carotene supplementation from palm oil as an adjuvant to enhance or modulate the

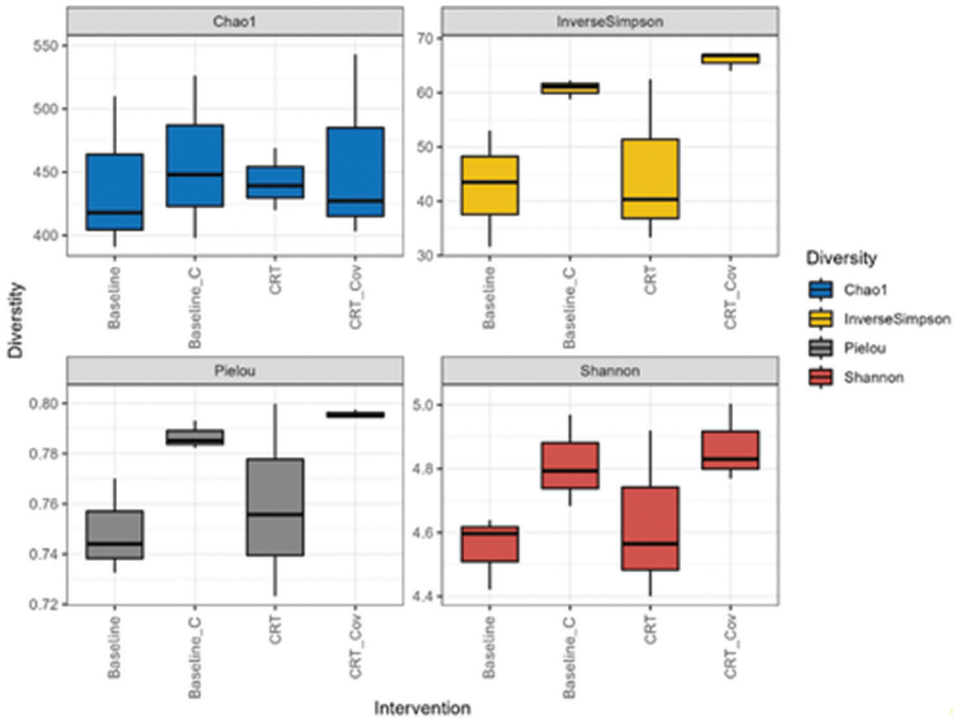

Figure 6. Box plots of alpha diversity indices (Chao1, Inverse Simpson, Pielou, and Shannon) of microbial diversity in feces of Baseline (fed with the vehicle), Baseline_C (fed with the vehicle and vaccinated with CoronaVac), CRT (fed with carotene), and CRT_Cov (fed with carotene and vaccinated with CoronaVac) groups. No significant differences were observed across the four groups in all indices. Data are presented as mean ± SD, derived from three mice (n = 3) per group.

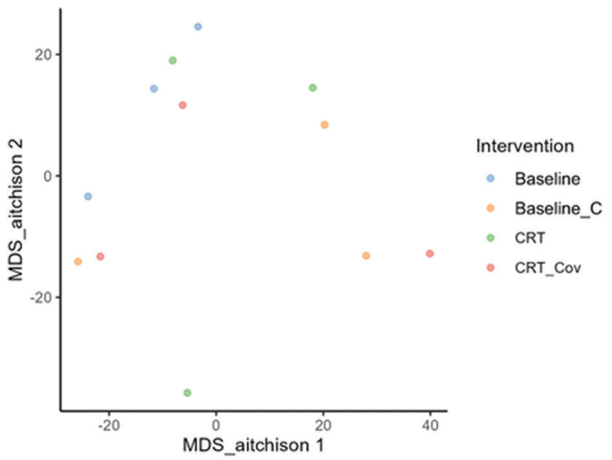

Figure 7. Scatter plot of principal coordinates analysis illustrating the beta diversity of microbial communities in feces from Baseline (fed with the vehicle), Baseline_C (fed with the vehicle and vaccinated with CoronaVac), CRT (fed with carotene), and CRT_Cov (fed with carotene and vaccinated with CoronaVac) groups. No significant differences were observed across the four groups. Data are derived from three mice (n=3) per group.
Abbreviation: MDS: Multidimensional scaling.

immune response to an inactivated COVID-19 vaccine were explored in a mouse model. The results from the flow-cytometry analysis showed no significant difference in the percentages of adaptive immune cells, such as B cells, $CD4^+$ Th cells, and $CD8^+$ CTLs, across the study groups. The daily supplementation of carotene did not significantly modulate lymphocyte counts in vaccinated and unvaccinated mice. The result aligns with an earlier random clinical trial, where the effect of daily β-carotene supplementation on immunity was investigated.[27] The β-carotene supplementation reported no significant changes in *in vitro* lymphocyte proliferation and production of IL-2. In addition, β-carotene supplementation resulted in no significant difference in profiles of leukocyte subsets ($CD3^+$ total T lymphocytes, $CD4^+$ Th cells, $CD8^+$ CTLs, and B cells). In contrast, the results from another random clinical trial demonstrated that moderate daily supplementation of β-carotene (15 mg/day for 26 days) enhanced cell-mediated immune responses in non-smoking males through upregulating the expression of major histocompatibility class II proteins, for example, the human leukocyte antigen-DR – a functional surface protein on monocytes associated with improved host immune response to antigenic stimulation.[28]

Humoral immunity was evaluated by quantification of antibody levels. In this study, daily carotene

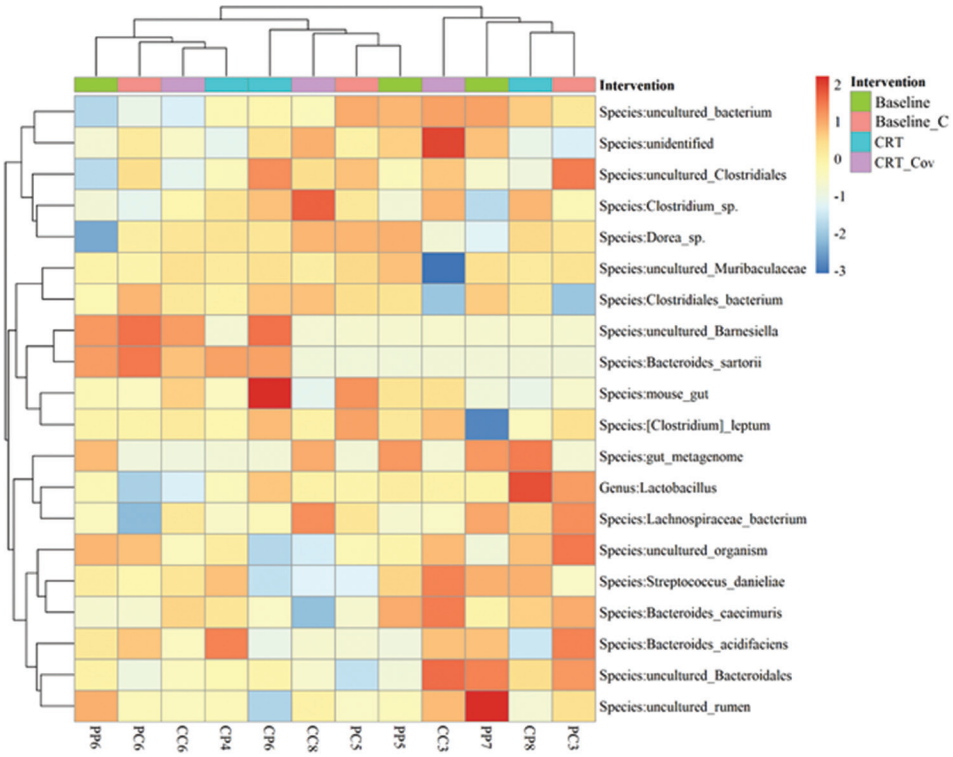

Figure 8. Taxonomic abundance cluster heatmap illustrating the abundance information of the top 20 phyla of all samples from Baseline (fed with the vehicle), Baseline_C (fed with the vehicle and vaccinated with CoronaVac), CRT (fed with carotene), and CRT_Cov (fed with carotene and vaccinated with CoronaVac) groups. The scale and legend in the upper right corner of the figure depict the colors in the heatmap associated with the relative abundance of operational taxonomic unit (y-axis) within each sample (x-axis).
Abbreviations: CC: Carotene vaccinated; CP: Carotene; PC: Baseline vaccinated; PP: Baseline.

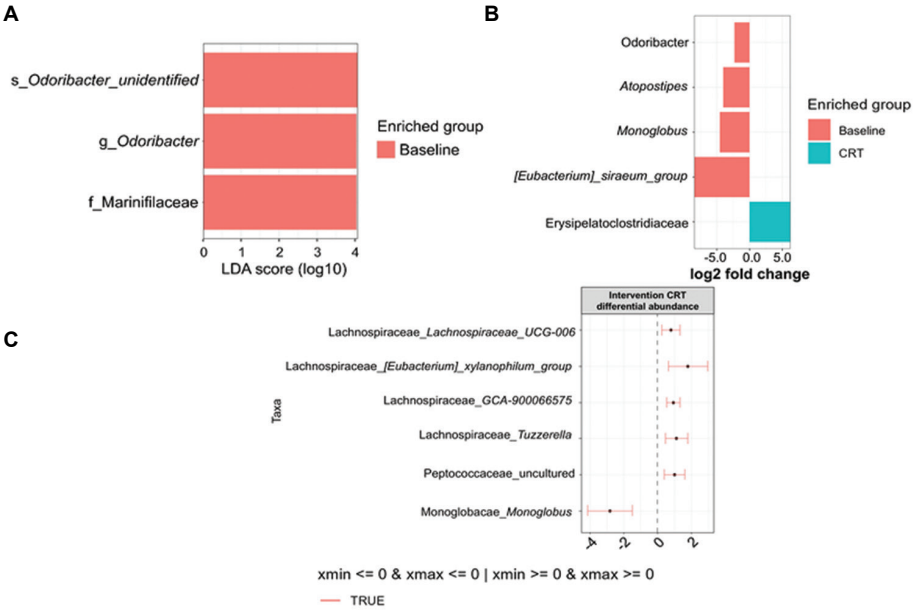

Figure 9. Comparison of differentially abundant bacterial taxa between unvaccinated groups receiving carotene supplementation (CRT) and vehicle palm oil (Baseline). (A) LEfSe histogram of linear discriminant analysis (LDA) scores for significant abundance differential in bacterial taxa. An LDA >4 represents species whose abundance shows differences between groups. (B) DESeq2 analysis graph showing log2 fold change to measure the significant abundance of the bacterial taxa (p<0.05) between groups. (C) Corncob plot using 5% false discovery rate-adjusted p-value (q-value) cutoff to measure the significant abundance of the bacterial taxa between groups. Data are derived from three mice (n=3) per group.

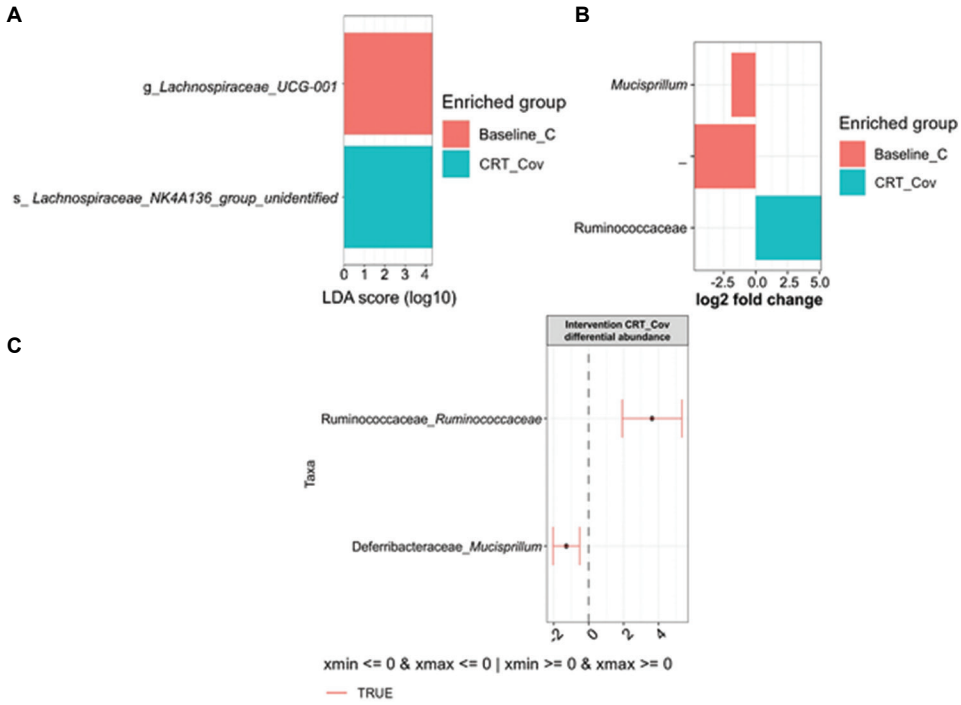

Figure 10. Comparison of differentially abundant bacterial taxa between vaccinated groups receiving carotene supplementation (CRT_Cov) and vehicle palm oil (Baseline_C). (A) LEfSe histogram of linear discriminant analysis (LDA) scores for significant abundance differential in bacterial taxa. An LDA >4 represents species whose abundance shows differences between groups. (B) DESeq2 analysis graph showing log2 fold change to measure the significant abundance of the bacterial taxa ($p< 0.05$) between groups. (C) Corncob plot using 5% false discovery rate-adjusted p-value (q-value) cutoff to measure the significant abundance of the bacterial taxa between groups. Data are derived from three mice (n=3) per group.

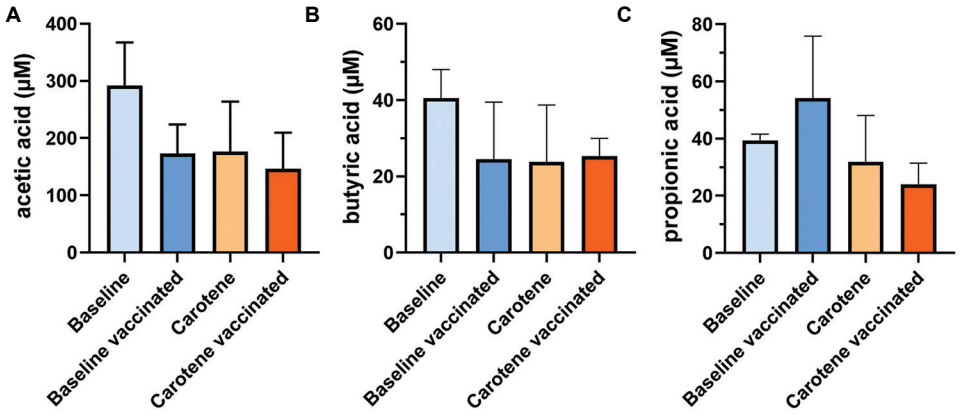

Figure 11. Quantification of short-chain fatty acids in mouse fecal samples after 70 days of nutritional interventions (carotene or vehicle) using gas chromatography-mass spectrometry. (A) Acetic acid. (B) Butyric acid. (C) Propionic acid. Data are presented as mean ± SD, derived from three mice (n=3) per group, and were analyzed using one-way ANOVA with Tukey *post hoc* test.
Notes: Baseline: mice fed with vehicle (palm oil); Baseline vaccinated: Mice fed with vehicle and vaccinated with CoronaVac; Carotene: mice fed with carotene; Carotene vaccinated: mice fed with carotene and vaccinated with CoronaVac.

supplementation reported no significant effect on SARS-CoV-2 IgG levels compared to the baseline group. A similar result was observed in Vitamin A dietary intervention in calves inoculated with an inactivated bovine coronavirus (BCoV) vaccine, where there were no significant differences in antibody responses (serum IgG_2, IgM, IgA and fecal IgA) between groups fed with high Vitamin A (3,300 U/kg) and low Vitamin A (1,100 U/kg).[29] However, the high Vitamin A-supplemented group displayed significantly higher serum IgG_1 titers than the low Vitamin A-supplemented group after two doses of the inactivated BCoV vaccine. Similar findings were also reported in influenza A-infected BALB/c mice supplemented with Vitamin A, where the control group (4,000 IU/kg diet)

reported a significantly higher IgG response than the high Vitamin A-supplemented group (250,000 IU/kg diet).[30]

The proliferation rate of splenocytes in response to an antigen represents the spleen's multiplication rate in response to the antigenic stimulus. This serves as an indicator of vaccine response, immune activation, and T-cell and B-cell responses. In this study, the splenocytes from vaccinated mice fed with carotene showed a higher proliferation rate ($p<0.05$) than those from vaccinated mice fed with the vehicle, suggesting that carotene supplementation can modulate the host immune system. A similar result was reported in a study on astaxanthin, a type of carotenoid, in BALB/c mice, where lipopolysaccharide (LPS)-induced lymphocyte proliferation was significantly increased by astaxanthin administration.[31]

Interferon-gamma is a pro-inflammatory cytokine produced by activated Th1 cells, CTLs, and NK cells.[32] This cytokine is pivotal in stimulating and modulating cell-mediated immune responses and class-switching antibodies to the IgG class.[7,31] Therefore, IFN-γ is a key biomarker to evaluate cellular immune response, where it is primarily produced by Th1 cells.[33] In this study, the differences in the levels of IFN-γ produced by antigen-stimulated splenocytes across all groups were not statistically significant ($p>0.05$), indicating that the supplementation of carotene did not affect the production of IFN-γ regardless of the status of vaccination. However, both the vaccinated control and carotene groups displayed elevated levels of IFN-γ compared to their unvaccinated counterparts, indicating the activation of T lymphocytes by the inactivated virus vaccine. In contrast to the present result, cultured splenocytes from BALB/c mice fed with β-carotene and immunized with ovalbumin were reported to produce higher IFN-γ and show increased IFN-γ mRNA expression compared to the control group.[34] In another study, supplementation of astaxanthin, a carotenoid, to BALB/c mice showed significantly higher IFN-γ production in response to LPS or concanavalin A.[31] The results of the present study suggest that daily supplementation of carotene after vaccination can increase SARS-CoV-2-specific humoral responses by promoting the proliferation of lymphocytes.

In the present study, daily carotene supplementation in unvaccinated BALB/c mice was observed to have reduced *Odoribacter* and *Monoglobus* in the gut microbiome compared to unvaccinated controls. *Odoribacter* is a member of the SCFA producers in a healthy, balanced gut microbiota.[35] *Monoglobus* is primarily represented by *Monoglobus pectinilyticus,* a gut bacterium that breaks down pectin.[36] On the other hand, carotene supplementation in vaccinated mice caused the enrichment of the Ruminococcaceae family and the reduction of the *Mucispirillum* genus compared to the vaccinated control group. The Ruminococcaceae family is a prominent butyrate producer.[37] *The Mucispirillum* genus, primarily represented by *Mucispirillum schaedleri*, is a mucus-resident intestinal bacterium in rodents and is considered a pathobiont, a commensal organism that may contribute to disease.[38] This indicates the potential of carotene supplementation to inhibit harmful bacteria in the gut. The findings from this study revealed that carotene supplements significantly decreased the abundance of SCFA producers (e.g., *Odoribacter*) and pectin-degrading bacteria in the feces of unvaccinated mice. In contrast, in the carotene-supplemented vaccinated group, there was an increase in the abundance of butyrate producers (e.g., Ruminococcaceae) and a decrease in the abundance of potential pathobionts (e.g., *Mucispirillum*) in the host gut microbiome. The Ruminococcaceae and *Odoribacter* enriched by carotene supplementation were reported to have a strong association with the metabolism and absorption of β-carotene.[39]

In this study, the GC-MS analysis revealed that carotene supplementation did not significantly modulate SCFA (e.g., acetic acid, butyric acid, and propionic acid) levels in the fecal samples. This result is in contrast to recent research that deployed an *in vitro* anaerobic fermentation model to study gut microbiome interaction with β-carotene, where β-carotene significantly increased the production of acetic acid and propionic acid compared to the control group.[10] The discrepancy in findings can be due to the difference in the research models, where quantification of SCFAs was affected by absorption of SCFAs in the colon but not in the *in vitro* model. Besides, this animal study was challenged by vaccination. The immunological challenge can cause an inflammatory reaction associated with gut dysbiosis, potentially inhibiting SCFA producers. This finding was supported by a recent study where COVID-19 patients reported significantly reduced SCFA levels.[19]

5. Conclusion

This study used the BALB/c mice model to explore the interaction of carotene supplementation with an inactivated SARS-CoV-2 virus vaccine. To evaluate the association between carotene and vaccine response, this study investigated the effect of carotene on immune parameters, gut microbiome, and SCFA levels. Carotene supplementation did not significantly affect the antibody levels related to the inactivated SARS-CoV-2 vaccine, IFN-γ levels, and fecal SCFA levels. However, it increases the proliferation rate of splenocytes in vaccinated mice.

Acknowledgments

The authors thank the Jeffrey Cheah School of Medicine, Monash University Malaysia, for supporting this study. The authors would like to thank PhytoGaia Sdn. Bhd. (Malaysia) for providing the carotene from palm oil (CaroGaia 30% OS) and Pharmaniaga Lifescience Sdn Bhd, Malaysia, for providing CoronaVac (Sinovac Biotech Ltd, China).

Funding

This study was supported by a research grant from the Jeffrey Cheah School of Medicine, Monash University Malaysia (STG-000056).

Conflict of interest

The authors declare that they have no competing interests.

Author contributions

Conceptualization: Ammu Kutty Radhakrishnan
Data curation: Kang Wei Tan
Formal analysis: Kang Wei Tan, Kar Wai Hong
Funding acquisition: Ammu Kutty Radhakrishnan
Investigation: Kang Wei Tan, Ammu Kutty Radhakrishnan
Methodology: Ammu Kutty Radhakrishnan
Project administration: Ammu Kutty Radhakrishnan
Resources: Saatheeyavaane Bhuvanendran, Uma Devi Palanisamy
Supervision: Saatheeyavaane Bhuvanendran, Kar Wai Hong, Uma Devi Palanisamy, Ammu Kutty Radhakrishnan
Writing – original draft: Kang Wei Tan
Writing – review & editing: Saatheeyavaane Bhuvanendran, Kar Wai Hong, Uma Devi Palanisamy, Ammu Kutty Radhakrishnan

Ethics approval and consent to participate

Ethics approval to carry out this study was obtained from the Animal Ethics Committee (AEC) of Monash University (AEC Project ID: 29899).

Consent for publication

Not applicable.

Availability of data

Data used in this work are available from the corresponding author upon reasonable request.

References

1. Amanat F, Krammer F. SARS-CoV-2 vaccines: Status report. *Immunity*. 2020;52:583-589.

   doi: 10.1016/j.immuni.2020.03.007

2. Pennisi F, Genovese C, Gianfredi V. Lessons from the COVID-19 pandemic: Promoting vaccination and public health resilience, a narrative review. *Vaccines* (*Basel*). 2024;12:891.

   doi: 10.3390/vaccines12080891

3. Lim WW, Mak L, Leung GM, Cowling BJ, Peiris M. Comparative immunogenicity of mRNA and inactivated vaccines against COVID-19. *Lancet Microbe*. 2021;2:e423.

   doi: 10.1016/S2666-5247(21)00177-4

4. Fu Z, Liang D, Zhang W, *et al.* Host protection against Omicron BA.2.2 sublineages by prior vaccination in spring 2022 COVID-19 outbreak in Shanghai. *Front Med*. 2023;17:562-575.

   doi: 10.1007/s11684-022-0977-3

5. Zeng G, Wu Q, Pan H, *et al.* Immunogenicity and safety of a third dose of CoronaVac, and immune persistence of a two-dose schedule, in healthy adults: Interim results from two single-centre, double-blind, randomised, placebo-controlled phase 2 clinical trials. *Lancet Infect Dis*. 2022;22:483-495.

   doi: 10.1016/s1473-3099(21)00681-2

6. Carr AC, Maggini S. Vitamin C and immune function. *Nutrients*. 2017;9:1211.

   doi: 10.3390/nu9111211

7. Chen Y, Yin S, Tong X, *et al.* Dynamic SARS-CoV-2-specific B-cell and T-cell responses following immunization with an inactivated COVID-19 vaccine. *Clin Microbiol Infect*. 2022;28:410-418.

   doi: 10.1016/j.cmi.2021.10.006

8. Yin J, Zhao Y, Huang F, *et al.* Immune response and homeostasis mechanism following administration of BBIBP-CorV SARS-CoV-2 inactivated vaccine. *Innovation* (*Camb*). 2023;4:100359.

   doi: 10.1016/j.xinn.2022.100359

9. Wang Y, Liu J, Burrows PD, Wang JY. B cell development and maturation. In: Wang JY, editor. *B Cells in Immunity and Tolerance*. Singapore: Springer Singapore; 2020. p. 1-22.

10. Ramljak D, Vukoja M, Curlin M, *et al.* Early response of $CD8^+$ T cells in COVID-19 patients. *J Pers Med*. 2021;11:1291.

    doi: 10.3390/jpm11121291

11. Gombart AF, Pierre A, Maggini S. A review of micronutrients and the immune system-working in harmony to reduce the risk of infection. *Nutrients*. 2020;12:236.

    doi: 10.3390/nu12010236

12. Hussain Y, Abdullah, Alsharif KF, *et al.* Therapeutic role of carotenoids in blood cancer: Mechanistic insights and therapeutic potential. *Nutrients*. 2022;14:1949.

    doi: 10.3390/nu14091949

13. Loganathan R, Subramaniam KM, Radhakrishnan AK,

Choo YM, Teng KT. Health-promoting effects of red palm oil: Evidence from animal and human studies. *Nutr Rev*. 2017;75:98-113.

doi: 10.1093/nutrit/nuw054

14. Iddir M, Brito A, Dingeo G, *et al.* Strengthening the immune system and reducing inflammation and oxidative stress through diet and nutrition: Considerations during the COVID-19 crisis. *Nutrients*. 2020;12:1562.

doi: 10.3390/nu12061562

15. Lewis ED, Meydani SN, Wu D. Regulatory role of vitamin E in the immune system and inflammation. *IUBMB Life*. 2019;71:487-494.

doi: 10.1002/iub.1976

16. Ávila-Román J, García-Gil S, Rodríguez-Luna A, Motilva V, Talero E. Anti-Inflammatory and anticancer effects of microalgal carotenoids. *Marine Drugs*. 2021;19:531.

doi: 10.3390/md19100531

17. Zainal Z, Abdul Rahim A, Khaza'ai H, Chang SK. Effects of palm oil tocotrienol-rich fraction (TRF) and carotenes in ovalbumin (OVA)-challenged asthmatic brown norway rats. *Int J Mol Sci*. 2019;20:1764.

doi: 10.3390/ijms20071764

18. Elefson SK, Greiner LL. The evaluation of the supplementation of vitamin A, beta-carotene, and oxidized beta-carotene in prepubertal gilts. *J Anim Sci.* 2023;101:skad103.

doi: 10.1093/jas/skad103

19. Liang Z, Wang N, Fan C, *et al.* Disturbance of adaptive immunity system was accompanied by a decrease in plasma short-chain fatty acid for patients hospitalized during SARS-CoV-2 infection after COVID-19 vaccination. *J Inflamm Res.* 2023;16:5261-5272.

doi: 10.2147/jir.S434860

20. Li Z, Dai Z, Shi E, *et al.* Study on the interaction between β-carotene and gut microflora using an *in vitro* fermentation model. *Food Sci Hum Wellness.* 2023;12:1369-1378.

doi: 10.1016/j.fshw.2022.10.030

21. Lynn DJ, Benson SC, Lynn MA, Pulendran B. Modulation of immune responses to vaccination by the microbiota: Implications and potential mechanisms. *Nat Rev Immunol*. 2022;22:33-46.

doi: 10.1038/s41577-021-00554-7

22. Liu XF, Shao JH, Liao YT, *et al.* Regulation of short-chain fatty acids in the immune system. *Front Immunol.* 2023;14:1186892.

doi: 10.3389/fimmu.2023.1186892

23. Takabayashi T, Yoshida K, Imoto Y, Schleimer RP, Fujieda S. Regulation of the expression of SARS-CoV-2 receptor angiotensin-converting enzyme 2 in nasal mucosa. *Am J Rhinol Allergy*. 2022;36:115-122.

doi: 10.1177/19458924211027798

24. Gray J, Guo B, Bearden R, Manka J. A fast, fully validated GC-MS method using a simplified pretreatment for the quantification of short and branched chain fatty acids in human stool. *J Mass Spectrom*. 2022;57:e4817.

doi: 10.1002/jms.4817

25. Kers JG, Saccenti E. The power of microbiome studies: Some considerations on which alpha and beta metrics to use and how to report results. *Front Microbiol.* 2022;12:796025.

doi: 10.3389/fmicb.2021.796025

26. Nearing JT, Douglas GM, Hayes MG, *et al.* Microbiome differential abundance methods produce different results across 38 datasets. *Nat Commun*. 2022;13:342.

doi: 10.1038/s41467-022-28034-z

27. Santos MS, Leka LS, Ribaya-Mercado JD, *et al.* Short-and long-term beta-carotene supplementation do not influence T cell-mediated immunity in healthy elderly persons. *Am J Clin Nutr.* 1997;66:917-924.

doi: 10.1093/ajcn/66.4.917

28. Hughes DA, Wright AJ, Finglas PM, *et al.* The effect of beta-carotene supplementation on the immune function of blood monocytes from healthy male nonsmokers. *J Lab Clin Med*. 1997;129:309-317.

doi: 10.1016/s0022-2143(97)90179-7

29. Jee J, Hoet AE, Azevedo MP, *et al.* Effects of dietary vitamin A content on antibody responses of feedlot calves inoculated intramuscularly with an inactivated bovine coronavirus vaccine. *Am J Vet Res.* 2013;74:1353-1362.

doi: 10.2460/ajvr.74.10.1353

30. Cui D, Moldoveanu Z, Stephensen CB. High-level dietary vitamin A enhances T-helper type 2 cytokine production and secretory immunoglobulin A response to influenza A virus infection in BALB/c mice. *J Nutr*. 2000;130:1132-1139.

doi: 10.1093/jn/130.5.1132

31. Lin KH, Lin KC, Lu WJ, Thomas PA, Jayakumar T, Sheu JR. Astaxanthin, a carotenoid, stimulates immune responses by enhancing IFN-γ and IL-2 secretion in primary cultured lymphocytes *in vitro* and *ex vivo*. *Int J Mol Sci.* 2015;17:44.

doi: 10.3390/ijms17010044

32. Dharra R, Kumar Sharma A, Datta S. Emerging aspects of cytokine storm in COVID-19: The role of proinflammatory cytokines and therapeutic prospects. *Cytokine.* 2023;169:156287.

doi: 10.1016/j.cyto.2023.156287

33. Thakur A, Pedersen LE, Jungersen G. Immune markers and correlates of protection for vaccine induced immune responses. *Vaccine.* 2012;30:4907-4920.

doi: 10.1016/j.vaccine.2012.05.049

34. Sato Y, Akiyama H, Suganuma H, *et al.* The feeding of beta-carotene down-regulates serum IgE levels and inhibits the type I allergic response in mice. *Biol Pharm Bull.* 2004;27:978-984.

doi: 10.1248/bpb.27.978

35. Hiippala K, Barreto G, Burrello C, *et al.* Novel odoribacter splanchnicus strain and its outer membrane vesicles exert immunoregulatory effects *in vitro*. *Front Microbiol*. 2020;11:575455.

doi: 10.3389/fmicb.2020.575455

36. Kim CC, Lunken GR, Kelly WJ, *et al.* Genomic insights from *Monoglobus pectinilyticus*: A pectin-degrading specialist bacterium in the human colon. *ISME J*. 2019;13:1437-1456.

doi: 10.1038/s41396-019-0363-6

37. Kim YJ, Jung DH, Park CS. Important roles of *Ruminococcaceae* in the human intestine for resistant starch utilization. *Food Sci Biotechnol*. 2024;33:2009-2019.

doi: 10.1007/s10068-024-01621-0

38. Loy A, Pfann C, Steinberger M, *et al.* Lifestyle and horizontal gene transfer-mediated evolution of *Mucispirillum schaedleri*, a core member of the murine gut microbiota. *mSystems*. 2017;2:e00171-16.

doi: 10.1128/msystems.00171-16

39. Shi E, Nie M, Wang X, *et al.* Polysaccharides affect the utilization of β-carotene through gut microbiota investigated by *in vitro* and *in vivo* experiments. *Food Res Int*. 2023;174:113592.

doi: 10.1016/j.foodres.2023.113592

Appendices

Table A1. Raw data for $CD3^+$ T lymphocytes from peripheral blood samples

Sample	% parent
Baseline 1	57.8
Baseline 2	67.8
Baseline 3	74.1
Baseline vaccinated 1	71.5
Baseline vaccinated 2	79.9
Baseline vaccinated 3	69.4
Carotene 1	74.1
Carotene 2	72.9
Carotene 3	59.9
Carotene vaccinated 1	24.0
Carotene vaccinated 2	69.0
Carotene vaccinated 3	53.7

Table A2. Raw data for splenocyte proliferation

Sample	% over baseline
Baseline vaccinated 1	91.2
Baseline vaccinated 2	82.8
Baseline vaccinated 3	97.2
Baseline vaccinated 4	94.2
Baseline vaccinated 5	87.3
Baseline vaccinated 6	96.0
Carotene 1	90.9
Carotene 2	128.3
Carotene 3	96.4
Carotene 4	143.5
Carotene 5	99.4
Carotene 6	87.1
Carotene vaccinated 1	139.9
Carotene vaccinated 2	163.3
Carotene vaccinated 3	90.4
Carotene vaccinated 4	121.9
Carotene vaccinated 5	194.2
Carotene vaccinated 6	124.6

ACCSCIENCE PUBLISHING

Microbes & Immunity

ORIGINAL RESEARCH ARTICLE

A proposal for biologically relevant classification of SARS-CoV-2 variants

Saja Al-Baidhani[1], Tarneem Sabra[1], Aslam Al-Baidhani[1], Mohammed Sallam[2,3,4], and Malik Sallam[1,5*]

[1]Department of Pathology, Microbiology and Forensic Medicine, School of Medicine, The University of Jordan, Amman, Jordan

[2]Department of Pharmacy, Mediclinic Parkview Hospital, Mediclinic Middle East, Dubai, United Arab Emirates

[3]Department of Management, Mediclinic Parkview Hospital, Mediclinic Middle East, Dubai, United Arab Emirates

[4]College of Medicine, Mohammed Bin Rashid University of Medicine and Health Sciences, Dubai, United Arab Emirates

[5]Department of Clinical Laboratories and Forensic Medicine, Jordan University Hospital, Amman, Jordan

Abstract

The present classification of severe acute respiratory syndrome coronavirus 2 (SARS-CoV-2) variants plays a central role in shaping public health policies, vaccine strategies, and global risk communication. However, existing designations of variants of concern (VOCs) rely on evolving epidemiological and phenotypic criteria rather than quantitative genetic divergence thresholds. In this study, we evaluated the genetic divergence of SARS-CoV-2 variants relative to human immunodeficiency virus type 1 (HIV-1), hepatitis C virus (HCV), and influenza A virus, and proposed a framework integrating genetic, functional, and epidemiological criteria for variant classification. Comparative phylogenetic analysis assessed the divergence of SARS-CoV-2 (*S*) relative to HIV-1 (*env*), HCV (*E1*), and influenza A virus (*HA*). Maximum likelihood phylogenies with bootstrap support were constructed using MEGA6, and pairwise genetic distances were calculated through the maximum composite likelihood model. Monte Carlo simulations (n = 1,000) using adjusted SARS-CoV-2 evolutionary rates (0.0006 – 0.003 substitutions/site/year) estimated time to reach divergence thresholds defined by other viruses. SARS-CoV-2 variants showed a maximum divergence of 0.006 substitutions/site – far below thresholds for HIV-1 (0.157), HCV (0.371), and influenza A (1.956). Projections estimate HIV-1-like divergence in 53.7 years, HCV-like in 126.8 years, and influenza A-like in 668.6 years. No present VOC met all proposed functional criteria: transmissibility, immune escape, disease severity, and global dominance. Omicron exhibited partial immune escape but insufficient divergence for lineage reclassification. While present classification supports short-term response, integrating evolutionary benchmarks would enhance their biological relevance as the virus continues to diversify. A new evidence-based framework is needed to reduce public alarm, guide rational policymaking, and prioritize durable countermeasures over variant-specific responses.

Keywords: Phylogeny; Classification; COVID-19; Lineage; Variant

***Corresponding author:**
Malik Sallam
(malik.sallam@ju.edu.jo)

Citation: Al-Baidhani S, Sabra T, Al-Baidhani A, Sallam M, Sallam M. A proposal for biologically relevant classification of SARS-CoV-2 variants. *Microbes & Immunity*. 2025;2(3):87-107.
doi: 10.36922/MI025190042

Received: May 10, 2025

1st revised: May 30, 2025

2nd revised: June 3, 2025

Accepted: June 4, 2025

Published online: June 17, 2025

1. Introduction

Severe acute respiratory syndrome coronavirus 2 (SARS-CoV-2) is a member of the family *Coronaviridae* that was first characterized in early 2020.[1-3] This virus is the causative agent of coronavirus disease 2019 (COVID-19) and long COVID.[4,5] COVID-19 has been recognized as the pandemic of the 21st century.[6] It ranges in manifestations from asymptomatic infections and mild cold-like illnesses to more severe forms that result in significant morbidity and mortality, especially in elderly patients with chronic illnesses.[7-11]

Like other members of *Coronaviridae*, SARS-CoV-2 has a genome comprising a positive-sense, single-stranded RNA with a linear configuration.[12,13] Despite the lack of accurate characterization of the exact origins of SARS-CoV-2, the early spread of the virus has been well documented.[14-18] Phylogenetic analyses of SARS-CoV-2 sequences from the early infections in China suggested that the first human cases likely occurred in late 2019.[19,20] The present evidence suggests that the emergence of SARS-CoV-2 resulted from recombination events between bat SARS-like coronaviruses and, possibly, coronaviruses found in pangolins, leading to cross-species transmission.[21-24] More recent research suggested that direct spillover from bats remains the most likely scenario, with limited genomic evidence supporting a significant role of pangolins in the emergence of SARS-CoV-2.[25,26]

The earliest available SARS-CoV-2 genomes were obtained from patients in December 2019.[27] These early viral sequences provided key insights into the genetic structure and early divergence of SARS-CoV-2.[3] Chinese researchers conducted phylogenetic analyses comparing these genomes with known bat and pangolin coronaviruses to infer the likely ancestral form of the virus.[28] Based on mutational differences, they identified an ancestral genome type, designated "S", and a more dominant derived type, labeled "L", to reflect specific amino acid substitutions.[29] Concurrently, Western researchers conducted independent analyses using similar methodologies but assigned different nomenclatures to describe the early divergence of SARS-CoV-2. Instead of "S" and "L," they labeled the ancestral strain as "A" and the derived strain as "B".[30-33] Over time, the B lineage continued to mutate, giving rise to sub-lineages, including B.1, which became the predominant SARS-CoV-2 lineage globally.[34] This lineage eventually diversified into major global variants of concern (VOCs), which the World Health Organization (WHO) formally labeled as Alpha, Beta, Gamma, Delta, and Omicron variants.[35] The early genomic studies illustrated the complex evolutionary dynamics of SARS-CoV-2, highlighting both early genetic bottlenecks and the subsequent rapid adaptation of the virus.[36]

During the initial phase of the COVID-19 pandemic, the relatively low number of infections limited the opportunities for genetic diversification within the SARS-CoV-2 genome. With fewer viral replication cycles, the accumulation of mutations was constrained, resulting in a lower frequency of SARS-CoV-2 variant emergence.[37] At this stage, mutations in the spike (S) protein, particularly within the receptor-binding domain (RBD), which mediates interaction with the human angiotensin-converting enzyme-2 (ACE2) receptor, were rarely observed.[37] As transmission increased globally, the virus evolved, with a positive selection of certain substitutions that conferred higher transmissibility (e.g., D614G).[38,39] Over time, specific S protein substitutions that enhanced SARS-CoV-2's ability to bind more efficiently to human cells became more prevalent and led to the emergence of genetic variants with epidemiological advantages. Notably, the Alpha (B.1.1.7) variant, first identified in the UK, and the Delta (B.1.617.2) variant, which originated in India, both demonstrated significantly higher transmission rates than earlier circulating strains.[40-42] These variants carried key S protein mutations, such as N501Y in the Alpha variant and L452R and P681R in the Delta variant, which enhanced their ability to infect host cells and possibly contributed to their global dominance at different phases during the pandemic.[43,44] The progressive emergence of more transmissible variants indicates the role of natural selection in shaping SARS-CoV-2 evolution, favoring mutations that increase infectivity while the virus continues to adapt to human hosts.[45]

At present, SARS-CoV-2 variants are designated as distinct viral lineages when they exhibit genetic changes deemed significant enough to warrant separate classification, as determined by the WHO Coronavirus Network (CoViNet).[35,46] Since the onset of the COVID-19 pandemic, the continuous evolution of SARS-CoV-2 has led to the identification of multiple VOCs and variants of interest (VOIs).[43,47,48] These designations have been based on the projected capacity of emerging variants to outcompete previously circulating strains through increased transmissibility or the necessity to adjust public health interventions.[49-51] This classification system has been important to facilitate epidemiological surveillance and risk assessment. However, its primary reliance on limited genetic divergence and evolving phenotypic criteria, rather than on consistent, functionally meaningful differentiation, highlights the opportunity for refining the system. Incorporating genetic and evolutionary benchmarks could enhance the alignment between nomenclature and the underlying virological or clinical significance of emerging SARS-CoV-2 variants.[52-54]

Certain SARS-CoV-2 variants are classified as VOCs due to their ability to maintain or enhance replication fitness despite increasing levels of population immunity – either through natural infection or vaccination.[43,45] These variants often exhibit mutations that provide a selective advantage, allowing them to spread more efficiently in partially immune populations.[55] A defining feature of many VOCs is the presence of mutations in the RBD of the S protein, which plays a critical role in host cell entry through the human ACE2 receptor.[56] Thus, the designation VOC is reserved for SARS-CoV-2 lineages in which specific genetic changes significantly enhance RBD binding affinity – as seen with substitutions such as N501Y – while also demonstrating epidemiological evidence of increased transmissibility.[57,58]

Before being categorized as a VOC, an emerging SARS-CoV-2 lineage is often first labeled as a VOI or, in some national surveillance frameworks, a variant under investigation.[35] If subsequent data confirm enhanced transmissibility, immune escape potential, or increased disease severity, the variant is formally designated as a VOC.[35] Once a variant reaches VOC status, it is systematically classified within the Pango nomenclature system, which provides detailed lineage assignments based on phylogenetic relationships.[48] In addition, the variant is assigned to specific clades within Nextstrain and Global Initiative on Sharing All Influenza Data (GISAID), two global platforms used for genomic epidemiology and viral evolution tracking.[59,60] These classification systems facilitate real-time monitoring of SARS-CoV-2 evolution, aiding in public health responses and vaccine adaptation strategies.

The WHO played a central role in the classification and monitoring of SARS-CoV-2 variants, regularly updating its framework to reflect emerging evidence on viral evolution, transmissibility, and immune escape potential.[35,47] Thus, the identification and designation of SARS-CoV-2 variants rely on genomic surveillance efforts, with submissions from member states analyzed through global platforms such as GISAID. This is followed by field investigations to assess the public health impact of SARS-CoV-2 variants.[61] Over time, the WHO expanded its classification system to include additional categories beyond VOCs. The updated framework now includes VOIs and variants under monitoring.[60] A VOI is defined as a variant possessing genetic changes that are predicted or known to affect viral characteristics, such as transmissibility, virulence, antibody evasion, therapeutic susceptibility, or detectability.[35,47] In addition, to be classified as a VOI, a variant must exhibit increasing circulation in at least one WHO region, raising concerns about potential global public health implications.[35] Other public health agencies, such as the United States Centers for Disease Control and Prevention (CDC), maintain independent classification criteria, which can lead to differences in the timing of variant de-escalation.[62,63] For example, the CDC, the European Centre for Disease Prevention and Control (ECDC), and the WHO de-escalated SARS-CoV-2 variants at different times, reflecting regional epidemiological assessments and risk evaluations.[35,64,65]

At this point, it is important to consider the foundational pillars in the field of virus evolution. It is well established that the accumulation of sufficient genetic divergence to produce a biologically distinct virus lineage – one with unique properties affecting transmission dynamics, pathogenicity, or immune interactions – typically requires several years of sustained evolutionary pressure.[66-70] The present classification framework for SARS-CoV-2, which designates new variants based on short-term genetic fluctuations, contradicts this fundamental understanding of viral evolution.[71] The issue is particularly pronounced in SARS-CoV-2 due to its genomic stability relative to other RNA viruses, such as human immunodeficiency virus type 1 (HIV-1), hepatitis C virus (HCV), and influenza A virus, all of which evolve under stronger selection pressures and exhibit markedly higher mutation rates.[72-75] Unlike HIV-1, HCV, and influenza A virus, SARS-CoV-2 possesses a proofreading exonuclease (nsp14-ExoN), a unique feature among the majority of RNA viruses that reduces the accumulation of replication errors.[76,77] This proofreading mechanism results in a significantly slower evolutionary rate for SARS-CoV-2, estimated between 0.0004 and 0.002 substitutions per site per year (s/s/y).[49,73,78] This evolutionary rate allows for gradual adaptation; however, it does not support the level of rapid divergence seen among other RNA viruses.[79] Consequently, it is plausible to assume that the frequent designation of SARS-CoV-2 variants as distinct entities, based on transient mutational changes rather than sustained functional divergence, represents a departure from well-established evolutionary virology principles.

Thus, the present study argues that the currently adopted classification of SARS-CoV-2 lineages has introduced significant challenges in COVID-19 risk communication. The existing SARS-CoV-2 classification systems are often the source of unnecessarily amplified public concern and inconsistent scientific justification that influences policy decisions, leading to a cycle of reactionary responses rather than well-balanced epidemiological measures. Accordingly, the present study aimed to: (1) Assess the genetic divergence of SARS-CoV-2 variants in comparison to established RNA virus speciation models (e.g., HIV-1,

HCV, and influenza A virus); (2) estimate the minimum evolutionary timeframe required for SARS-CoV-2 to reach a level of genetic divergence equivalent to that observed in HIV-1, HCV, and influenza A virus; and (3) propose a complementary classification framework for SARS-CoV-2 that is based on evolutionary and phylogenetic principles.

2. Materials and methods

2.1. Study design, dataset acquisition, and sequence selection

This study aimed to propose a practical and evolutionarily informed classification framework for SARS-CoV-2, grounded in a conservative, objective threshold of genetic divergence that could support the identification of biologically distinct lineages as the virus continues to evolve. To achieve this, the evolutionary divergence of SARS-CoV-2 variants was compared with that of three well-characterized RNA viruses – HIV-1, HCV, and influenza A virus. These viruses were selected as their lineage differentiation is associated with substantial biological and functional differences in transmissibility, immune evasion, and pathogenesis.

The viral genomes and corresponding genes chosen for analysis were: (1) SARS-CoV-2: *S* gene (3,822 bases); (2) HIV-1: *env* gene (2,592 bases); (3) HCV: *E1* gene (576 bases); and (4) influenza A virus: *HA* gene (1,707 bases). These regions were selected due to their relevance in viral entry, immune evasion, and vaccine targeting, besides being recognized as rapidly evolving genomic regions of each virus.[80-83] Full-length viral sequences were retrieved from the Los Alamos HIV Database, Los Alamos HCV Database, GenBank Influenza Virus Database, and NCBI Virus Database.[84-87] Selection criteria included: (1) Complete coding sequences (removal of sequences with large gaps or ambiguous bases, defined as >1% nucleotide base); (2) diversity in collection date and geographical origin to ensure representation of global viral evolution; (3) exclusion of recombinant sequences, except where recombination is inherent to viral evolution (e.g., HIV-1 circulating recombinant forms [CRFs]); and (4) at least 40 representative sequences per viral subtype/lineage to ensure robust phylogenetic reconstruction.[88] The selection of 50 (SARS-CoV-2), 58 (HIV-1), 40 (HCV), and 49 (influenza A virus) sequences adhered to this standard.

2.2. Selection of viral subtypes/lineages

To ensure a comprehensive comparison of SARS-CoV-2 genetic divergence with well-characterized RNA viruses, representative subtypes and lineages for HIV-1, HCV, and influenza A virus were selected based on their global prevalence and established phylogenetic classification. For SARS-CoV-2, sequences from the major VOCs were included in the analysis. These variants were selected based on their distinct S protein mutations and their role in altering transmissibility, immune escape, and vaccine efficacy.

HIV-1 exhibits significant genetic diversity, with distinct subtypes and CRFs contributing to its global dissemination. The following subtypes/CRFs, representing the most common lineages, were selected: A1, B, C, D, CRF01_AE, and CRF02_AG.[89] These subtypes were chosen due to their high epidemiological relevance and established divergence patterns, which serve as a benchmark for evaluating the evolutionary dynamics of SARS-CoV-2.[90]

HCV classification is based on well-defined genotypes and subtypes, which exhibit substantial genetic diversity.[91] The following subtypes were selected: subtype 1a, subtype 1b, subtype 3a, and subtype 4a. These subtypes represent widely studied lineages with distinct evolutionary trajectories, providing an appropriate comparison for assessing SARS-CoV-2 divergence. Influenza A virus evolves through antigenic drift and shift, leading to the emergence of distinct subtypes with significant genetic and antigenic variation. The following subtypes were included: H1N1 and H3N2.[92] These subtypes were selected as they represent the dominant circulating influenza lineages over the past century, providing a well-documented model of viral evolution and antigenic variation. For SARS-CoV-2, sequences from the five major VOCs designated by the WHO were analyzed, representing key evolutionary lineages that have dominated transmission waves globally: Alpha (B.1.1.7), Beta (B.1.351), Gamma (P.1), Delta (B.1.617.2), and Omicron (B.1.1.529).[43]

2.3. Sequence alignment and genetic distance estimation

Multiple sequence alignments were performed separately for HIV-1, HCV, influenza A, and SARS-CoV-2 using MAFFT v7.490, employing the L-INS-i algorithm, which optimizes alignment accuracy for sequences with frequent insertions and deletions, particularly in the HIV-1 *env* and influenza *HA* genes.[93] Alignment quality was manually reviewed in MEGA6, and sequences with poor alignment were excluded.[94] Genetic distances were estimated using the maximum composite likelihood (MCL) model, with rate variation among sites modeled using a gamma distribution (shape parameter = 1). Codon positions included 1st, 2nd, and 3rd coding positions, as well as non-coding regions.[94,95] All positions containing gaps or missing data were removed before analysis. The final alignment of HIV-1 (n = 58) consisted of 2,214 nucleotide positions; HCV (n = 40) consisted of 513 nucleotide positions; influenza

A virus (n = 49) consisted of 939 nucleotide positions; and SARS-CoV-2 (n = 50) consisted of 3,089 nucleotide positions. Evolutionary analyses were conducted using MEGA6 to compute pairwise genetic distances across all sequence groups.[94]

To enhance the temporal signal in assessing the genetic divergence of the viruses, we included sequences spanning multiple years and epidemic phases as follows. For HIV-1, the sequence collection years spanned 1993 – 2017, from 20 countries, including Argentina, Australia, Brazil, Botswana, China, Cyprus, Spain, Ethiopia, Finland, Indonesia, India, Iran, Kenya, Nigeria, Sweden, Thailand, Tanzania, Uganda, UK, and US. For HCV, the sequence collection years spanned 1993 – 2023, from 15 countries, including Australia, Switzerland, China, Cuba, Germany, Egypt, Spain, France, Ireland, India, Japan, Pakistan, Thailand, the UK, and the US. For influenza A, sequences were collected in multiple locations in Sweden spanning 1992 – 2010. For SARS-CoV-2, sequences were collected during 2020 – 2025 from Canada, Ghana, Japan, New Zealand, and several locations in the US, including Arizona, California, the District of Columbia, Iowa, Indiana, Michigan, Minnesota, North Carolina, Nevada, New Jersey, North Carolina, Oklahoma, Oregon, Pennsylvania, South Carolina, South Carolina, and Washington.

2.4. Maximum likelihood phylogenetic analysis

To assess evolutionary relationships and determine whether SARS-CoV-2 variants exhibit lineage divergence comparable to that observed in HIV-1, HCV, and influenza A virus, maximum likelihood (ML) phylogenetic trees were constructed using MEGA6.[94,95] The MCL model was employed for nucleotide substitution, with rate variation among sites modeled using a gamma distribution (shape parameter = 1). The analysis included all nucleotide sequences, with codon positions (first, second, third, and non-coding regions) considered. Sequences containing gaps or missing data were removed before analysis.[94,95] An unrooted ML tree was generated with 100 ultrafast bootstrap replicates to evaluate branch support, with bootstrap values exceeding 70% considered statistically significant.[96] The resulting tree was visualized using FigTree software to facilitate the interpretation of lineage relationships.[97] The inclusion of ≥40 sequences per virus provided sufficient phylogenetic resolution.[96,98]

2.5. Defining the genetic divergence threshold for variant classification

To establish an objective cutoff for defining distinct viral variants, the genetic distances of SARS-CoV-2 were compared to the following benchmarks: (1) HIV-1 subtypes (*env* region) mean divergence; (2) HCV subtypes (*E1* region) mean divergence; and (3) influenza A virus subtypes (*HA* gene) mean divergence. ANOVA and Kruskal–Wallis tests were used to compare mean genetic divergence values among viral groups, and the analysis was conducted using IBM SPSS Statistics for Windows, Version 26.0 (IBM Corp, United States). It was hypothesized that if SARS-CoV-2 variants do not surpass the established genetic divergence thresholds derived from HIV-1, HCV, and influenza A virus, this would indicate that their present classification is driven more by transient mutations than by meaningful virological differentiation.

2.6. Estimation of speciation time for SARS-CoV-2 based on genetic distances compared to HIV-1, HCV, and influenza A virus

To estimate the time required for SARS-CoV-2 to reach speciation-level divergence, we compared its genetic distances to those observed in HIV-1, HCV, and influenza A virus. Speciation thresholds were defined based on the minimum genetic distances observed between recognized subtypes or genotypes in these viruses. Using the established evolutionary rate of SARS-CoV-2 (0.0004 – 0.002 s/s/y), we applied the formula: Years = Genetic distance threshold/evolutionary rate. The evolutionary rate of SARS-CoV-2 was set at 0.0004 – 0.002 s/s/y, consistent with published estimates.[17,51,99-103] To evaluate how recombination affects divergence, an adjusted evolutionary rate model was incorporated based on the estimated recombination frequency in SARS-CoV-2 genomes (~2.7% recombinant ancestry).[104,105] A 1.5× acceleration factor was applied, as recombination has been shown to elevate the viral evolutionary rate,[106,107] yielding adjusted evolutionary rates: lower bound, 0.0006 s/s/y; upper bound, 0.003 s/s/y. Monte Carlo simulation was performed by generating 1,000 random evolutionary rates sampled uniformly from the adjusted range. Simulated rate values and calculated time estimates were compiled into a structured dataset and analyzed using the IBM SPSS Statistics for Windows, Version 26.0 (IBM Corp, United States). Descriptive statistics (mean, standard deviation, and 95% confidence intervals [CIs]) were computed for the estimated time required to reach each threshold.

2.7. Basis of the proposal of new SARS-CoV-2 classification scheme

To establish a robust and biologically meaningful classification system for SARS-CoV-2 variants, a two-pronged methodological approach was employed, integrating (1) genetic divergence thresholds derived from well-characterized viral evolution patterns, and (2) functional impact criteria identified through a comprehensive review of literature on viral pathogenesis,

transmissibility, and immune escape mechanisms. Genetic divergence thresholds were established by analyzing the evolutionary distances between recognized subtypes or genotypes of HIV-1, HCV, and influenza A virus, as outlined in the sections above.

A review of the literature was conducted in PubMed/MEDLINE to identify key functional parameters that have historically defined viral lineages in other RNA viruses, including HIV-1, HCV, influenza A virus, and previous SARS-CoV-2 designated as VOCs. The exact search strategy, concluded on 31 January 2025, was: (("SARS-CoV-2" OR "COVID-19" OR "HIV-1" OR "Hepatitis C Virus" OR "HCV" OR "Influenza A") AND ("variant of concern" OR "VOC" OR "subtype" OR "genotype" OR "lineage" OR "clade") AND ("transmissibility" OR "replication fitness" OR "R0" OR "immune escape" OR "neutralizing antibodies" OR "vaccine resistance" OR "vaccine escape" OR "clinical severity" OR "hospitalization" OR "mortality" OR "epidemiological dominance" OR "variant persistence" OR "lineage replacement")).

Criteria were categorized into four virologically relevant domains: (1) Transmissibility: Evidence of increased replication fitness[40,91,108-112]; (2) Immune escape potential: ≥2-fold reduction in neutralizing antibody effectiveness, impacting vaccine efficacy, or convalescent immunity[92,113]; (3) Clinical impact: Increased hospitalization, mortality, or multisystem complications compared to prior circulating variants[114-119]; and (4) Epidemiological dominance: Variant must persist for >12 months, indicating sustained selective advantage.[89,120-122]

3. Results

3.1. HIV-1 *env* dataset description and ML phylogenetic analysis

A total of 58 full-length HIV-1 *env* sequences were analyzed, representing six major subtypes and CRFs. The ML phylogenetic tree robustly supported the classification of these subtypes into distinct lineages, with bootstrap values exceeding 0.99, indicating high confidence in the inferred evolutionary relationships (Figure 1). The distances ranged from 0.157 s/s (A vs. CRF02_AG) to 0.235 s/s (D vs. CRF01_AE), with an overall mean divergence of 0.21 s/s. The highest divergence was observed between subtypes D and CRF01_AE (0.235 s/s), whereas the lowest was found between subtypes A and CRF02_AG (0.157 s/s) (Table 1).

3.2. HCV *E1* dataset and evolutionary distance estimation

A total of 40 HCV *E1* sequences were analyzed, representing four major subtypes: 1a, 1b, 3a, and 4a. The dataset was curated to ensure full-length coding sequences, with all ambiguous bases and incomplete sequences removed before analysis. The final alignment contained a total of 2,214 nucleotide positions, with discrete clustering observed in the ML phylogenetic analysis (Figure 2).

The evolutionary divergence between subtypes was assessed using pairwise genetic distances (Table 2). The genetic distances among HCV subtypes ranged from 0.371 s/s (1a vs. 1b) to 0.674 s/s (3a vs. 4a), reflecting the well-documented high genetic diversity of HCV. The mean divergence across all subtype comparisons was 0.57 s/s, which is notably higher than that observed in HIV-1 *env* sequences.

3.3. Influenza A virus dataset and evolutionary distance analysis

The influenza dataset included 49 full-length *HA* sequences, representing two major subtypes, H1 and H3, as indicated in the ML phylogenetic tree (Figure 3). The genetic divergence between these subtypes was estimated at 1.956 s/s, which is substantially higher than the divergence observed in both HIV-1 and HCV subtypes.

3.4. SARS-CoV-2 dataset and evolutionary distance analysis

The SARS-CoV-2 *S* sequence dataset in the ML phylogenetic analysis showed a clear separation into five different statistically supported monophyletic clades (Figure 4). Pairwise genetic distance analysis of SARS-CoV-2 variants revealed minimal divergence, with nucleotide substitution rates ranging from 0.002 to 0.006 s/s. The highest genetic distance was observed between Omicron and Beta (0.006 s/s) and Omicron and Alpha (0.006 s/s), while the lowest was between Beta and Gamma (0.002 s/s). Variants Delta, Beta, and Gamma exhibited similar divergence levels relative to Alpha (0.003 – 0.004 s/s), indicating limited evolutionary separation. These findings demonstrate that SARS-CoV-2 variants remain within a constrained genetic space, with divergence levels substantially lower than those observed in HIV-1 subtypes, HCV genotypes, or influenza A virus subtypes (Table 3).

3.5. Establishing the genetic divergence threshold based on sequences analyzed

To objectively classify viral genetic divergence, three evolutionary divergence thresholds were established based on the minimum observed genetic distances in HIV-1, HCV, and influenza A virus. Three thresholds, shown in Figure 5, are as follows: low divergence, below 0.157 s/s (based on HIV-1 subtype minimum); moderate divergence, between 0.157 and 0.371 s/s (based on HCV subtype minimum); and high divergence, above 0.371 s/s (with influenza A virus defining the upper bound at

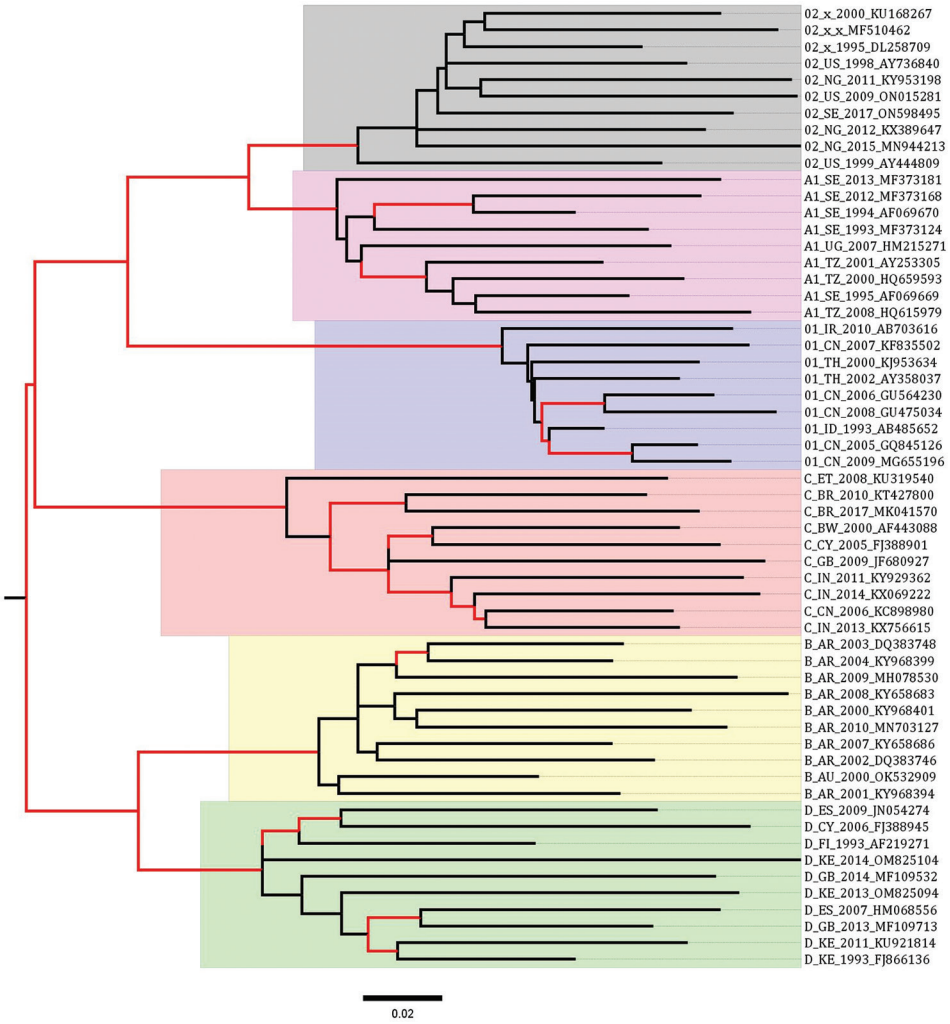

Figure 1. Maximum likelihood phylogenetic tree of HIV-1 subtypes/CRFs. Statistically supported branches are highlighted in red. The tree was visualized using the FigTree software.
Abbreviations: CRF: Circulating recombinant form; HIV-1: Human immunodeficiency virus 1.

1.956 s/s). HCV exhibited the highest mean genetic distance (0.5747 s/s, 95% CI: 0.4619 – 0.6874), consistent with the established differentiation of HCV genotypes. HIV-1 displayed moderate divergence (0.2159 s/s, 95% CI: 0.2043 – 0.2274), reflecting known subtype diversification. SARS-CoV-2 demonstrated extremely low divergence (0.004 s/s, 95% CI: 0.00299 – 0.00501), with all pairwise genetic distances ranging from 0.002 to 0.006 s/s, placing it well within the low divergence threshold. One-way ANOVA revealed highly significant differences in mean genetic distances among viral groups ($F = 606.821$, $p<0.001$), confirming that SARS-CoV-2 exhibits markedly lower divergence compared to HIV-1 and HCV. Kruskal–Wallis test further confirmed significant divergence differences ($H = 26.75$, $df = 3$, $p<0.001$).

3.6. Speciation time for SARS-CoV-2 based on genetic distances compared to HIV-1, HCV, and influenza A virus

Using 1,000 Monte Carlo-simulated evolutionary rates sampled uniformly from the adjusted range of 0.0006 to 0.003 s/s/y – to reflect SARS-CoV-2's empirically observed substitution rate, modified to account for recombination – we estimated the time required for the virus to reach genetic divergence thresholds comparable to those defining well-established subtypes of HIV-1, HCV, and influenza A virus.

For the HIV-1 divergence benchmark of 0.157 s/s, the estimated mean time for SARS-CoV-2 to reach an equivalent level of genetic divergence was 53.7 years (95% CI: 52.0 – 55.3), corresponding to a projected speciation

year of 2074 (range: 2046 – 2148). The median estimate was 43.8 years, or the year 2064, with a right-skewed distribution reflecting variability in substitution rates. For HCV-level divergence (0.371 s/s), the mean estimated timeframe was 126.8 years (95% CI: 123.0 – 130.6), corresponding to a projected divergence year of 2147 (range: 2082 – 2324), with a median of 103.5 years (year 2124). For the influenza A virus threshold (1.956 s/s), the mean estimated time to comparable divergence was 668.6 years (95% CI: 648.4 – 688.7), translating to a projected year of 2689 (range: 2346 – 3620), with a median of 545.7 years, or the year 2566 (Figure 6).

Table 1. Estimates of evolutionary divergence over sequence pairs between HIV-1 subtypes/CRFs

HIV-1 species 1	HIV-1 species 2	Genetic distance (s/s)
CRF01_AE	C	0.231
CRF02_AG	CRF01_AE	0.200
CRF02_AG	C	0.227
A	CRF02_AG	0.157
A	CRF01_AE	0.203
A	C	0.223
B	D	0.188
B	A	0.220
B	CRF02_AG	0.223
B	CRF01_AE	0.226
B	C	0.227
D	A	0.219
D	CRF02_AG	0.230
D	CRF01_AE	0.235
D	C	0.229

Abbreviations: CRFs: Circulating recombinant forms; HIV-1: Human immunodeficiency virus 1; s/s: Substitutions per site.

3.7. Application of the new literature-based classification system to existing SARS-CoV-2 variants

To evaluate whether existing SARS-CoV-2 variants met the criteria for variant classification, each was assessed using the new literature-based classification system as follows: (1) Genetic distance analysis: None of the examined SARS-CoV-2 variants exceeded the moderate divergence threshold (0.157 s/s); (2) Functional and epidemiological review: While some variants demonstrated increased transmissibility and immune escape, none met all classification functional criteria. Omicron sub-lineages exhibited notable immune evasion but did not substantially increase clinical severity or hospitalization rates beyond prior VOCs; and (3) Longitudinal surveillance: No SARS-CoV-2 variant maintained dominance for >12 months or necessitated a fundamental vaccine update, which would indicate a stable antigenic drift pattern. These findings suggest that the present classification of SARS-CoV-2 variants as distinct lineages is not supported by genetic, virological, or epidemiological data. Under

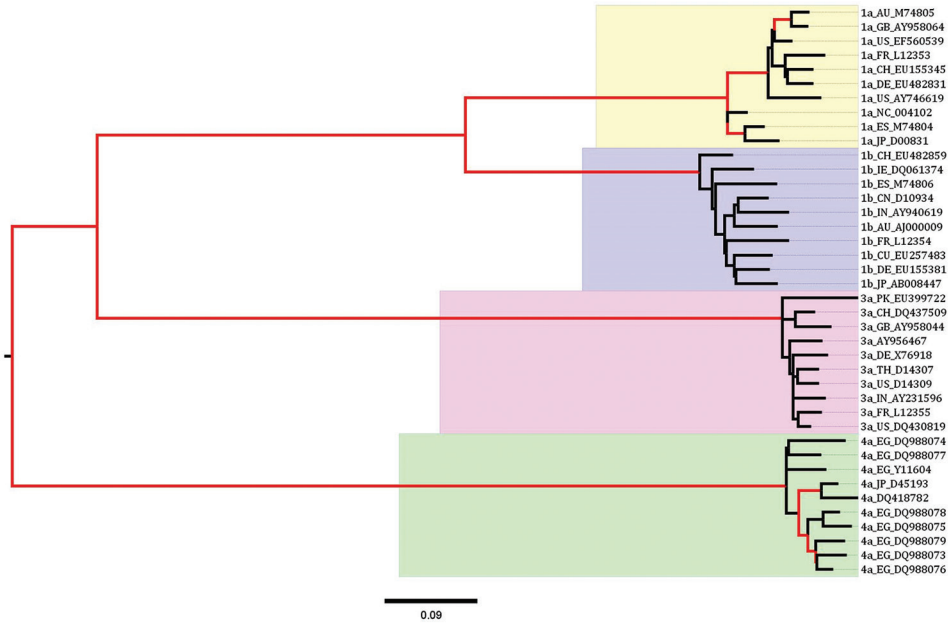

Figure 2. Maximum likelihood phylogenetic tree of HCV subtypes. Statistically supported branches are highlighted in red. The tree was visualized using the FigTree software.
Abbreviation: HCV: Hepatitis C virus.

the suggested classification system, none of the examined SARS-CoV-2 variants qualify as VOCs by both genetic and functional impact criteria, reinforcing the need for a revised classification framework based on objective thresholds.

Table 2. Estimates of evolutionary divergence over sequence pairs between HCV subtypes

HCV species 1	HCV species 2	Genetic distance (s/s)
1a	1b	0.371
1a	3a	0.613
1b	3a	0.554
1a	4a	0.599
1b	4a	0.637
3a	4a	0.674

Abbreviations: HCV: Hepatitis C virus; s/s: Substitutions per site.

4. Discussion

Although the present SARS-CoV-2 classification schemes played a role in early variant detection and response planning, several shortcomings remain that could be addressed with a complementary evolutionary and biologically based system. First, the present schemes overgeneralize risk, frequently triggering disproportionate public reactions before sufficient epidemiological data are available. Second, they lack robust quantitative severity metrics, often prioritizing genetic alterations over concrete clinical outcomes or real-world vaccine effectiveness. Third, they inadvertently amplify public anxiety by reinforcing the notion that each new variant constitutes an existential crisis, rather than a predictable feature of viral evolution.[123,124] A shift toward a refined, biologically relevant classification system is therefore needed. Rather than

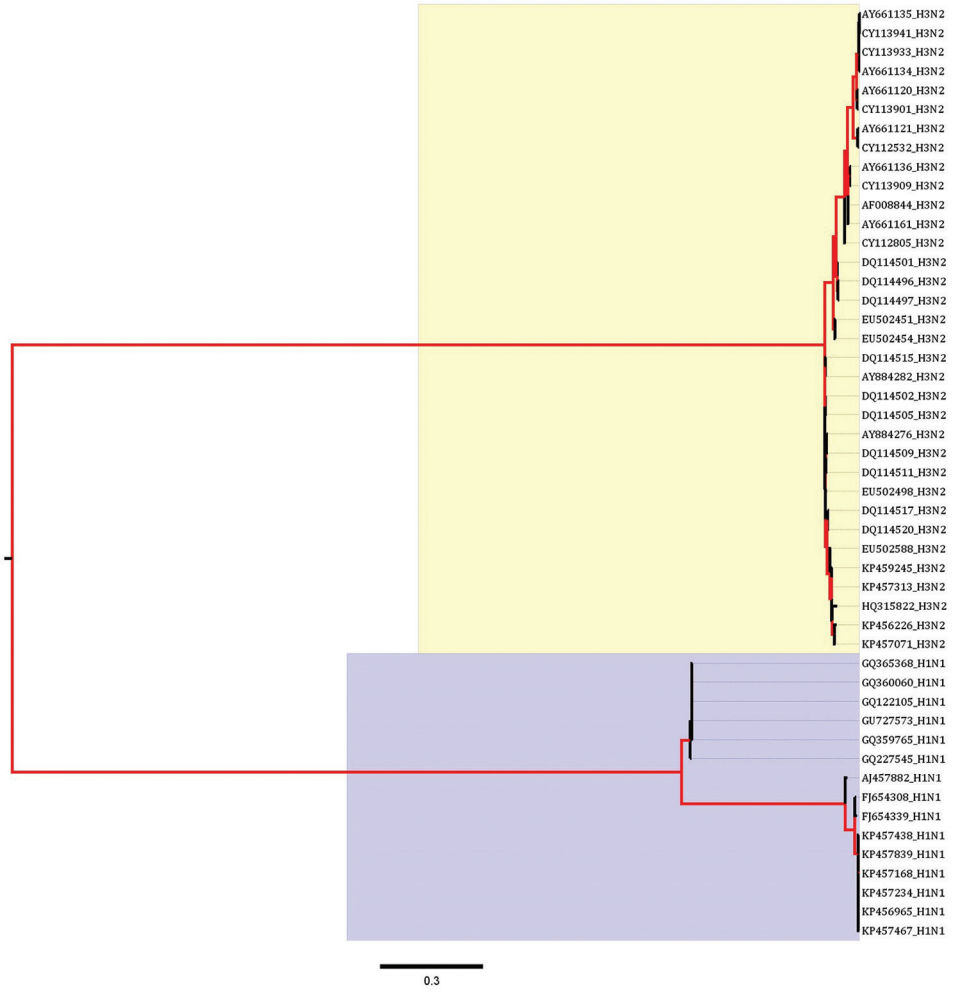

Figure 3. Maximum likelihood phylogenetic tree of influenza A virus subtypes. Statistically supported branches are highlighted in red. The tree was visualized using the FigTree software.

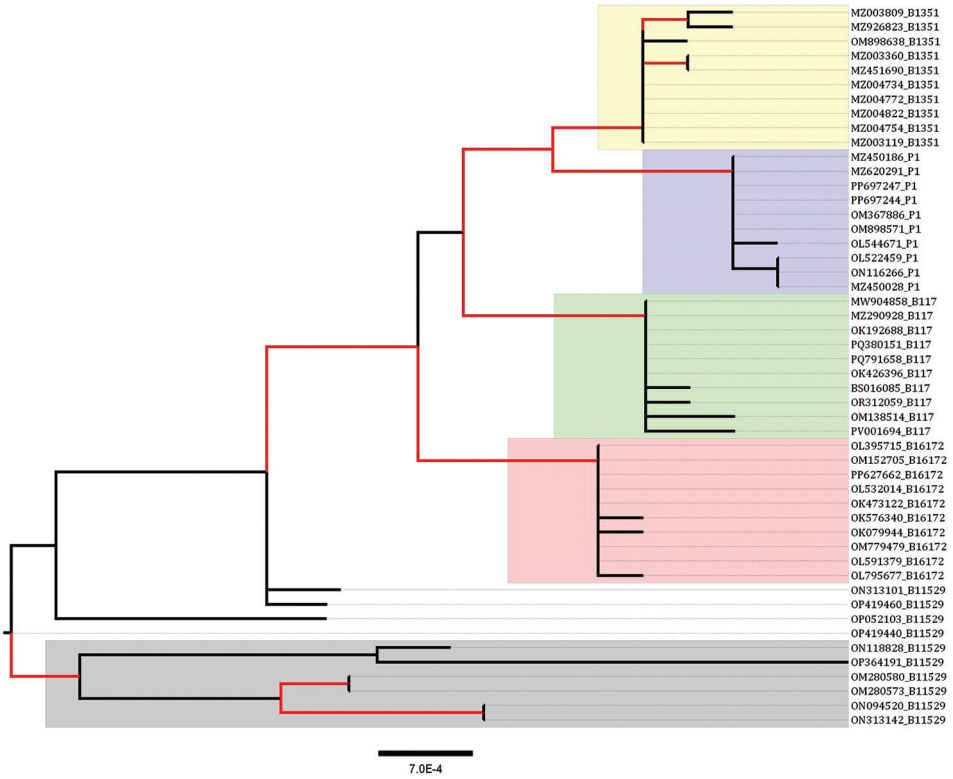

Figure 4. Maximum likelihood phylogenetic tree of SARS-CoV-2 VOCs. Statistically supported branches are highlighted in red. The tree was visualized using the FigTree software.
Abbreviations: SARS-CoV-2: Severe acute respiratory syndrome coronavirus 2; VOCs: Variants of concern.

Table 3. Estimates of evolutionary divergence over sequence pairs between SARS-CoV-2 VOCs

SARS-CoV-2 species 1	SARS-CoV-2 species 2	Genetic distance (s/s)
Omicron	Delta	0.005
Omicron	Beta	0.006
Delta	Beta	0.003
Omicron	Gamma	0.005
Delta	Gamma	0.003
Beta	Gamma	0.002
Omicron	Alpha	0.006
Delta	Alpha	0.003
Beta	Alpha	0.003
Gamma	Alpha	0.004

Abbreviations: SARS-CoV-2: Severe acute respiratory syndrome coronavirus 2; s/s: Substitutions per site; VOCs: Variants of concern.

abandoning existing surveillance efforts, a new approach would re-anchor SARS-CoV-2 variant designation in a long-term phylogenetic context – improving public health communication, reducing overreaction, and aligning public health policy with actual risk.

The recurrent emergence of new SARS-CoV-2 variants has repeatedly led to heightened concern. These concerns were amplified by media coverage with reactive health policy shifts despite limited evidence of substantial biological divergence of these variants.[125] From Alpha to Omicron and its subsequent sub-lineages, the actual epidemiological impact of these variants has exhibited substantial variability.[126,127] While certain mutations have been associated with enhanced transmissibility, immune evasion, or altered pathogenicity, the magnitude of these changes is often overstated in public discussions.[114,128-130] The assumption that every newly designated variant introduces a profound shift in SARS-CoV-2 behavior lacks consistent empirical validation. Most SARS-CoV-2 variants remain genetically and phenotypically constrained within a narrow evolutionary space, exhibiting only minor incremental changes rather than the transformative antigenic shifts observed in viruses such as influenza A virus.[131,132]

The classification of SARS-CoV-2 variants has dominated scientific discourse and public health decision-making, yet findings from the present study reveal fundamental flaws in the system currently in use. The

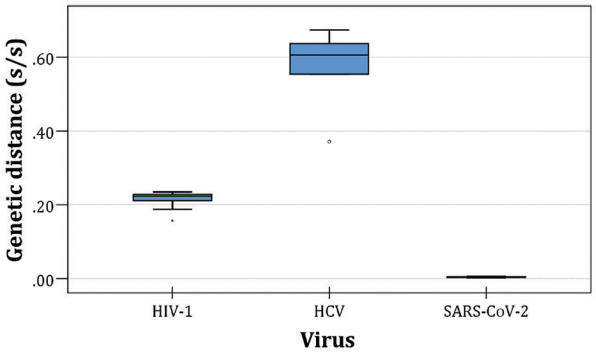

Figure 5. Genetic distance distributions among HIV-1, HCV, and SARS-CoV-2
Notes: Circles indicate mild outliers (1.5 – 3× interquartile range (IQR) from Q1 or Q3); asterisks indicate extreme outliers (>3× IQR).
Abbreviations: HCV: Hepatitis C virus; HIV-1: Human immunodeficiency virus 1; SARS-CoV-2: Severe acute respiratory syndrome coronavirus 2; s/s: Substitutions per site.

existing system, which rapidly designates emerging lineages as VOCs based on relatively minor genetic mutations, lacks quantifiable thresholds rooted in evolutionary virology. This study establishes a comparative framework by analyzing genetic divergence in well-characterized RNA viruses, including HIV-1, HCV, and influenza A virus, to determine whether SARS-CoV-2 variants exhibit levels of genetic differentiation that justify their classification as distinct viral entities. Results indicated that SARS-CoV-2 genetic distances are orders of magnitude below those observed in these benchmark viruses, demonstrating that the repeated designation of SARS-CoV-2 variants has been driven more by reactionary classification than by true viral evolution.

The classification of RNA viruses into lineages, variants, subtypes, clades, or genotypes has historically been based on genetic divergence thresholds that correlate with functional, epidemiological, or antigenic differentiation.[133-135] In this study, HIV-1 subtype classification was defined by a minimum genetic distance of 0.157 s/s, with clear distinctions in antigenicity, immune evasion, and drug resistance between HIV-1 subtypes/CRFs, as indicated by previous studies.[136-138] In addition, HCV subtypes exhibited even greater divergence (≥0.371 s/s), with genetic differences that impact both viral pathogenesis and treatment responses, as indicated by a multitude of previous studies.[139-142] Influenza A virus subtypes, which undergo antigenic shift, demonstrate a genetic divergence of approximately 1.956 s/s, corresponding to profound structural and functional changes in the hemagglutinin (HA) protein that drive immune escape and reinfection dynamics.[143,144]

In contrast, the analysis revealed that SARS-CoV-2 variants exhibited a maximum genetic distance of only

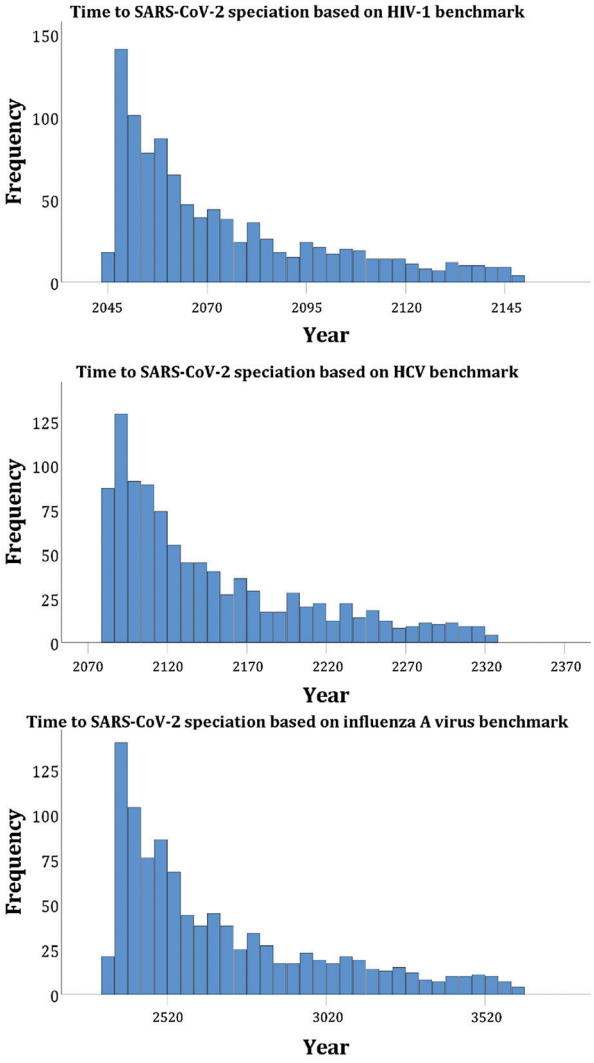

Figure 6. Projected time required for SARS-CoV-2 to reach speciation-level divergence based on comparative viral benchmarks
Abbreviations: HCV: Hepatitis C virus; HIV-1: Human immunodeficiency virus 1; SARS-CoV-2: Severe acute respiratory syndrome coronavirus.

0.006 s/s, placing them significantly below the minimum divergence threshold established for the HIV-1 subtype. This indicates that the widely publicized SARS-CoV-2 variants, including Alpha, Delta, and Omicron, fall within the range of normal intra-lineage variation rather than approaching the level of divergence that would justify classification as separate viral lineages. The absence of substantial genetic separation challenges the rationale behind the present SARS-CoV-2 classification system. Emerging data from the later stages of the COVID-19 pandemic (2023 – 2024) support the view that SARS-CoV-2 continues to evolve within a constrained genetic landscape.[145] For example, Markov *et al.*[49] described the appearance of VOCs as "shift-

like" events – abrupt, mutation-rich transitions following prolonged periods of undetected evolution. These contrast with the more gradual, "drift-like" evolution observed within the Omicron lineage.[49] Complementary CDC genomic surveillance during 2023 – 2024 indicated that dominant Omicron sub-lineages (e.g., XBB.1.5, JN.1) remained genetically close to earlier variants.[146,147]

To further contextualize the slow evolutionary trajectory of SARS-CoV-2, the time required for the virus to reach genetic divergence thresholds observed in HIV-1, HCV, and influenza A was modeled. Using the estimated evolutionary rate of SARS-CoV-2 (0.0004 – 0.002 s/s per year), the timeframes necessary for the accumulation of genetic distances comparable to those of other RNA viruses were calculated as follows: On average, HIV-1-like divergence would require 54 years; HCV-like divergence would require 127 years; and influenza A virus-like divergence would require 669 years. Even under accelerated evolutionary scenarios that incorporate recombination events, the time required for SARS-CoV-2 to evolve into a distinct viral lineage is projected to exceed the present pandemic timeline. This finding disputes the variant-driven narrative that suggests SARS-CoV-2 is undergoing rapid evolutionary shifts with each new lineage designation. Instead, the data support a preliminary conclusion that SARS-CoV-2 remains evolutionarily constrained, undergoing relatively slow genetic drift rather than true speciation.

As stated earlier, the WHO classification framework for SARS-CoV-2 variants is not entirely based on established genetic divergence thresholds but rather on epidemiological trends and qualitative assessments of transmissibility, immune escape, and severity.[35] However, the findings of this study suggest several contradictory aspects. Variant designations are applied inconsistently, with transient genetic mutations (e.g., D614G, N501Y) serving as the primary justification for labeling variants, despite similar mutations occurring in other viruses without warranting separate classification.[45,148]

Further supporting the hypothesis that some SARS-CoV-2 variant classifications may lack robust biological justification is the consistent observation that functional changes attributed to SARS-CoV-2 variants are quantitatively minor, particularly in comparison to antigenic shifts in influenza A virus.[75,149] While Omicron sub-lineages exhibit a 3 – 4-fold reduction in neutralizing antibody titers, this pales in comparison to the differences observed between HIV-1 subtypes/CRFs, highlighting the exaggerated portrayal of SARS-CoV-2 mutations as profound evolutionary shifts.[150,151] Thus, the epidemiological dominance of a SARS-CoV-2 variant at a given time point was often misinterpreted as increased viral fitness, without sufficient consideration of immune landscape effects, stochastic founder effects, and shifting population-level immunity in shaping variant emergence.[43] By relying on short-term epidemiological observations rather than virological principles, the present classification system of SARS-CoV-2 VOCs appears to promote an illusion of continuous viral emergence, despite genetic evidence indicating relative evolutionary stability of SARS-CoV-2, as shown by Lv *et al.*[71]

A more rigorous and biologically grounded framework for classifying SARS-CoV-2 variants would complement the existing system by providing clearer genetic and functional thresholds. This integrative approach could enhance the present SARS-CoV-2 classification schemes, offering additional context for long-term surveillance while preserving their relevance for rapid public health response. This approach would help to ensure that SARS-CoV-2 variant classifications are based on measurable evolutionary changes, rather than transient mutations that have contributed to public anxiety and misdirected public health responses.[123,124] A robust classification system must first define genetic divergence thresholds aligned with the established evolutionary dynamics of RNA viruses. In the case of HIV-1, HCV, and influenza A virus, genetic distances serve as a key determinant of whether a viral strain is classified as a distinct subtype/CRF, genotype/sub-genotype, or lineage.

While genetic divergence serves as the foundation of viral classification, the functional consequences of mutations must also be considered. A variant should not be designated solely based on genetic alterations, but rather on whether these changes confer a meaningful impact on transmission, immune evasion, or disease severity. Functional criteria must also be met in conjunction with genetic divergence thresholds to ensure that only biologically significant variants are designated as VOCs. These functional criteria include: (1) A demonstrable increase in transmissibility compared to the previously dominant variant; (2) a significant reduction in neutralizing antibody titers, confirmed in real-world immunological studies rather than isolated *in vitro* assays, indicating a meaningful immune escape advantage; (3) a significant increase in hospitalization rates attributable to increased intrinsic virulence, rather than confounding factors such as healthcare system burden or case misclassification; and (4) sustained epidemiological dominance lasting ≥12 months, ensuring that the emergent variant represents a sustained shift in viral evolution rather than a transient lineage fluctuation.

To put these criteria into practical aspects, influenza emerges as a stark example with antigenic shifts between

H1N1 and H3N2 being associated with near-complete immune escape and requiring substantial vaccine reformulation with a long period of circulation.[152,153] In contrast, no SARS-CoV-2 variant has maintained epidemiological dominance for over 12 months, a key criterion for distinguishing transient genetic shifts from long-term evolutionary changes. For instance, while Delta emerged as the dominant strain for several months, it was rapidly displaced by Omicron, which, in turn, has continued to generate multiple sub-lineages without a single, stable successor.[154] This pattern strongly suggests that SARS-CoV-2 evolution is characterized by alternating variant prevalence rather than sustained antigenic evolution, a hallmark of viruses undergoing immune-driven lineage differentiation. On the other hand, HIV-1 subtypes/CRFs, HCV genotypes/subtypes, and influenza A subtypes maintain long-term epidemiological dominance, persisting for decades despite selective pressures from immune responses and antiviral therapies.[138,141]

An important aspect that motivated this study can be presented as follows. By failing to incorporate both genetic divergence thresholds and functional impact assessments, the present WHO SARS-CoV-2 VOCs classification system may have resulted in unnecessary alarm and misdirected public health interventions.[155,156] The repeated reclassification of variants might have eroded public trust by creating the impression that SARS-CoV-2 is undergoing rapid, unpredictable evolutionary leaps, despite evidence indicating that it remains a genetically stable virus with a slow rate of change. This has also led to inefficient resource allocation, with disproportionate emphasis placed on variant-specific vaccine formulations, booster campaigns, and travel restrictions, rather than investing in broad-spectrum immunological strategies that provide durable protection against viral evolution.[47]

The potential misclassification of SARS-CoV-2 variants could have far-reaching consequences, influencing public health policies, economic stability, and scientific priorities, often in ways that lack a solid virological foundation. Reactive policy decisions, including travel bans, lockdowns, and stringent restrictions, were hastily implemented in response to the emergence of Beta, Gamma, and Omicron, despite these variants exhibiting genetic distances well within the bounds of normal intra-lineage variation.[157,158] Such responses were not only scientifically unjustified but also economically disruptive, fueling cycles of uncertainty that undermined long-term pandemic planning. Compounding this issue, the frequent and often sensationalized designation of new variants has significantly eroded public trust in health authorities. The portrayal of SARS-CoV-2 as an unpredictable, rapidly evolving virus – despite genomic evidence indicating relatively slow evolutionary change – has led to widespread misinformation, fostering public skepticism toward vaccination efforts and pandemic control measures.[159] In addition, scientific resources have been misallocated, with an excessive focus on sequencing minor genetic mutations rather than investing in broadly protective vaccines, long-term antiviral solutions, and cross-reactive immunological strategies. This relentless pursuit of tracking and naming every emerging sub-lineage has diverted focus from more sustainable public health interventions, including endemic virus management and the development of durable, pan-coronavirus strategies better suited for long-term mitigation efforts.

Building on the findings of this study, several areas for future research are warranted. Comparative genomic analyses should be expanded to include other coronaviruses – such as SARS-CoV-1, Middle East respiratory syndrome coronavirus (MERS-CoV), and endemic human coronaviruses – to establish divergence thresholds that are biologically tailored to the coronavirus family, rather than relying solely on benchmarks derived from HIV-1, HCV, and influenza A virus. Evolutionary rate modeling should be extended to longer timeframes, incorporating host adaptation, immune-driven selection, and antiviral pressure, all of which may alter divergence trajectories over time. Given the unique RNA proofreading mechanisms in coronaviruses, future work should also assess the role of recombination in shaping long-term evolution. Studies should investigate whether observed genetic divergence corresponds to antigenic drift by utilizing neutralization assays across multiple viral proteins beyond the spike. Moreover, large-scale meta-analyses are needed to clarify whether specific mutations consistently associate with increased clinical severity. Variant-specific models should be integrated into real-world vaccine effectiveness studies to better quantify the impact of mutations on breakthrough infections and the duration of immunity. Finally, the framework proposed in this study could be integrated with existing nomenclature systems such as Pango and the WHO variant classifications. By delineating transient, antigenically responsive sub-lineages from those exhibiting sustained phylogenetic divergence, this approach could provide a complementary strategy that improves evolutionary resolution and may help prevent overinterpretation of SARS-CoV-2 genomic changes, thereby reducing unnecessary public health interventions.

Finally, this study is subject to several limitations that should be taken into account as follows. First, SARS-CoV-2 has circulated in humans for a relatively short period, and while evolutionary projections were made based on the

present mutation rates, unforeseen selective pressures may alter these trajectories. Second, although SARS-CoV-2 has exhibited limited divergence to date, the potential for future recombination or adaptive mutations remains. Third, while the analysis included the most epidemiologically significant SARS-CoV-2 variants, it may not capture the evolutionary dynamics of rare or geographically restricted lineages. Fourth, evolutionary rate estimates are constrained by the availability and geographic distribution of sequencing data, which may overrepresent certain SARS-CoV-2 variants due to sequencing concentration in high-income countries. Fifth, although recombination was incorporated into the modeling, its true long-term impact on divergence is not fully understood. Sixth, inferences about transmissibility were drawn from epidemiological data rather than direct experimental comparisons, which were beyond the scope of this study. Finally, while the proposed classification system aims to guide future policy and research, its global adoption will require coordination and consensus among international public health authorities with potentially divergent priorities.

5. Conclusion

The classification of SARS-CoV-2 variants has profoundly shaped public health policy, vaccine development, and global perceptions throughout the pandemic. However, the analysis suggests that many of these classifications have not been consistently anchored in robust virological criteria, highlighting an opportunity to enhance the present system with more biologically grounded standards. Comparative genomic analyses demonstrate that the maximum divergence among SARS-CoV-2 variants (0.006 s/s) is substantially below the thresholds used to define subtypes in HIV-1, HCV, or influenza A virus. Even under accelerated evolutionary scenarios, the virus would require centuries to reach divergence levels warranting lineage designation. These findings challenge the prevailing narrative of rapid, unpredictable viral evolution and instead suggest that SARS-CoV-2 remains evolutionarily constrained. The frequent and inconsistent designation of VOCs has led to public confusion, reactionary policy decisions, and the diversion of scientific resources. To address these issues, an evidence-based framework integrating genetic, functional, and epidemiological criteria is proposed to classify SARS-CoV-2 variants. Under this proposed framework, none of the existing SARS-CoV-2 VOCs meet the combined genetic and functional thresholds typically required for lineage-level classification in other RNA viruses. Rather than replacing present classification systems, the proposed approach advocates for a paradigm shift that distinguishes persistent evolutionary patterns from short-term genetic fluctuations – to support more proportionate, evidence-based responses in future phases of the pandemic.

Acknowledgments

None.

Funding

None.

Conflict of interest

The authors declare they have no competing interests.

Author contributions

Conceptualization: Malik Sallam
Data curation: All authors
Formal analysis: Saja Al-Baidhani, Malik Sallam
Investigation: All authors
Methodology: All authors
Project administration: Malik Sallam
Supervision: Malik Sallam
Validation: Saja Al-Baidhani, Malik Sallam
Visualization: Malik Sallam
Writing – original draft: Malik Sallam
Writing – review & editing: All authors

Ethics approval and consent to participate

Not applicable.

Consent for publication

Not applicable.

Availability of data

The data presented in this study are available on request from the corresponding author (Malik Sallam).

References

1. Gorbalenya AE, Baker SC, Baric RS, *et al*. The species severe acute respiratory syndrome-related coronavirus: Classifying 2019-nCoV and naming it SARS-CoV-2. *Nat Microbiol*. 2020;5(4):536-544.

   doi: 10.1038/s41564-020-0695-z

2. Lu R, Zhao X, Li J, *et al*. Genomic characterisation and epidemiology of 2019 novel coronavirus: Implications for virus origins and receptor binding. *Lancet*. 2020;395(10224):565-574.

   doi: 10.1016/s0140-6736(20)30251-8

3. Zhou P, Yang XL, Wang XG, *et al*. A pneumonia outbreak associated with a new coronavirus of probable bat origin. *Nature*. 2020;579(7798):270-273.

   doi: 10.1038/s41586-020-2012-7

4. Rosen CJ. Viral variants, vaccinations, and long covid - new insights. *N Engl J Med*. 2024;391(6):561-562.

doi: 10.1056/NEJMe2407575

5. He F, Deng Y, Li W. Coronavirus disease 2019: What we know? *J Med Virol*. 2020;92(7):719-725.

   doi: 10.1002/jmv.25766

6. Joseph S, Kutty Narayanan A. Covid 19-the 21st century pandemic: The novel coronavirus outbreak and the treatment strategies. *Adv Pharm Bull*. 2022;12(1):34-44.

   doi: 10.34172/apb.2022.005

7. Sah P, Fitzpatrick MC, Zimmer CF, *et al*. Asymptomatic SARS-CoV-2 infection: A systematic review and meta-analysis. *Proc Natl Acad Sci U S A*. 2021;118(34):e2109229118.

   doi: 10.1073/pnas.2109229118

8. Gandhi RT, Lynch JB, Del Rio C. Mild or moderate Covid-19. *N Engl J Med*. 2020;383(18):1757-1766.

   doi: 10.1056/NEJMcp2009249

9. Çelik I, Öztürk R. From asymptomatic to critical illness: Decoding various clinical stages of COVID-19. *Turk J Med Sci*. 2021;51(Si-1):3284-3300.

   doi: 10.3906/sag-2107-137

10. Nikolich-Zugich J, Knox KS, Rios CT, Natt B, Bhattacharya D, Fain MJ. SARS-CoV-2 and COVID-19 in older adults: What we may expect regarding pathogenesis, immune responses, and outcomes. *GeroScience*. 2020;42(2):505-514.

    doi: 10.1007/s11357-020-00186-0

11. Boyton RJ, Altmann DM. The immunology of asymptomatic SARS-CoV-2 infection: What are the key questions? *Nat Rev Immunol*. 2021;21(12):762-768.

    doi: 10.1038/s41577-021-00631-x

12. Naqvi AAT, Fatima K, Mohammad T, *et al*. Insights into SARS-CoV-2 genome, structure, evolution, pathogenesis and therapies: Structural genomics approach. *Biochim Biophys Acta Mol Basis Dis*. 2020;1866(10):165878.

    doi: 10.1016/j.bbadis.2020.165878

13. Rahimi A, Mirzazadeh A, Tavakolpour S. Genetics and genomics of SARS-CoV-2: A review of the literature with the special focus on genetic diversity and SARS-CoV-2 genome detection. *Genomics*. 2021;113(1 Pt 2):1221-1232.

    doi: 10.1016/j.ygeno.2020.09.059

14. Alwine JC, Casadevall A, Enquist LW, Goodrum FD, Imperiale MJ. A critical analysis of the evidence for the SARS-CoV-2 origin hypotheses. *mSphere*. 2023;8(2):e0011923.

    doi: 10.1128/msphere.00119-23

15. Hao YJ, Wang YL, Wang MY, *et al*. The origins of COVID-19 pandemic: A brief overview. *Transbound Emerg Dis*. 2022;69(6):3181-3197.

    doi: 10.1111/tbed.14732

16. Boni MF, Lemey P, Jiang X, *et al*. Evolutionary origins of the SARS-CoV-2 sarbecovirus lineage responsible for the COVID-19 pandemic. *Nat Microbiol*. 2020;5(11):1408-1417.

    doi: 10.1038/s41564-020-0771-4

17. Pereson MJ, Mojsiejczuk L, Martínez AP, Flichman DM, Garcia GH, Di Lello FA. Phylogenetic analysis of SARS-CoV-2 in the first few months since its emergence. *J Med Virol*. 2021;93(3):1722-1731.

    doi: 10.1002/jmv.26545

18. Canuti M, Bianchi S, Kolbl O, *et al*. Waiting for the truth: is reluctance in accepting an early origin hypothesis for SARS-CoV-2 delaying our understanding of viral emergence? *BMJ Glob Health*. 2022;7(3):e008386.

    doi: 10.1136/bmjgh-2021-008386

19. Pekar JE, Magee A, Parker E, *et al*. The molecular epidemiology of multiple zoonotic origins of SARS-CoV-2. *Science*. 2022;377(6609):960-966.

    doi: 10.1126/science.abp8337

20. Bukin YS, Bondaryuk AN, Kulakova NV, Balakhonov SV, Dzhioev YP, Zlobin VI. Phylogenetic reconstruction of the initial stages of the spread of the SARS-CoV-2 virus in the Eurasian and American continents by analyzing genomic data. *Virus Res*. 2021;305:198551.

    doi: 10.1016/j.virusres.2021.198551

21. Domingo JL. What we know and what we need to know about the origin of SARS-CoV-2. *Environ Res*. 2021;200:111785.

    doi: 10.1016/j.envres.2021.111785

22. Latinne A, Hu B, Olival KJ, *et al*. Origin and cross-species transmission of bat coronaviruses in China. *Nat Commun*. 2024;15(1):10705.

    doi: 10.1038/s41467-024-55384-7

23. Voskarides K. SARS-CoV-2: Tracing the origin, tracking the evolution. *BMC Med Genomics*. 2022;15(1):62.

    doi: 10.1186/s12920-022-01208-w

24. Lopes LR, de Mattos Cardillo G, Paiva PB. Molecular evolution and phylogenetic analysis of SARS-CoV-2 and hosts ACE2 protein suggest Malayan pangolin as intermediary host. *Braz J Microbiol*. 2020;51(4):1593-1599.

    doi: 10.1007/s42770-020-00321-1

25. Samson S, Lord É, Makarenkov V. Assessing the emergence time of SARS-CoV-2 zoonotic spillover. *PLoS One*. 2024;19(4):e0301195.

    doi: 10.1371/journal.pone.0301195

26. Ruiz-Aravena M, McKee C, Gamble A, *et al*. Ecology, evolution and spillover of coronaviruses from bats. *Nat Rev Microbiol*. 2022;20(5):299-314.

    doi: 10.1038/s41579-021-00652-2

27. Holmes EC, Goldstein SA, Rasmussen AL, *et al*. The origins of

SARS-CoV-2: A critical review. *Cell*. 2021;184(19):4848-4856.

doi: 10.1016/j.cell.2021.08.017

28. Zhang T, Wu Q, Zhang Z. Probable pangolin origin of SARS-CoV-2 associated with the COVID-19 outbreak. *Curr Biol*. 2020;30(7):1346-1351.e2.

doi: 10.1016/j.cub.2020.03.022

29. Tang X, Ying R, Yao X, *et al*. Evolutionary analysis and lineage designation of SARS-CoV-2 genomes. *Sci Bull*. 2021;66(22):2297-2311.

doi: 10.1016/j.scib.2021.02.012

30. Rambaut A, Holmes EC, O'Toole Á, *et al*. A dynamic nomenclature proposal for SARS-CoV-2 lineages to assist genomic epidemiology. *Nat Microbiol*. 2020;5(11):1403-1407.

doi: 10.1038/s41564-020-0770-5

31. Forster P, Forster L, Renfrew C, Forster M. Phylogenetic network analysis of SARS-CoV-2 genomes. *Proc Natl Acad Sci U S A*. 2020;117(17):9241-9243.

doi: 10.1073/pnas.2004999117

32. Lemey P, Hong SL, Hill V, *et al*. Accommodating individual travel history and unsampled diversity in Bayesian phylogeographic inference of SARS-CoV-2. *Nat Commun*. 2020;11(1):5110.

doi: 10.1038/s41467-020-18877-9

33. Worobey M, Pekar J, Larsen BB, *et al*. The emergence of SARS-CoV-2 in Europe and North America. *Science*. 2020;370(6516):564-570.

doi: 10.1126/science.abc8169

34. Hill V, Du Plessis L, Peacock TP, *et al*. The origins and molecular evolution of SARS-CoV-2 lineage B.1.1.7 in the UK. *Virus Evol*. 2022;8(2):veac080.

doi: 10.1093/ve/veac080

35. World Health Organization. *Tracking SARS-CoV-2 Variants*; 2025. Available from: https://www.who.int/activities/tracking-SARS-CoV-2-variants [Last accessed on 2025 May 09].

36. Essabbar A, El Mazouri S, Boumajdi N, *et al*. Temporal dynamics and genomic landscape of SARS-CoV-2 after four years of evolution. *Cureus*. 2024;16(2):e53654.

doi: 10.7759/cureus.53654

37. Brüssow H. COVID-19: Emergence and mutational diversification of SARS-CoV-2. *Microb Biotechnol*. 2021;14(3):756-768.

doi: 10.1111/1751-7915.13800

38. Korber B, Fischer WM, Gnanakaran S, *et al*. Tracking changes in SARS-CoV-2 spike: Evidence that D614G increases infectivity of the COVID-19 virus. *Cell*. 2020;182(4):812-827.e19.

doi: 10.1016/j.cell.2020.06.043

39. Sallam M, Ababneh NA, Dababseh D, Bakri FG, Mahafzah A. Temporal increase in D614G mutation of SARS-CoV-2 in the Middle East and North Africa. *Heliyon*. 2021;7(1):e06035.

doi: 10.1016/j.heliyon.2021.e06035

40. Earnest R, Uddin R, Matluk N, *et al*. Comparative transmissibility of SARS-CoV-2 variants Delta and Alpha in New England, USA. *Cell Rep Med*. 2022;3(4):100583.

doi: 10.1016/j.xcrm.2022.100583

41. Sallam M, Mahafzah A. Molecular analysis of SARS-CoV-2 genetic lineages in Jordan: Tracking the introduction and spread of COVID-19 UK variant of concern at a country level. *Pathogens*. 2021;10(3):302.

doi: 10.3390/pathogens10030302

42. Chouikha A, Fares W, Laamari A, *et al*. Molecular epidemiology of SARS-CoV-2 in Tunisia (North Africa) through several successive waves of COVID-19. *Viruses*. 2022;14(3):624.

doi: 10.3390/v14030624

43. Carabelli AM, Peacock TP, Thorne LG, *et al*. SARS-CoV-2 variant biology: Immune escape, transmission and fitness. *Nat Rev Microbiol*. 2023;21(3):162-177.

doi: 10.1038/s41579-022-00841-7

44. Pondé RAA. Physicochemical effect of the N501Y, E484K/Q, K417N/T, L452R and T478K mutations on the SARS-CoV-2 spike protein RBD and its influence on agent fitness and on attributes developed by emerging variants of concern. *Virology*. 2022;572:44-54.

doi: 10.1016/j.virol.2022.05.003

45. Perez-Gomez R. The development of SARS-CoV-2 variants: The gene makes the disease. *J Dev Biol*. 2021;9(4):58.

doi: 10.3390/jdb9040058

46. Harris E. WHO launches broad coronavirus surveillance network. *JAMA*. 2024;331(19):1615.

doi: 10.1001/jama.2024.6724

47. Otto SP, Day T, Arino J, *et al*. The origins and potential future of SARS-CoV-2 variants of concern in the evolving COVID-19 pandemic. *Curr Biol*. 2021;31(14):R918-R929.

doi: 10.1016/j.cub.2021.06.049

48. O'Toole Á, Pybus OG, Abram ME, Kelly EJ, Rambaut A. Pango lineage designation and assignment using SARS-CoV-2 spike gene nucleotide sequences. *BMC Genomics*. 2022;23(1):121.

doi: 10.1186/s12864-022-08358-2

49. Markov PV, Ghafari M, Beer M, *et al*. The evolution of SARS-CoV-2. *Nat Rev Microbiol*. 2023;21(6):361-379.

doi: 10.1038/s41579-023-00878-2

50. Shahhosseini N, Babuadze GG, Wong G, Kobinger GP. Mutation signatures and *in silico* docking of novel SARS-CoV-2

variants of concern. *Microorganisms*. 2021;9(5):926.

doi: 10.3390/microorganisms9050926

51. Tao K, Tzou PL, Nouhin J, *et al*. The biological and clinical significance of emerging SARS-CoV-2 variants. *Nat Rev Genet*. 2021;22(12):757-773.

doi: 10.1038/s41576-021-00408-x

52. Subissi L, Otieno JR, Worp N, *et al.* An updated framework for SARS-CoV-2 variants reflects the unpredictability of viral evolution. *Nat Med*. 2024;30(9):2400-2403.

doi: 10.1038/s41591-024-02949-0

53. Giovanetti M, Benedetti F, Campisi G, *et al*. Evolution patterns of SARS-CoV-2: Snapshot on its genome variants. *Biochem Biophys Res Commun*. 2021;538:88-91.

doi: 10.1016/j.bbrc.2020.10.102

54. Hussain B, Wu C. Evolutionary and phylogenetic dynamics of SARS-CoV-2 variants: A genetic comparative study of Taiyuan and Wuhan Cities of China. *Viruses*. 2024;16(6):907.

doi: 10.3390/v16060907

55. Zabidi NZ, Liew HL, Farouk IA, *et al.* Evolution of SARS-CoV-2 variants: Implications on immune escape, vaccination, therapeutic and diagnostic strategies. *Viruses*. 2023;15(4):944.

doi: 10.3390/v15040944

56. Kumar R, Srivastava Y, Muthuramalingam P, *et al*. Understanding mutations in human SARS-CoV-2 spike glycoprotein: A systematic review & meta-analysis. *Viruses*. 2023;15(4):856.

doi: 10.3390/v15040856

57. Bhattacharya M, Chatterjee S, Lee SS, Dhama K, Chakraborty C. Antibody evasion associated with the RBD significant mutations in several emerging SARS-CoV-2 variants and its subvariants. *Drug Resist Updat*. 2023;71:101008.

doi: 10.1016/j.drup.2023.101008

58. Liu Y, Liu J, Plante KS, *et al*. The N501Y spike substitution enhances SARS-CoV-2 infection and transmission. *Nature*. 2022;602(7896):294-299.

doi: 10.1038/s41586-021-04245-0

59. Oude Munnink BB, Worp N, Nieuwenhuijse DF, *et al*. The next phase of SARS-CoV-2 surveillance: Real-time molecular epidemiology. *Nat Med*. 2021;27(9):1518-1524.

doi: 10.1038/s41591-021-01472-w

60. Parums V. Editorial: Revised world health organization (WHO) terminology for variants of concern and variants of interest of SARS-CoV-2. *Med Sci Monit*. 2021;27:e933622.

doi: 10.12659/msm.933622

61. Chen Z, Azman AS, Chen X, *et al*. Global landscape of SARS-CoV-2 genomic surveillance and data sharing. *Nat Genet*. 2022;54(4):499-507.

doi: 10.1038/s41588-022-01033-y

62. CDC COVID-19 Response Team. SARS-CoV-2 B.1.1.529 (Omicron) variant-United States, December 1-8, 2021. *MMWR Morb Mortal Wkly Rep.* 2021;70(50):1731-1734.

doi: 10.15585/mmwr.mm7050e1

63. Lambrou AS, Shirk P, Steele MK, *et al.* Genomic surveillance for SARS-CoV-2 variants: predominance of the delta (B.1.617.2) and Omicron (B.1.1.529) variants-United States, June 2021-January 2022. *MMWR Morb Mortal Wkly Rep.* 2022;71(6):206-211.

doi: 10.15585/mmwr.mm7106a4

64. The European Centre for Disease Prevention and Control. *ECDC De-escalates BA.2, BA.4 and BA.5 from its List of Variants of Concern*; 2025. Available from: https://www.ecdc.europa.eu/en/news-events/ecdc-de-escalates-ba2-ba4-and-ba5-its-list-variants-concern [Last accessed on 2025 May 09].

65. Kanuri S, Chen A, Barnett D, Hsu E. CDC policy changes during the COVID-19 pandemic. *Open J Soc Sci*. 2024;12:174-200.

doi: 10.4236/jss.2024.126009

66. Dolan PT, Whitfield ZJ, Andino R. Mechanisms and concepts in RNA virus population dynamics and evolution. *Annu Rev Virol*. 2018;5(1):69-92.

doi: 10.1146/annurev-virology-101416-041718

67. Woo HJ, Reifman J. Quantitative modeling of virus evolutionary dynamics and adaptation in serial passages using empirically inferred fitness landscapes. *J Virol*. 2014;88(2):1039-1050.

doi: 10.1128/jvi.02958-13

68. Lancaster KZ, Pfeiffer JK. Viral population dynamics and virulence thresholds. *Curr Opin Microbiol*. 2012;15(4):525-530.

doi: 10.1016/j.mib.2012.05.007

69. Jin T, Yin J. Patterns of virus growth across the diversity of life. *Integr Biol (Camb)*. 2021;13(2):44-59.

doi: 10.1093/intbio/zyab001

70. Pybus OG, Rambaut A. Evolutionary analysis of the dynamics of viral infectious disease. *Nat Rev Genet*. 2009;10(8):540-550.

doi: 10.1038/nrg2583

71. Lv JX, Liu X, Pei YY, *et al.* Evolutionary trajectory of diverse SARS-CoV-2 variants at the beginning of COVID-19 outbreak. *Virus Evol.* 2024;10(1):veae020.

doi: 10.1093/ve/veae020

72. Grellet E, L'Hôte I, Goulet A, Imbert I. Replication of the coronavirus genome: A paradox among positive-strand

RNA viruses. *J Biol Chem*. 2022;298(5):101923.

doi: 10.1016/j.jbc.2022.101923

73. Gupta S, Gupta D, Bhatnagar S. Analysis of SARS-CoV-2 genome evolutionary patterns. *Microbiol Spectr*. 2024;12(2):e0265423.

doi: 10.1128/spectrum.02654-23

74. Fischer W, Giorgi EE, Chakraborty S, *et al*. HIV-1 and SARS-CoV-2: Patterns in the evolution of two pandemic pathogens. *Cell Host Microbe*. 2021;29(7):1093-1110.

doi: 10.1016/j.chom.2021.05.012

75. Wang X, Li J, Liu H, Hu X, Lin Z, Xiong N. SARS-CoV-2 versus influenza A virus: Characteristics and co-treatments. *Microorganisms*. 2023;11(3):580.

doi: 10.3390/microorganisms11030580

76. Tahir M. Coronavirus genomic nsp14-ExoN, structure, role, mechanism, and potential application as a drug target. *J Med Virol*. 2021;93(7):4258-4264.

doi: 10.1002/jmv.27009

77. Robson F, Khan KS, Le TK, *et al*. Coronavirus RNA proofreading: Molecular basis and therapeutic targeting. *Mol Cell*. 2020;79(5):710-727.

doi: 10.1016/j.molcel.2020.07.027

78. Simmonds P. Rampant C→U hypermutation in the genomes of SARS-CoV-2 and other coronaviruses: Causes and consequences for their short- and long-term evolutionary trajectories. *mSphere*. 2020;5(3):e00408-20.

doi: 10.1128/mSphere.00408-20

79. Neher RA. Contributions of adaptation and purifying selection to SARS-CoV-2 evolution. *Virus Evol*. 2022;8(2):veac113.

doi: 10.1093/ve/veac113

80. Liu J, Wu Y, Gao GF. A structural voyage toward the landscape of humoral and cellular immune escapes of SARS-CoV-2. *Immunol Rev*. 2025;330(1):e70000.

doi: 10.1111/imr.70000

81. Tong Y, Lavillette D, Li Q, Zhong J. Role of hepatitis C virus envelope glycoprotein E1 in virus entry and assembly. *Front Immunol*. 2018;9:1411.

doi: 10.3389/fimmu.2018.01411

82. Beretta M, Migraine J, Moreau A, *et al*. Common evolutionary features of the envelope glycoprotein of HIV-1 in patients belonging to a transmission chain. *Sci Rep*. 2020;10(1):16744.

doi: 10.1038/s41598-020-73975-4

83. Xu C, Zhang N, Yang Y, *et al*. Immune escape adaptive mutations in hemagglutinin are responsible for the antigenic drift of Eurasian avian-like H1N1 swine influenza viruses. *J Virol*. 2022;96(16):e0097122.

doi: 10.1128/jvi.00971-22

84. Kuiken C, Korber B, Shafer RW. HIV sequence databases. *AIDS Rev*. 2003;5(1):52-61.

85. Kuiken C, Yusim K, Boykin L, Richardson R. The Los Alamos hepatitis C sequence database. *Bioinformatics*. 2005;21(3):379-384.

doi: 10.1093/bioinformatics/bth485

86. Calhoun VC, Hatcher EL, Yankie L, Nawrocki EP. Influenza sequence validation and annotation using VADR. *Database (Oxford)*. 2024;2024:baae091.

doi: 10.1093/database/baae091

87. Brister JR, Ako-Adjei D, Bao Y, Blinkova O. NCBI viral genomes resource. *Nucleic Acids Res*. 2015;43(Database issue):D571-D577.

doi: 10.1093/nar/gku1207

88. Drummond AJ, Ho SY, Phillips MJ, Rambaut A. Relaxed phylogenetics and dating with confidence. *PLoS Biol*. 2006;4(5):e88.

doi: 10.1371/journal.pbio.0040088

89. Abecasis A, Vandamme AM. Origin and distribution of HIV-1 subtypes. In: Hope TJ, Stevenson M, Richman D, editors. *Encyclopedia of AIDS*. Berlin: Springer New York; 2014. p. 1-16.

90. Hemelaar J, Elangovan R, Yun J, *et al*. Global and regional molecular epidemiology of HIV-1, 1990-2015: A systematic review, global survey, and trend analysis. *Lancet Infect Dis*. 2019;19(2):143-155.

doi: 10.1016/s1473-3099(18)30647-9

91. Smith DB, Bukh J, Kuiken C, *et al*. Expanded classification of hepatitis C virus into 7 genotypes and 67 subtypes: Updated criteria and genotype assignment web resource. *Hepatology*. 2014;59(1):318-327.

doi: 10.1002/hep.26744

92. Petrova VN, Russell CA. The evolution of seasonal influenza viruses. *Nat Rev Microbiol*. 2018;16(1):47-60.

doi: 10.1038/nrmicro.2017.118

93. Katoh K, Standley DM. MAFFT multiple sequence alignment software version 7: Improvements in performance and usability. *Mol Biol Evol*. 2013;30(4):772-780.

doi: 10.1093/molbev/mst010

94. Tamura K, Stecher G, Peterson D, Filipski A, Kumar S. MEGA6: Molecular evolutionary genetics analysis version 6.0. *Mol Biol Evol*. 2013;30(12):2725-2729.

doi: 10.1093/molbev/mst197

95. Tamura K, Nei M, Kumar S. Prospects for inferring very large phylogenies by using the neighbor-joining method.

Proc Natl Acad Sci U S A. 2004;101(30):11030-11035.

doi: 10.1073/pnas.0404206101

96. Ren A, Ishida T, Akiyama Y. Assessing statistical reliability of phylogenetic trees via a speedy double bootstrap method. *Mol Phylogenet Evol.* 2013;67(2):429-435.

doi: 10.1016/j.ympev.2013.02.011

97. Rambaut A, Drummond A. *FigTree v1. 3.1 Institute of Evolutionary Biology*. Scotland: University of Edinburgh. 2010.

98. Lemoine F, Gascuel O. The Bayesian phylogenetic bootstrap and its application to short trees and branches. *Mol Biol Evol.* 2024;41(11):msae238.

doi: 10.1093/molbev/msae238

99. Candido DS, Claro IM, de Jesus JG, *et al.* Evolution and epidemic spread of SARS-CoV-2 in Brazil. *Science*. 2020;369(6508):1255-1260.

doi: 10.1126/science.abd2161

100. Tegally H, Wilkinson E, Lessells RJ, *et al.* Sixteen novel lineages of SARS-CoV-2 in South Africa. *Nat Med*. 2021;27(3):440-446.

doi: 10.1038/s41591-021-01255-3

101. Tegally H, Wilkinson E, Giovanetti M, *et al.* Detection of a SARS-CoV-2 variant of concern in South Africa. *Nature*. 2021;592(7854):438-443.

doi: 10.1038/s41586-021-03402-9

102. Day T, Gandon S, Lion S, Otto SP. On the evolutionary epidemiology of SARS-CoV-2. *Curr Biol*. 2020;30(15):R849-R857.

doi: 10.1016/j.cub.2020.06.031

103. Faria NR, Mellan TA, Whittaker C, *et al.* Genomics and epidemiology of the P.1 SARS-CoV-2 lineage in Manaus, Brazil. *Science*. 2021;372(6544):815-821.

doi: 10.1126/science.abh2644

104. Focosi D, Maggi F. Recombination in coronaviruses, with a focus on SARS-CoV-2. *Viruses*. 2022;14(6):1239.

doi: 10.3390/v14061239

105. Turakhia Y, Thornlow B, Hinrichs A, *et al.* Pandemic-scale phylogenomics reveals the SARS-CoV-2 recombination landscape. *Nature*. 2022;609(7929):994-997.

doi: 10.1038/s41586-022-05189-9

106. Simon-Loriere E, Holmes EC. Why do RNA viruses recombine? *Nat Rev Microbiol*. 2011;9(8):617-626.

doi: 10.1038/nrmicro2614

107. Xiao Y, Rouzine IM, Bianco S, *et al.* RNA recombination enhances adaptability and is required for virus spread and virulence. *Cell Host Microbe*. 2016;19(4):493-503.

doi: 10.1016/j.chom.2016.03.009

108. van Dorp L, Richard D, Tan CCS, Shaw LP, Acman M, Balloux F. No evidence for increased transmissibility from recurrent mutations in SARS-CoV-2. *Nat Commun*. 2020;11(1):5986.

doi: 10.1038/s41467-020-19818-2

109. Davies NG, Abbott S, Barnard RC, *et al.* Estimated transmissibility and impact of SARS-CoV-2 lineage B.1.1.7 in England. *Science*. 2021;372(6538):eabg3055.

doi: 10.1126/science.abg3055

110. Gutierrez B, Márquez S, Prado-Vivar B, *et al.* Genomic epidemiology of SARS-CoV-2 transmission lineages in Ecuador. *Virus Evol.* 2021;7(2):veab051.

doi: 10.1093/ve/veab051

111. Hassan AS, Pybus OG, Sanders EJ, Albert J, Esbjörnsson J. Defining HIV-1 transmission clusters based on sequence data. *Aids*. 2017;31(9):1211-1222.

doi: 10.1097/qad.0000000000001470

112. Hedskog C, Parhy B, Chang S, *et al.* Identification of 19 novel hepatitis C virus subtypes-further expanding HCV classification. *Open Forum Infect Dis*. 2019;6(3):ofz076.

doi: 10.1093/ofid/ofz076

113. Takeshita M, Nishina N, Moriyama S, *et al.* Immune evasion and chronological decrease in titer of neutralizing antibody against SARS-CoV-2 and its variants of concerns in COVID-19 patients. *Clin Immunol*. 2022;238:108999.

doi: 10.1016/j.clim.2022.108999

114. Mahilkar S, Agrawal S, Chaudhary S, *et al.* SARS-CoV-2 variants: Impact on biological and clinical outcome. *Front Med (Lausanne)*. 2022;9:995960.

doi: 10.3389/fmed.2022.995960

115. Quintero AM, Eisner M, Sayegh R, *et al.* Differences in SARS-CoV-2 clinical manifestations and disease severity in children and adolescents by infecting variant. *Emerg Infect Dis*. 2022;28(11):2270-2280.

doi: 10.3201/eid2811.220577

116. Cojocaru C, Cojocaru E, Turcanu AM, Zaharia DC. Clinical challenges of SARS-CoV-2 variants (Review). *Exp Ther Med*. 2022;23(6):416.

doi: 10.3892/etm.2022.11343

117. Parczewski M, Scheibe K, Witak-Jędra M, Pynka M, Aksak-Wąs B, Urbańska A. Infection with HIV-1 subtype D adversely affects the live expectancy independently of antiretroviral drug use. *Infect Genet Evol.* 2021;90:104754.

doi: 10.1016/j.meegid.2021.104754

118. Baeten JM, Chohan B, Lavreys L, *et al.* HIV-1 subtype D infection is associated with faster disease progression than subtype A in spite of similar plasma HIV-1 loads. *J Infect*

Dis. 2007;195(8):1177-1180.

doi: 10.1086/512682

119. Palm AA, Esbjörnsson J, Månsson F, *et al.* Faster progression to AIDS and AIDS-related death among seroincident individuals infected with recombinant HIV-1 A3/CRF02_AG compared with sub-subtype A3. *J Infect Dis*. 2014;209(5):721-728.

doi: 10.1093/infdis/jit416

120. Dorp CHV, Goldberg EE, Hengartner N, Ke R, Romero-Severson EO. Estimating the strength of selection for new SARS-CoV-2 variants. *Nat Commun*. 2021;12(1):7239.

doi: 10.1038/s41467-021-27369-3

121. Tongo M, Harkins GW, Dorfman JR, *et al.* Unravelling the complicated evolutionary and dissemination history of HIV-1M subtype A lineages. *Virus Evol.* 2018;4(1):vey003.

doi: 10.1093/ve/vey003

122. Bedford T, Riley S, Barr IG, *et al*. Global circulation patterns of seasonal influenza viruses vary with antigenic drift. *Nature*. 2015;523(7559):217-220.

doi: 10.1038/nature14460

123. Kwon Y, Park J, An E, Jung S, Kweon K. Impact of omicron-variant SARS-CoV-2 infection on depression and anxiety: A community-based study in Korea. *Psychiatry Investig*. 2024;21(4):415-421.

doi: 10.30773/pi.2023.0323

124. Feng X, Yang C, Yang H, *et al*. Anxiety, depression, and somatic symptom disorders in health care workers at high altitude during the rapid spread of the SARS-CoV-2 Omicron variant: A prospective cohort study. *Front Psychiatry*. 2022;13:1018391.

doi: 10.3389/fpsyt.2022.1018391

125. Janik E, Niemcewicz M, Podogrocki M, Majsterek I, Bijak M. The emerging concern and interest SARS-CoV-2 variants. *Pathogens*. 2021;10(6):633.

doi: 10.3390/pathogens10060633

126. Hattab D, Amer MFA, Al-Alami ZM, Bakhtiar A. SARS-CoV-2 journey: From alpha variant to omicron and its sub-variants. *Infection*. 2024;52(3):767-786.

doi: 10.1007/s15010-024-02223-y

127. Andre M, Lau LS, Pokharel MD, *et al.* From alpha to omicron: How different variants of concern of the SARS-Coronavirus-2 impacted the world. *Biology (Basel)*. 2023;12(9):1267.

doi: 10.3390/biology12091267

128. Thakur S, Sasi S, Pillai SG, *et al.* SARS-CoV-2 mutations and their impact on diagnostics, therapeutics and vaccines. *Front Med (Lausanne)*. 2022;9:815389.

doi: 10.3389/fmed.2022.815389

129. Hirabara SM, Serdan TDA, Gorjao R, *et al.* SARS-COV-2 Variants: Differences and potential of immune evasion. *Front Cell Infect Microbiol*. 2021;11:781429.

doi: 10.3389/fcimb.2021.781429

130. Jabeen M, Shoukat S, Shireen H, Bao Y, Khan A, Abbasi AA. Unraveling the genetic variations underlying virulence disparities among SARS-CoV-2 strains across global regions: Insights from Pakistan. *Virol J*. 2024;21(1):55.

doi: 10.1186/s12985-024-02328-8

131. Telenti A, Hodcroft EB, Robertson DL. The evolution and biology of SARS-CoV-2 variants. *Cold Spring Harb Perspect Med*. 2022;12(5):a041390.

doi: 10.1101/cshperspect.a041390

132. Kim H, Webster RG, Webby RJ. Influenza virus: Dealing with a drifting and shifting pathogen. *Viral Immunol*. 2018;31(2):174-183.

doi: 10.1089/vim.2017.0141

133. Burrell CJ, Howard CR, Murphy FA. Chapter 2 - Classification of viruses and phylogenetic relationships. In: Burrell CJ, Howard CR, Murphy FA, editors. *Fenner and White's Medical Virology*. 5th ed. United States: Academic Press; 2017. p. 15-25.

134. Moya A, Holmes EC, González-Candelas F. The population genetics and evolutionary epidemiology of RNA viruses. *Nat Rev Microbiol*. 2004;2(4):279-288.

doi: 10.1038/nrmicro863

135. Geretti AM. HIV-1 subtypes: Epidemiology and significance for HIV management. *Curr Opin Infect Dis*. 2006;19(1):1-7.

doi: 10.1097/01.qco.0000200293.45532.68

136. Nastri BM, Pagliano P, Zannella C, *et al.* HIV and drug-resistant subtypes. *Microorganisms*. 2023;11(1):221.

doi: 10.3390/microorganisms11010221

137. Santoro MM, Perno CF. HIV-1 genetic variability and clinical implications. *ISRN Microbiol*. 2013;2013:481314.

doi: 10.1155/2013/481314

138. Rambaut A, Posada D, Crandall KA, Holmes EC. The causes and consequences of HIV evolution. *Nat Rev Genet*. 2004;5(1):52-61.

doi: 10.1038/nrg1246

139. Echeverría N, Moratorio G, Cristina J, Moreno P. Hepatitis C virus genetic variability and evolution. *World J Hepatol*. 2015;7(6):831-845.

doi: 10.4254/wjh.v7.i6.831

140. Martinez MA, Franco S. Therapy implications of hepatitis C virus genetic diversity. *Viruses*. 2020;13(1):41.

doi: 10.3390/v13010041

141. Sallam M, Khalil R. Contemporary insights into hepatitis C

virus: A comprehensive review. *Microorganisms*. 2024;12(6):1035.

doi: 10.3390/microorganisms12061035

142. Le Guillou-Guillemette H, Vallet S, Gaudy-Graffin C, *et al.* Genetic diversity of the hepatitis C virus: Impact and issues in the antiviral therapy. *World J Gastroenterol*. 2007;13(17):2416-2426.

doi: 10.3748/wjg.v13.i17.2416

143. Wu NC, Wilson IA. Influenza hemagglutinin structures and antibody recognition. *Cold Spring Harb Perspect Med*. 2020;10(8):a038778.

doi: 10.1101/cshperspect.a038778

144. Wu NC, Wilson IA. A perspective on the structural and functional constraints for immune evasion: Insights from influenza virus. *J Mol Biol*. 2017;429(17):2694-2709.

doi: 10.1016/j.jmb.2017.06.015

145. Faraji N, Zeinali T, Joukar F, *et al.* Mutational dynamics of SARS-CoV-2: Impact on future COVID-19 vaccine strategies. *Heliyon*. 2024;10(9):e30208.

doi: 10.1016/j.heliyon.2024.e30208

146. Ma KC, Shirk P, Lambrou AS, *et al.* Genomic surveillance for SARS-CoV-2 variants: circulation of omicron lineages - United States, January 2022-May 2023. *MMWR Morb Mortal Wkly Rep.* 2023;72(24):651-656.

doi: 10.15585/mmwr.mm7224a2

147. Ma KC, Castro J, Lambrou AS, *et al.* Genomic surveillance for SARS-CoV-2 variants: Circulation of omicron XBB and JN.1 lineages - United States, May 2023-September 2024. *MMWR Morb Mortal Wkly Rep.* 2024;73(42):938-945.

doi: 10.15585/mmwr.mm7342a1

148. Grabowski F, Preibisch G, Giziński S, Kochańczyk M, Lipniacki T. SARS-CoV-2 variant of concern 202012/01 has about twofold replicative advantage and acquires concerning mutations. *Viruses*. 2021;13(3):392.

doi: 10.3390/v13030392

149. Havasi A, Visan S, Cainap C, Cainap SS, Mihaila AA, Pop LA. Influenza A, influenza B, and SARS-CoV-2 similarities and differences - a focus on diagnosis. *Front Microbiol*. 2022;13:908525.

doi: 10.3389/fmicb.2022.908525

150. Gruell H, Vanshylla K, Korenkov M, *et al.* SARS-CoV-2 Omicron sublineages exhibit distinct antibody escape patterns. *Cell Host Microbe*. 2022;30(9):1231-1241.e6.

doi: 10.1016/j.chom.2022.07.002

151. Stefic K, Bouvin-Pley M, Braibant M, Barin F. Impact of HIV-1 diversity on its sensitivity to neutralization. *Vaccines (Basel)*. 2019;7(3):74.

doi: 10.3390/vaccines7030074

152. van de Sandt CE, Kreijtz JH, Rimmelzwaan GF. Evasion of influenza A viruses from innate and adaptive immune responses. *Viruses*. 2012;4(9):1438-1476.

doi: 10.3390/v4091438

153. Nuwarda RF, Alharbi AA, Kayser V. An overview of influenza viruses and vaccines. *Vaccines (Basel)*. 2021;9(9):1032.

doi: 10.3390/vaccines9091032

154. Santiago GA, Volkman HR, Flores B, *et al.* SARS-CoV-2 omicron replacement of delta as predominant variant, Puerto Rico. *Emerg Infect Dis*. 2023;29(4):855-857.

doi: 10.3201/eid2904.221700

155. Zhao H, Han K, Gao C, *et al.* VOC-alarm: Mutation-based prediction of SARS-CoV-2 variants of concern. *Bioinformatics*. 2022;38(14):3549-3556.

doi: 10.1093/bioinformatics/btac370

156. Salehi-Vaziri M, Fazlalipour M, Seyed Khorrami SM, *et al.* The ins and outs of SARS-CoV-2 variants of concern (VOCs). *Arch Virol*. 2022;167(2):327-344.

doi: 10.1007/s00705-022-05365-2

157. Tegally H, Wilkinson E, Tsui JL, *et al.* Dispersal patterns and influence of air travel during the global expansion of SARS-CoV-2 variants of concern. *Cell*. 2023;186(15):3277-3290.e16.

doi: 10.1016/j.cell.2023.06.001

158. Chen S, Guo L, Xie Y, *et al.* Government responses to the COVID-19 pandemic of the Gulf Cooperation Council countries: Good practices and lessons for future preparedness. *Glob Health Res Policy*. 2024;9(1):10.

doi: 10.1186/s41256-024-00349-y

159. Kisa S, Kisa A. A comprehensive analysis of COVID-19 misinformation, public health impacts, and communication strategies: Scoping review. *J Med Intern Res*. 2024;26:e56931.

doi: 10.2196/56931

ACCSCIENCE PUBLISHING

Microbes & Immunity

ORIGINAL RESEARCH ARTICLE

A comprehensive statistical analysis of COVID-19 trends: Global and United States insights through ARIMA, regression, and spatial models

Zhihao Lei[1,2*]

[1]School of Mathematics, University of Edinburgh, Edinburgh, Scotland, United Kingdom

[2]Department of Biostatistics, School of Public Health, Brown University, Providence, Rhode Island, United States of America

Abstract

The COVID-19 pandemic has driven the need for accurate data analysis and forecasting to support public health decision-making. This study applied autoregressive integrated moving average (ARIMA) models and ARIMA models with exogenous variables to predict short-term trends in confirmed COVID-19 cases across several regions, including the United States of America, Asia, Europe, and Africa. Model performance was compared between ARIMA and the automated model selection function, auto.arima, and anomaly detection was performed to investigate discrepancies between predicted and observed case numbers. Additionally, the study explored the relationship between vaccination rates and new case trends while also examining the influence of socioeconomic factors—such as gross domestic product per capita, human development index, and healthcare resources availability—on COVID-19 incidence across countries. The findings provide valuable insights into the effectiveness of predictive models and highlight the significant role of socioeconomic factors in the spread of the virus, thereby contributing to the development of more effective strategies for future epidemic prevention and control.

Keywords: Autoregressive integrated moving average model; COVID-19; Public health; Socioeconomic factors; Time series forecasting; Vaccination rates

***Corresponding author:**
Zhihao Lei
(Z.Lei-6@sms.ed.ac.uk)

Citation: Lei Z. A comprehensive statistical analysis of COVID-19 trends: Global and United States insights through ARIMA, regression, and spatial models. *Microbes & Immunity*. 2025;2(3):108-129. doi: 10.36922/MI025040007

Received: January 22, 2025

Revised: April 9, 2025

Accepted: May 12, 2025

Published online: June 18, 2025

1. Introduction

Since the onset of the COVID-19 pandemic in late 2019, the pandemic has had profound and widespread effects on global public health, economies, and daily life. As of 2024, it continues to pose challenges to healthcare systems worldwide, underscoring the ongoing need for accurate forecasting of case trends for effective policy-making decisions and intervention strategies. Statistical modeling, particularly time series analysis, has proven to be a valuable tool in predicting the trajectory of the pandemic and supporting the development of effective public health responses.[1]

Among the range of statistical models, the autoregressive integrated moving average (ARIMA) model has been widely employed in epidemiological studies for short-term forecasting due to its simplicity and effectiveness in modeling temporal data.[2] ARIMA

models have been utilized to predict COVID-19 case trends across different countries, often producing reasonably accurate forecasts over limited time horizons.[3] However, the accuracy of ARIMA-based forecasts can vary significantly depending on the region and time period, influenced by factors such as viral mutations, government interventions, and changes in population behavior.[4] One notable limitation of ARIMA models is their exclusive reliance on historical data, without considering external factors that might influence future trends—such as vaccination rates, policy changes, or behavioral adaptations—which introduces greater uncertainty in long-term predictions.

To address these limitations, the ARIMA with exogenous variables (ARIMAX) model incorporates external variables—such as vaccination rates—to enhance its predictive capabilities. By incorporating vaccination data, the model enables researchers to assess the potential impact of vaccination campaigns on future case trends, providing a more comprehensive understanding of epidemic dynamics.[5] Although previous studies have shown that vaccination plays a crucial role in mitigating the spread of COVID-19—leading to significant reductions in new case numbers following mass immunization efforts[6]—most of these studies are region-specific or limited to particular periods and do not fully capture the complex interactions between vaccination efforts, virus mutations, and policy interventions.

In addition to time series forecasting, examining the relationship between COVID-19 incidence and socioeconomic factors is crucial. Previous research has highlighted the influence of indicators—such as gross domestic product (GDP) per capita, healthcare infrastructure, and other socioeconomic variables—in shaping the impact of the pandemic across different regions.[7] For example, countries with greater healthcare spending and more robust medical systems tend to manage the crisis more effectively, resulting in lower mortality rates and more effective containment strategies.[8] However, most of the existing research relies on single-variable analyses and does not fully capture the complex, multifaceted interactions among socioeconomic factors, which may contribute to significant disparities in COVID-19 outcomes across different countries.

This study aims to advance existing research by applying both ARIMA and ARIMAX models to predict short-term COVID-19 case trends in the United States (US) and globally. In the ARIMAX model, vaccination rates are incorporated as an exogenous variable to enhance predictive accuracy and provide deeper insights into the relationship between vaccination efforts and new case trends. Discrepancies between predicted and actual case numbers are examined to investigate potential causes for forecast anomalies, such as policy changes and virus mutations. Additionally, the study explores the socioeconomic factors—including GDP per capita, healthcare resources, and human development index (HDI)—on COVID-19 case numbers across countries. This multidimensional approach allows for a more comprehensive comparison of ARIMA and ARIMAX models performance, while also offering valuable perspectives on the broader determinants of the pandemic's spread, contributing to future epidemic prevention and control strategies.

2. Data collection

To conduct a comprehensive analysis of the COVID-19 pandemic and its associated factors, a diverse set of datasets was obtained from reputable sources, including the World Health Organization (WHO), Centers for Disease Control and Prevention, World Bank, and other national and international agencies. These datasets were selected based on their relevance, comprehensiveness, and frequency of updates to ensure that the analysis reflects the most accurate and current information available. As shown in Table 1, the data include daily and weekly reports of COVID-19 cases, deaths, and vaccination trends, alongside key socioeconomic indicators such as GDP per capita, HDI, Gini index, healthcare expenditures, and healthcare infrastructure data. These variables were essential for modeling the progression of the pandemic and for evaluating the impact of various factors on infection rates.

All statistical analyses were conducted using R version 4.4.3.

3. Methodology

3.1. Theoretical basis of the ARIMA model

The ARIMA model is a statistical method commonly used for analyzing and forecasting time series data. The general form of an ARIMA model with order (p, d, q) is represented by the following equation:

$$\phi(B)\nabla^d x_t = \theta(B)\varepsilon_t \quad \text{(I)}$$

where:

(i) $\nabla^d = (1-B)^d$ is the differencing operator, with B representing the backshift operator,[9]

(ii) $\phi(B) = 1-\phi_1 B - \cdots - \phi_p B^p$ is the autoregressive (AR) coefficient polynomial,[9]

(iii) $\theta(B) = 1-\theta_1 B - \cdots - \theta_q B^q$ is the moving average (MA) coefficient polynomial,[9]

(iv) ε_t denotes white noise error terms that satisfy the following properties: $E(\varepsilon_t) = 0$, Var $(\varepsilon_t) = \sigma^2$,

(v) $E(\varepsilon_t \varepsilon_s) = 0$ for $s \neq t$,[9]

Table 1. Overview of key datasets

Data source	Data description	Link
WHO	Daily COVID-19 case and death data reported to the WHO, updated weekly and incorporating corrections to historical records based on newly received information	https://data.who.int/dashboards/covid19/data?n=c
United Nations Development Programme	The HDI measures key dimensions of human development, such as a long and healthy life, access to education, and a decent standard of living	https://hdr.undp.org/data-center/human-development-index#/indices/HDI
CDC	COVID-19 vaccination trends in the US at both national and jurisdictional levels, regularly updated to reflect changes over time	https://data.cdc.gov/Vaccinations/
	Archived weekly data on COVID-19 cases and deaths in the US, providing state-level trends and historical records	https://data.cdc.gov/Case-Surveillance/Weekly-United-States-COVID-19-Cases-and-pwn4-m3yp/about_data
	County-level data on COVID-19 vaccinations in the US, including detailed trends and demographic breakdowns	https://data.cdc.gov/Vaccinations/COVID-19-Vaccinations-in-the-United-Stat8×kx-amqh/about_data
World Bank	GDP per capita (in current US$), representing the monetary value of all final goods and services produced per person in a given year	https://data.worldbank.org/indicator/NY.GDP.PCAP.CD
	The Gini index measures the distribution of income across a population, representing inequality	https://data.worldbank.org/indicator/SI.POV.GINI
	Current health expenditure per capita (in current US$) represents the average national spending on healthcare per individual	https://data.worldbank.org/indicator/SH.XPD.CHEX.PC.CD
	Hospital beds per 1,000 people, indicating the availability of healthcare infrastructure	https://data.worldbank.org/indicator/SH.MED.BEDS.ZS
	Population density, measured as the number of people per km^2 of land area, reflects how concentrated a population is within a specific area	https://data.worldbank.org/indicator/EN.POP.DNST
Bureau of Economic Analysis	GDP and personal income by state for the first quarter of 2024, providing insights into regional economic performance	https://www.bea.gov/data/gdp/gdp-state
US Census Bureau	Historical population density data (1910 – 2020) provides population density trends over the past century	https://www.census.gov/data/tables/time-series/dec/density-data-text.html
	State population totals and components of change from 2020 to 2023, highlighting trends in population growth, decline, and migration patterns	https://www.census.gov/data/tables/time-series/demo/popest/2020s-state-total.html
Kaiser Family Foundation	Healthcare expenditures per capita by state of residence, providing detailed insights into state-level spending on healthcare	https://www.kff.org/other/state-indicator/health-spending-per-capita/?currentTimeframe=0&sortModel=%7B%22colId%22:%22Location%22%22sort%22:%22asc%22%7D
	Number of hospital beds per 1,000 people by ownership type, providing insights into the distribution and availability of healthcare resources	https://www.kff.org/other/state-indicator/beds-by-ownership/?currentTimeframe=0&sortModel=%7B%22colId%22:%22Location%22%22sort%22:%22asc%22%7D

Abbreviations: GDP: Gross domestic product; HDI: Human development index; US: United states; WHO: World health organization.

(vi) $E(x_s \varepsilon_t) = 0$ for all $s < t$, ensuring that the noise terms are uncorrelated with past values of the series.[10]

The ARIMA model consists of three main components:

(i) Autoregressive: Captures the relationship between a current observation and its past (lagged) values.[9]

(ii) Integrated: Represents the differencing of observations required to achieve stationarity in the time series.[9]

(iii) Moving average: Models the relationship between a current observation and the residual errors from an MA model applied to past (lagged) observations.[9]

The ARIMA modeling process began with a stationarity test, commonly conducted using the augmented Dickey–Fuller test.[11] If the time series is found to be non-stationary, transformations such as differencing or logarithmic scaling are typically applied to achieve stationarity.[10] Model identification involved determining the orders of the model, specifically the values of p and q, which represent the AR and MA terms, respectively. This step is usually performed by analyzing the autocorrelation function (ACF) and partial autocorrelation function (PACF) plots.[9] The differencing order (d) was determined based on the transformations applied during the stationarity testing phase.

Following model identification, the parameters ϕ_i and θ_j were estimated, typically using maximum likelihood estimation.[10] Model validation was then performed using statistical tests such as the Ljung-Box test to ensure that the residuals exhibited white noise behavior, indicating that the model adequately captured the time series structure.[12] Model selection was based on information criteria such as the Akaike information criterion (AIC) or Bayesian information criterion (BIC), with preference given to the model with the lowest criterion value.[13] Finally, once validated, the model was employed to forecast future values of the time series.[9]

Figure 1 summarizes this process, illustrating the sequence of steps from stationarity assessment to forecasting.

3.2. Rolling window cross-validation and comparison with auto.arima

In this study, rolling window cross-validation was used to evaluate the performance of ARIMA models for time series forecasting. The primary goal was to identify the optimal ARIMA model parameters by minimizing the root mean squared error (RMSE) and to compare the results with those obtained from the automated model selection function, auto.arima.[14]

Rolling window cross-validation is a method specifically designed for time series data as it preserves the temporal order of the data. In each iteration, the model was trained on a fixed-length window of historical data and validated on the subsequent observation. This approach ensures that the evaluation reflects real-world forecasting conditions, where future values must be predicted using only past data.[15] For each ARIMA model evaluated, the one-step-ahead forecast errors were calculated, and RMSE was used as the primary evaluation metric. RMSE is given:

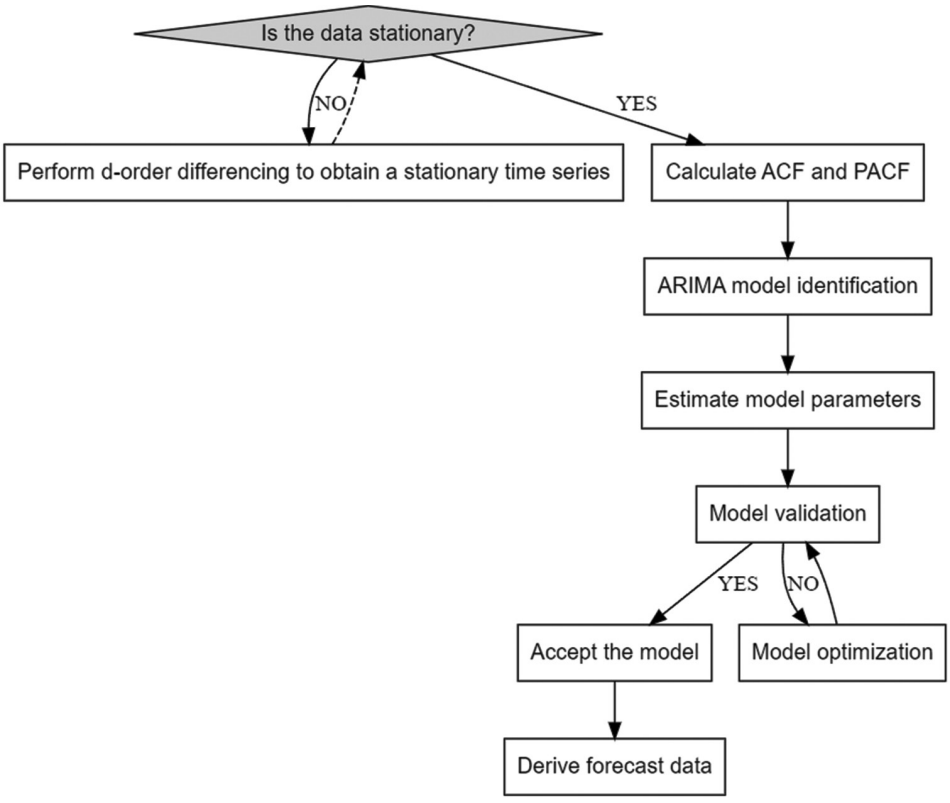

Figure 1. The autoregressive integrated moving average model construction flow chart
Abbreviations: ACF: Autocorrelation function; ARIMA: Autoregressive integrated moving average; PACF: Partial autocorrelation function.

$$\text{RMSE} = \sqrt{\frac{1}{n}\sum_{i=1}^{n}\left(x_i - \breve{x}_i\right)^2} \quad \text{(II)}$$

where x_i is the actual value, and $\hat{x}_i$ is the predicted value. Lower RMSE values indicate better model performance.[16]

A grid search was conducted across various combinations of the p and q parameters, with the d-order fixed at 1. This process was parallelized to efficiently explore the parameter space.[14] RMSE was used as the evaluation metric due to its effectiveness in quantifying average prediction errors while placing greater emphasis on larger errors.[17] This characteristic makes RMSE particularly useful in contexts where significant forecasting errors could lead to significant consequences, as it penalizes large discrepancies more heavily than other metrics, such as mean absolute error (MAE). Additionally, since RMSE is measured in the same units as the original data, it provides results that are interpretable in practical applications.

To compare the performance between manual and automated model selections, the auto.arima function was employed. This function automatically identifies the optimal ARIMA model by optimizing information criteria such as the AIC or BIC.[18] While auto.arima provides a rapid and efficient global fit over the entire dataset, rolling window cross-validation offers a more robust evaluation by assessing the model's predictive performance across different time periods.[19] This approach enabled a detailed comparison of the consistency and reliability of automated versus manually selected models.

By visualizing the RMSE values across various parameter combinations, the best-performing model identified through rolling window cross-validation was compared with the model selected by auto.arima. This comparison provided insights into the trade-offs between automated selection and manual tuning in ARIMA-based time series forecasting.

3.3. Anomaly detection

Anomaly detection in time series data is crucial for identifying irregular patterns, such as sudden spikes in COVID-19 case numbers. In this study, a statistical approach was employed to detect anomalies directly from the time series data without fitting a complex model like ARIMA. This method, known as residual-based anomaly detection, identifies outliers based on their deviation from expected behavior within the data.[14]

The anomaly detection approach relies on statistical rules that identify observations as anomalies when they significantly deviate from surrounding values. Specifically, outliers are detected by analyzing the residuals after accounting for typical patterns in the time series.[20] In this study, the residuals were examined, and points were classified as outliers if their deviation from the local mean exceeded a certain threshold.

The theoretical basis for this method involves identifying points that significantly deviate from the local mean or expected value of the time series. Mathematically, a data point x_t is considered an outlier if it satisfies the condition:

$$|x_t - \mu| > k \times \sigma \quad \text{(III)}$$

where:

(i) μ represents the local mean,

(ii) σ is the standard deviation of the surrounding data points,

(iii) k is a threshold factor that determines the sensitivity of the detection.[21]

Typically, k is set to values such as 2 or 3, corresponding to confidence intervals commonly used in outlier detection.[20]

This method is particularly effective for detecting additive outliers, which appear as sudden spikes or drops in the time series—events that may result from external shocks such as the emergence of a new COVID-19 variant.[14] Identifying and analyzing these outliers provides valuable insights into how unexpected events influence overall trends, enabling more informed adjustments to forecasting models.

The detected anomalies were then visualized in a time series plot, highlighting points of significant deviation to facilitate further investigation and model adjustments.[21]

3.4. Theoretical basis of the ARIMAX model

To improve the accuracy of time series forecasting, the ARIMAX model was employed, integrating external factors into the standard ARIMA model. This extension allows the model to account for factors beyond the inherent patterns in the target time series.[14] In this study, vaccination rates were included as an exogenous variable to determine whether they would improve forecast accuracy compared to the ARIMA model, which relied solely on historical time series data.

The ARIMAX model expanded upon the ARIMA framework by introducing exogenous regressors—external variables believed to influence the dependent variable. Mathematically, the ARIMAX model is expressed as:

$$y_t = \phi_0 + \sum_{i=1}^{p}\phi_i y_{t-i} + \sum_{j=1}^{q}\theta_j \epsilon_{t-j} + \epsilon_t + \sum_{k=1}^{r}\beta_k X_{t-k} \quad \text{(IV)}$$

where:
(i) y_t represents the value of the dependent variable at time t,
(ii) ϕ_i are the AR coefficients,
(iii) θ_j are the MA coefficients,
(iv) ϵ_t is the error term,
(v) X_{t-k} represents the exogenous variable lagged by k periods.[22]

Exogenous variables were incorporated to capture additional influences on the time series that could not be explained solely by its historical values.[9]

The ARIMAX model was fitted using an automated selection of ARIMA parameters (p, d, and q) while incorporating the selected exogenous variable. Model performance was evaluated by comparing the ARIMAX model against the ARIMA model using standard evaluation metrics, such as AIC, RMSE, and MAE.[14,16]

Model forecasts were generated for a holdout period to assess predictive accuracy. The inclusion of exogenous variables in the ARIMAX model enables an assessment of whether incorporating external factors can improve the forecasting performance and provide a more comprehensive understanding of the dynamics affecting the time series. This comparison between ARIMA and ARIMAX models provided insights into the benefits and limitations of incorporating external factors into the forecasting process.[22]

3.5. Evaluating the impact of vaccination on new COVID-19 cases

To analyze the relationship between vaccination rates and the number of new COVID-19 cases, several statistical methods were employed, including Granger causality testing, segmented regression, and regression discontinuity design (RDD). These methods support a clearer understanding of both the temporal relationships and potential causal effects of vaccination on the incidence of new cases.[9,14]

3.5.1. Granger causality test

The Granger causality test was employed to evaluate whether past vaccination rates provided predictive information for future new COVID-19 case numbers. This test determines whether one time series provides statistically significant information for forecasting another time series, suggesting a potential causal relationship.[23] In this context, the null hypothesis states that vaccination rates do not Granger-cause new COVID-19 cases—implying that past vaccination rates do not provide additional predictive value for future case numbers after accounting for past cases. A detailed mathematical formulation of the model is provided in the Supplementary File.

It is important to note that the Granger causality test does not confirm true causality in a philosophical or structural sense but rather indicates that past values of one series are useful in predicting another.

3.5.2. Segmented regression analysis and Chow test

Segmented regression analysis was employed to quantify the impact of vaccination on the trend of new COVID-19 cases. This method estimates changes in trends before and after an intervention, such as the introduction of a vaccination program.[24] The resulting coefficients provide estimates of the immediate change in case numbers and the change in the trend following the intervention.

To validate these findings, a Chow test was conducted to assess the presence of a structural break at the intervention point. This test evaluates whether the relationship between time and new COVID-19 cases differs significantly before and after the intervention.[25] Rejecting the null hypothesis indicates a statistically significant change in the trend post-intervention. A detailed mathematical formulation of both the segmented regression model and the Chow test is provided in the Supplementary File.

3.5.3. RDD

An RDD was employed to estimate the causal effect of vaccine introduction on new COVID-19 cases, using the start of mass vaccination as the cutoff point.[26] RDD assumes that observations just before and after the cutoff are comparable except for the treatment effect. This effect is estimated by comparing new COVID-19 cases immediately before and after vaccination introduction. The parameter of interest (β) represents the effect of the intervention at the cutoff. A non-parametric approach was used to flexibly model the relationship between time and new cases on either side of the cutoff. Detailed mathematical formulation and implementation of the RDD model are provided in the Supplementary File.

While RDD strengthens causal inference through a quasi-experimental design, it remains dependent on the assumption that other confounding factors vary continuously at the cutoff. As such, it does not provide definitive proof of causality.

3.6. Regression analysis of COVID-19 infection rates and determinants

3.6.1. Linear regression analysis of COVID-19 infection rates and economic development

To investigate the relationship between COVID-19 infection rates and economic development, a linear regression analysis was conducted with the infection rate as the dependent variable and GDP per capita as

the independent variable. This analysis aimed to assess whether a country's economic development is associated with its COVID-19 infection rate. Additionally, Pearson's and Spearman's correlation coefficients, along with the maximal information coefficient (MIC), were calculated to evaluate the strength of linear relationships.[27] Pearson's correlation measured the strength of linear relationships, Spearman's assessed the monotonic relationships, and MIC captured both linear and nonlinear associations. Detailed mathematical formulations for these analyses are provided in the Supplementary File.

3.6.2. Multiple regression analysis with additional socioeconomic and health variables

To further investigate the determinants of COVID-19 infection rates, a multiple regression model was employed, incorporating additional variables such as the HDI, Gini coefficient, health expenditure per capita, number of hospital beds per 1,000 people, and population density. This analysis was used to evaluate the relative influence of various socioeconomic and healthcare-related factors on COVID-19 infection rates across various countries.[28] Interaction terms were included to explore potential synergistic effects between variables.[29] The detailed mathematical formulation of the expanded regression model is provided in the Supplementary File.

3.6.3. Addressing multicollinearity: Stepwise regression, principal component regression (PCR), and partial least squares (PLS)

Given the potential for multicollinearity among socioeconomic and healthcare-related predictors, several strategies were implemented to improve model interpretability and estimation stability. First, stepwise regression was employed to refine the linear model by iteratively adding or removing predictors based on their statistical significance. The selection process aimed to minimize the AIC, balancing model fit with complexity.[30] To further evaluate multicollinearity, the variance inflation factor (VIF) was calculated for each predictor. Variables with VIF values exceeding 10 were considered to exhibit significant multicollinearity, which can inflate the variance of coefficient estimates and reduce model reliability.[31]

To address multicollinearity more robustly, two-dimensionality reduction techniques were applied: PCR and PLS regression. Both methods transformed the original set of correlated predictors into a smaller set of uncorrelated components, which were then used in place of the original variables in regression analysis.[32]

The PCR analysis constructed components solely based on the variance structure of the predictor variables, identifying principal components that captured the largest proportion of variance in the input space.[33] These components were then used to predict the dependent variable, regardless of their relevance to it. In contrast, PLS regression incorporated information from both the predictors and the response variable during component extraction, enabling it to select components most relevant for predicting the outcome by maximizing the covariance between predictors and response.[34]

The appropriate number of components for each method was determined using cross-validation procedures, and model performance was assessed based on the mean squared error of prediction (MSEP). Full mathematical formulations and implementation details for both PCR and PLS are provided in Supplementary File.

3.7. Spatial autocorrelation and hotspot analysis of COVID-19 cases

In this study, spatial analysis techniques were applied to examine the distribution of COVID-19 infection rates across various regions. Moran's *I* was calculated to assess global spatial autocorrelation, and the Getis-Ord Gi* statistic was performed to identify local hotspots and coldspots. The results were visualized using traditional red-blue color schemes, effectively highlighting areas with significant spatial clustering of high or low infection rates.[35,36]

3.7.1. Spatial autocorrelation: Moran's I

Moran's *I* is a widely used measure of global spatial autocorrelation that quantifies the degree of spatial clustering of a variable across geographical regions.[37] It identifies whether similar values (e.g., infection rates) tend to cluster spatially. A positive Moran's *I* indicates that similar values clustered together, while a negative value indicates that dissimilar values are adjacent. For this analysis, a spatial weights matrix was generated based on shared boundaries between geographic regions, and Moran's *I* was calculated to assess the overall spatial autocorrelation of COVID-19 infection rates.[35] The detailed mathematical formulation of Moran's *I* is provided in the Supplementary File.

3.7.2. Hotspot analysis: Getis-ord Gi statistic*

The Getis-Ord Gi* statistic is a local spatial statistic used to identify geographic hotspots and coldspots, representing areas with significant clustering of high or low values, such as COVID-19 infection rates. Hotspots indicate clusters of high values, while coldspots indicate clusters of low values. The significance of these clusters is determined by comparison with a reference distribution under the null hypothesis of spatial randomness.[38] For this analysis, the Getis-Ord Gi* statistic was calculated using a spatial

weights matrix to identify regions with statistically significant clustering of high or low infection rates.[36] The detailed mathematical formulation of the Getis-Ord Gi* statistic is provided in the Supplementary File.

4. Results and discussion

4.1. Short-term forecasting and anomaly detection in COVID-19 case counts using ARIMA models

To evaluate the short-term predictive performance of ARIMA models on COVID-19 case counts, forecasts were generated for four distinct time periods using training data from prior months. Predictive accuracy was assessed by comparing these forecasts with actual observed data.

The first forecast, covering September 27 – December 27, 2020, utilized data from January 5 to September 27, 2020. As shown in Figure 2A, the forecast generally follows the actual case trajectory, though deviations near the end of the period highlight the model's limitations in capturing sudden changes in the data. The ACF and PACF plots (Figure 2B and C) reveal some residual autocorrelation, highlighting potential areas for model improvement. The Ljung-Box test yields a p=0.3746, indicating no significant residual autocorrelation.

The second forecast, covering December 27, 2020 – March 28, 2021, utilized data up to December 27, 2020. Figure 2D illustrates a closer alignment between the predicted and actual observed cases, with only minor deviations. The ACF and PACF plots (Figure 2E and F) further support the model's adequacy, though some residual correlations persist. The Ljung-Box test for this period yields a p=0.6327, further indicating that residual autocorrelation is not a concern.

The third forecast, covering March 28 – June 27, 2021, was generated using data up to March 28, 2021. As illustrated in Figure 2G, the model closely aligns with the actual case counts throughout the period, demonstrating strong predictive capability. The corresponding ACF and PACF plots (Figure 2H and I) show that the model effectively captures the data's temporal structure, though the Ljung-Box test yields a p=0.0728, suggesting the presence of minor residual autocorrelation.

In the final forecast period, covering September 26 – December 26, 2021, the model included data from January 3, 2021, to September 26, 2021. As illustrated in Figure 2J, the model maintains strong performance, with forecasts closely aligning with the actual case counts. The ACF and PACF plots (Figure 2K and L) indicate that the model has successfully captured the underlying patterns, with the Ljung-Box test demonstrating a p=0.2876, indicating minimal residual autocorrelation.

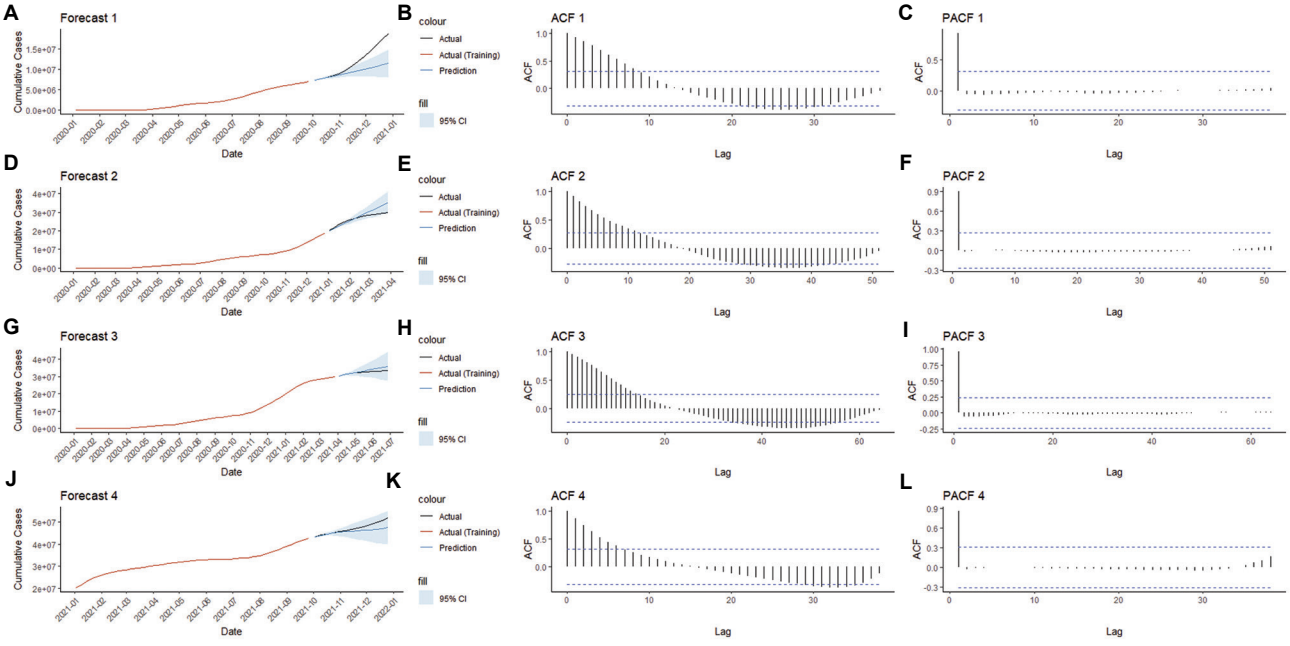

Figure 2. ARIMA model analysis of COVID-19 case forecasts in the United States across four time periods. First forecast period: Actual versus predicted (A), ACF (B) and PACF (C); second forecast period: Actual versus predicted (D), ACF (E) and PACF (F); third forecast period: Actual versus predicted (G), ACF (H) and PACF (I); and fourth forecast period: Actual versus predicted (J), ACF (K) and PACF (L).
Abbreviations: ACF: Autocorrelation function; CI: Confidence interval; PACF: Partial autocorrelation function; USA: United States of America.

Throughout these periods, the ARIMA model demonstrates consistent predictive accuracy, although the residual autocorrelation observed in the ACF and PACF plots highlights areas for further refinement to improve model performance. These findings indicate that while the ARIMA model effectively captures overall trends, it does not fully account for short-term dependencies or sudden structural changes in the data. The presence of residual autocorrelation—especially mild positive lags at short intervals—suggests the presence of unmodeled impacts, such as seasonal effects or external shocks. To address this, ARIMAX models incorporating vaccination rates as exogenous variables were then explored, with the findings discussed in Section 4.5, demonstrating improved performance in certain forecasting scenarios.

Among the four forecast periods analyzed using ARIMA models, the first forecast period demonstrates the lowest predictive accuracy. Several factors may contribute to this discrepancy between the predicted and actual observed data. One possibility is the inherent limitation of the ARIMA model itself—a linear model designed to predict future values based on past data. This model may struggle to capture sudden nonlinear changes or external shocks that occur during the forecast period. ARIMA models assume a degree of stationarity in the data. Therefore, structural breaks or sudden shifts in the underlying time series can reduce the reliability of the model's predictions.

Additionally, significant outliers or unexpected spikes in COVID-19 cases during the forecast period can affect predictive accuracy. Such anomalies may result from the emergence of new virus variants, changes in public health policies, or sudden shifts in public behavior. These rapid increases in case numbers reduce the effectiveness of models trained solely on historical data.

To investigate this hypothesis, outlier detection analysis was conducted on data from January 5 to December 27, 2020. The identified outliers, shown in Table 2 and illustrated in Figure S1, highlight key dates where significant anomalies were observed. These anomalies correspond to periods with sharp increases in case counts, suggesting that forecast discrepancies may be linked to these sudden and unexpected changes.

As shown in Table 2, significant outliers were detected on November 8, November 15, and December 13, 2020, corresponding to sharp rises in cumulative cases. These dates likely reflect specific events or conditions that triggered case surges, such as the emergence of more transmissible variants or changes in testing or reporting practices.

To explore potential anomalies in COVID-19 case trends, an outlier detection analysis was performed on cumulative case data for both the US and global datasets. This analysis aimed to identify time points where actual case numbers significantly deviated from expected trends, potentially indicating periods associated with the emergence and spread of new COVID-19 variants.

Table 2. The detected outliers in COVID-19 cases in the United States of America from January 5 to December 27, 2020

Date reported (year 2020)	Cumulative cases
November 8	9,920,253
November 15	10,925,098
December 13	16,012,396

Figure 3A displays the detected outliers in COVID-19 cases in the US from January 5 to December 27, 2020, with a summary of these outliers provided in Table S1. Notably, several of these dates align with the emergence of significant COVID-19 variants—such as the Omicron variant (B.1.1.529)—which was first identified in November 2021 in South Africa and Botswana.[39] Other variants—such as BQ.1 and BQ.1.1—spread rapidly in late 2022, contributing to the increased number of cases that may have reduced predictive accuracy.[40] Figure 3B presents the time series plot of COVID-19 cases in the US, highlighting the detected outliers.

Further analysis was conducted on a global scale, with the results presented in Figure S2. The corresponding dates and case numbers for the detected global outliers are summarized in Table S1. Similar to the US data, these global outliers correspond to key dates when emerging variants—such as XBB, CH.1.1, and BF.7—were identified and began spreading across various regions, leading to significant increases in case numbers.[41] These variants, first reported in late 2022 and early 2023, significantly impacted regions such as Asia and Europe, leading to significant deviations from the predicted trends.[42]

The detected outliers in both the US and global datasets highlight the significant impact of emerging COVID-19 variants on the spread of the virus. Although the Alpha (B.1.1.7) and Gamma (P.1) variants were not explicitly captured by the outlier detection process—possibly due to their emergence near the end of 2020—the trend illustrated in Figure 3A (US outlier detection plot) exhibits a marked increase in cases during this period.[39] This surge aligns with the period when Alpha and Gamma variants began to spread rapidly, suggesting that their enhanced transmissibility and potential for immune evasion contributed to the surge in case numbers. Consequently, almost all significant surges in the data correspond with the emergence of new variants.

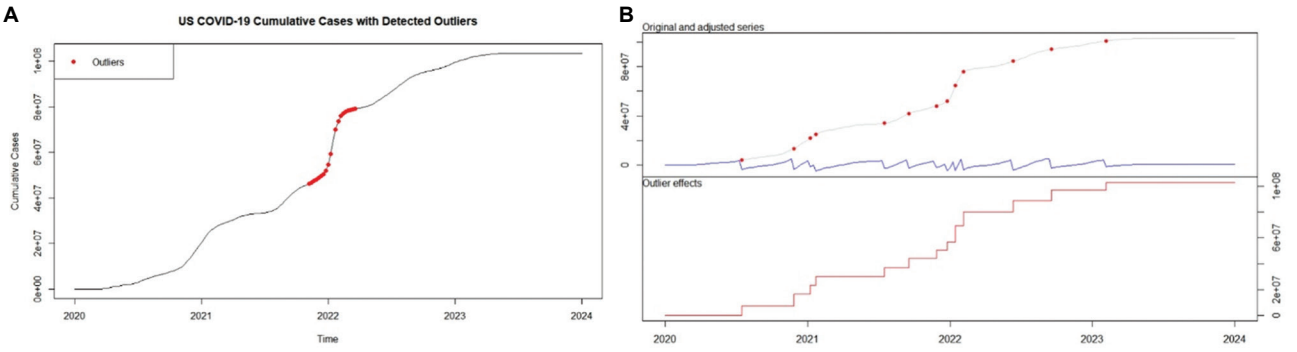

Figure 3. Outlier detection and time series plot of cumulative COVID-19 cases in the United States from January 2020 to December 2023. (A) Detected outliers in the cumulative COVID-19 case data. (B) Time series plot of cumulative COVID-19 cases with detected outliers.
Abbreviation: US: United States.

The outlier dates listed in Tables 1 and 2 closely align with the timelines of variant emergence and global spread. For example, the sharp rise in the US case counts observed between November 2021 and February 2022 aligns with the emergence of the Omicron variant and its subvariants.[40] Similarly, the global spikes identified from late 2021 through 2022 align with the spread of Omicron and its subvariants, further supporting the notion that these variants had a significant impact on the accuracy of predicted versus actual case numbers.

4.2. Regional COVID-19 forecasting across continents

The ARIMA model was employed to forecast COVID-19 cases across various continents, including Asia, Europe, Africa, the Americas, and South America. To isolate trends specific to South America, the Americas dataset excluded Canada, the US, and Mexico. Figure S3 illustrates the forecast results for each continent, with predictions covering the period from January 2020 to early 2021.

In Asia, the ARIMA model's predictions closely align with the actual observed data, effectively capturing the overall upward trend in COVID-19 cases. The prediction intervals encompass the actual case numbers, indicating the model's robustness in this region.

In Europe, the ARIMA model's predictions are less accurate, as the predicted cases significantly deviate from the actual observed data. This discrepancy is particularly evident toward the end of 2020 when a sharp and sudden increase in COVID-19 cases occurred—an event the ARIMA model failed to predict effectively. Based on the forecast's patterns, the earlier anomaly detection for the US and global data, and reports from the WHO on emerging variants, it is plausible to attribute this rapid rise to the Alpha variant (B.1.1.7). First detected in September 2020 in the United Kingdom, this variant was the first to be classified by the WHO as a "variant of concern." Its high transmissibility likely contributes to the significant increase in cases, which is not fully captured by the ARIMA model, thereby highlighting the challenges of forecasting during periods of rapid epidemiological change.

In Africa, the model demonstrates a good fit with the actual observed data, although the sharp rise in cases toward the end of the year pushes the limits of the prediction interval—similar to the pattern observed in Europe. In the Americas, the ARIMA model demonstrates good performance, with predictions closely matching the rapid increase in case numbers. Despite this region experiencing one of the most significant surges in cases, the predictions remain within the confidence intervals, indicating the model's robustness in capturing the trend.

In South America, after excluding the northern countries, the ARIMA model continues to show good model performance. The predicted cases remain within reasonable bounds compared to the observed data, similar to the other continents.

Across all regions, the Ljung-Box test p-values remain well above the 0.05 threshold, indicating no significant autocorrelation in the residuals. This suggests that the ARIMA models successfully capture the temporal patterns of COVID-19 case progression in each region. Occasional underestimations, particularly during rapid case surges, highlight the challenges posed by the pandemic's dynamic nature and the emergence of new variants that earlier model training data may not fully capture. Nonetheless, the ARIMA models demonstrate robust overall performance across various regions, providing valuable insights into the transmission of COVID-19 during the forecast periods.

4.3. Rolling window cross-validation and comparison with auto.arima

In the previous ARIMA forecasting efforts, the auto.arima function was used to automatically select the model parameters *p, d*, and *q*. This function optimizes the model by minimizing the AIC, which balances the model fit and complexity by penalizing excessive parameters. This approach offers several advantages—including speed, automation, and generally reliable results. However, relying solely on AIC may not always produce the most accurate forecasts, especially when working with nonstationary time series or for long-term predictions.

To explore whether other parameter selection methods could improve forecast accuracy, a rolling window cross-validation technique was applied to optimize the *p* and *q* parameters, while the *d* parameter remains fixed as determined by the auto.arima function. The differencing order *d* is fixed because it addresses the time series' stationarity by removing trends or seasonality—a concept well-supported by statistical theory. For example, once a time series is made stationary through differencing, the order of *d* generally remains unchanged to maintain that stationarity, even as *p* and *q* are adjusted.

In this analysis, the period where ARIMA predictions significantly diverged from the actual observed data—such as in the US and Europe from January 5 to December 27, 2020—was examined. These discrepancies are primarily due to sudden surges in cases associated with the emergence of new variants, highlighting the limitations of traditional ARIMA models in capturing such sudden changes.

The rolling window cross-validation approach was employed to evaluate different combinations of *p* and *q* based on the RMSE metric. This approach, which assesses out-of-sample performance across multiple training windows, is particularly valuable for forecasting nonstationary time series with evolving patterns. Table 3 summarizes the RMSE values for the US's ARIMA model using parameters selected through cross-validation, compared to those obtained using auto.arima, while Figure 4A provides a heatmap visualizing RMSE across different *p* and *q* combinations.

As illustrated in Figure 4A, the RMSE heatmap shows that the cross-validated ARIMA parameters (p=2, q = 2) achieve better performance compared to the auto.arima parameters (p=1, q = 0). The heatmap provides a comprehensive view of how different combinations of *p* and *q* affect forecast accuracy, with lower RMSE values indicating better performance.

Furthermore, Figure 4B compares the forecasted COVID-19 cases in the US using ARIMA models with parameters selected by auto.arima and cross-validation. While both models exhibit significant deviations from the actual observed data due to the sudden surge in cases, the cross-validated model's predictions are more closely aligned with the actual observed data than those of auto.arima. This suggests that the cross-validation approach can improve forecast accuracy under certain conditions.

Table 3. Comparison of RMSE values for ARIMA models with parameters selected by auto.arima and cross-validation for COVID-19 case data in the United States

Model	ARIMA parameters			RMSE
	p	*d*	*q*	
auto.arima	1	2	0	27,648.12
Cross-validation-based ARIMA	2	2	2	22,949.3

Abbreviations: ARIMA: Autoregressive integrated moving average; RMSE: Root mean squared error.

A similar approach was employed in the European ARIMA model. Table S2 presents the RMSE values comparing parameters selected by cross-validation and auto.arima, while the RMSE heatmap in Figure S4A visualizes the model performance across different combinations of *p* and *q*.

Figure S4B compares the forecasted COVID-19 cases in Europe using ARIMA models with parameters selected by auto.arima and cross-validation. The forecast line generated by the cross-validated model aligns more closely with the actual observed data than that of auto.arima, although both models show notable deviations from the actual trajectory. These findings are consistent with the results observed in the US, highlighting the potential advantages of using cross-validation for parameter selection in ARIMA models when dealing with highly volatile and non-stationary time series data.

4.4. The effect of vaccination on new COVID-19 cases

Beginning in December 2020, global vaccination efforts against COVID-19 raised a critical question of whether the vaccination campaigns effectively reduce the number of new COVID-19 cases. To address this issue, several statistical methods were applied, including the Granger causality test, segmented regression analysis, the Chow test, and RDD.

The Granger causality test was performed to evaluate whether the number of vaccinated individuals could predict future new COVID-19 cases while accounting for past case counts. Two models were compared: One incorporating lags of both new cases and vaccination counts, and another including only lags of new cases.

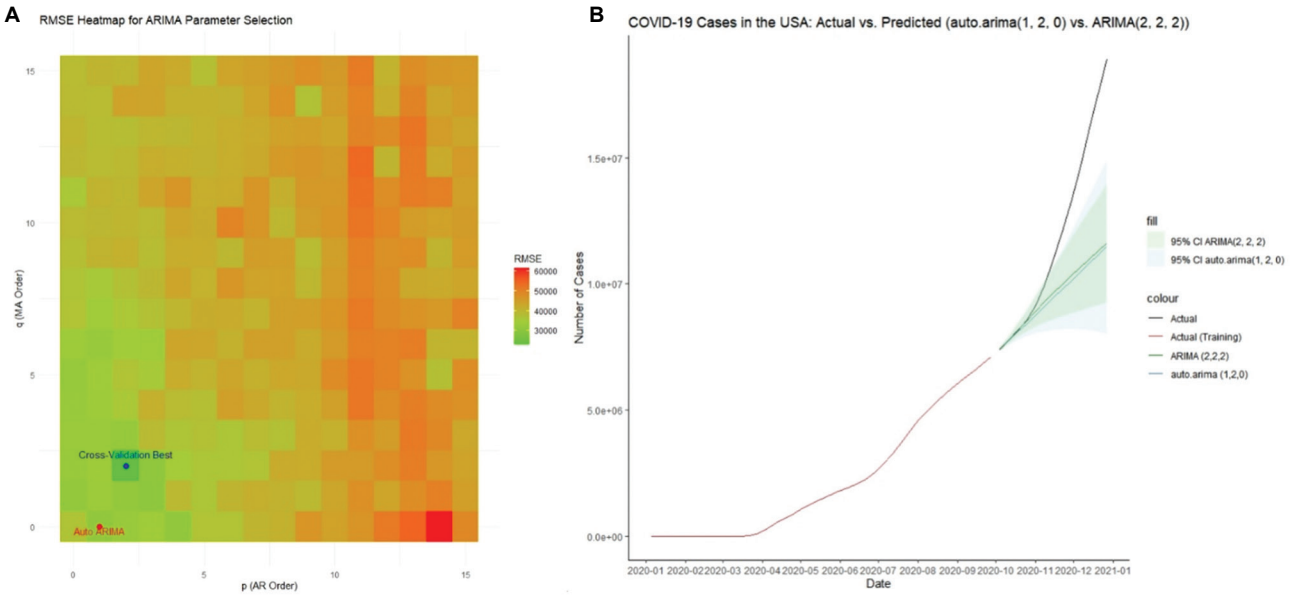

Figure 4. Performance and forecasts of ARIMA models for COVID-19 cases in the United States of America. (A) Heatmap of RMSE for ARIMA models with parameters selected by auto.arima and cross-validation for COVID-19 cases in the United States. (B) Forecast comparison of COVID-19 cases in the United States for ARIMA models with parameters selected by auto.arima and cross-validation.
Abbreviations: ARIMA: Autoregressive integrated moving average; CI: Confidence interval; MA: Moving average; RMSE: Root mean squared error; USA: United States of America.

The results demonstrate no significant causal relationship between vaccination numbers and a reduction in new cases, as evidenced by an *F*-statistic of 0.24 and a p=0.9746. This suggests that the inclusion of vaccination data does not improve the predictive power of the model within the tested lags. Specifically, with a lag of 7 (equivalent to 49 days), the Granger causality test demonstrates no significant effect of vaccination on new cases during this period, as shown in Table 4.

To further investigate the potential impact of vaccination on the trend in COVID-19 cases, segmented regression analysis was employed by introducing a breakpoint at the onset of the vaccination campaign. The regression model included time—an indicator for the post-intervention period—and the interaction between time and the post-intervention phase. The analysis shows that while the overall trend in new cases has a positive slope (β = 18,987, p=0.0214), the interaction term (time–post-intervention) is negative and significant (β = −24,115, p=0.0044), indicating a reduction in the growth rate of new cases following the intervention. However, the post-intervention indicator itself is not statistically significant (p=0.31), which is consistent with the results of the Granger causality test, further suggesting that the immediate effect of vaccination on reducing new cases is not significant. Regardless, the significant negative interaction term suggests that vaccination has a significant long-term effect in reducing new cases, indicating a beneficial impact over time. Figure 5A illustrates the segmented regression results, showing how the predicted number of cases diverges from the actual cases over time. As shown in Table S3, the segmented regression results clearly reflect these trends.

Table 4. The Granger causality test results

Model	Lags	Res. Df	Df	*F*	Pr(> *F*)
Model 1 (new cases and vaccination counts)	New cases=1:7; vaccination counts=1:7	151	-	-	-
Model 2 (new cases only)	New cases=1:7	158	−7	0.24	0.9746

Notes: Df: Degrees of freedom; F: F-statistic; Pr(> F): *P*-value; Res.Df: Residual degrees of freedom.

Additionally, the Chow test was conducted to assess the presence of a structural break at the intervention point. The test provides strong evidence of a structural change, with a $p=6.437\times10^{-6}$, indicating that the introduction of the vaccination campaign significantly alters the underlying relationship between time and new cases. This finding is consistent with the results of the segmented regression analysis, suggesting that vaccination leads to a structural shift in the trend of new cases.

Finally, RDD analysis was applied to further validate these findings. This method focused on the sharp change in the trend of new cases at the intervention point, yielding a conventional coefficient estimate of 76,662.154 with a

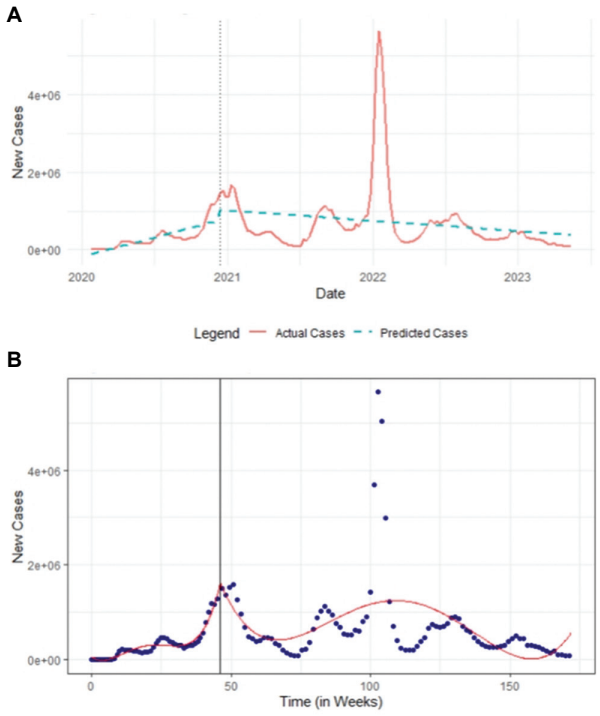

Figure 5. Segmented and regression discontinuity analysis of COVID-19 cases. (A) Segmented regression analysis of COVID-19 cases. (B) Regression discontinuity plot, where blue points represent the observed data and the red line indicates the fitted regression discontinuity model. The vertical black line marks the intervention date (December 13, 2020).

non-significant p=0.636. This suggests that while there may be an observable shift in the trend of new cases at the intervention point, it is not statistically significant at conventional levels. As shown in Table S4, the RDD results further support the idea that the immediate impact of vaccination is not statistically significant. Figure 5B provides a visualization of the RDD results, highlighting the discontinuity at the intervention point. The non-significant result from the RDD analysis is consistent with the findings from both the Granger causality test and the segmented regression analysis, indicating that the immediate impact of vaccination is not significant.

4.5. Forecast on COVID-19 cases using ARIMAX model, with vaccination rates as the exogenous variable

Based on the results in the previous section, where vaccination demonstrates a significant long-term impact on the reduction of new COVID-19 cases, a logical extension was made to incorporate the number of vaccinations as an exogenous variable in ARIMAX models. It was hypothesized that the inclusion of this variable could improve forecast accuracy compared to the standard ARIMA model, which does not account for such external factors.

To test this hypothesis, the dataset starting from December 13, 2020—the beginning of the vaccination campaign—was employed. Given the evidence that the impact of vaccination is more pronounced over time, the first forecast period selected spanned from January 5, 2020, to June 27, 2021—approximately 6 months after vaccination began. This period was used to predict the cumulative number of cases for the subsequent 3 months. Following this, the training data period was gradually extended across 3 time periods:

(i) January 5, 2020 – June 27, 2021,
(ii) January 5, 2020 – December 26, 2021,
(iii) January 5, 2020 – September 25, 2022.

Figures 6, S5, and S6 compare the ARIMA and ARIMAX model predictions across these periods, while Tables 5, S5, and S6 present the evaluation metrics (AIC, RMSE, and MAE) for both models.

These results indicate that the ARIMAX model generally produces forecasts that are closer to the actual data than those of the ARIMA model, as evidenced by lower RMSE and MAE values in certain time periods. However, in some cases, the ARIMAX model exhibits greater deviation from the actual data, resulting in higher RMSE values. Notably, improvements in RMSE and MAE do not always correspond to lower AIC values. For example, in the third period, although the ARIMAX model provides more accurate predictions (reflected by lower RMSE and MAE values), its AIC value is higher than that of the ARIMA model. This highlights the trade-off between model complexity and goodness-of-fit inherent in the AIC calculations.

4.6. Multivariate regression analysis of global COVID-19 infection rates

To investigate the factors influencing COVID-19 infection rates across different countries, it was initially hypothesized that countries with advanced healthcare systems and greater access to medical resources would exhibit lower infection rates. However, an analysis of the top 10 countries by infection rate as of December 31, 2023 (Figure S7) contradicts this assumption. Several highly developed countries, including Luxembourg, Denmark, and Austria, appear among those with the highest infection rates, challenging the initial hypothesis.

To further examine this relationship, a linear regression analysis was conducted using GDP per capita as an indicator of a country's level of development and the COVID-19 infection rate as the outcome variable. The scatterplot with the fitted regression line is illustrated in

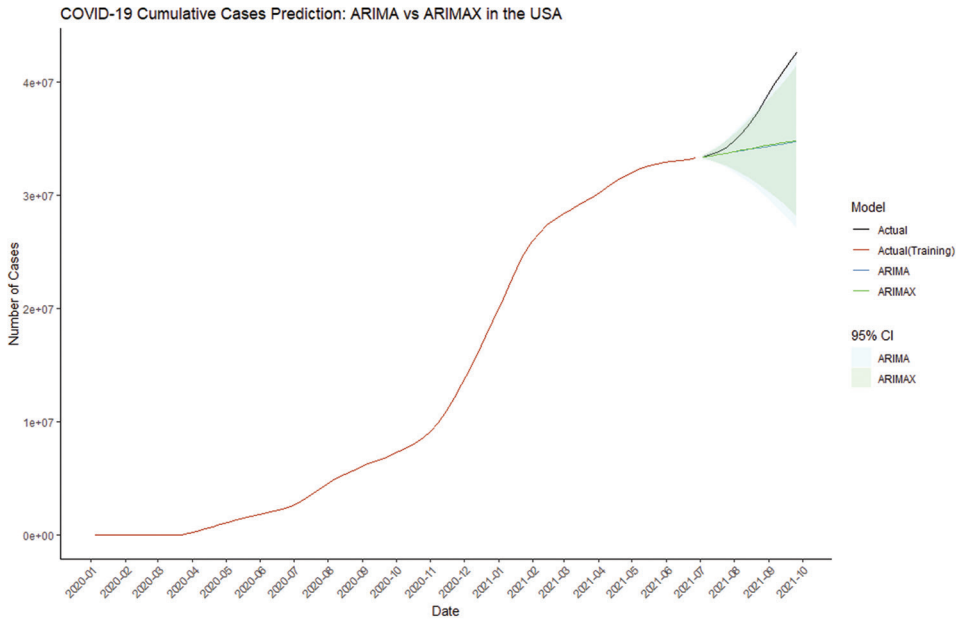

Figure 6. Comparison between ARIMA and ARIMAX models for the first forecast period
Abbreviations: ARIMA: Autoregressive integrated moving average; ARIMAX: Autoregressive integrated moving average with exogenous variables; CI: Confidence interval; USA: United States of America.

Table 5. Comparison between ARIMA and ARIMAX models for the first forecast period

Model	AIC	RMSE	MAE
ARIMA	1,919.556	4,082,257	3,063,789
ARIMAX	1,919.935	4,011,124	3,004,951

Abbreviations: AIC: Akaike information criterion; ARIMA: autoregressive integrated moving average; ARIMAX: autoregressive integrated moving average with exogenous variables; MAE: Mean absolute error; RMSE: Root mean squared error.

Figure 7. The analysis (Table 6) demonstrates a statistically significant positive relationship between GDP per capita and infection rate, with the regression coefficient for GDP per capita being positive and highly significant ($p<2\times10^{-16}$). This suggests that countries with higher GDP per capita tend to have higher reported infection rates. However, the model yields a relatively low R^2 value of 0.4763, suggesting that GDP per capita accounts for approximately 47.63% of the variance in infection rates.

In addition to the regression analysis, three correlation metrics were calculated to further assess the relationship between GDP per capita and COVID-19 infection rate. Pearson's correlation coefficient yields a value of 0.6902, which indicates a moderately strong positive linear relationship between the two variables. Spearman's rank correlation coefficient is higher, at 0.8593, suggesting a strong monotonic relationship. Additionally, the MIC yields a value of 0.7256, reflecting a strong association that may capture nonlinear relationships between GDP per capita and infection rate. Collectively, these correlation measures suggest that higher GDP per capita is associated with increased infection rates, although other factors likely contribute to the remaining unexplained variance.

The relatively low infection rates observed among low-GDP per capita countries may reflect underreporting due to limited testing capacity rather than true differences in transmission. Testing data is sparse and inconsistent across countries, especially in low-income regions, making it difficult to correct this effect quantitatively. Nonetheless, this under-detection is a plausible contributor to the observed pattern.

Given the relatively low R^2, it is evident that factors beyond GDP per capita may influence infection rates. Therefore, the model was expanded to incorporate additional variables that could plausibly affect infection rates, including HDI, Gini coefficient, health expenditure per capita, the number of hospital beds per 1,000 people, and population density. The resulting multivariate regression model incorporated both main effects and interaction terms among these variables.

The analysis reveals a more complex relationship between the predictors and the infection rate. While GDP per capita remains a significant factor (p=0.0065), other variables like health expenditure and certain interaction terms also emerge as significant predictors.

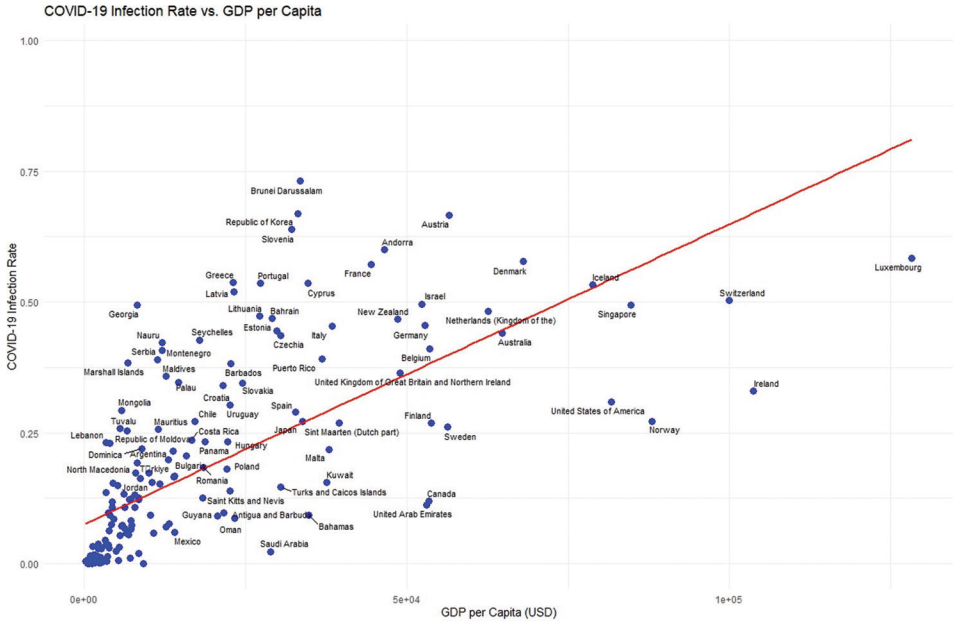

Figure 7. The scatterplot with fitted regression line
Abbreviations: GDP: Gross domestic product; USD: United States dollars.

Table 6. Linear regression results: Infection rate versus gross domestic product (GDP) per capita

Coefficients	Estimate	Standard error	*t*-value	Pr(>|*t*|)
(Intercept)	7.523×10^{-2}	1.254×10^{-2}	6.001	1.05×10^{-8}***
GDP per capita	5.736×10^{-6}	4.470×10^{-7}	12.831	$<2\times10^{-16}$***

Notes: Residuals: Minimum=−0.3404; first quartile: −0.0784; median=−0.0503; maximum=0.4639. Residual standard error=0.1352 on 181 degrees of freedom. Multiple R^2=0.4763; adjusted R^2=0.4734; *F*-statistic=164.6 on 1 and 181 degrees of freedom; $p=2.2\times10^{-16}$. Three asterisks (***) represent $p<0.001$.

For example, the interaction between GDP per capita and HDI (p=0.0064), as well as between GDP per capita and the Gini coefficient (p=0.0297), are both statistically significant. These findings suggest that the effect of GDP per capita on infection rates is moderated by a country's level of HDI and income inequality. Additionally, the interaction between HDI and health expenditure (p=0.0007) is also significant, suggesting that their combined effect significantly influences infection rates. The detailed results of the regression analysis, including coefficients, standard errors, *t*-values, and *p*-values, are provided in Table S7.

Despite these findings, the model's R^2 increased significantly to 0.8179, indicating that approximately 81.79% of the variance in infection rates can be explained by the expanded set of predictors and their interactions. However, residual plots (Figure 8A) reveal potential issues with model fit, including non-constant variance (heteroscedasticity) and deviations from normality, as indicated by the *Q*–*Q* plot.

The scatterplot matrix (Figure 8B) and coefficient plot (Figure S8) further illustrate the complexity of the relationships among the predictors. The scatterplot matrix shows the correlations between variables, with some expected relationships, such as a positive correlation between GDP per capita and HDI (0.729) and a negative correlation between GDP per capita and the Gini coefficient (−0.330). The coefficient plot shows the magnitude and direction of the effects, with GDP per capita, health expenditure, and certain interaction terms having the most pronounced impacts on infection rates.

4.7. Addressing multicollinearity in the regression model

The initial multivariate regression model, which incorporated interaction terms, significantly improved the model's explanatory power, as indicated by a significant increase in the R^2 value. However, this complexity introduced severe multicollinearity, as evidenced by extremely high VIF values. Predictors such as GDP per capita, HDI, and health expenditure, along with their interaction terms, exhibited VIF values in the tens of thousands, indicating that multicollinearity is indeed a significant problem. This multicollinearity can destabilize regression coefficients and complicate their interpretation, thereby necessitating a more rigorous approach to model simplification and stabilization.

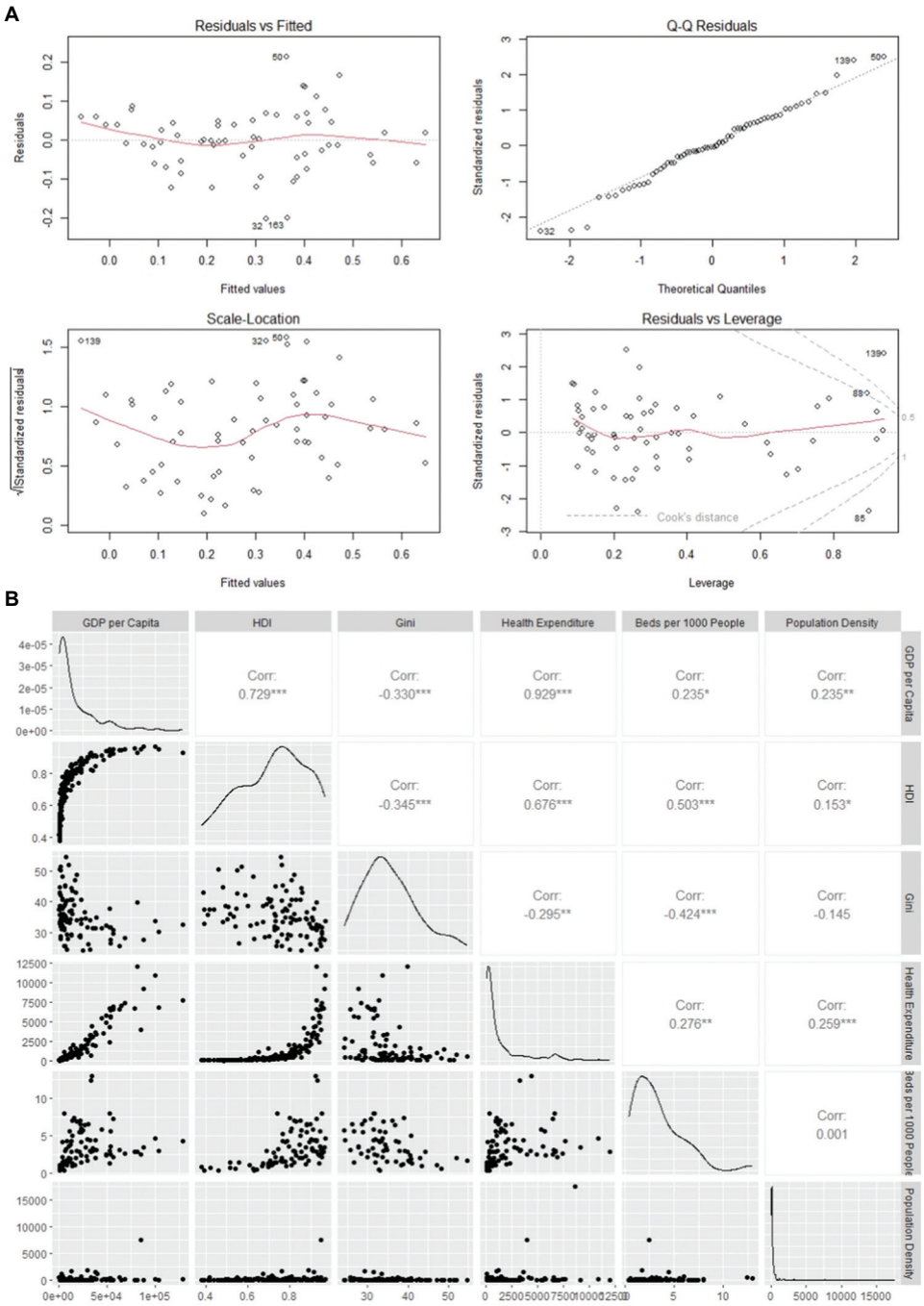

Figure 8. Diagnostic residual plots and correlation analysis of model predictors. (A) Residual plots and (B) scatterplot matrix.
Note: Asterisks (*) indicate levels of statistical significance: $p<0.05$ (*), $p<0.01$ (**), and $p<0.001$ (***).
Abbreviations: GDP: Gross domestic product; HDI: Human development index.

To address these issues, stepwise regression was employed as an initial strategy to reduce model complexity by removing less significant predictors. The simplified model retained key variables and interaction terms that contributed meaningfully to the model's explanatory power while excluding those with minimal impact. Although the resulting model was more manageable, notable multicollinearity persisted, with several VIF values remaining high, albeit reduced from their initial levels.

To further address the issue of multicollinearity, alternative approaches such as PLS and PCR were

employed. These techniques are specifically designed to mitigate multicollinearity by transforming the predictor variables into a set of uncorrelated components.

The PLS and PCR models were applied to the dataset, with each method aiming to reduce the dimensionality of the predictor variables while maximizing the explained variance in the response variable—namely, the infection rate. In particular, the PLS analysis—as shown in Table 7—is effective, demonstrating 67.22% of the variance in infection rates using five components—identified as the optimal number of components through cross-validation (Figure 9). Beyond these components, the model's MSEP begins to increase, suggesting that additional components may introduce noise rather than improve predictive accuracy.

In addition to the error plot, Table S9 provides detailed cross-validation results for each model. This table presents the MSEP for different numbers of components, highlighting how the error decreases as the number of components increases up to five and then rises with the inclusion of additional components. These results support the findings illustrated in Figure 9, which identify five components as optimal.

The component loadings from the PLS model, as illustrated in the heatmap (Figure S9), highlight the contribution of each variable to the principal components. Predictors such as GDP per capita, HDI, and health expenditure demonstrate significant loadings on the first few components, indicating their strong influence on the model. Additionally, more complex interactions—such as those between GDP per capita and population density or health expenditure and population density—play critical roles in the later components.

In addition to the heatmap, detailed PLS loadings are provided in Table S10. This table lists the specific loading values for each variable across the first five components, further illustrating the contributions and interactions among variables in shaping the principal components.

By reducing the predictors into principal components, the PLS model provides a more stable set of coefficients, as shown by the reduced VIF values and improved interpretability of the regression coefficients. The final regression coefficients obtained from the PLS model (Table S11) reveal both the direct and interaction effects of the predictor variables on infection rates, offering a clearer insight into the complex underlying relationships.

In contrast, PCR (Table S8) demonstrates similar results but with slightly lower explained variance for the same number of components. While PCR effectively reduces multicollinearity, this comes at the cost of reduced predictive power compared to PLS. Specifically, PCR explains 59.43% of the variance in infection rates using six components, increasing to 75.81% with 17 components, but it does not exceed the overall performance of the PLS model.

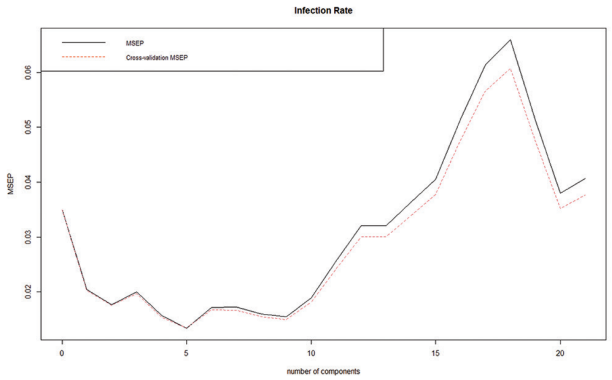

Figure 9. Cross-validation mean squared error plot for the partial least squares model analysis
Abbreviation: MSEP: Mean squared error of prediction.

Table 7. The partial least squares analysis results showing variance explained by the number of components

Number of components	Predictor variables (%)	Infection rates (%)
1	47.98	48.67
2	66.98	55.79
3	81.77	59.75
4	88.76	65.34
5	94.81	67.22
6	97.28	70.14
7	98.05	72.68
8	98.92	73.76
9	99.48	73.93
10	99.78	74.10
11	99.85	74.56
12	99.90	75.47
13	99.95	75.98
14	99.97	76.27
15	99.98	76.49
16	99.99	76.84
17	99.99	77.45
18	100.00	77.79
19	100.00	78.81
20	100.00	81.62
21	100.00	81.79

4.8. Spatial autocorrelation and hotspot analysis of COVID-19 cases across states in the United States

A spatial autocorrelation and hotspot analysis of COVID-19 cases across states in the US was conducted. Spatial autocorrelation assessed the degree to which COVID-19 cases are geographically clustered, while hotspot analysis identified regions with significantly high or low case counts.

Using the most recent COVID-19 case data across states in the US, the number of cases per 100,000 people was calculated to account for population differences. Figure 10A illustrates the spatial distribution of these normalized case counts. States with higher case rates per 100,000 people are shown in red, while those with lower rates are shown in blue. Notably, Alaska and several southern states exhibit particularly high case rates.

In addition to the spatial visualization, Table S12 presents the detailed rankings of the top 10 and bottom 10 states based on COVID-19 cases/100,000 people. Alaska reports the highest case rates, with 40,576.16 cases/100,000 people, followed by Rhode Island and Kentucky. Conversely, New York, Maryland, and Oregon report the lowest case rates, with New York ranking lowest with 18,251.51 cases/100,000 people.

To further understand the spatial pattern, Moran's *I* test—a commonly used measure of spatial autocorrelation—was conducted. The results demonstrate a Moran's *I* value of 0.1578 with a p=0.0317, indicating a significant positive spatial autocorrelation. This suggests that states with high COVID-19 case rates tend to be geographically clustered rather than randomly distributed.

To identify specific clusters of high or low case rates, the Getis-Ord Gi* statistic was employed, providing a measure of local spatial clustering. As shown in Figure 10B, the hotspot analysis reveals several hotspots and coldspots. Southern states—such as Arkansas, Georgia, and Mississippi, as well as parts of Texas and Ohio—are identified as hotspots, with high Gi* values, indicating significant clustering of high case rates. Conversely, states like Alaska, Delaware, New Hampshire, and Vermont are identified as coldspots, suggesting significant clustering of low case rates.

In addition, Table S13 lists the top 10 hotspot and coldspot states along with their corresponding Gi* values. For instance, Arkansas has the highest Gi* value of 1.0004, indicating that it is a significant hotspot, while Alaska has the lowest Gi* value of −1.2373, making it a prominent coldspot. These detailed Gi* values provide a quantitative basis for understanding the spatial clustering patterns observed in the map.

For Alaska, given that it does not share borders with any other state, Washington is designated as its sole neighbor. Despite this adjustment, Alaska—which has the highest infection rate among all states—is classified as a coldspot in the Getis-Ord Gi* hotspot analysis. This counterintuitive result may be due to the isolation of Alaska, where the absence of adjacent states reduces the influence of its high case rate on surrounding areas. Additionally, its high infection rate does not align with a broader regional trend, causing the Gi* statistic to categorize it as a coldspot rather than a hotspot. This highlights the importance of considering geographic and relational context in spatial analyses, particularly for isolated regions.

Figure 10. Geographic distribution and hotspot analysis of COVID-19 cases/100,000 people across the United States of America. (A) COVID-19 cases/100,000 people by state. (B) Getis-Ord Gi* hotspot analysis of COVID-19 cases/100,000 people.

5. Conclusion

The comprehensive statistical analysis of COVID-19 trends—employing ARIMA, ARIMAX, multiple regression, and spatial autocorrelation models—provides valuable insights into the dynamics of the pandemic both globally and within the US. These findings highlight the strengths and limitations of different modeling approaches and the complexity of factors influencing COVID-19 case numbers.

The ARIMA models demonstrate robust performance in predicting short-term COVID-19 trends, particularly when case dynamics follow relatively stable patterns.[14] However, the models show limitations when sudden changes occur in infection rates, such as those caused by sudden policy shifts or the emergence of new virus variants.[43] These situations often reduce predictive accuracy, suggesting that while ARIMA models effectively capture general trends, they may require augmentation or combination with other models to better account for sudden, non-linear changes.[44]

The ARIMAX models, which incorporate exogenous variables such as vaccination data, provide a more nuanced analysis by accounting for external influences on COVID-19 case numbers.[22] However, the effectiveness of the ARIMAX model depends heavily on the specific characteristics of the time period and the data. For instance, during periods when the impact of vaccination on case numbers is delayed or less pronounced, the model struggles to accurately capture the true relationship between variables.[45] This is particularly evident when vaccine uptake is gradual or when vaccination effects take time to appear in the population. Under these conditions, the model may overestimate or underestimate the influence of vaccination, leading to skewed forecasts.[46]

Several challenges arise in applying the ARIMAX model. Firstly, the model assumes a direct and linear effect of the exogenous variable (vaccination rates) on the dependent variable (COVID-19 cases), which may not fully capture the complex, non-linear relationships involved.[14] Factors such as varying vaccine efficacy, the emergence of new virus variants, shifts in public behavior, and policy interventions (e.g., lockdowns, mask mandates) influence the effectiveness of vaccination efforts in reducing case numbers.[47] If these factors are not properly incorporated, the ARIMAX model may incorrectly attribute changes in case numbers to vaccination, leading to inaccurate predictions.

Moreover, including vaccination data as an exogenous variable introduces the risk of multicollinearity, particularly if the vaccination rates correlate with other factors influencing the spread of COVID-19. Multicollinearity causes instability in coefficient estimates, reducing the reliability of the model's predictions.[31] In some cases, this instability leads the ARIMAX model to perform worse than the simpler ARIMA model, which does not encounter this complication.

Timing also plays a crucial role in the performance of the ARIMAX model. The effects of vaccination on COVID-19 cases often involve variable and unpredictable lags.[45] If the model fails to capture the appropriate lag structure, it could lead to inaccurate predictions. For example, the time required for immunity to develop post-vaccination or differences in response across population groups can cause mismatches between vaccination data and observed case changes, further complicating the accuracy of ARIMAX predictions.

Additionally, the ARIMAX model carries a risk of overfitting, especially when it becomes overly complex in relation to the available data. Overfitting occurs when the model captures noise or random fluctuations in the training data as meaningful patterns, reducing its predictive accuracy on new data.[32] This issue becomes more pronounced when vaccination data are included, as the added complexity could reduce the model's generalizability.

In the multiple regression analysis, several socioeconomic factors emerge as significant predictors of COVID-19 case numbers. For example, previous research indicates that factors such as population density, median income, and access to healthcare services demonstrate strong correlations with case numbers.[48] These findings highlight the unequal impact of the pandemic across various demographic groups and regions. Specifically, areas with higher population density and lower income levels tend to report higher case numbers, likely due to the challenges in practicing social distancing and the limited access to healthcare services.[8]

The regression analysis further emphasizes the importance of incorporating a broad range of socioeconomic factors when assessing the spread of COVID-19. However, the model also reveals certain limitations. The relationships between the independent variables and COVID-19 case numbers are not always linear, suggesting the need for more advanced modeling approaches that can capture these complexities.[29] Moreover, the presence of interaction effects among the variables, such as the combined impact of income and healthcare access, suggests that future models should explore these interactions to better understand the pandemic's dynamics.

Spatial autocorrelation analyses provide additional insights, particularly regarding the geographic clustering

of COVID-19 cases. The results reveal significant spatial clusters of high infection rates, suggesting that local factors—such as public health policies, population density, and mobility patterns—play crucial roles in the spread of the virus.[35] These findings suggest that a one-size-fits-all approach is insufficient for managing the pandemic, highlighting the necessity of region-specific strategies.

In conclusion, while the ARIMA and ARIMAX models serve as valuable tools for understanding and predicting COVID-19 trends, their limitations underscore the need for more complex models that can effectively capture the dynamic and non-linear nature of the pandemic.[47] The multiple regression analysis highlights the crucial role of socioeconomic factors in determining COVID-19 case numbers, suggesting that public health interventions should be tailored to address these disparities. The spatial autocorrelation analysis further emphasizes the importance of region-specific strategies in controlling the spread of the virus. Future research should focus on refining these models, incorporating more real-time data, and improving the granularity of spatial analyses to enhance their predictive accuracy and applicability in public health decision-making. Additionally, the effect of vaccination on COVID-19 case numbers, as explored through various statistical techniques, highlights the critical role of timely and effective vaccination efforts in controlling the pandemic. However, the variability in outcomes across different regions suggests that a tailored, region-specific approach is essential for optimizing public health responses.

Acknowledgments

I would like to express my sincere gratitude to my supervisor, Dr. Wen Zhang, for his invaluable guidance, insightful feedback, and continuous support throughout the entire process of my research and thesis writing. His expertise, patience, and encouragement have been instrumental in the successful completion of this work.

Funding

None.

Conflict of interest

The author declares no conflicts of interest.

Author contributions

This is a single-authored article.

Ethics approval and consent to participate

Not applicable.

Consent for publication

Not applicable.

Availability of data

All datasets used in this study are listed in Table 1.

References

1. Lai CC, Shih TP, Ko WC, Tang HJ, Hsueh PR. Severe acute respiratory syndrome coronavirus 2 (SARS-CoV-2) and coronavirus disease-2019 (COVID-19): The epidemic and the challenges. *Int J Antimicrob Agents*. 2020;55(3):105924.

   doi: 10.1016/j.ijantimicag.2020.105924

2. Adhikari R, Agrawal RK. An introductory study on time series modeling and forecasting. *arXiv [Preprint]*; 2013.

   doi: 10.48550/arXiv.1302.6613

3. Benvenuto D, Giovanetti M, Vassallo L, Angeletti S, Ciccozzi M. Application of the ARIMA model on the COVID-2019 epidemic dataset. *Data Brief*. 2020;29:105340.

   doi: 10.1016/j.dib.2020.105340

4. Petropoulos F, Makridakis S. Forecasting the novel coronavirus COVID-19. *PLoS One*. 2020;15(3):e0231236.

   doi: 10.1371/journal.pone.0231236

5. Bontempi E, Vergalli S, Squazzoni F. Understanding COVID-19 diffusion requires an interdisciplinary, multi-dimensional approach. *Environ Res*. 2020;188:109814.

   doi: 10.1016/j.envres.2020.109814

6. Paltiel AD, Zheng A, Schwartz JL. Speed versus efficacy: Quantifying potential tradeoffs in COVID-19 vaccine deployment. *Ann Intern Med*. 2021;174(4):568-570.

   doi: 10.7326/M20-7866

7. Islam N, Khunti K, Dambha-Miller H, Kawachi I, Marmot M. COVID-19 mortality: A complex interplay of sex, gender and ethnicity. *Eur J Public Health*. 2020;30(5):847-848.

   doi: 10.1093/eurpub/ckaa150

8. Bambra C, Riordan R, Ford J, Matthews F. The COVID-19 pandemic and health inequalities. *J Epidemiol Community Health*. 2020;74(11):964-968.

   doi: 10.1136/jech-2020-214401

9. Box GE, Jenkins GM, Reinsel GC, Ljung GM. *Time Series Analysis: Forecasting and Control*. 5th ed. United States: John Wiley and Sons; 2015.

10. Hamilton JD. Time Series Analysis. United States: Princeton University Press; 1994.

11. Dickey DA, Fuller WA. Distribution of the estimators for autoregressive time series with a unit root. *J Am Stat Assoc*. 1979;74(366a):427-431.

    doi: 10.1080/01621459.1979.10482531

12. Ljung GM, Box GE. On a measure of lack of fit in time series models. *Biometrika*. 1978;65(2):297-303.

doi: 10.1093/biomet/65.2.297

13. Akaike H. A new look at the statistical model identification. In: Parzen E, Tanabe K, Kitagawa G, editors. *Selected Papers of Hirotugu Akaike*. Germany: Springer; 1994. p. 215-232.

doi: 10.1007/978-1-4612-1694-0_16

14. Hyndman RJ, Athanasopoulos G. *Forecasting: Principles and practice*. Australia: OTexts; 2018.

15. Bergmeir C, Benítez JM. On the use of cross-validation for time series predictor evaluation. *Inform Sci.* 2012;191: 192-213.

doi: 10.1016/j.ins.2011.12.028

16. Chai T, Draxler RR. Root mean square error (RMSE) or mean absolute error (MAE)? - Arguments against avoiding RMSE in the literature. *Geosci Model Dev*. 2014;7(3):1247-1250.

doi: 10.5194/gmd-7-1247-2014

17. Willmott CJ, Matsuura K. Advantages of the mean absolute error (MAE) over the root mean square error (RMSE) in assessing average model performance. *Climate Res*. 2005;30(1):79-82.

18. Hyndman RJ, Khandakar Y. Automatic time series forecasting: The forecast package for R. *J Stat Softw*. 2008;27(3):1-22.

doi: 10.18637/jss.v027.i03

19. Tashman LJ. Out-of-sample tests of forecasting accuracy: An analysis and review. *Int J Forecasting*. 2000;16(4):437-450.

doi: 10.1016/S0169-2070(00)00065-0

20. Chandola V, Banerjee A, Kumar V. Anomaly detection: A survey. *ACM Comput Surv.* 2009;41(3):1-58.

doi: 10.1145/1541880.1541882

21. Aggarwal CC. *Outlier Analysis*. 2nd ed. Germany: Springer; 2017.

22. Pankratz A. *Forecasting with Dynamic Regression Models*. United States: John Wiley and Sons; 1991.

23. Granger CWJ. Investigating causal relations by econometric models and cross-spectral methods. *Econometrica.* 1969;37(3):424-438.

doi: 10.2307/1912791

24. Wagner AK, Soumerai SB, Zhang F, Ross-Degnan D. Segmented regression analysis of interrupted time series studies in medication use research. *J Clin Pharm Ther*. 2002;27(4):299-309.

doi: 10.1046/j.1365-2710.2002.00430.x

25. Chow GC. Tests of equality between sets of coefficients in two linear regressions. *Econometrica*. 1960;28(3):591-605.

doi: 10.2307/1910133

26. Imbens GW, Lemieux T. Regression discontinuity designs: A guide to practice. *J Econometrics*. 2008;142(2):615-635.

doi: 10.1016/j.jeconom.2007.05.001

27. Mukaka MM. A guide to appropriate use of correlation coefficient in medical research. *Malawi Med J*. 2012;24(3):69-71.

28. Kutner MH, Nachtsheim CJ, Neter J, Li W. *Applied Linear Statistical Models*. 5th ed. United Staes: McGraw-Hill/Irwin; 2005.

29. Montgomery DC, Peck EA, Vining GG. *Introduction to Linear Regression Analysis.* 5th ed. United States: John Wiley and Sons; 2012.

30. Burnham KP, Anderson DR. *Model Selection and Multimodel Inference: A Practical Information-Theoretic Approach*. 2nd ed. Germany: Springer; 2004.

31. O'Brien RM. A caution regarding rules of thumb for variance inflation factors. *Qual Quant.* 2007;41(5):673-690.

doi: 10.1007/s11135-006-9018-6

32. James G, Witten D, Hastie T, Tibshirani R. *An Introduction to Statistical Learning: With Applications in R*. Germany: Springer; 2013.

33. Jolliffe IT. *Principal Component Analysis*. 2nd ed. Germany: Springer; 2002.

34. Wold S, Sjöström M, Eriksson L. PLS-regression: A basic tool of chemometrics. *Chemometr Intell Lab Syst.* 2001;58(2):109-130.

doi: 10.1016/S0169-7439(01)00155-1

35. Anselin L. Local indicators of spatial association-LISA. *Geograph Anal*. 1995;27(2):93-115.

doi: 10.1111/j.1538-4632.1995.tb00338.x

36. Ord JK, Getis A. Local spatial autocorrelation statistics: Distributional issues and an application. *Geograph Anal.* 1995;27(4):286-306.

doi: 10.1111/j.1538-4632.1995.tb00912.x

37. Cliff AD, Ord JK. *Spatial Processes: Models and Applications.* Billerica, MA: Pion; 1981.

38. Getis A, Ord JK. The analysis of spatial association by use of distance statistics. *Geograph Anal.* 1992;24(3):189-206.

doi: 10.1111/j.1538-4632.1992.tb00261.x

39. World Health Organization. *Classification of Omicron (B.1.1.529): SARS-CoV-2 Variant of Concern*. Available from: https://www.who.int/news/item/26-11-2021-classification-of-omicron-(b.1.1.529)-sars-cov-2-variant-of-concern [Last accessed on 2021 Nov 26].

40. World Health Organization. *Tracking SARS-CoV-2 Variants*; 2022. Available from: https://www.who.int/en/activities/tracking-sars-cov-2-variants [Last accessed on 2025 Jun 16].

41. World Health Organization. *Update on Omicron Subvariants and the Global COVID-19 Situation*; 2022. Available from:

https://www.who.int/news-room/feature-stories/detail/update-on-omicron-subvariants-and-the-global-covid-19-situation [Last accessed on 2024 Sep 24].

42. World Health Organization. *Weekly Epidemiological Update on COVID-19*; 2023. Available from: https://www.who.int/publications/m/item/weekly-epidemiological-update-on-covid-19 [Last accessed on 2023 Jan 11].
43. Chowell G, Hyman JM, Castillo-Chavez C. *Mathematical and Statistical Estimation Approaches in Epidemiology.* Germany: Springer; 2021.
44. Liu Z, Magal P, Seydi O, Webb G. Predicting the cumulative number of cases for the COVID-19 epidemic in China from early data. *Math Biosci Eng*. 2020;17(4):3040-3051.

    doi: 10.3934/mbe.2020172
45. Li Q, Guan X, Wu P, *et al*. Early transmission dynamics in Wuhan, China, of novel coronavirus-infected pneumonia. *N Engl J Med*. 2020;382(13):1199-1207.

    doi: 10.1056/NEJMoa2001316
46. Hernández-Orallo E, Chiner-Oms Á, Rubio-Soler M, *et al*. The importance of considering the impact of COVID-19 variants in forecasting models. *J Ambient Intell Hum Comput*. 2022;13(7):3285-3298.

    doi: 10.1007/s12652-021-03113-x
47. Gao Q, Hu Y, Dai H, *et al*. Modeling COVID-19 with ARIMA and ARIMAX models: A case study in China. *IEEE Access*. 2022;10:55089-55102.

    doi: 10.1109/ACCESS.2022.3182134
48. Wooldridge JM. *Introductory Econometrics: A Modern Approach*. 6th ed. United States: Cengage Learning; 2016.

ACCSCIENCE PUBLISHING

Microbes & Immunity

ORIGINAL RESEARCH ARTICLE

Cellular and molecular characteristics of low-grade central nervous system tumors revealing modulations in Ki-67/propidium iodide, MMP2, VEGFR2, and CD11b/Iba1: Analyses of post-operative samples

Krishnendu Ghosh[1,2,3], Pritha Bhattacharjee[2], and Anirban Ghosh[1,4*]

[1]Immunobiology Laboratory, Department of Zoology, Panihati Mahavidyalaya (West Bengal State University), Sodepur, West Bengal, India

[2]Environmental Epigenomics Laboratory, Department of Environmental Science, University of Calcutta, Kolkata, West Bengal, India

[3]Department of Pathology, Carver College of Medicine, University of Iowa, Iowa City, Iowa, United States of America

[4]Cell Development and Immunobiology Laboratory, Department of Zoology, School of Sciences, Netaji Subhas Open University, Kolkata, West Bengal, India

***Corresponding author:**
Anirban Ghosh
(anirbanghosh@wbnsou.ac.in; aghosh06@gmail.com)

Citation: Ghosh K, Bhattacharjee P, Ghosh A. Cellular and molecular characteristics of low-grade central nervous system tumors revealing modulations in Ki-67/propidium iodide, MMP2, VEGFR2, and CD11b/Iba1: Analyses of post-operative samples. *Microbes & Immunity*. 2025;2(3):130-144. doi: 10.36922/MI025190040

Received: May 8, 2025

Revised: June 5, 2025

Accepted: June 6, 2025

Published online: July 16, 2025

Abstract

The World Health Organization's 2016 and 2021 classifications of central nervous system (CNS) tumors emphasize the integration of histopathological and molecular profiling for improved prognostic and therapeutic precision. Understanding the molecular hallmarks of low-grade CNS tumors is essential for enabling precision therapies and minimizing off-target effects while preventing malignant transformation. This study investigated key oncogenic features in surgically resected low-grade CNS tumors of varying cellular lineages and anatomical locations, alongside associated clinical metadata. Tumors were histologically classified and analyzed for molecular markers using immunohistochemistry, immunofluorescence microscopy, and flow cytometry. Assessed hallmarks included proliferation (Ki-67, propidium iodide index), invasiveness (matrix metalloproteinase [MMP]-2), neovascularization (vascular endothelial growth factor receptor 2 [VEGFR2], epigenetic modulation (DNA methyltransferase 1 [DNMT1], and immune microenvironment (Cluster of Differentiation 11b [CD11b], Iba1, silver-gold macrophage staining). Statistical analyses included *t*-tests, one-way ANOVA, and Kruskal–Wallis tests ($p<0.05$). In diffuse astrocytoma and myxopapillary ependymoma, a proliferation–invasion dichotomy was observed, with lower-proliferative ependymomas exhibiting higher MMP-2 expression. Astrocytomas exhibited elevated DNMT1 expression, indicative of increased epigenetic alterations. Immune profiling revealed tumor-specific differences: $CD11b^+$ macrophages were more prominent in meningiomas, while $Iba1^+$ microglia were enriched in astrocytomas, reflecting distinct immune microenvironments. Despite their low-grade classification, these tumors demonstrated hallmark cancer characteristics, variably expressed across astrocytoma, ependymoma, and meningioma. The combined assessment of Ki-67, MMP-2, VEGFR2, DNMT1, CD11b, and Iba1 provides a prognostically informative and therapeutically exploitable profile. These findings support the integration of molecular profiling into risk stratification and adjunctive

treatment strategies to improve prognosis and reduce malignant progression in low-grade CNS tumors.

Keywords: Low-grade tumor; Astrocytoma; Ependymoma; Meningioma; Proliferation; Neo-vascularization; Invasion; Immune microenvironment

1. Introduction

Primary central nervous system (CNS) tumors represent a broad category of malignancies with an incidence rate of approximately 5 – 10 cases/100,000 individuals in India. Although they account for only 2 – 2.5% of all malignancy cases, they are associated with significant morbidity and mortality.[1] A foundational cross-sectional study analyzing 39,509 cancer patient records from multiple hospitals and institutions in Kolkata, India, reported that 2.4% of all CNS malignancies were primary CNS tumors, among which 60% were gliomas, followed by meningioma, medulloblastomas, primitive neuroectodermal tumors, and others.[2] Another prospective epidemiological study reported that 59.6% of all astrocytic tumors were high-grade astrocytomas, which account for 38.7% of all astrocytic neoplasms in the study population.[3] More recently, a clinico-epidemiological study from Gauhati Medical College, Assam, India, reported that 30% of all diagnosed brain tumors were glioblastoma multiforme, followed by 15% each for grade II and grade III astrocytomas.[4]

CNS tumors are found to be more common in males and frequently occur in individuals aged 40 – 60 years. Over two decades of surveillance have shown an increasing trend in CNS tumor incidence in the Indian population, with overall poor due to the relatively high prevalence of gliomas despite recent therapeutic advancements.[1,2,5] Similarly, data from the Central Brain Tumor Registry of the United States indicate that malignant brain tumors are higher in males, with a modest increase in overall survival in recent years; however, outcomes in elderly glioblastoma multiforme patients have demonstrated only marginal improvement.[6]

These findings suggest that the middle-aged Indian population is more susceptible to glial-origin CNS tumors than others, with prognosis heavily dependent on early diagnosis and treatment modules. Since radiological assessments are often limited by diagnostic variability, and other non-invasive diagnostic methods remain elusive,[7] molecular profiling has emerged as a critical tool for identifying detailed tumor phenotypes – essential for accurate prognostication and personalized therapeutic interventions.[8] Accordingly, molecular profiling is now prominently featured in the revised editions of the World Health Organization (WHO) Classification of Tumors of the CNS, particularly the 4th and 5th editions. In 2016, the WHO introduced integrated molecular and histological criteria for CNS tumor classification, which were further expanded in the 2021 edition with greater emphasis on molecular characterization.[9,10] The importance of these changes is increasingly evident as tumor samples reveal molecular features that are either type- or grade-specific, or in some cases, shared across subtypes.

The molecular characterization of CNS tumors has advanced significantly with the identification of key biomarkers. Ki-67 is a reliable marker of cell proliferation, with expression levels markedly elevated in high-grade tumors.[11] Matrix metalloproteinase (MMP)-2 shows moderate expression in low-grade gliomas, reflecting limited invasiveness and an intact blood–brain barrier (BBB), but becomes significantly upregulated in high-grade tumors, facilitating extracellular matrix degradation and invasive growth.[12] Vascular endothelial growth factor receptor 2 (VEGFR2) is minimally expressed in low-grade tumors, indicating relatively stable vascular architecture and limited angiogenesis, but is highly expressed in advanced CNS neoplasms, where it is related to pathological angiogenesis and microvascular proliferation.[13] Immune markers, such as Cluster of Differentiation 11b (CD11b), a leukocyte/macrophage marker, and Iba1, a CNS macrophage/microglia marker, play important roles in shaping the tumor immune microenvironment. In high-grade CNS tumors, expression levels of CD11b and Iba1 increase substantially, reflecting an altered immune landscape with greater invasion potential.[14] Moreover, tumor-associated macrophages in high-grade tumors tend to polarize toward the CD206^{+} M2 phenotype, which promotes pro-tumorigenic activity – a feature largely absent in low-grade tumors.[15] DNA methyltransferase 1 (DNMT1) also displays grade-specific expression, remaining relatively low in low-grade tumors, consistent with stable DNA methylation patterns. In contrast, DNMT1 is significantly upregulated in high-grade tumors, contributing to widespread CpG island hypermethylation and silencing of tumor suppressor gene.[16] Given the strong associations between these molecular markers, tumor phenotypes,

and their prognostic and therapeutic relevance, the present study incorporated Ki-67, MMP-2, VEGFR2, CD11b, Iba1, and DNMT1 for characterization.

In the present work, we analyzed histopathology and molecular hallmarks of three types of low-grade CNS tumors: spinal myxopapillary ependymoma, fibroblastic meningioma, and diffuse astrocytoma. Low-grade CNS tumors pose considerable clinical challenges due to their unpredictable progression and the lack of reliable prognostic biomarkers. Present diagnostic modalities often fail to predict which tumors will undergo malignant transformation, when this transition might occur, and how aggressively the disease may evolve. Consequently, therapeutic strategies remain suboptimal, adversely affecting patient outcomes.

Moreover, the tumor microenvironment and cellular dynamics that drive progression from indolent to aggressive phenotypes remain poorly characterized, representing a critical knowledge gap in neuro-oncological research. Accordingly, this study aimed to: (i) conduct a comparative analysis of key molecular ontogenic profiles between glial and non-glial low-grade CNS tumors to reveal physiological differences; (ii) determine whether these molecular hallmarks represent viable, subtype-specific therapeutic targets; and (iii) explore whether these molecular characterizations could inform the development of targeted therapies with improved efficacy and reduced off-target toxicity.

Although limited by a small sample size, this study offers a unique contribution to understanding the molecular landscape of low-grade CNS tumors. It may aid in diagnosis, risk stratification, and therapeutic decision-making. Ultimately, this approach seeks to bridge fundamental tumor biology with clinical application, offering potential pathways for early intervention strategies that could prevent malignant transformation and enable more effective targeted therapies.

2. Methodology

2.1. Tumor samples, histology, and metadata

Post-operative CNS tumor tissues were collected from the Bangur Institute of Neurosciences, Institute of Post Graduate Medical Education and Research (IPGME&R), Kolkata, India. Samples were preserved in (i) 10% buffered formalin (CDH, India) for histopathological and immunohistochemical analysis, (ii) 4% paraformaldehyde (MERCK, India) for immunofluorescence studies, and (iii) serum-free Dulbecco's Modified Eagle Medium (DMEM) (Gibco Invitrogen, United States of America [USA]) for live cell isolation and flow cytometry.

Formalin-fixed tissues were processed with embedding and sectioned at 10 μm using a microtome (WESWOX, India). Sections were mounted on glass slides, deparaffinized through alcoholic dehydration, stained with hematoxylin and eosin (Merck, India), and observed under a bright field microscope (TS100F Eclipse, Nikon Corp., Japan). Images were captured using a CCD camera (DS-Fi2-U3, Nikon Corp., Japan).

Tumor type and grade were determined by a collaborating pathologist based on histological features, following the 2016 WHO classification of CNS tumors. A total of 10 low-grade tumor samples were obtained: three spinal myxopapillary ependymomas, four fibroblastic meningiomas, and three diffuse astrocytomas. These tumors are frequently underdiagnosed and are typically identified only after progression to higher-grade lesions, which limits the number of available samples. Additional clinical data included magnetic resonance imaging (MRI) scans with T1- and T2-weighted contrast-enhanced imaging and magnetic resonance spectroscopy (MRS), focusing on N-acetylaspartate (NAA) peaks and choline/creatine ratios. The use of post-operative human tumor tissues adhered to ethical guidelines approved by the Institutional Ethical Committee, IPGME&R, Kolkata (vide Memo No. Inst/IEC/553, dated January 15, 2014).

2.2. Silver/gold (SG) staining of paraffin-embedded tissue

Silver staining and gold toning were performed on 10 μm paraffin-embedded tissue sections. After fixation and deparaffinization, sections were stained using freshly prepared ammoniacal silver carbonate (CDH, India), followed by rinsing in 10% formalin. Subsequently, the sections were toned in gold chloride (Loba Chemie, India) and then fixed in sodium thiosulfate (MERCK, India). Microscopic analysis was carried out using the same imaging system as described in Section 2.1. Images were acquired using the NIS Element-BR software (Nikon Corp., Japan) to identify electron-dense macrophages and microglia.

2.3. Tissue preparation for immunofluorescence microscopy

Tissues were fixed in 4% paraformaldehyde (MERCK, India), washed, and stored in phosphate-buffered saline (PBS; CDH, India) at 4°C. Specimens were sectioned at a thickness of 10 μm, and separate immunofluorescence staining protocols were applied using the following antibodies: glial fibrillary acidic protein (GFAP)-Alexa Fluor 488-conjugated monoclonal antibody (mAb) (Cat. No. 561449, BD Pharmingen, USA), CD11b-FITC mAb (Cat. No. 101205, BioLegend, USA), and Iba1 mAb

(Cat. No. ab5076, Abcam, USA) with a PE-conjugated, anti-mouse, human cross-reactive polyclonal secondary antibody (Cat. No. ab98742, Abcam, USA). In addition, VEGFR2 mAb (Cat. No. sc-6251, Santacruz, USA) was used with a TRITC-conjugated secondary antibody (Cat No. ab6786, Abcam, USA), and MMP-2 mAb (Cat. No. NB200-114, Novus Biologicals, USA) was paired with a FITC-conjugated secondary antibody (Cat. No. ab6785, Abcam, USA).

Non-conjugated primary antibodies were used at a 1:500 dilution, while conjugated primary and secondary antibodies were used at a 1:1000 dilution. All antibodies were diluted in 5% fetal bovine serum (GIBCO, USA) in PBS. Incubations were performed in a dark, humid chamber. A blocking-permeabilizing buffer was prepared using 5% FBS in PBS containing 0.25% Tween-20 (MERCK, India). Fluorescence imaging was conducted using the previously mentioned microscope equipped with EpiFL-B2A and EpiFL-G2A filters (for Alexa Fluor 488/FITC and PE/TRITC, respectively; Nikon Corp., Japan). Images were captured and processed using the previously mentioned CCD camera and imaging software. Mean fluorescence intensity (MFI) was quantified, plotted, and subjected to statistical analysis.

2.4. Immunohistochemistry with counterstaining

Tissue sections were incubated at 54°C overnight, then hydrated and washed with PBS. Blocking was performed using 3% bovine serum albumin (LOBA, India), followed by overnight incubation with non-conjugated Ki-67 mAb (Cat. No. sc-23900, Santacruz, USA) and DNMT1 mAb (Cat. No. sc-271729, Santacruz, USA) at a 1:200 dilution. The slides were then washed and incubated with a horseradish peroxidase-conjugated secondary antibody (Cat. No. ab97030; Abcam, USA) at 1:500 in ×1 PBS. Development was achieved using 3,3-diaminobenzidine (SRL, India) in buffered H_2O_2 (1M TRIS, pH 7.4) supplemented with 0.5% cupric sulfate, in the dark for 20 minutes. Sections were counterstained with hematoxylin (Merck, India), followed by graded alcohol dehydration, air drying, and mounting. Slides were examined using the same microscopic system. For Ki-67 quantification, the number of Ki-67-positive cells were counted and divided by the total number of cells within each microscopical field to calculate the proliferative index. Data were tabulated, graphed, and statistically analyzed.

2.5. Cell isolation, culture, and immunophenotyping

Freshly excised tumor samples were aseptically collected in serum-free DMEM at 4 – 6°C and mechanically minced. Samples were enzymatically dissociated using 0.25% trypsin-ethylenediaminetetraacetic acid (EDTA) (Sigma Aldrich, USA). FBS (MP Biomedicals, USA) was added to neutralize trypsin, and the suspension was filtered through a 70 µm nylon mesh (HiMedia, India). The filtrate was centrifuged and resuspended in DMEM. Cells were counted and seeded in 60 mm culture dishes (Greiner, Germany) at a density of 2×10^6 cells in DMEM supplemented with 10% FBS and 2% antibiotic-antimycotic solution (HiMedia, India). Cultures were maintained in a humidified incubator at 37°C with 5% CO_2 (New Brunswick, Eppendorf, United Kingdom) for 2 days. Following incubation, cells were detached using Accutase (Sigma-Aldrich, USA), washed, and fixed with 4% paraformaldehyde. Cell pellets were treated with permeabilizing blocking buffer (5% FBS in PBS with 0.5% Tween-20) and then washed. Immunostaining was performed using MMP-2 mAb (Cat. No. NB200-114, Novus Biologicals, USA) at a 1:500 dilution and a PE-conjugated secondary antibody (Cat. No. ab97024, Abcam, USA) at a 1:700 dilution. After staining, pellets were washed and analyzed using a BD-FACS Verse flow cytometer with Verse-Suit 1.0 software (BD Biosciences, USA).

2.6. Cell cycle analysis from paraffin-fixed tissue

Cell cycle ploidy analysis was performed on paraffin-embedded tumor tissues as previously described.[10,17] Briefly, 90 µm ribbons were sectioned from paraffinized tissue blocks and treated with xylene (MERCK, India). The resulting pellet was collected through centrifugation, subjected to descending alcohol gradation, and washed repeatedly with PBS. Antigen retrieval was performed using citrate buffer, followed by incubation. Samples were then digested with 0.25% trypsin-EDTA, washed in PBS, and filtered through a 70 µm nylon mesh. The filtrate was centrifuged and resuspended in PBS. RNaseA (1 mg/mL; Invitrogen, USA) was added and incubated at 37°C. Propidium iodide (PI; 0.5 mg/mL; Life Technologies, USA) was then added, followed by incubation. Samples were analyzed using the BD Accuri C5 flow cytometer (BD Biosciences, USA). The cumulative percentage of cells in the S+G2M phases was used as an indicator of proliferation and was subsequently graphed and analyzed statistically.

2.7. Statistical analysis

All experiments were performed in triplicate for each sample. Depending on the data distribution and experimental design, non-parametric tests and/or *t*-tests were applied. Statistical significance was assessed using the Kruskal–Wallis test and nested one-way ANOVA, performed with GraphPad Prism® 10 for Windows 64-bit, version 10.4.2 (633). A $p \leq 0.05$ was considered statistically significant. Additional statistical tests were employed where appropriate. Full statistical details, including significance levels, are provided in the figure legends.

3. Results

3.1. Histopathological findings, MRI metadata, and evaluation of glial/non-glial nature

Histopathological analysis at ×100 and ×400 magnifications revealed distinct architectural features for each tumor type. Ependymoma exhibited lobulated, island-like patterns with hyalinized fibrovascular cores and characteristic perivascular pseudorosettes (Figures 1B and 1C). Meningioma demonstrated classic "whorling" formations resulting from interlacing fascicles of fibroblastic origin (Figure 1F and 1G). In diffuse fibrillary astrocytoma, we noted increased glial cell density and a prominent fibrillary network (Figure 1J and 1K). Among the astrocytoma specimens, nuclear atypia and pleomorphism – hallmarks of malignancy – were most pronounced. Vascular proliferation was most extensive in astrocytoma, followed by lobular-specific vascular islands in ependymoma and moderate, sprouting vasculature in meningioma.

Dystrophic microcalcifications were most abundant within the lobules of ependymoma, moderately dispersed in astrocytoma, and sparse in meningioma. Each tumor type exhibited a distinct histoarchitectural profile. The progressive increase in nuclear atypia and vascular proliferation from meningioma to ependymoma to astrocytoma suggests an escalating degree of biological aggressiveness, even within low-grade classifications.

MRI of myxopapillary spinal ependymoma (Figure 1A) revealed a heterogeneous lesion extending from L1 to L5, with a loss of normal lumbar curvature. The lesion appeared iso- to hyperintense on T2-weighted images. MRS demonstrated a markedly elevated choline peak and a significantly reduced NAA peak. In meningioma (Figure 1E), imaging revealed a large extra-axial mass in the midline basifrontal region, showing intense post-contrast enhancement. The mass appeared iso- to hypointense on T1 and iso- to mildly hyperintense on T2-weighted sequences,

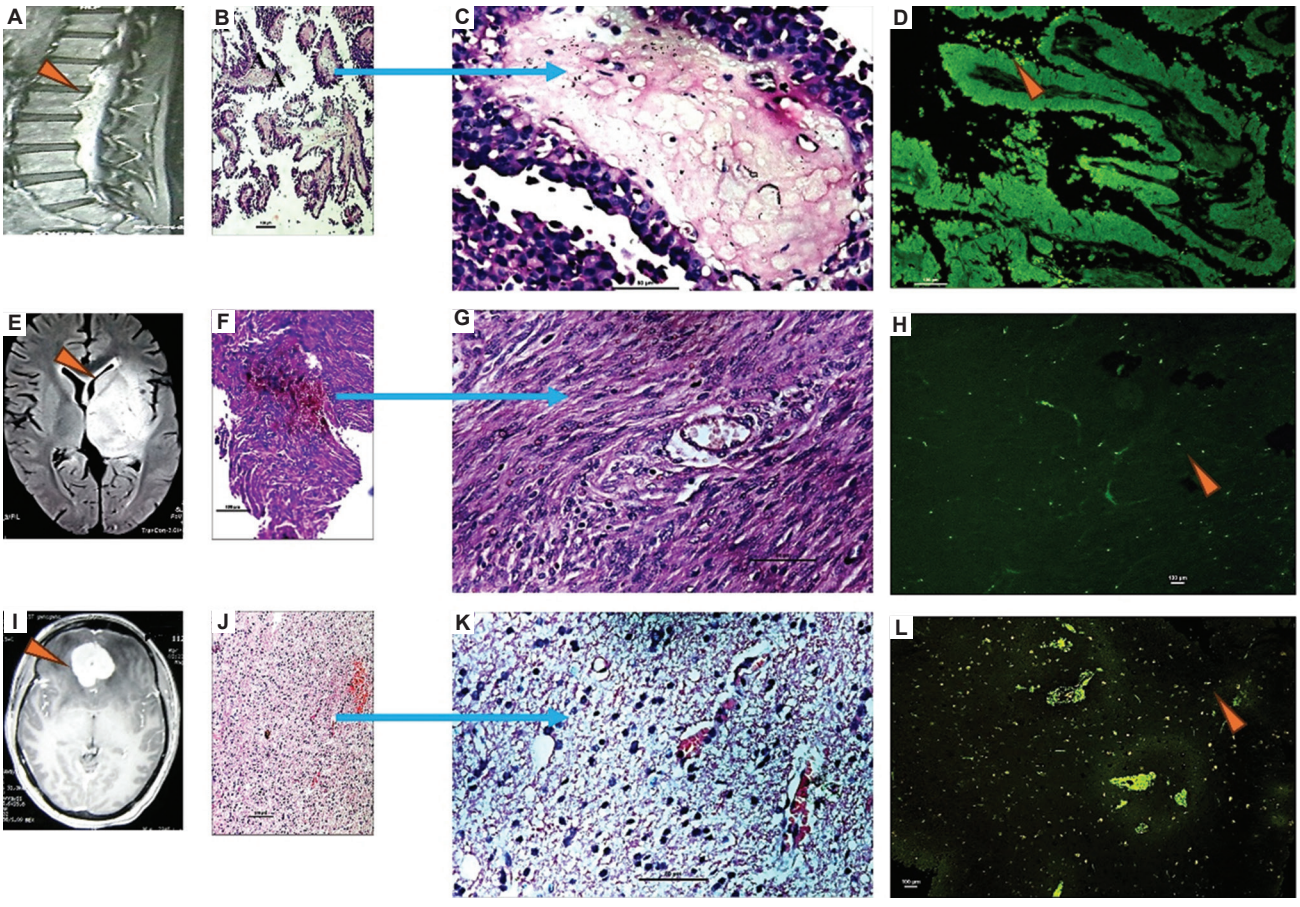

Figure 1. Radiological, histopathological, and immunofluorescence analysis of tumor samples. Low-grade spinal myxopapillary ependymoma: T1- and T2-weighted magnetic resonance (MR) images of (A); Hematoxylin and eosin (H&E)-stained histopathological sections at ×100 (scale bar: 100 μm) and ×400 (scale bar: 50 μm) magnification (B and C); Glial fibrillary acidic protein (GFAP) immunofluorescence (D), with glial cells indicated by orange arrows; Low-grade fibroblastic meningioma: MR images (E); H&E-stained sections at ×100 (scale bar: 100 μm) and ×400 (scale bar: 50 μm) magnification (F and G); GFAP immunofluorescence, with glial cells indicated by orange arrows (H); Low-grade diffuse astrocytoma: MR images (I); H&E-stained sections at ×100 (scale bar: 100 μm) and ×400 (scale bar: 50 μm) magnification (J and K); GFAP immunofluorescence, with glial cells indicated by orange arrows (L).

with mild midline shift and compression effects. MRS indicated increased choline and predominantly reduced NAA levels. Intracranial diffuse astrocytoma (Figure 1I) demonstrated an ill-marginated region of altered signal intensity in the left temporo-parietal region, appearing hypointense on T1 and hyperintense on T2-weighted images. The lesion was associated with a distinct mass effect and midline shift. MRS showed highly elevated choline levels and significantly reduced NAA peaks. Across all tumor types, consistently increased choline and reduced NAA levels reflected altered cellular metabolism characteristic of neoplastic transformation. Among these, astrocytoma displayed the most pronounced metabolic disruption, consistent with its higher malignant potential.

GFAP immunofluorescence revealed extensive astrocytic involvement in low-grade astrocytoma (Figure 1L), with numerous GFAP-positive cells indicating glial hypercellularity. Spinal ependymoma exhibited significantly fewer GFAP-positive cells (Figure 1D), while meningioma demonstrated minimal GFAP expression (Figure 1H), consistent with its origin from GFAP-negative meningio-epithelial cells.

3.2. Immunocytochemistry and immunofluorescence assay corroborates cell-cycle, proliferation, and neo-angiogenesis

Immunohistochemical analysis of Ki-67 expression revealed distinct proliferative profiles among the three tumor types. Astrocytoma demonstrated the highest Ki-67 expression (Figure 2C), whereas ependymoma (Figure 2A) and meningioma (Figure 2B) exhibited comparatively lower expression. Quantitative assessment of Ki-67-positive cell indices yielded mean values of 0.62 ± 0.09 for ependymoma, 1.34 ± 0.36 for meningioma, and 2.1 ± 0.16 for astrocytoma. Statistical analysis confirmed significant differences in proliferative indices across all tumor types, with the most marked disparity observed between ependymoma and astrocytoma (Figure 2D).

Flow cytometric analysis using PI staining corroborated the Ki-67 findings. Cell cycle distribution analysis demonstrated that astrocytoma exhibited the highest percentage of cells in active proliferative phases (S+G2/M: 20.40 ± 2.06%) (Figure 2I and 2J), followed by meningioma (S+G2/M: 12.60 ± 0.70%) (Figure 2G and 2H) and ependymoma (S+G2/M: 8.63 ± 0.51%) (Figure 2E and 2F). Comparative analysis revealed statistically significant differences, confirming that astrocytoma displayed markedly elevated proliferative activity relative to the other two tumor types (Figure 2K).

Given that neoangiogenesis represents a fundamental hallmark of malignancy, we further assessed the angiogenic potential of these tumors through VEGFR2-targeted immunofluorescence using TRITC-conjugated antibodies. Qualitative examination revealed enhanced neovascularization in astrocytoma (Figure 2N) compared to meningioma (Figure 2M) and spinal ependymoma (Figure 2L). Quantitative analysis of MFI values demonstrated statistically significant differences: astrocytoma (59.66 ± 2.55), ependymoma (30.10 ± 2.38), and meningioma (21.35 ± 2.35) (Figure 2O).

These findings collectively indicate a progressive increase in angiogenic activity that correlates with the observed proliferative indices. This suggests a coordinated upregulation of both proliferative and angiogenic signaling pathways in astrocytoma, distinguishing it from other low-grade CNS tumor types.

3.3. MMP-2 expression and invasive potential in low-grade tumor types

Flow cytometric analysis revealed that the MFI of MMP-2-PE was highest in ependymoma (Figure 3A), followed by astrocytoma (Figure 3C), and with the lowest expression observed in meningioma (Figure 3B). To further assess gelatinase-dependent invasiveness, we conducted immunofluorescence using MMP-2-FITC. Ependymoma (Figure 3D) exhibited intense, regionally clustered MMP-2 expression, in contrast to the sparse and scattered signal in meningioma (Figure 3E) and the diffuse moderate expression pattern in astrocytoma (Figure 3F). Quantitative analysis of MFI values showed statistically significant differences in MMP-2 expression across tumor types (Figure 3G). Notably, ependymoma, despite its lower proliferative index, demonstrated the highest MMP-2 expression (62.03 ± 9.50), followed by astrocytoma (40.90 ± 2.04) and meningioma (21.30 ± 2.62).

These findings suggest an inverse relationship between proliferative activity and MMP-2-mediated invasive potential, with ependymomas demonstrating the highest gelatinase-dependent invasiveness despite limited proliferation. This observation highlights ependymomas as a potentially underexplored therapeutic target for MMP-2 inhibitors. Furthermore, profiling MMP-2 expression may serve as a diagnostic tool for personalized treatment strategies for low-grade CNS tumors.

3.4. Immune cell infiltration profiles in the studied low-grade CNS tumors based on silver-gold staining, CD11b, and Iba1 expression

SG histochemical staining was employed to visualize electron-dense mononuclear immune cell populations within the tumor microenvironment, leveraging the differential affinity of metallic ions for cytoplasmic

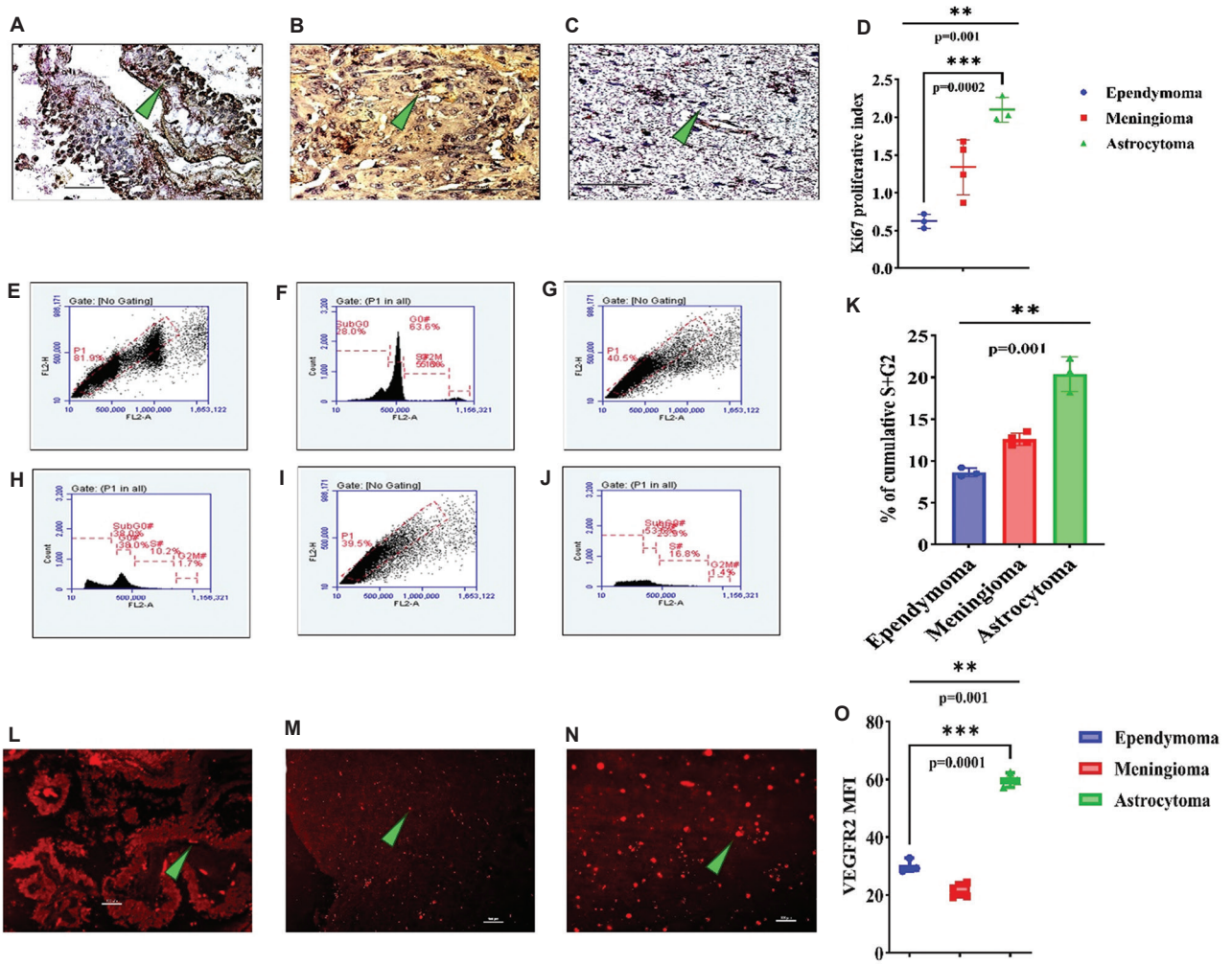

Figure 2. Evaluation of cellular proliferation and associated neoangiogenesis. Ki-67 immunohistochemistry showing proliferative activity (areas marked with green arrows) in: (A) low-grade spinal myxopapillary ependymoma (scale bars: 50 µm; magnification: ×400), (B) low-grade meningioma (scale bars: 50 µm; magnification: ×400), and (C) low-grade astrocytoma (scale bars: 50 µm; magnification: ×400). (D) Quantified Ki-67 proliferative indices plotted and analyzed ***$p \leq 0.001$ ($p=0.0002$; ependymoma versus astrocytoma, unpaired *t*-test); **$p \leq 0.01$ ($p=0.001$; all tumors, Kruskal–Wallis test). Cell cycle analysis using propidium iodide: (E and F) low-grade spinal myxopapillary ependymoma, (G and H) low-grade meningioma, (I and J) low-grade astrocytoma. (K) Cumulative S+G2 phase percentages plotted, with **$p \leq 0.01$ ($p=0.001$; Kruskal–Wallis test). VEGFR2-TRITC IF images (×100, scale bar: 100 µm) (areas marked with green arrows) showing angiogenesis: (L) low-grade spinal myxopapillary ependymoma, (M) low-grade meningioma, (N) low-grade astrocytoma. (O) Box plot of VEGFR2 mean fluorescence intensity data: ***$p \leq 0.001$ ($p=0.0001$; ependymoma vs. astrocytoma, *t*-test); **$p \leq 0.01$ ($p=0.001$; all tumors, Kruskal–Wallis test).
Abbreviations: VEGFR2: Vascular endothelial growth factor receptor 2; TRITC: Tetramethylrhodamine; IF: Immunofluorescence.

components of immune cells. At low magnification (×100), ependymomas (Figure 4A) and astrocytomas (Figure 4E) exhibited comparable levels of immune cell density, whereas meningiomas showed substantially greater infiltration (Figure 4C). High-magnification imaging (×400) revealed the characteristic dark punctate staining of activated macrophages and microglia. Quantitative analysis revealed statistically significant differences in SG-positive cell density across tumor subtypes. Meningiomas exhibited the highest immune cell infiltration (62 ± 3.40; Figure 4D), representing a 1.9-fold increase over ependymomas (32 ± 3.60; Figure 4B) and a 3.4-fold increase over astrocytomas (18 ± 2.5; Figure 4F). *Post hoc* analysis confirmed significant pairwise differences among all tumor groups (Figure 4G), indicating distinct immune microenvironments among CNS tumor subtypes.

Immunofluorescence analysis using CD11b revealed that meningiomas exhibited the highest MFI (27.57 ± 1.23; Figure 4I), followed by ependymomas (9.73 ± 0.60; Figure 4H) and astrocytoma (4.8 ± 0.55; Figure 4J). This

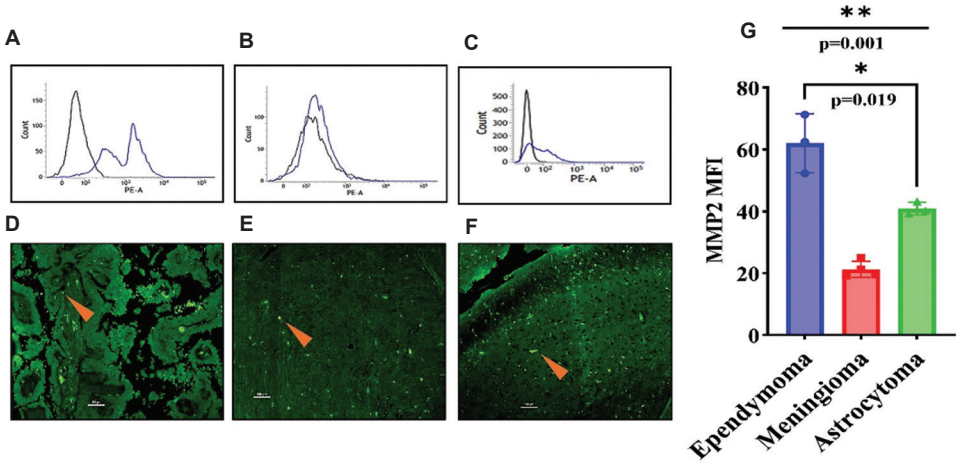

Figure 3. Evaluation of gelatinase-dependent invasiveness. Flow cytometry with PE-conjugated MMP-2 for (A) low-grade spinal myxopapillary ependymoma, (B) low-grade meningioma, (C) low-grade astrocytoma. MMP-2-FITC immunofluorescence images (×100, scale bar: 100 µm) (MMP-2 positive regions marked with orange arrows): (D) low-grade spinal myxopapillary ependymoma, (E) low-grade meningioma, (F) low-grade astrocytoma. (G) Mean fluorescence intensity data plotted: *$p \leq 0.05$ ($p=0.019$; ependymoma vs. astrocytoma, *t*-test); **$p \leq 0.01$ ($p=0.001$; all tumors, Kruskal–Wallis test).
Abbreviations: MMP-2: Matrix metalloproteinase 2; FITC: Fluorescein isothiocyanate.

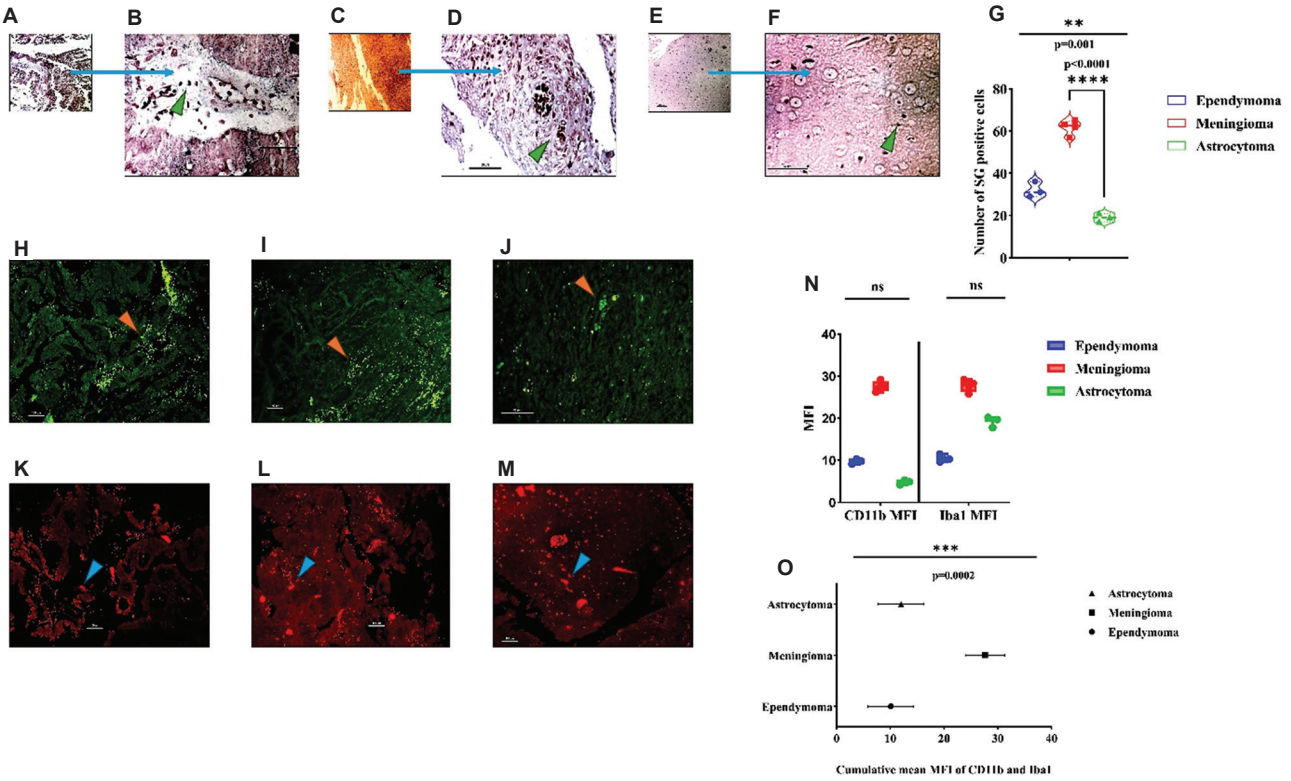

Figure 4. Evaluation of tumor-associated immune cells. Silver-gold (SG)-stained tissue sections at ×100 (scale bar: 100 µm) and ×400 (scale bar: 50 µm) magnification showing SG-positive immune cells (green arrows): (A and B) low-grade spinal myxopapillary ependymoma, (C and D) low-grade meningioma, (E and F) low-grade astrocytoma. (G) Violin plot comparing SG-positive cells density: ****$p \leq 0.0001$ (ependymoma vs. astrocytoma, *t*-test); **$p \leq 0.001$ (Kruskal–Wallis test); Immunofluorescence using CD11b-FITC (for detecting leukocytes, marked with orange arrows): (H) low-grade spinal myxopapillary ependymoma, (I) low-grade meningioma, (J) low-grade astrocytoma. Immunofluorescence using Iba1-PE (for detecting macrophage, marked with blue arrows): (K) ependymoma, (L) meningioma, (M) astrocytoma. (N) Clustered box plot for MFI values of CD11b-FITC and PE-Iba1: Not statistically significant (Kruskal–Wallis test). (O) Comparison of mean MFI (cumulative) of both CD11b and Iba1 across tumors analyzed through nested one-way ANOVA: ***$p \leq 0.001$.
Abbreviations: FITC: Fluorescein isothiocyanate; MFI: Mean fluorescence intensity.

pattern was consistent with the SG staining results and confirms a predominance of $CD11b^+$ myeloid cells in meningioma microenvironments.

In contrast, Iba1 immunofluorescence, which marks both resting and activated microglia, revealed a different pattern. Meningiomas exhibited the highest Iba1 MFI (27.72 ± 1.44; Figure 4L), followed by astrocytomas (19.23 ± 1.26; Figure 4M), and ependymomas (10.46 ± 0.96; Figure 4K). Although individual group comparisons for Iba1 did not reach statistical significance, these trends provided insights into the relative contributions from resident microglia and infiltrating macrophages (Figure 4N). Nested one-way ANOVA incorporating cumulative MFI values for CD11b and Iba1 revealed statistically significant differences in total mononuclear immune cell infiltration among all tumor subtypes (Figure 4O). This integrated analysis indicates that, despite variability in individual marker expression, each CNS tumor subtype exhibits a distinct immune microenvironment signature.

Astrocytomas exhibited a pronounced Iba1-predominant profile (Iba1:CD11b = 4:1), indicating preferential activation of resident microglial populations rather than recruitment of peripheral macrophages. This pattern aligns with the relative preservation of BBB in lower-grade astrocytic tumors, which limits peripheral immune cell infiltration while favoring localized microglial activation. These findings suggest that therapeutic strategies targeting microglial function, such as colony-stimulating factor 1 receptor (CSF1R) inhibitors or microglial repolarization agents, may be particularly effective in preventing tumor progression in astrocytomas. In addition, our observation of an inverse correlation between immune cell density and tumor aggressiveness challenges the conventional association between inflammation and malignancy in CNS tumors. The high immune cell infiltration in typically benign meningiomas, compared to the sparse immune presence in more aggressive astrocytomas, suggests that immune cell abundance may be a defining component of the CNS tumor microenvironment rather than a mere consequence of malignancy.

3.5. DNMT1 expression and epigenetic regulation patterns

Immunohistochemical analysis of DNMT1 expression in fixed tumor sections revealed distinct epigenetic patterns across CNS tumor subtypes. DNMT1-positive cells, identified by dark brown nuclear staining, demonstrated minimal expression in ependymomas (Figure 5A), a focal patchy distribution in meningiomas (Figure 5B), and markedly elevated expression in astrocytomas (Figure 5C). These findings suggest that differential epigenetic regulatory mechanisms may be operative across these tumor types.

The observed gradient of DNMT1 expression (ependymoma < meningioma < astrocytoma) implies that epigenetic dysregulation may serve as a key driver distinguishing indolent from more aggressive CNS tumors. This finding supports the notion that epigenetic alterations contribute significantly to malignant transformation. The elevated DNMT1 expression observed in astrocytomas identifies this tumor type as a potential candidate for methyltransferase inhibitor therapy, which could reverse the epigenetic silencing of tumor suppressor genes and potentially prevent progression to higher-grade malignancy.

4. Discussion

Comprehensive molecular characterization of low-grade CNS neoplasms represents a significant gap in the present neuro-oncological research, particularly when compared to their high-grade counterparts – particularly within the glioma spectrum.[1,18] This disparity may partly result from the often-subtle clinical manifestation of low-grade CNS tumors, resulting in delayed diagnosis or underreporting. However, such tumors can occasionally exhibit unexpected complications and poor prognostic outcomes.[19-21]

To address this gap, we conducted a study on selected low-grade primary CNS tumors, including grade I meningioma and ependymoma, and grade II diffused astrocytoma (noting that grade I astrocytomas are extremely

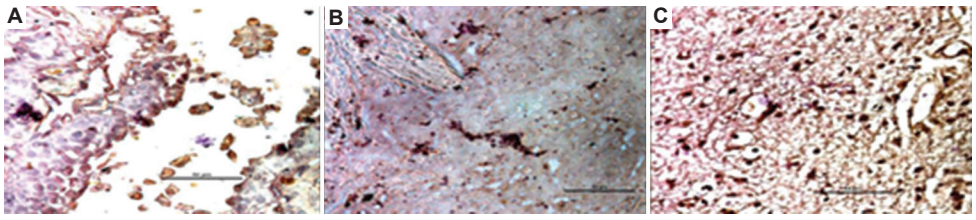

Figure 5. Epigenetic marker analysis. DNMT1 immunochemical imaging (×400, scale bar: 50 μm) showing methylation (brown patchy areas): (A) low-grade spinal myxopapillary ependymoma, (B) low-grade meningioma, and (C) low-grade astrocytoma.
Abbreviation: DNMT1: DNA methyltransferase 1.

rare and typically undiagnosed). Despite the limited sample size, our investigation revealed distinct patterns of cellular organization, proliferative potential, and tissue architecture. These features were closely associated with biological behavior and carry significant prognostic implications. Our findings highlight the critical need for enhanced molecular stratification strategies for low-grade CNS tumors. Such approaches could improve prognostic accuracy and guide therapeutic decisions. This preliminary investigation suggests an emerging pattern that may support prognostic assessment in low-grade CNS tumors.

Immunohistochemical and flow cytometric analyses revealed that neoplastic proliferation in WHO grade II diffuse astrocytomas – as quantified by GFAP immunoreactivity and Ki-67 index – demonstrated strong correlations with tumor cell proliferative activity and patient median overall survival.[22] Complementary demographic analyses conducted in South Indian populations corroborate these findings, demonstrating statistically significant associations between tumor proliferative capacity and clinical outcomes.[23] Although myxopapillary ependymomas comprise approximately 15% of all intramedullary spinal cord neoplasms and are traditionally classified as benign lesions with low Ki-67 indices, our molecular profiling paradoxically revealed elevated MMP-2 expression at both the cellular and tissue-architectural levels. This observation indicates an inverse correlation between proliferation and invasive potential, revealing a critical paradigm in CNS tumor biology. MMPs orchestrate extracellular matrix degradation, facilitate basement membrane disruption, and promote tumor cell invasion and potential metastasis. Previous investigations have documented significant correlations between elevated MMP-2 and MMP-14 expression levels across WHO grade I–III ependymomas and enhanced invasive behavior, which in turn correlate with poorer patient survival outcomes.[24]

Our comparative analysis of VEGFR2 expression, reflecting neoangiogenic activity, revealed heterogeneous patterns in myxopapillary ependymomas. These patterns suggest the presence of focal angiogenic switching in areas of gross total resection, despite the typically low proliferative indices observed. The angiogenic switch is governed by complex regulatory networks involving growth factor signaling pathways (e.g., epidermal growth factor, platelet-derived growth factor, and transforming growth factor) and tissue inhibitors of metalloproteinases modulation, which are influenced by tumor cells, stromal fibroblasts, infiltrating macrophages, and other immune cells. These elements collectively regulate MMP expression and VEGFR2-mediated signaling cascades.[25-27]

Taken together, our findings support a proliferation–invasion dichotomy with associated angiogenic implications among low-grade CNS tumors. Based on the molecular profiles observed, we propose that combination therapy targeting both MMP activity and neo-vasculogenesis may enhance treatment efficacy in low-grade spinal ependymoma. Similarly, dual inhibition of cell proliferation and neo-vasculogenesis may offer therapeutic benefits in low-grade astrocytic tumors. These approaches hold promise for preventing malignant progression while minimizing off-target cytotoxic effects.

Our previous investigations demonstrated a progressive accumulation of both brain-resident microglia and infiltrating macrophages across the malignancy spectrum from WHO grade II to grade IV astrocytomas. These myeloid cell populations play key roles in orchestrating extracellular matrix remodeling, which correlates directly with patient morbidity indices.[28] In the present study, quantitative analysis revealed the highest density of SG-stained, electron-dense microglia and macrophages in meningioma specimens, compared to astrocytomas and ependymomas. These findings were further corroborated through immunophenotyping using CD11b and Iba1 markers.

Previous reports have shown that the extradural location and arachnoid-derived origin of meningiomas – outside the constraints of the BBB – facilitate immune cell infiltration. In particular, meningiomas overexpress monocyte chemoattractant protein-1 (MCP-1), leading to the accumulation of tumor-associated macrophages of monocytic lineage and $CD8^+$ tumor-infiltrating lymphocytes. These immune cell populations are frequently associated with peri-tumoral edema, reflecting the complex interplay between tumor-secreted chemokines and vascular permeability factors. Conversely, the relatively sparse $CD11b^+$ cell populations observed in low-grade astrocytomas are consistent with the preserved integrity of the BBB. Tight junction proteins, such as claudin-5, occludin, and zonula occludens-1 help maintain BBB selectivity, thereby restricting the trans-endothelial migration of circulating monocytes and other peripheral immune effector cells at early stages of tumor development.[29,30] This barrier function, coupled with the typically low expression of MCP-1, limits peripheral monocyte recruitment. Instead, these tumors demonstrate predominant activation of brain-resident $Iba1^+$ microglia, which contribute to tumor progression through the evolving tumor–immune synapse.[31,32]

The differential abundance and spatial organization of resident microglia versus infiltrating macrophages within

Table 1. Comparative profiles of low-grade ependymoma, meningioma, and astrocytoma

Experimental parameters	Defining characteristics	WHO grade I myxopapillary ependymoma	WHO grade I fibrous meningioma	WHO grade II diffuse astrocytoma
Site of occurrence	Sub-regional location (as seen in MRI)	Extradural, spinal, involving the spinal canal extending from L1 – L5	Extracranial, midline basifrontal region	Intracranial, left temporo-parietal region
Magnetic resonance imaging (MRI)	T1	Hypointense	Iso to hypointense	Hypointense
	T2	Overall iso- to hyperintense	Iso to hyperintense	Markedly hyperintense
	Midline shift	Mild to negligible	Mild	Vividly observed
	Mass effect	Mild to negligible	Mild	Vividly observed
Magnetic resonance spectroscopy	Choline peak	High	High	High
	NAA peak	Low	Very low	Low
Histopathology under bright field microscopy	Hematoxylin and eosin staining (observed both in×10 [lower] and×40 [higher] magnification)	Lobulated islands, hyalinized fibrovascular core, perivascular pseudo-rosettes, lobulated blood islands, dystrophic micro-calcification	"Whorling" intercrossing fascicles, vascular sprouting, dystrophic micro-calcification	Fibrillary astrocytic processes, pleomorphic nucleus, conspicuous neovascularization, dystrophic micro-calcification
Astrocytic glial origin and proliferation	IF with GFAP-Alexa Fluor 488 to measure expressional intensity	Moderate	Least	Maximum
Gross proliferation	Proliferative index with IHC with Ki-67-HRP+hematoxylin counterstaining	Minimum (index value 0.62±0.09 SD)	Intermediate (index value1.34±0.36 SD)	Maximum (index value 2.1±0.16 SD)
	Tissue cell cycle analysis with PI	Total percentage of S+G2/M is minimum (8.63±0.51% SD)	Total percentage of S+G2/M is intermediate (12.60±0.70% SD)	Total percentage of S+G2/M is maximum (20.40±2.06% SD)
Angiogenic switching or neovascularization	IF with VEGFR2-TRITC to measure levels of angiogenic receptor expression (MFI)	Clustered/Patchy (30.1±2.38 SD)	Lowest (21.35±2.35 SD)	Highest (59.66±2.55 SD)
Metastatic nature or invasiveness	Cellular FC with MMP-2-PE	Highest	Intermediate	Lowest
	IF with MMP-2-FITC (MFI)	Regional intense expression (62.03±9.50 SD)	Low scattered expression (21.3±2.62 SD)	Diffused moderate expression (40.9±2.04 SD)
Association of mononuclear monocytic lineage Immune cells	S/G staining on fixed tissue (positive cells)	Moderate (32±3.60 SD)	Highest (62±3.40 SD)	Lowest (19±2 SD)
	IF with CD11b-FITC (MFI)	Moderate (9.73±0.60 SD)	Highest (27.57±1.23 SD)	Lowest (4.8±0.55 SD)
	IF with Iba1-PE (MFI)	Lowest (10.46±0.96 SD)	Highest (18.927.72±1.44 SD)	Moderate (19.23±1.26 SD)
Epigenetic alteration	Global methylation pattern detection by IHC with DNMT1-HRP+hematoxylin counterstaining	Scarce	Patchy and moderate	Diffuse but intense

Abbreviations: CD11b: Cluster of Differentiation 11b; DNMT1: DNA methyl transferase 1; FC: Flow cytometry; FITC: Fluorescein isothiocyanate; GFAP: Glial fibrillary acidic protein; HRP: Horse radish peroxidase; IHC: Immunohistochemistry; IF: Immunofluorescence; Ki-67: Kiel cell proliferating antigen protein 67; L1 – L5: Lumber region 1 – 5; MFI: Mean fluorescence index; MMP-2: Matrix metalloproteinase 2; NAA: N-acetylaspartate; PE: Phycoerythrin; PI: Propidium iodide; TRITC: Tetramethylrhodamine; SD: Standard deviation; S/G: Silver-gold staining; VEGFR2: Vascular endothelial growth factor receptor 2.

CNS tumors represent a fundamental pathophysiological determinant of tumor progression, therapeutic response, and clinical outcomes.[33] These immune microenvironmental characteristics are emerging as critical prognostic factors that merit further investigation.

Our findings support the development of precision therapeutic strategies that target microglia to prevent malignant progression in low-grade astrocytomas. CSF1R antagonists may effectively disrupt the CSF1/CSF1R signaling axis,[34] which is essential for microglial survival,

proliferation, and pro-tumorigenic M2 polarization. In addition, microglial repolarization strategies – employing CD40 agonists and/or STAT6 pathway inhibitors – may facilitate phenotypic switching from pro-tumorigenic M2 to anti-tumorigenic M1 activation states, thereby restraining transformation to higher-grade malignancies.[35,36]

In another aspect of the present study, DNMT1 expression across low-grade CNS tumor subtypes revealed the highest immunoreactivity in WHO grade II astrocytoma specimens, followed by intermediate levels in ependymomas. Non-glial meningiomas demonstrated moderate DNMT1 expression, suggesting distinct epigenetic regulatory mechanisms across tumor types. In our previous research, we observed a general trend of increasing epigenetic perturbation with higher glioma grades. However, a comprehensive analysis of epigenetic alterations in post-operative CNS tumor samples across different subtypes remains largely unexplored and may offer prognostic benefits.[37,38] The present study highlights the need for further rigorous investigations involving epigenomic profiling of grade-specific CNS neoplasms. Such studies could provide meaningful prognostic insights and facilitate the identification of novel therapeutic targets, including DNMT inhibitors, histone deacetylase (HDAC) inhibitors, O6-methylguanine-DNA methyltransferase (MGMT) inhibitors, and isocitrate dehydrogenase inhibitors. These agents may block malignant transformation through epigenetic reprogramming while reducing therapeutic resistance and minimizing off-target side effects.[39,40]

In summary, histopathological evaluation alone is insufficient for guiding anti-neoplastic treatment strategies. Prognostic success lies in understanding the functional potential of tumor cells and their microenvironmental interactions. Therefore, molecular characterizations at the cellular and tissue levels are indispensable for revealing hallmark tumor features, including proliferation, invasion, metastasis, neo-vasculogenic potency, and immune cell infiltration.[41]

Integrating cellular and molecular data with histopathological assessment is thus crucial for the rational design of effective anti-cancer treatment regimens. These findings underscore the importance of molecular and genetic tumor characterization, as emphasized in several recent studies.[10,42,43] Moreover, they highlight the need to examine inter- and intra-tumoral cellular organization within the CNS microenvironment – a highly influential factor influencing tumor progression and dissemination, even in low-grade lesions. To improve outcomes for patients with CNS tumors, including prolonged survival and enhanced quality of life, such diagnostic advancements must be incorporated at the early stages of clinical decision-making.

5. Conclusion

The study of low-grade CNS tumor samples from a hospital-based population revealed a non-linear and heterogeneous biological landscape (Table 1). The pathophysiological dynamics observed in WHO grade II diffuse astrocytomas and myxopapillary ependymomas – particularly the inverse correlations between proliferative capacity, invasive potential, and neoangiogenic activity – highlight the necessity of multimodal therapeutic approaches. These findings suggest that targeting interdependent oncogenic pathways simultaneously may be more effective than conventional single-agent strategies. For low-grade ependymomas, the strategic combination of MMP inhibitors with anti-angiogenic agents could synergistically disrupt the invasion–angiogenesis axis while minimizing the cytotoxic effects associated with anti-proliferative therapies. In contrast, patients with low-grade astrocytomas may benefit from the use of anti-proliferative agents, such as temozolomide in combination with therapies tailored to their unique molecular characteristics. These could include CSF1/CSF1R pathway antagonists or microglial repolarization agents targeting Iba1$^+$ microglial activity, anti-angiogenic therapies, and/or epigenetic reprogramming agents, such as DNMT inhibitors, MGMT inhibitors, and HDAC inhibitors. In low-grade meningiomas, where CD11b$^+$ macrophage infiltration is facilitated by their extradural location and absence of BBB constraints, immunotherapeutic interventions may hold particular promise, such as mTOR inhibitors (e.g., everolimus), CDK4/6 inhibitors, anti-invasive agents, and/or epigenetic modifiers depending on the minute biological properties of the tumor and physiological tolerance of the patients. Overall, this preliminary investigation suggests that several key hallmarks of cancer – proliferation, invasion, angiogenesis, and immune cell infiltration – may manifest distinctly even at early tumor grades, depending on CNS tumor subtype. Recognizing and addressing these subtype-specific patterns is essential for advancing personalized therapeutic strategies and optimizing clinical outcomes in patients with low-grade brain tumors.

Acknowledgments

The authors acknowledge Prof. S.N. Ghosh at the Neurosurgery Unit, Bangur Institute of Neurosciences (BIN), Institute of Post Graduate Medical Education and Research (IPGME&R), Kolkata, for helping in the collection of post-operative tumor samples, and Prof. Uttara Chatterjee of Pathology Department of IPGME&R for identifying and grading tumor samples.

Funding

This work was supported by the Council of Scientific and Industrial Research (CSIR), Government of India, through Project No. 37(1587)/13/EMR-II, and was partially supported by the Indian Council of Medical Research (ICMR) under project grant No. 61/8/2011-BMS, awarded to Dr. Anirban Ghosh as principal investigator.

Conflict of interest

The authors declare they have no competing interests.

Author contributions

Conceptualization: Anirban Ghosh
Data curation: Krishnendu Ghosh
Formal analysis: Krishnendu Ghosh
Funding acquisition: Anirban Ghosh
Investigation: Krishnendu Ghosh, Anirban Ghosh
Methodology: Krishnendu Ghosh
Project administration: Anirban Ghosh
Resources: Pritha Bhattacharjee, Anirban Ghosh
Supervision: Pritha Bhattacharjee, Anirban Ghosh
Validation: Pritha Bhattacharjee, Anirban Ghosh, Krishnendu Ghosh
Writing – original draft: Krishnendu Ghosh
Writing – review & editing: All authors

Ethics approval and consent to participate

The present study involved collection of post-operative human tumor samples, which was approved by the Institutional Ethical Committee (IEC) at the Institute of Post Graduate Medical Education and Research (IPGME&R), Kolkata, West Bengal, India (Human Ethical Clearance Memo No: Inst/IEC/553 dated January 15, 2014). The specimen collection was performed together with our collaborating neurosurgeon and clinical pathologist mentioned in the Acknowledgments section. Informed consent was obtained from the human subjects (patients' next keen) abiding by the World Medical Association- Declaration of Helsinki, 64th general assembly, Brazil, 2013.

Consent for publication

Informed consent was obtained from the human subjects (patients' next keen) to publish their data.

Availability of data

All the materials are owned by the authors and will be available from the corresponding authors upon reasonable request.

References

1. Dasgupta A, Gupta T, Jalali R. Indian data on central nervous tumors: A summary of published work. *South Asian J Cancer*. 2016;5(3):147-153.

   doi: 10.4103/2278-330X.187589

2. Ghosh A, Sarkar S, Begum Z, *et al*. The first cross sectional survey on intracranial malignancy in Kolkata, India: Reflection of the State of the art in Southern West Bengal. *Asian Pacific J Cancer Prev*. 2004;5(3):259.

3. Jalali R, Datta D. Prospective analysis of incidence of central nervous tumors presenting in a tertiary cancer hospital from India. *J Neurooncol*. 2008;87(1):111-114.

   doi: 10.1007/S11060-007-9487-Z

4. Paul M, Goswami S, Goutham Raj C, Bora G. Clinico-epidemiological profile of primary brain tumours in North-Eastern region of India: A retrospective single institution study. *Asian Pacific J Cancer Care*. 2023;8(2):333-336.

   doi: 10.31557/apjcc.2023.8.2.333-336

5. Yeole BB. Trends in the brain cancer incidence in India. *Asian Pac J Cancer Prev*. 2008;9(2):267-270.

6. Miller KD, Ostrom QT, Kruchko C, *et al*. Brain and other central nervous system tumor statistics, 2021. *CA A Cancer J Clin*. 2021;71(5):381-406.

   doi: 10.3322/CAAC.21693

7. Gao H, Jiang X. Progress on the diagnosis and evaluation of brain tumors. *Cancer Imaging*. 2013;13(4):466-481.

   doi: 10.1102/1470-7330.2013.0039

8. Park SH, Won J, Kim SI, *et al*. Molecular testing of brain tumor. *J Pathol Transl Med*. 2017;51(3):205-223.

   doi: 10.4132/jptm/2017.03.08

9. Louis DN, Perry A, Reifenberger G, *et al*. The 2016 World Health Organization classification of tumors of the central nervous system: A summary. *Acta Neuropathol*. 2016;131(6):803-820.

   doi: 10.1007/s00401-016-1545-1

10. Louis DN, Perry A, Wesseling P, *et al*. The 2021 WHO classification of tumors of the central nervous system: A summary. *Neuro Oncol*. 2021;23(8):1231-1251.

    doi: 10.1093/neuonc/noab106

11. Sincevičiūtė R, Vaitkienė P, Urbanavičiūtė R, Steponaitis G, Tamašauskas A, Skiriutė D. MMP2 is associated with glioma malignancy and patient outcome. *Int J Clin Exp Pathol*. 2018;11(6):3010-3018.

12. Seyedmirzaei H, Shobeiri P, Turgut M, Hanaei S, Rezaei N. VEGF levels in patients with glioma: A systematic review and meta-analysis. *Rev Neurosci*. 2020;32(2):191-202.

    doi: 10.1515/revneuro-2020-0062

13. Zheng Y, Graeber MB. Microglia and brain macrophages as drivers of glioma progression. *Int J Mol Sci*. 2022;23(24):15612.

doi: 10.3390/ijms232415612

14. Vidyarthi A, Agnihotri T, Khan N, *et al*. Predominance of M2 macrophages in gliomas leads to the suppression of local and systemic immunity. *Cancer Immunol Immunother*. 2019;68(12):1995-2004.

doi: 10.1007/s00262-019-02423-8

15. Rajendran G, Shanmuganandam K, Bendre A, Muzumdar D, Goel A, Shiras A. Epigenetic regulation of DNA methyltransferases: DNMT1 and DNMT3B in gliomas. *J Neurooncol*. 2011;104(2):483-494.

doi: 10.1007/s11060-010-0520-2

16. Zhao Y, Gan L, Ren L, Lin Y, Ma C, Lin X. Factors influencing the blood-brain barrier permeability. *Brain Res*. 2022;1788:147937.

doi: 10.1016/j.brainres.2022.147937

17. Alanen KA, Joensuu H, Klemi PJ. DNA ploidy and cell-cycle analysis in pancreatic and ampullary carcinoma: Flow cytometric study of formalin-fixed paraffin-embedded tissue. *Virchows Arch A Pathol Anat Histopathol*. 1991;419(3):255-256.

doi: 10.1007/BF01626357

18. Bready D, Placantonakis DG. Molecular pathogenesis of low-grade glioma. *Neurosurg Clin N Am*. 2019;30(1):17-25.

doi: 10.1016/j.nec.2018.08.011

19. Yrysov K, Arstanbekov N, Mamytov M, Akmataliev A, Turganbaev B, Vityala Y. Postoperative complications in patients with intracranial meningiomas who underwent surgery. *Biomedicine*. 2023;43(3):34-40.

doi: 10.51248/.v43i3.2886

20. Chang JH, Chang JW, Choi JY, Park YG, Chung SS. Complications after gamma knife radiosurgery for benign meningiomas. *J Neurol Neurosurg Psychiatry*. 2003;74(2):226-230.

doi: 10.1136/jnnp.74.2.226

21. Bertrand KC, Klimo P. Recent advancements in ependymoma: Challenges and therapeutic opportunities. *Pediatr Neurosurg*. 2023;58(5):307-312.

doi: 10.1159/000530868

22. Thotakura M, Tirumalasetti N, Krishna R. Role of Ki-67 labeling index as an adjunct to the histopathological diagnosis and grading of astrocytomas. *J Cancer Res Ther*. 2014;10(3):641-645.

doi: 10.4103/0973-1482.139154

23. Shivaprasad NV, Satish S, Ravishankar S, Vimalambike MG. Ki-67 immunostaining in astrocytomas: Association with histopathological grade - a South Indian study. *J Neurosci Rural Pract*. 2016;7(4):510-514.

doi: 10.4103/0976-3147.188626

24. Akyurek S, Chang EL, Yu TK, *et al*. Spinal myxopapillary ependymoma outcomes in patients treated with surgery and radiotherapy at M.D. Anderson cancer center. *J Neurooncol*. 2006;80(2):177-183.

doi: 10.1007/s11060-006-9169-2.

25. Snuderl M, Chi SN, De Santis SM, *et al*. Prognostic value of tumor microinvasion and metalloproteinases expression in intracranial pediatric ependymomas. *J Neuropathol Exp Neurol*. 2008;67(9):911-920.

doi: 10.1097/NEN.0b013e318184f413

26. Chen X, Li C, Che X, Chen H, Liu Z. Spinal myxopapillary ependymomas: A retrospective clinical and immunohistochemical study. *Acta Neurochir (Wien)*. 2016;158(1):101-107.

doi: 10.1007/s00701-015-2637-8

27. Ghosh K, Ghosh S, Chatterjee U, Chaudhuri S, Anirban A. Microglial contribution to glioma progression: An immunohistochemical study in Eastern India. *Asian Pac J Cancer Prev*. 2016;17(6):2767-2773.

28. Sato K, Kuratsu J, Takeshima H, Yoshimura T, Ushio Y. Expression of monocyte chemoattractant protein-1 in meningioma. *J Neurosurg*. 1995;82(5):874-878.

doi: 10.3171/jns.1995.82.5.0874

29. Lochhead JJ, Yang J, Ronaldson PT, Davis TP. Structure, function, and regulation of the blood-brain barrier tight junction in central nervous system disorders. *Front Physiol*. 2020;11:914.

doi: 10.3389/fphys.2020.00914

30. Yan D, Kowal J, Akkari L, *et al*. Inhibition of colony stimulating factor-1 receptor abrogates microenvironment-mediated therapeutic resistance in gliomas. *Oncogene*. 2017;36(43):6049-6058.

doi: 10.1038/onc.2017.261

31. Kvisten M, Mikkelsen VE, Stensjøen AL, Solheim O, Van Der Want J, Torp SH. Microglia and macrophages in human glioblastomas: A morphological and immunohistochemical study. *Mol Clin Oncol*. 2019;11(1):31-36.

doi: 10.3892/mco.2019.1856

32. Gutmann DH, Kettenmann H. Microglia/brain macrophages as central drivers of brain tumor pathobiology. *Neuron*. 2019;104(3):442-449.

doi: 10.1016/j.neuron.2019.08.028

33. Dubuc AM, Mack S, Unterberger A, Northcott PA, Taylor MD. The epigenetics of brain tumors. *Methods Mol Biol*. 2012;863:139-153.

doi: 10.1007/978-1-61779-612-8_8

34. Van Hooren L, Vaccaro A, Ramachandran M, *et al*. Agonistic CD40 therapy induces tertiary lymphoid structures but impairs responses to checkpoint blockade in glioma. *Nat Commun*. 2021;12(1):4127.

doi: 10.1038/s41467-021-24347-7

35. Tang F, Wang Y, Zeng Y, Xiao A, Tong A, Xu J. Tumor-associated macrophage-related strategies for glioma immunotherapy. *NPJ Precis Oncol*. 2023;7(1):78.

doi: 10.1038/s41698-023-00431-7

36. Skouras P, Markouli M, Papadatou I, Piperi C. Targeting epigenetic mechanisms of resistance to chemotherapy in gliomas. *Criti Rev Oncol Hematol.* 2024;104:104532.

doi: 10.1016/j.critrevonc.2024.104532

37. Ghosh K, Ghosh S, Chatterjee U, Bhattacharjee P, Ghosh A. Dichotomy in growth and invasion from low- to high-grade glioma cellular variants. *Cell Mol Neurobiol*. 2022;42(7):2219-2234.

doi: 10.1007/s10571-021-01096-1

38. Hanahan D, Weinberg RA. Hallmarks of cancer: The next generation. *Cell*. 2011;144(5):646-674.

doi: 10.1016/j.cell.2011.02.013

39. McClellan BL, Haase S, Nunez FJ, *et al*. Impact of epigenetic reprogramming on antitumor immune responses in glioma. *J Clin Invest*. 2023;133(2):e163450.

doi: 10.1172/JCI163450

40. Liu Y, Ali H, Khan F, Pang L, Chen P. Epigenetic regulation of tumor-immune symbiosis in glioma. *Trends Mol Med*. 2024;30(5):429-442.

doi: 10.1016/j.molmed.2024.02.004

41. Wang H, Diaz AK, Shaw TI, *et al*. Deep multiomics profiling of brain tumors identifies signaling networks downstream of cancer driver genes. *Nat Commun*. 2019;10(1):3718.

doi: 10.1038/s41467-019-11661-4

42. Ghosh A, Chaudhuri S. Tissue-free non-invasive diagnostic methodology for brain tumour: Present scenario and future direction. *Biomedicine*. 2019;44(1):39-45.

doi: 10.51248/.v44i1.4045

43. Heiden T, Castaños-Vélez E, Andersson LC, Biberfeld, P. Combined analysis of DNA ploidy, proliferation, and apoptosis in paraffin-embedded cell material by flow cytometry. *Lab Invest*. 2019;80(8):1207-1213.

doi: 10.1038/labinvest.3780128

ACCSCIENCE PUBLISHING

Microbes & Immunity

MINI-REVIEW

Candida hyphae and healthspan: Hypothesis

Patrick W. Chambers*

Department of Pathology, Torrance Memorial Medical Center, Torrance, California, United States of America

Abstract

Candida is traditionally considered an opportunistic pathogen. However, recent research, accelerated by COVID-19, has raised thought-provoking questions about the limitations of this view. Dietary carbohydrates and ethanol have been shown to enable its pathogenic transition. Its hyphae express epitopes that may initiate celiac and Crohn's diseases. Hyphal mannan is potentially linked to Gq-coupled G-protein coupled receptors. Antibodies to these receptors include chemotactic cytokine receptors, which may mediate the escape of latent Epstein–Barr virus. *Candida* hyphae induce mast cells to release histamine and tryptase, which are associated with paroxysmal orthostatic tachycardia syndrome, mast cell activation syndrome, and hypermobility spectrum disorder—conditions frequently observed in long COVID (LC). Hyphae are also implicated in periodontitis, a condition linked to and potentially serving as a sentinel risk indicator for cancer, dementia, autoimmune disease, atherosclerotic cardiovascular disease, and chronic diseases in general. *Candida* yeast and hyphae can produce their own indoleamine dioxygenase (IDO), which antagonizes host IDO, impacting tryptophan metabolism. Altered tryptophan metabolism is observed in cancer, dementia, autoimmune diseases, and LC. *Candida* overgrowth (CO) also releases candidalysin, a toxin that suppresses competing intestinal bacteria, triggers inflammasomes, and causes hypercitrullination, a process associated with several autoimmune diseases and cancers. In addition, CO produces aspartyl protease, leading to the release of zonulin from intestinal epithelial cells, which increase intestinal and endothelial permeability – hallmarks of autoimmune diseases. *Candida*-induced acetaldehyde amplifies the harmful effects of a genetic variant, highly prevalent in Americans, linked to cancer, dementia, and autoimmune diseases. The gut microbiome is increasingly recognized as critical to overall health, and hyphae may play a major role in determining its composition. In this review, the roles of cholecalciferol, tryptophan, and magnesium in counteracting the yeast-to-hyphae transition and invasion are explored. The approach presented here is conceptual rather than empirical.

Keywords: Periodontitis; Mast cell; Cancer; Dementia; Zonulin; *Candida*; Microbiome

***Corresponding author:**
Patrick W. Chambers
(pwc@gte.net)

Citation: Chambers PW. *Candida* hyphae and healthspan: Hypothesis. *Microbes & Immunity.* 2025;2(3):145-161.
doi: 10.36922/mi.4736

Submitted: September 2, 2024

Revised: September 9, 2024

Accepted: November 11, 2024

Published online: December 12, 2024

1. Introduction

The overarching goal for humanity is to enhance both the quality and length of life. Although life expectancy has generally increased due to technological advancements, the quality of life has often declined. A growing deficit in proper diet and exercise has significantly contributed to this deterioration. The vital importance

of the gut microbiome is now recognized as a primary determinant of overall health. Data from long COVID (LC) research may have elevated *Candida* from a mere opportunist to a key player in healthspan. Traditionally considered incidental or opportunistic, more recent findings suggest that invasive *Candida* plays a critical and wide-ranging pathogenic role, even in individuals who are not overtly immunocompromised. *Candida* has now been identified as a collaborator with numerous other pathogens. The overconsumption of refined carbohydrates and alcohol has unleashed *Candida*, the primary hyphae-producing gut fungus, which is normally present as a commensal organism in its yeast form. These hyphae release candidalysin, a toxin capable of inducing autoantibodies. As Hippocrates observed, "All diseases begin in the gut," and the gut, in turn, begins in the mouth. In this context, *Candida* potentiates pathogenic bacteria, and it is unsurprising that periodontitis (and *Candida*) has been linked to pervasive health issues, including autoimmune diseases, cancer, dementia, atherosclerotic cardiovascular disease (ASCVD), and other systemic conditions. *Candida* overgrowth (CO)-induced periodontitis may serve as a pre-cursor to a shortened healthspan; however, the precise mechanisms remain unclear. Several distinct but overlapping mechanisms have been proposed:

1) Hyphal aspartyl protease induces the release of zonulin
2) Hyphal epitopes generate autoantibodies
3) Candidalysin induces the production of citrullinated peptide antibodies
4) Citrullinated autoantibodies facilitate Epstein–Barr virus (EBV) escape
5) Hyphae stimulate mast cells to release histamine and tryptase
6) Altered tryptophan metabolism (ATM) results from fungal indoleamine dioxygenase (IDO)
7) *Candida*-induced acetaldehyde suppresses methionine synthase
8) Histone deacetylase release is triggered by *Candida.*

2. Inflammaging, *Candida*, and periodontitis

Aging is characterized by systemic chronic inflammation, known as inflammaging,[1] and is associated with autoimmunity,[2] dementia,[3] and cancer.[4] Periodontitis triggers inflammaging[5] and is directly linked to cancer risk,[6] dementia,[7,8] and autoimmune diseases, including systemic lupus erythematosus (SLE),[9,10] systemic sclerosis,[11] Hashimoto's disease,[12] and multiple sclerosis.[13]

Porphyromonas gingivalis has been implicated in the generation of anti-citrullinated protein antibodies (ACPAs) in patients with rheumatoid arthritis (RA), indicating a direct biological link between periodontitis and RA.[14]

Periodontitis is also linked to ASCVD[15] and obesity.[16] Gut profiling revealed an elevated abundance and diversity of *Candida* species among people who are obese.[17] Indeed, periodontitis is associated with systemic disease in general[18] and specifically with the NOD-, LRR-, and pyrin domain-containing protein 3 (NLRP3) inflammasome[19] and transglutaminase,[20] both CO markers.[21] Periodontitis is directly related to COVID-19 severity[22] and is also linked to LC.[23] *Candida* is directly associated with periodontitis, dysphagia, and hyposalivation.[24] CO may precede and potentiate *P. gingivalis*[25] in addition to *Treponema denticola*, *Tannerella forsythia*, and other periodontopathic bacteria, inducing periodontitis.[26] Refined carbohydrates increase the risk of periodontitis and CO.[27] CO can be both the cause and effect of xerostomia,[28] a frequent oral complaint in LC.[29] *Candida* and periodontitis are also linked to zonulin,[30] the primary determinant of intestinal and endothelial permeability. In a study of 33 patients with various inflammatory and autoimmune diseases, 60% of those with high zonulin levels tested positive for yeast overgrowth.[31] Additional links between zonulin, autoimmune disease, and *Candida* have recently been reported. Zonulin is a biomarker for the development of celiac disease[32] and is elevated in inflammatory bowel disease (IBD).[33] CO has recently been implicated in the etiology of ulcerative colitis.[34] It may be a primary determinant of chronic disease because invading hyphae present mannan epitopes that appear to elicit Gq proteins coupled to G-protein coupled receptor (GPCR) antibodies.[35] Gq is one of the four types of G alpha protein, which also include Gi, Gs, and G12/13. Gq proteins are associated with chronic diseases.[36] They can also induce pain[37,38] and loss of taste/smell.[39] The effects of histamine[40] and bradykinin[41] are also dependent on Gq-coupled GPCRs. These interconnecting linkages are shown in Figure 1.

3. Hyphal protease and zonulin

Candida hyphae secrete aspartyl protease, which activates the protease-activated receptor 2,[42] leading to zonulin release from intestinal epithelial cells.[43] Zonulin is directly associated with increased intestinal and endothelial permeability. Yeast overgrowth is reported in most individuals with elevated zonulin levels.[31] Aspartyl protease facilitates hyphae development, biofilm formation, host invasion, and immune evasion. Biofilm formation contributes to cancer progression,[44] dementia,[45] periodontitis, ASCVD,[46] and autoimmune diseases.[47]

4. Hyphal epitopes and autoantibodies

Candida hyphal epitopes include a hyphal wall protein that mimics gliadin, associated with celiac disease. Mannan is another hyphal epitope that may bind lectins

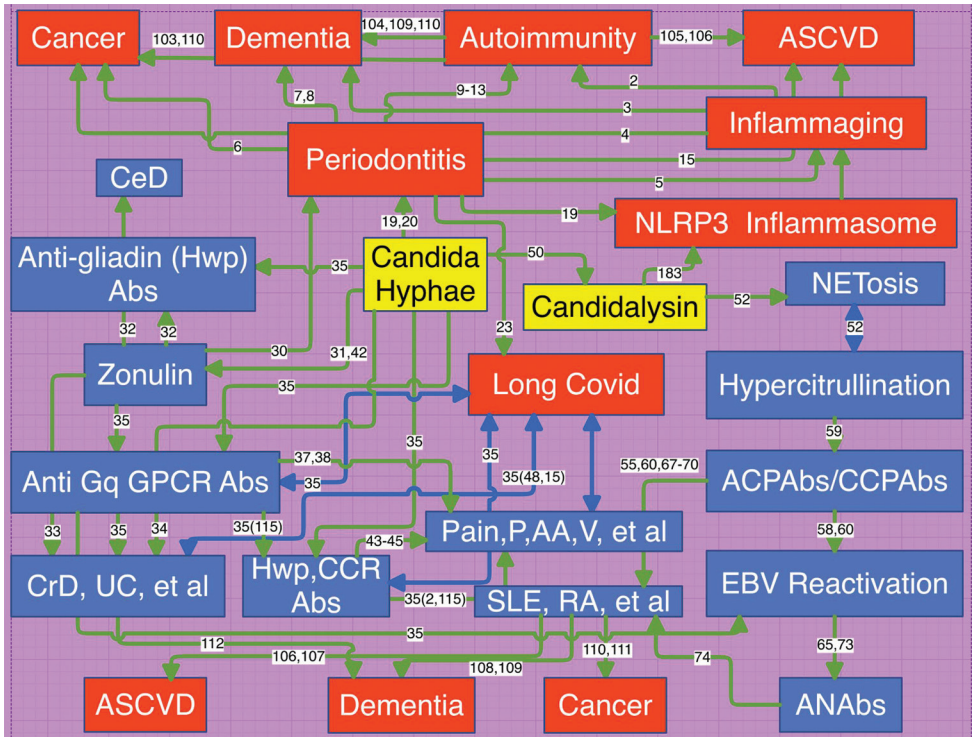

Figure 1. Diagrammatic representation of *Candida* hyphal growth linked to various autoimmune diseases and associated markers

Notes: Numbers indicate references. Green arrows indicate promotion, blue arrows indicate bidirectional relationships, and red boxes indicate impacts on healthspan. See the glossary for additional abbreviations.

Abbreviations: AA: Alopecia areata; ACP: Anti-citrullinated protein; ANA: Antinuclear antibody; CCP: Cyclic citrullinated peptide; CCR: Chemotactic cytokine receptor; CeD: Celiac disease; CrD: Crohn's disease; EBV: Epstein–Barr virus; GPCR: G-protein coupled receptor; Hwp: Hyphal wall protein; P: Psoriasis; UC: Ulcerative colitis; V: Vitiligo.

linked to Gq-coupled GPCRs[35] and chemotactic cytokine receptors (CCRs). GPCRs associated with Gq-coupled GPCRAbs may contribute to dysfunction in taste, smell, and histamine/bradykinin release, as well as various LC symptoms. CCRs, which are also Gq-coupled GPCRs, may mediate pain[48] and are implicated in psoriasis,[49] alopecia areata,[50] and vitiligo[51]—all of which are common in LC.

5. Hyphae candidalysin and citrullinated autoantibodies

Candida hyphae release candidalysin, which triggers citrullination and drives the formation of neutrophil extracellular traps (NETs) and additional citrullination.[52] Candidalysin-induced hypercitrullination can lead to the production of ACPAs, which are associated with autoimmune diseases[53] and periodontitis.[54] ACPAs have been implicated in RA, multiple sclerosis, Alzheimer's disease, psoriatic arthritis, SLE, and juvenile idiopathic arthritis.[55] NETs release numerous citrullinated antigens, driving further ACPA production, which can, in turn, generate more NETs.[56] Anti-cyclic citrullinated peptide antibodies (CCPAbs), a subset of ACPAs, are associated with severe COVID-19[57] and are a hallmark of RA. ACPAs are reported in 5 – 10% of primary Sjögren's syndrome cases.[58] *Candida*, periodontal pathogens, and EBV have been linked to both RA and periodontitis.[59] ACPAs are observed in up to 50% of patients with SLE and arthritis (Rhupus).[60] Alopecia areata and vitiligo, which are observed in both SLE and LC, involve aberrant CCRs[61] that bind to gliadin, mimicked by hyphal wall epitopes (Figure 1), specifically CXCR3.[62] *Candida* and candidalysin are associated not only with inflammation and autoimmune diseases but also with cancer.[63]

6. Hypercitrullination and antinuclear antibodies (ANAs)

B lymphocytes bearing CCP receptors normally tolerate circulating CCP antigens,[64] but when exposed to hypercitrullination, B lymphocytes may produce CCPAbs[53] Although EBV-laden B lymphocytes are present in virtually all humans,[65] EBV typically remains latent. EBV reactivation could occur through the loss of viral surveillance by T-cell receptors (Gq-coupled GPCRs)[35] or through hypercitrullination-induced CCPAbs targeting

EBV-laden B cells,[53] leading to the release of EBV nuclear antigen (ENA) into the general circulation. This reactivation correlates with the coincident appearance of ANAs and ENA.[66] Such CCPAb activity has been observed in RA[67] and SLE.[68,69] ANAs are positive in approximately one-fourth of postural orthostatic tachycardia syndrome (POTS) cases.[70] EBV reactivation has been reported in up to 27% of those with COVID-19[71] and 68% of those with LC.[72] The released but viable EBV may not only generate ANAs against ENA secreted by the virus but also shuttle between immune and epithelial cells,[65] inducing autoimmune diseases related to intracellular ENA. Examples include SLE, multiple sclerosis, RA, IBD, celiac disease, type 1 diabetes, and juvenile idiopathic arthritis.[73] Autoantibodies induced by different regions of ENA may cross-react with SLE autoantigens such as SmB, SmD, and Ro.[74]

7. Hyphae and mast cells/histamine/tryptase

This section explores the connections between hyphae, periodontitis, candidalysin-induced antibodies, and the trifecta of POTS, mast cell activation syndrome (MCAS), and hypermobility spectrum disorder (HSD). Mast cells are recognized as biomarkers of periodontitis,[75,76] and hyphae associated with periodontitis can activate mast cells.[77] The incidence of periodontitis is higher in individuals with LC compared to controls.[78] Anticardiolipin antibodies (antiphospholipid antibodies) are detected in 15 – 20% of individuals with periodontitis.[79] Oral symptoms in POTS include refractory periodontitis, xerostomia, dysgeusia, and burning mouth.[80] Periodontal disease in HSD is primarily genetic in origin,[81] although CO may exacerbate it. Mast cells are key players in periodontitis[82] and are also prominent in dementia,[83] cancer,[84] ASCVD,[85] and autoimmune diseases. Tryptase- and chymase-positive mast cells are frequently found in skin biopsies from individuals with systemic and cutaneous lupus.[86] Mast cells collaborate with ACPAs in RA[87] and play significant roles in Sjögren's syndrome,[88] Graves' disease,[89] IBD,[90] and various other autoimmune diseases, including multiple sclerosis, psoriasis, and atopic dermatitis.[91] Mast cells and tryptase serve as crucial links in the trifecta of HSD, MCAS, and POTS and may also contribute to antiphospholipid syndrome (APS)[92] (Figure 2).

ACPAs activate mast cells, which are associated with RA, spondyloarthritis, psoriatic arthritis, and HSD,[93] all observed in LC.[94] MCAS and HSD are linked,[95] as are POTS/MCAS[96] and POTS/HSD. Nearly 80% of patients with HSD displayed POTS.[97] MCAS,[98] HSD,[99] and POTS[100] are all linked to SLE, as is APS.[101,102] In a large community-based survey, the most common autoimmune conditions coexistent with SLE were Hashimoto thyroiditis (6%), celiac disease (3%), Sjögren syndrome (3%), and RA (2%).[100]

8. ATM in cancer, dementia, autoimmunity, and ASCVD

These diseases collectively contribute to the reduction of both healthspan and lifespan. Their pathogenesis is complex; however, they appear to be interconnected. Autoimmune diseases are associated with cancer,[103] dementia,[104] and ASCVD.[105] Specifically, SLE and RA are linked to ASCVD,[106,107] dementia,[108,109] and cancer.[110,111] In addition, IBD has been associated with dementia.[112]

Candida may actively contribute to this linkage not only through hyphae and candidalysin-induced autoantibodies but also through yeast/hyphae release of IDO and D_3 deficiency. CO is a growing concern due to the increasing prevalence of (1) a more sedentary lifestyle with reduced sunlight exposure and (2) the nutritional decline of the Western diet, characterized by higher consumption of alcohol, refined sugars, and processed meats. This is significant because IDO expression has been detected in both the yeast and hyphal forms of *Candida*.[113] IDO metabolizes tryptophan, which opposes the transition of commensal yeast to its pathogenic hyphal form.[113] Pathogenesis seems to proceed through ATM, a physiological abnormality central to various diseases, including LC.[114] ATM has also been reported in periodontitis[115] and is a hallmark of most chronic inflammatory diseases.[116] The IDO-releasing potential of CO[113] may not only induce ATM but may also be potentiated by it.[117] Moreover, short-chain fatty acids (SCFAs) produced by gut bacteria inhibit *Candida* hyphal invasion[118] and help prevent ATM.[119]

9. *Candida* and ATM

Increasing interest in the gut microbiome and ATM has underscored their underappreciated roles in cancer,[120] autoimmune disease,[121] dementia,[122,123] and chronic inflammation.[124] CO may potentiate ATM[113] due to the following mechanisms:

1) *Candida* expresses its own IDO, which shares 31% homology with mammalian IDO
2) Tryptophan inhibits fungal IDO, while fungal IDO inhibits tryptophan
3) Interferon-gamma (IFN-γ) drives mammalian IDO activity
4) Fungal IDO promotes yeast-to-hyphae morphogenesis
5) Tryptophan, mammalian IDO, and IFN-γ inhibit yeast-to-hyphae morphogenesis
6) Fungal IDO and mammalian IDO are antagonists and are typically balanced in individuals with a healthy gut microbiome.

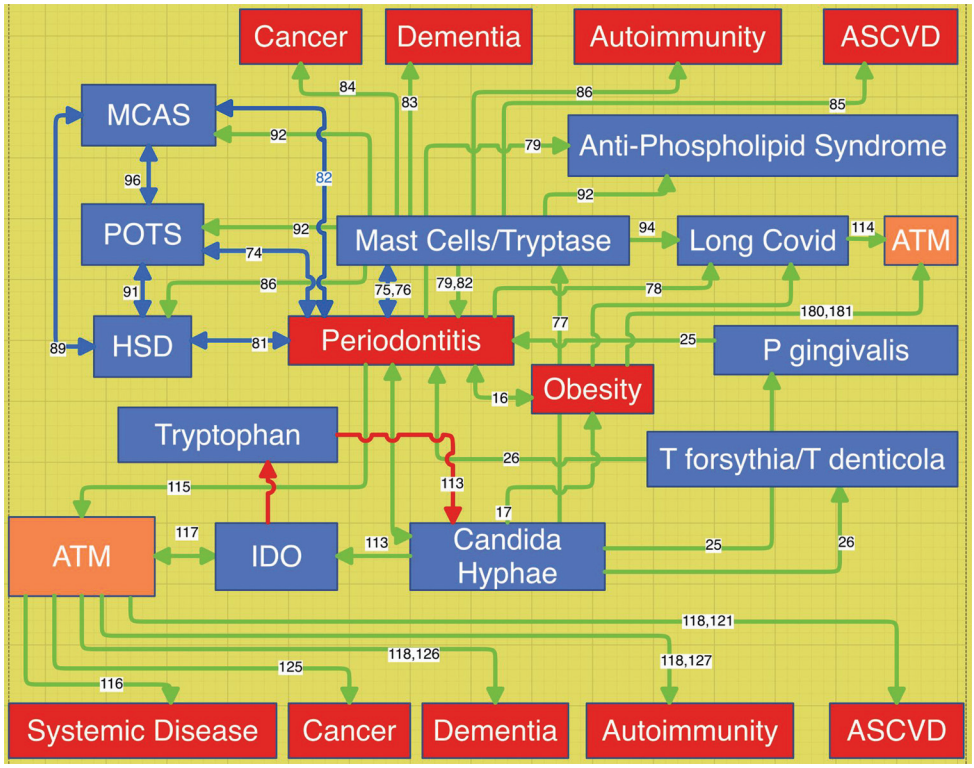

Figure 2. Diagrammatic representation (in continuation of Figure 1) of *Candida* hyphae involvement in ATM, promoting the growth of *Porphyromonas gingivalis*, *Treponema denticola*, and *Tannerella forsythia*

Notes: Numbers indicate references. Green arrows indicate promotion, red arrows indicate inhibition, blue arrows indicate bidirectional relationships, and red boxes indicate impacts on healthspan.

Abbreviations: ATM: Altered tryptophan metabolism; HSD: Hypermobility spectrum disorder; IDO: Indoleamine dioxygenase; MCAS: Mast cell activation syndrome; POTS: Postural orthostatic tachycardia syndrome.

Recent research has highlighted the critical role of the aryl hydrocarbon receptor (AhR) in aging,[125] dementia, autoimmune disease, cancer,[126] and ASCVD.[127] AhR activity depends on its ligands. For instance, nuclear factor kappa-light-chain-enhancer (NF-κB) mediates the NLRP3 inflammasome, whereas kynurenines—AhR ligands—accelerate aging and neurodegeneration. In contrast, indoles derived from intestinal bacteria act as ligands that counteract these effects.[125] ATM disrupts the immune response-dependent function of AhR. Elevated IDO levels and abnormal AhR signaling have been observed in Alzheimer's disease.[120] In addition, AhR has been shown to play a protective role in periodontitis.[128] These findings suggest that a sustained increase in IDO release by *Candida* hyphae, accompanied by a reduction in indole and SCFA levels and an increase in kynurenine and NF-κB levels, may result in unopposed detrimental AhR ligands. Such an imbalance could significantly influence healthspan.

This biochemical relationship between *Candida*, tryptophan, IDO, AhR, and SCFAs (e.g., butyrate) may associate CO with diseases characterized by ATM, such as cancer, dementia, autoimmunity, and ASCVD. Furthermore, it may link CO to diseases associated with a gut microbiome deficient in both biodiversity and SCFAs, such as LC, myalgic encephalomyelitis/chronic fatigue syndrome, and fibromyalgia. The association between CO and butyrate—a GLP-1 agonist similar to semaglutide (Ozempic®)—may further implicate CO in dementia,[129,130] cancer,[131] and obesity.

10. Therapeutic interventions

The active form of vitamin D ($1,25(OH)_2D_3$) supports intestinal barrier integrity, enhances microbial biodiversity, and increases bacterial butyrate production. Notably, it is less widely recognized that D_3 independently inhibits yeast-to-hyphae morphogenesis. This unique effect of D_3 is not mediated through endocrine, intracrine, autocrine, or paracrine pathways but instead reflects an intra-alimentary fungicidal property independent of host receptors.[132,133] The significant but underappreciated benefits of D_3 in this context are often underestimated. Could supplemental D_3 provide benefits that match or surpass those derived from solar exposure?

Tryptophan, a neutral or non-polar amino acid, is one of the nine essential amino acids. It inhibits hyphal

morphogenesis and fungal IDO.[113] This is especially critical for individuals with COVID-19 and LC. Intestinal epithelial cells are rich in ACE2 receptors, which must form a complex with B_0AT, a neutral amino acid transporter, to enable tryptophan absorption.[134] The loss of ACE2 receptor-bearing cells due to SARS-CoV-2 invasion may explain the low levels of tryptophan and serotonin reported in COVID-19 and LC.[135] (Figure 3). This leaves fungal IDO unopposed and suggests that *Candida* might act as a collaborator with SARS-CoV-2. Methionine, another essential neutral amino acid, is critical for methylation (Figure 4). Aberrant methylation, which is linked to cancer, dementia, and autoimmune disease, is facilitated by the 677T methylenetetrahydrofolate reductase (MTHFR) variant allele. According to the Centers for Disease Control and Prevention (CDC), most Americans carry this allele.[136] Acetaldehyde, elevated in CO, inhibits methionine synthase,[137] further compromising methylation in such individuals (Figure 4). This methylation deficiency may pre-dispose them to COVID-19 and LC.[138] Furthermore, CO may exacerbate this vulnerability.

Intestinal bacterial cytochrome P450 enzymes metabolize tryptophan into its indole derivatives (Figure 3),[139] which enhances the integrity of both intestinal and brain barriers. All CYP450 enzymes require Mg^{2+}[140], highlighting its critical role and the importance of the Ca: Mg ratio. Dietary calcium and magnesium compete for absorption through the calcium-sensing receptor. Mg^{2+} is also necessary for converting tryptophan to serotonin (for mood regulation) and serotonin to melatonin (for sleep). It serves as a required cofactor for multiple steps in the synthesis of the active form of vitamin D from D_3 and is essential for its transport by the vitamin D-binding protein. In addition, Mg^{2+} is required for methylation (Figure 4), exacerbating risks associated with CO and the 677T allele. Magnesium exhibits fungicidal properties *in vitro*.[141] In 1989, Jean Durlach, founder of the International Society for Development of Research on Magnesium, reported that a ratio of 2.0 (cation concentrations in mmol/volume) was the ideal target. A high Ca: Mg ratio is characteristic of conditions such as cancer, autoimmune diseases,[142] and ASCVD,[143] with the optimal ratio being between 1.7 and 2.8.[144] The Asian diet is typically low in calcium, whereas the Western diet is often deficient in magnesium.[145] According to the National Health and Nutrition Examination Survey, the mean dietary Ca: Mg intake ratio for Americans has

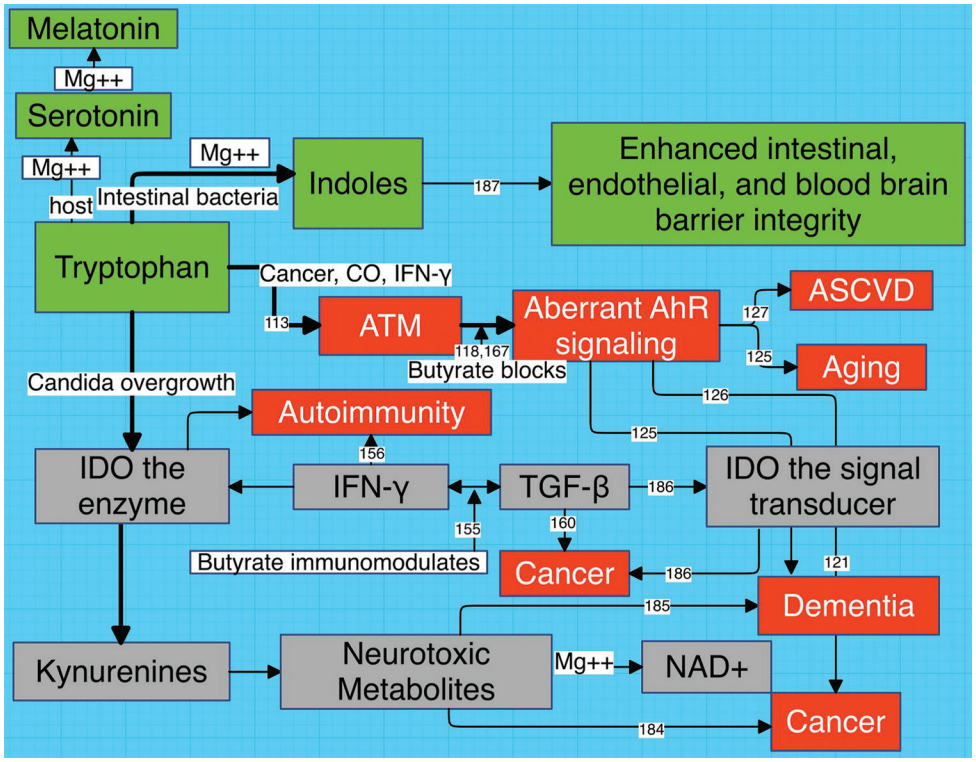

Figure 3. Altered tryptophan metabolism (ATM) characterizes long COVID, autoimmunity, cancer, dementia, and other diseases. Interferon-gamma (IFN-γ) and transforming growth factor beta (TGF-β) counterbalance each other: TGF-β governs tolerogenesis, with excessive levels leading to tolerance of cancer antigens and insufficient levels resulting in intolerance of host antigens. *Candida* can release its own indoleamine dioxygenase (IDO), contributing to ATM and potentiating cancer and dementia.
Notes: Numbers indicate references. Arrow thickness denotes pathway preference.
Abbreviations: AhR: Aryl hydrocarbon receptor; NAD^+: Oxidized nicotinamide adenine dinucleotide.

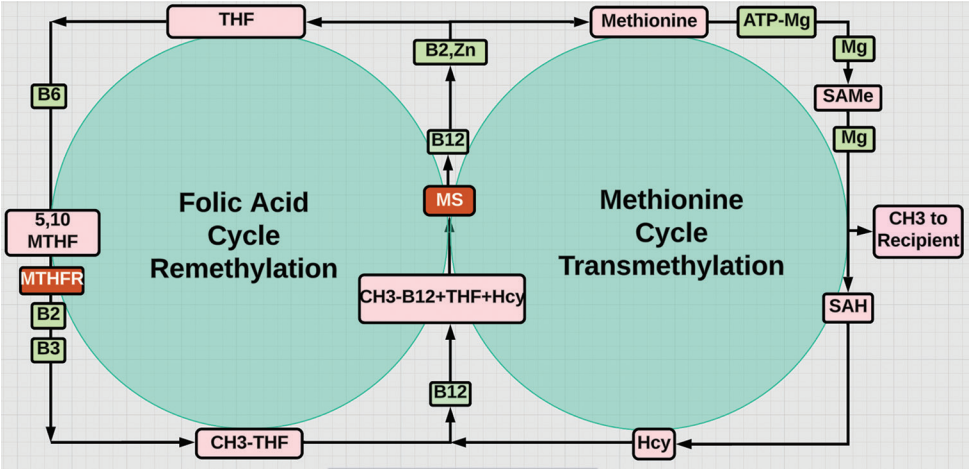

Figure 4. The MTHFR variant allele, present in the majority of Americans, and methionine synthetase (MS), suppressed by acetaldehyde, both highlighted in red, contribute to impair methylation.
Notes: Cofactors are shown in green. Molecules are shown in pink.
Abbreviations: Hcy: Homocysteine; MS: Methionine synthetase; MTHFR: Methylenetetrahydrofolate reductase; SAH: S-Adenosyl homocysteine; SAMe: S-Adenosyl methionine; THF: Tetrahydrofolate.

increased from 2.6 in 1977 to over 3.0 since 2000. When this ratio falls outside its recommended range, similar diseases tend to emerge, such as dementia,[145,146] colon cancer,[144] and ASCVD.[144]

Candida morphogenesis, virulence, biofilm formation, and dissemination are regulated by fungal histone deacetylase (HDAC), particularly Sirtuin2.[147] Sirtuin2 is NAD^+-dependent and may be upregulated through the kynurenine pathway (Figure 3). The dietary inclusion of a pre-biotic (e.g., d-mannose), probiotic (e.g., yogurt), and post-biotic (e.g., butyrate) can counteract CO. Bifidobacteria stimulate butyrogenic bacteria,[148] whereas lactobacilli enhance butyrate absorption.[149] Both dominate the colony-forming units in probiotics. Lactobacilli significantly inhibit *Candida* hyphal morphogenesis and biofilm formation.[150] Butyrate, a potent HDAC inhibitor,[153] suppresses *Candida*.[152,153] HDAC also plays a critical role in carcinogenesis[154] and is associated with dementia,[155] autoimmune diseases, and even periodontitis.[156] Autism spectrum disorder should also be considered part of this list.[157] Butyrate immunomodulates IFN-γ and transforming growth factor beta,[158] which are cytokine reciprocals linked to autoimmune disease[159] and cancer,[161] respectively (Figure 3). In summary, probiotics containing bifidobacteria and lactobacilli may enhance healthspan.[161] They work synergistically through butyrate to promote longevity.[162] The HDAC-inhibiting properties of butyrate have been directly linked to increased lifespan.[163]

Candida thrives on a diet high in refined carbohydrates and alcohol, both of which are metabolized to acetaldehyde (rate-limiting step). Acetaldehyde is associated not only with short-term effects such as brain fog and fatigue but also with cancer[164] and dementia.[165] Alcohol metabolism elevates homocysteine levels (while reducing B_9 and B_{12}),[166] which is linked to cancer,[167] dementia,[168] and autoimmune disease.[169] The active forms of folate (B_9) and cyanocobalamin (B_{12}) depend on methylation, a process compromised in individuals with the 677T allele. The risks of cancer and dementia are further elevated in those carrying the 677T MTHFR allele.[170,171] According to the CDC, nearly half of American adults have pre-diabetes or diabetes, conditions driven by increasing insulin resistance now linked to CO.[172] Recent research indicates that methylation may play a role in the development of systemic insulin resistance.[173] Consequently, CO, which is associated with aberrant DNA methylation and histone deacetylation, may drive disease through dual pathogenic mechanisms involving the epigenome (Figure 4).

Exercise reversibly enhances gut biodiversity.[174]

In summary, achieving an optimal gut microbiome through therapeutic approaches involves the following:

1) Vitamin D3 supplementation
2) Adequate levels of tryptophan
3) Maintaining a Ca: Mg ratio close to 2.0
4) Incorporating pre-biotics, probiotics, and post-biotics
5) Following a diet that moderates the intake of refined carbohydrates and ethanol
6) Engaging in exercise.

11. Conclusion

The described linkages are thought-provoking but do not establish a cause-and-effect relationship. Furthermore,

the magnitude of any such impact remains unknown. However, as reducing dietary refined carbohydrates and alcohol intake is beneficial in numerous other ways, the therapeutic approach appears straightforward. Vitamin D3 and tryptophan both counteract the yeast-to-hyphae transition, whereas magnesium seems to exhibit fungicidal properties.[141] Although incorporating sun exposure and supplemental vitamin D3[132,133] into one's routine is unequivocally advantageous, consuming tryptophan in amounts exceeding 4.5 g/day may be ill-advised.[175] Low-dose tryptophan can enhance mood and sleep. Most individuals following a Western diet have an elevated body mass index and insulin resistance, which is linked to CO.[176] This condition can be mitigated by introducing a lactobacilli-rich probiotic,[172] which not only exhibits anticandidal properties[177] but also helps modulate the immune response.[178] Bifidobacteria and lactobacilli may significantly contribute to enhancing healthspan.[161] The Western diet, typically high in calcium and low in magnesium, also upregulates zonulin,[179] a factor contributing to increased intestinal permeability. Obesity is directly associated with ATM in both children and adults[180,181] and is the leading factor potentially explaining the otherwise inexplicable increase in early-onset cancers. *Candida* may ultimately be recognized as a key facilitator, not only for other pathogens but also for many autoantibodies – such as anti-gliadin antibodies, anti-Gq-coupled GPCR antibodies, anti-CCR antibodies, ACPAs, and ANAs – that link cancer, dementia, ASCVD, and systemic diseases.

In summary, a healthy gut microbiome is increasingly recognized as critical for healthspan and is characterized by the following:

1) High biodiversity
2) Microbiota rich in butyrogenic bacteria and their facilitators, such as lactobacilli and bifidobacteria[148,149]
3) Optimal tryptophan metabolism, defined by a balance between host IDO and fungal IDO

CO opposes these conditions and promotes the following:

1) Aberrant methylation, such as the 677T allele found in most Americans[136] (epigenetic)
2) Insulin resistance, present in nearly half of the population
3) DNA histone deacetylation (epigenetic), contributes to pre-mature aging.[163]

Although these conclusions are conceptual and not empirically validated, they align with the 2,400-year-old adage of Hippocrates. Although not all diseases originate in the gut, the gut microbiome appears to play a central role in initiating or potentiating most diseases, even those driven by epigenetic abnormalities. Diet and exercise[182]—and their impact on the gut microbiome—are clearly within our control.

Acknowledgments

None.

Funding

None.

Conflict of interest

The author declares no conflict of interest.

Author contributions

This is a single-authored article.

Ethics approval and consent to participate

Not applicable.

Consent for publication

Not applicable.

Availability of data

Not applicable.

References

1. Li X, Li C, Zhang W, Wang Y, Qian P, Huang H. Inflammation and aging: Signaling pathways and intervention therapies. *Signal Transduct Target Ther*. 2023;8:239.

   doi: 10.1038/s41392-023-01502-8

2. Santos-Moreno P, Burgos-Angulo G, Martinez-Ceballos MA, *et al*. Inflammaging as a link between autoimmunity and cardiovascular disease: The case of rheumatoid arthritis. *RMD Open*. 2021;7(1):e001470.

   doi: 10.1136/rmdopen-2020-001470

3. Mekli K, Lophatananon A, Maharani A, Nazroo JY, Muir KR. Association between an inflammatory biomarker score and future dementia diagnosis in the population-based UK Biobank cohort of 500,000 people. *PLoS One*. 2023;18(7):e0288045.

   doi: 10.1371/journal.pone.0288045

4. Berben L, Floris G, Wildiers H, Hatse S. Cancer and aging: Two tightly interconnected biological processes. *Cancers* (*Basel*). 2021;13(6):1400.

   doi: 10.3390/cancers13061400

5. Zhu L, Tang Z, Hu R, Gu M, Yang, Y. *Ageing and Inflammation in Periodontium*. Encyclopedia; 2024. Available from: https://encyclopedia.pub/entry/51981 [Last accessed on 2024 Dec 09].

6. Kim EH, Nam S, Park CH, *et al*. Periodontal disease and cancer risk: A nationwide population-based cohort study. *Front Oncol*. 2022;12:901098.

   doi: 10.3389/fonc.2022.901098

7. Guo H, Chang S, Pi X, *et al*. The effect of periodontitis on dementia and cognitive impairment: A meta-analysis. *Int J Environ Res Public Health*. 2021;18(13):6823.

   doi: 10.3390/ijerph18136823

8. Lundergan W, Parthasarathy K, Knight N. Periodontitis and Alzheimer's disease: Is there a connection? *Oral*. 2024;4(1):61-73.

   doi: 10.3390/oral4010006

9. Rutter-Locher Z, Smith TO, Giles I, Sofat N. Association between systemic lupus erythematosus and periodontitis: A systematic review and meta-analysis. *Front Immunol*. 2017;8:1295.

   doi: 10.3389/fimmu.2017.01295

10. Hussain SB, Leira Y, Zehra SA, *et al*. Periodontitis and systemic lupus erythematosus: A systematic review and meta-analysis. *J Periodontal Res*. 2022;57(1):1-10.

    doi: 10.1111/jre.12936

11. Stanomir A, Micu IC, Picoş A, *et al*. Periodontitis burden in diffuse versus limited systemic sclerosis subtypes: A pilot study. *Curr Health Sci J*. 2023;49(2):280-287.

    doi: 10.12865/CHSJ.49.02.280

12. Patil BS, Patil S, Gururaj TR. Probable autoimmune causal relationship between periodontitis and Hashimotos thyroidits: A systemic review. *Niger J Clin Pract*. 2011;14(3):253-261.

    doi: 10.4103/1119-3077.86763

13. Tsimpiris A, Tsolianos I, Grigoriadis A, Tsimtsiou Z, Goulis DG, Grigoriadis N. Association of chronic periodontitis with multiple sclerosis: A systematic review and meta-analysis. *Mult Scler Relat Disord*. 2023;77:104874.

    doi: 10.1016/j.msard.2023.104874

14. de Molon RS, Rossa C Jr., Thurlings RM, Cirelli JA, Koenders MI. Linkage of periodontitis and rheumatoid arthritis: Current evidence and potential biological interactions. *Int J Mol Sci*. 2019;20(18):4541.

    doi: 10.3390/ijms20184541

15. Skipina TM, Elhawary MM, Soliman EZ. Periodontal disease is associated with elevated atherosclerotic cardiovascular disease risk score. *Am J Med Sci*. 2022;364(3):327-332.

    doi: 10.1016/j.amjms.2022.04.002

16. Kim CM, Lee S, Hwang W, *et al*. Obesity and periodontitis: A systematic review and updated meta-analysis. *Front Endocrinol* (*Lausanne*). 2022;13:999455.

    doi: 10.3389/fendo.2022.999455

17. Shoukat M, Ullah F, Tariq MN, Din G, Khadija B, Faryal R. Profiling of potential pathogenic *Candida* species in obesity. *Microb Pathog*. 2023;174:105894.

    doi: 10.1016/j.micpath.2022.105894

18. Bhuyan R, Bhuyan SK, Mohanty JN, Das S, Juliana N, Juliana IF. Periodontitis and its inflammatory changes linked to various systemic diseases: A review of its underlying mechanisms. *Biomedicines*. 2022;10(10):2659.

    doi: 10.3390/biomedicines10102659

19. Isola G, Polizzi A, Santonocito S, Alibrandi A, Williams RC. Periodontitis activates the NLRP3 inflammasome in serum and saliva. *J Periodontol*. 2022;93(1):135-145.

    doi: 10.1002/JPER.21-0049

20. Matarese G, Currò M, Isola G, *et al*. Transglutaminase 2 up-regulation is associated with RANKL/OPG pathway in cultured HPDL cells and THP-1-differentiated macrophages. *Amino Acids*. 2015;47(11):2447-2455.

    doi: 10.1007/s00726-015-2039-5

21. Reyna-Beltrán E, Iranzo M, Calderón-González KG, *et al*. The *Candida albicans* ENO1 gene encodes a transglutaminase involved in growth, cell division, morphogenesis, and osmotic protection. *J Biol Chem*. 2018;293(12):4304-4323.

    doi: 10.1074/jbc.M117.810440

22. Gupta S, Mohindra R, Singla M, *et al*. The clinical association between periodontitis and COVID-19. *Clin Oral Investig*. 2022;26(2):1361-1374.

    doi: 10.1007/s00784-021-04111-3

23. Lloyd-Jones G, Pontes CC, Molayem S, Chapple ILC. The oral-vascular-pulmonary infection route: A pathogenic mechanism linking oral health status to acute and post-acute COVID-19. *Curr Oral Health Rep*. 2023;10:163-174.

    doi: 10.1007/s40496-023-00354-z

24. Suresh Unniachan A, Krishnavilasom Jayakumari N, Sethuraman S. Association between *Candida* species and periodontal disease: A systematic review. *Curr Med Mycol*. 2020;6(2):63-68.

    doi: 10.18502/CMM.6.2.3420

25. Bartnicka D, Gonzalez-Gonzalez M, Sykut J, *et al*. *Candida albicans* shields the periodontal killer *Porphyromonas gingivalis* from recognition by the host immune system and supports the bacterial infection of gingival tissue. *Int J Mol Sci*. 2020;21(6):1984.

    doi: 10.3390/ijms21061984

26. Shigeishi H, Nakamura M, Oka I, *et al*. The associations of periodontopathic bacteria and oral *Candida* with periodontal inflamed surface area in older adults receiving supportive periodontal therapy. *Diagnostics* (*Basel*). 2021;11(8):1397.

    doi: 10.3390/diagnostics11081397

27. Liu W, Zhang W, Ye M. Association between carbohydrate-to-fiber ratio and the risk of periodontitis. *J Dent Sci*. 2024;19:246-253.

    doi: 10.1016/j.jds.2023.04.012

28. Molek M, Florenly F, Lister INE, Wahab TA, Lister C, Fioni F. Xerostomia and hyposalivation in association with oral candidiasis: A systematic review and meta-analysis. *Evid Based Dent*. 2022.

    doi: 10.1038/s41432-021-0210-2

29. Patel D, Louca C, Machuca Vargas, C. Oral manifestations of long COVID and the views of healthcare professionals. *Br Dent J*. 2024;236:111-116.

    doi: 10.1038/s41415-023-6715-7

30. Wright CD. *Zonulin as a Mediator of Psychological Stress and Periodontal Disease*. Graduate Theses, Dissertations, and Problem Reports; 2022. p. 11331. Available from: https://researchrepository.wvu.edu/etd/11331 [Last accessed on 2024 Dec 09].

31. Abigail E, Haytham E. *Assessment of the Relevance of Intestinal Zonulin Test for Inflammatory Conditions in An Integrated Clinical Setting*; 2018. Available from: https://api.semanticscholar.org/corpusid:53624540 [Last accessed on 2024 Dec 09].

32. DaFonte TM, Valitutti F, Kenyon V, *et al*. Zonulin as a biomarker for the development of celiac disease. *Pediatrics*. 2024;153(1):e2023063050.

    doi: 10.1542/peds.2023-063050

33. Caviglia GP, Dughera F, Ribaldone DG, *et al*. Serum zonulin in patients with inflammatory bowel disease: A pilot study. *Minerva Med*. 2019;110(2):95-100.

    doi: 10.23736/S0026-4806.18.05787-7

34. Jangi S, Hsia K, Zhao N, *et al*. Dynamics of the gut mycobiome in patients with ulcerative colitis. *Clin Gastroenterol Hepatol*. 2024;22(4):821-830.e7.

    doi: 10.1016/j.cgh.2023.09.023

35. Chambers P. *Candida and Long Covid: Mannan Not from Heaven*. London: Qeios; 2024.

    doi: 10.32388/JE31EO.5

36. Riemekasten G, Petersen F, Heidecke H. What makes antibodies against G protein-coupled receptors so special? A novel concept to understand chronic diseases. *Front Immunol*. 2020;11:564526.

    doi: 10.3389/fimmu.2020.564526

37. Xie AX, Madayag A, Minton SK, McCarthy KD, Malykhina AP. Sensory satellite glial Gq-GPCR activation alleviates inflammatory pain via peripheral adenosine 1 receptor activation. *Sci Rep.* 2020;10:14181.

    doi: 10.1038/s41598-020-71073-z

38. Li H, Wang R, Lu Y, Xu X, Ni J. Targeting G protein-coupled receptor for pain management. *Brain Circ*. 2017;3(2):109-113.

    doi: 10.4103/bc.bc_3_17

39. An SS, Liggett SB. Taste and smell GPCRs in the lung: Evidence for a previously unrecognized widespread chemosensory system. *Cell Signal*. 2018;41:82-88.

    doi: 10.1016/j.cellsig.2017.02.002

40. Chan CK, Liao SY, Zhang YL, Xu A, Tse HF, Vanhoutte PM. Protective effects of histamine on Gq-mediated relaxation in regenerated endothelium. *Am J Physiol Heart Circ Physiol*. 2014;306(2):H286-H290.

    doi: 10.1152/ajpheart.00733.2013

41. Shen J, Zhang D, Fu Y, Chen A, Yang X, Zhang H. Cryo-EM structures of human bradykinin receptor-G_q proteins complexes. *Nat Commun*. 2022;13(1):714.

    doi: 10.1038/s41467-022-28399-1

42. Kumar R, Rojas IG, Edgerton M. *Candida albicans* Sap6 initiates oral mucosal inflammation via the protease activated receptor PAR2. *Front Immunol*. 2022;13:912748.

    doi: 10.3389/fimmu.2022.912748

43. Yu J, Shen Y, Zhou N. Advances in the role and mechanism of zonulin pathway in kidney diseases. *Int Urol Nephrol*. 2021;53:2081-2088.

    doi: 10.1007/s11255-020-02756-9

44. Choi E, Murray B, Choi S. Biofilm and cancer: Interactions and future directions for cancer therapy. *Int J Mol Sci*. 2023;24(16):12836.

    doi: 10.3390/ijms241612836

45. Chakravarthi ST, Joshi SG. An association of pathogens and biofilms with Alzheimer's disease. *Microorganisms*. 2021;10(1):56.

    doi: 10.3390/microorganisms10010056

46. Tonelli A, Lumngwena EN, Ntusi NAB. The oral microbiome in the pathophysiology of cardiovascular disease. *Nat Rev Cardiol*. 2023;20:386-403.

    doi: 10.1038/s41569-022-00825-3

47. Miller AL, de Anda J, Wong GCL, Tükel Ç. Amyloid-containing biofilms and autoimmunity. *Curr Opin Struct Biol*. 2022;75:102435.

    doi: 10.1016/j.sbi.2022.102435

48. Aloyouny AY, Bepari A, Rahman I. Evaluating the role of $CXCR_3$ in pain modulation: A literature review. *J Pain Res*. 2020;13:1987-2001.

    doi: 10.2147/JPR.S254276

49. Hedrick MN, Lonsdorf AS, Hwang ST, Farber JM. CCR6 as a possible therapeutic target in psoriasis. *Expert Opin Ther Targets*. 2010;14(9):911-922.

doi: 10.1517/14728222.2010.504716

50. Ito T, Kageyama R, Nakazawa S, Honda T. Understanding the significance of cytokines and chemokines in the pathogenesis of alopecia areata. *Exp Dermatol*. 2020;29(8):726-732.

doi: 10.1111/exd.14129

51. He Q, Yuan Q, Shan H, *et al*. Mechanisms of ligand recognition and activation of melanin-concentrating hormone receptors. *Cell Discov*. 2024;10:48.

doi: 10.1038/s41421-024-00679-8

52. Unger L, Skoluda S, Backman E, *et al*. *Candida albicans* induces neutrophil extracellular traps and leucotoxic hypercitrullination via candidalysin. *EMBO Rep*. 2023;24(11):e57571.

doi: 10.15252/embr.202357571

53. Ciesielski O, Biesiekierska M, Panthu B, Soszyński M, Pirola L, Balcerczyk A. Citrullination in the pathology of inflammatory and autoimmune disorders: Recent advances and future perspectives. *Cell Mol Life Sci*. 2022;79(2):94.

doi: 10.1007/s00018-022-04126-3

54. Martos R, Tar I, Nagy AC, Csősz É, Kiss C, Márton I. Hypercitrullination and anti-citrullinated protein antibodies in chronic apical periodontitis, a laboratory investigation. Does autoimmunity contribute to the pathogenesis? *Int Endod J*. 2023;56(5):584-592.

doi: 10.1111/iej.13903

55. Alghamdi M, Alasmari D, Assiri A, *et al*. An overview of the intrinsic role of citrullination in autoimmune disorders. *J Immunol Res*. 2019;2019:7592851.

doi: 10.1155/2019/7592851

56. Liu J, Gao J, Wu Z, *et al*. Anti-citrullinated protein antibody generation, pathogenesis, clinical application, and prospects. *Front Med* (*Lausanne*). 2022;8:802934.

doi: 10.3389/fmed.2021.802934

57. Roghani SA, Dastbaz M, Lotfi R, *et al*. The development of anticyclic citrullinated peptide (anti-CCP) antibody following severe COVID-19. *Immun Inflamm Dis*. 2024;12(5):e1276.

doi: 10.1002/iid3.1276

58. Payet J, Belkhir R, Gottenberg JE, *et al*. ACPA-positive primary Sjögren's syndrome: True primary or rheumatoid arthritis-associated Sjögren's syndrome? *RMD Open*. 2015;1(1):e000066.

doi: 10.1136/rmdopen-2015-000066

59. Paksoy T, Ustaoglu G, Tasci M, Demirci M, Unlu O, Yasar MF. Assessment of Epstein-Barr virus, *Candida albicans*, and some periodontal pathogens in rheumatoid arthritis patients with periodontitis. *North Clin Istanb*. 2023;10(4):490-500.

doi: 10.14744/nci.2023.58998

60. Ceccarelli F, Perricone C, Colasanti T, *et al*. Anti-carbamylated protein antibodies as a new biomarker of erosive joint damage in systemic lupus erythematosus. *Arthritis Res Ther*. 2018;20:126.

doi: 10.1186/s13075-018-1622-z

61. Lammers KM, Lu R, Brownley J, *et al*. Gliadin induces an increase in intestinal permeability and zonulin release by binding to the chemokine receptor $CXCR_3$. *Gastroenterology*. 2008;135(1):194-204.e3.

doi: 10.1053/j.gastro.2008.03.023

62. Rork JF, Rashighi M, Harris JE. Understanding autoimmunity of vitiligo and alopecia areata. *Curr Opin Pediatr*. 2016;28(4):463-469.

doi: 10.1097/MOP.0000000000000375

63. Ho J, Camilli G, Griffiths JS, Richardson JP, Kichik N, Naglik JR. *Candida albicans* and candidalysin in inflammatory disorders and cancer. *Immunology*. 2021;162(1):11-16.

doi: 10.1111/imm.13255

64. Yamada H, Ozawa T, Kishi H, *et al*. Cutting edge: B cells expressing cyclic citrullinated peptide-specific antigen receptor are tolerized in normal conditions. *J Immunol*. 2018;201(12):3492-3496.

doi: 10.4049/jimmunol.1800826

65. Houen G, Trier NH. Epstein-barr virus and systemic autoimmune diseases. *Front Immunol*. 2021;11:587380.

doi: 10.3389/fimmu.2020.587380

66. Cuomo L, Cirone M, Di Gregorio AO, *et al*. Elevated antinuclear antibodies and altered anti-Epstein-Barr virus immune responses. *Virus Res*. 2015;195:95-99.

doi: 10.1016/j.virusres.2014.09.014

67. Pratesi F, Tommasi C, Anzilotti C, Chimenti D, Migliorini P. Deiminated epstein-barr virus nuclear antigen 1 is a target of anti-citrullinated protein antibodies in rheumatoid arthritis. *Arthritis Rheum*. 2006;54:733-741.

doi: 10.1002/art.21629

68. Skare TL, Nisihara R, Barbosa BB, da Luz A, Utiyama S, Picceli V. Anti-CCP in systemic lupus erythematosus patients: A cross sectional study in Brazilian patients. Clin *Rheumatol*. 2013;32(7):1065-1070.

doi: 10.1007/s10067-013-2213-7

69. Draborg AH, Duus K, Houen G. Epstein-Barr virus and systemic lupus erythematosus. *Clin Dev Immunol*. 2012;2012:370516.

doi: 10.1155/2012/370516

70. Ashangari C, Asghar SF, Syed S, Sulema A. Abstract 116: Antinuclear antibody levels study in postural orthostatic

tachycardia syndrome. *Circ Cardiovasc Qual Outcomes*. 2016;9.

doi: 10.1161/circoutcomes.9.suppl_2.116

71. Bernal KDE, Whitehurst CB. Incidence of Epstein-Barr virus reactivation is elevated in COVID-19 patients. *Virus Res*. 2023;334:199157.

doi: 10.1016/j.virusres.2023.199157

72. Gold JE, Okyay RA, Licht WE, Hurley DJ. Investigation of long COVID Prevalence and its relationship to Epstein-Barr virus reactivation. *Pathogens*. 2021;10(6):763.

doi: 10.3390/pathogens10060763

73. Harley JB, Chen X, Pujato M, *et al*. Transcription factors operate across disease loci, with EBNA2 implicated in autoimmunity. *Nat Genet*. 2018;50(5):699-707.

doi: 10.1038/s41588-018-0102-3

74. James JA, Harley JB, Scofield RH. Epstein-Barr virus and systemic lupus erythematosus. *Curr Opin Rheumatol*. 2006;18(5):462-467.

doi: 10.1097/01.bor.0000240355.37927.94

75. Trimarchi M, Lauritano D, Ronconi G, *et al*. Mast cell cytokines in acute and chronic gingival tissue inflammation: Role of IL-33 and IL-37. *Int J Mol Sci*. 2022;23(21):13242.

doi: 10.3390/ijms232113242

76. Lagdive SS, Lagdive SB, Mani A, *et al*. Correlation of mast cells in periodontal diseases. *J Indian Soc Periodontol*. 2013;17(1):63-67.

doi: 10.4103/0972-124X.107500

77. Yu M, Song XT, Liu B, Luan TT, Liao SL, Zhao ZT. The emerging role of mast cells in response to fungal infection. *Front Immunol*. 2021;12:688659.

doi: 10.3389/fimmu.2021.688659

78. Louisa M, Amalina A, Putranto RA, Komala ON, Anggraini W. Periodontal disease severity in patients with long COVID and non-COVID-19. *Dent J*. 2024;57(1):50-55.

doi: 10.20473/j.djmkg.v57.i1.p50-55

79. Schenkein HA, Berry CR, Burmeister JA, *et al*. Anti-cardiolipin antibodies in sera from patients with periodontitis. *J Dent Res*. 2003;82(11):919-922.

doi: 10.1177/154405910308201114

80. Brooks JK, Francis LA. Postural orthostatic tachycardia syndrome: Dental treatment considerations. *J Am Dent Assoc*. 2006;137(4):488-493.

doi: 10.14219/jada.archive.2006.0221

81. Kapferer-Seebacher I, Pepin M, Werner R, *et al*. Periodontal ehlers-danlos syndrome is caused by mutations in C1R and C1S, which encode subcomponents C_1r and C_1s of complement. *Am J Hum Genet*. 2016;99(5):1005-1014.

doi: 10.1016/j.ajhg.2016.08.019

82. Kak MM, Bharali J, Rastogi P, Chaubey KK. Role of mast cells in periodontal health and disease: A comparative study. *Int J Appl Dent Sci*. 2021;7(4):113-116.

doi: 10.22271/ORAL.2021.V7.I4B.1361

83. Jones MK, Nair A, Gupta M. Mast cells in neurodegenerative disease. *Front Cell Neurosci*. 2019;13:171.

doi: 10.3389/fncel.2019.00171

84. Guo X, Sun M, Yang P, Meng X, Liu R. Role of mast cells activation in the tumor immune microenvironment and immunotherapy of cancers. *Eur J Pharmacol*. 2023;960:176103.

doi: 10.1016/j.ejphar.2023.176103

85. Kovanen PT, Bot I. Mast cells in atherosclerotic cardiovascular disease - Activators and actions. *Eur J Pharmacol*. 2017;816:37-46.

doi: 10.1016/j.ejphar.2017.10.013

86. Kaczmarczyk-Sekuła K, Dyduch G, Kostański M, *et al*. Mast cells in systemic and cutaneous lupus erythematosus. *Pol J Pathol*. 2015;66(4):397-402.

doi: 10.5114/pjp.2015.57253

87. Suurmond J, Dorjée AL, Boon MR, *et al*. Mast cells are the main interleukin 17-positive cells in anticitrullinated protein antibody-positive and -negative rheumatoid arthritis and osteoarthritis synovium. *Arthritis Res Ther*. 2015;17:354.

doi: 10.1186/s13075-015-0847-3

88. Nakae S, Suto H, Berry GJ, Galli SJ. Mast cell-derived TNF can promote Th17 cell-dependent neutrophil recruitment in ovalbumin-challenged OTII mice. *Blood*. 2007;109:3640-3648.

doi: 10.1182/blood-2006-09-046128

89. Kenna T, Brown MA. The role of IL-17-secreting mast cells in inflammatory joint disease. *Nat Rev Rheumatol*. 2012;9:375-379.

doi: 10.1038/nrrheum.2012.205

90. De Zuani M, Dal Secco C, Frossi B. Mast cells at the crossroads of microbiota and IBD. *Eur J Immunol*. 2018;48(12):1929-1937.

doi: 10.1002/eji.201847504

91. Kempuraj D, Tagen M, Iliopoulou BP, *et al*. Luteolin inhibits myelin basic protein-induced human mast cell activation and mast cell-dependent stimulation of Jurkat T cells. *Br J Pharmacol*. 2008;155:1076-1084.

doi: 10.1038/bjp.2008.356

92. Schofield JR. Persistent antiphospholipid antibodies, mast cell activation syndrome, postural orthostatic tachycardia syndrome and post-COVID syndrome: 1 year on. *Eur J Case Rep Intern Med*. 2021;8(3):002378.

doi: 10.12890/2021_002378

93. Gutowski Ł, Kanikowski S, Formanowicz D. Mast cell involvement in the pathogenesis of selected musculoskeletal diseases. *Life* (*Basel*). 2023;13(8):1690.

doi: 10.3390/life13081690

94. Sumantri S, Rengganis I. Immunological dysfunction and mast cell activation syndrome in long COVID. *Asia Pac Allergy*. 2023;13(1):50-53.

doi: 10.5415/apallergy.0000000000000022

95. Monaco A, Choi D, Uzun S, Maitland A, Riley B. Association of mast-cell-related conditions with hypermobile syndromes: A review of the literature. *Immunol Res*. 2022;70(4):419-431.

doi: 10.1007/s12026-022-09280-1

96. Kohno R, Cannom DS, Olshansky B, *et al.* Mast cell activation disorder and postural orthostatic tachycardia syndrome: A clinical association. *J Am Heart Assoc*. 2021;10(17):e021002.

doi: 10.1161/JAHA.121.021002

97. Gazit Y, Nahir AM, Grahame R, Jacob G. Dysautonomia in the joint hypermobility syndrome. *Am J Med*. 2003;115:33-40.

doi: 10.1016/S0002-9343(03)00235-3

98. Wang Y, Wang T, Cai M, Zhu S, Song L, Wang Q. Expression and existence forms of mast cell activating molecules and their antibodies in systemic lupus erythematosus. *Immun Inflamm Dis*. 2022;10(2):235-240.

doi: 10.1002/iid3.567

99. Gumà M, Olivé A, Roca J, *et al*. Association of systemic lupus erythematosus and hypermobility. *Ann Rheum Dis*. 2002;61:1024-1026.

doi: 10.1136/ard.61.11.1024

100. Shaw BH, Stiles LE, Bourne K, *et al*. The face of postural tachycardia syndrome - insights from a large cross-sectional online community-based survey. *J Intern Med*. 2019;286(4):438-448.

doi: 10.1111/joim.12895

101. Abu-Shakra M, Gladman DD, Urowitz MB, Farewell V. Anticardiolipin antibodies in systemic lupus erythematosus: Clinical and laboratory correlations. *Am J Med*. 1995;99(6):624-628.

doi: 10.1016/s0002-9343(99)80249-6

102. Meroni PL, Tsokos GC. Editorial: Systemic lupus erythematosus and antiphospholipid syndrome. *Front Immunol*. 2019;10:199.

doi: 10.3389/fimmu.2019.00199

103. Mangani D, Yang D, Anderson AC. Learning from the nexus of autoimmunity and cancer. *Immunity*. 2023;56(2):256-271.

doi: 10.1016/j.immuni.2023.01.022

104. Weaver DF. Alzheimer's disease as an innate autoimmune disease (AD^2): A new molecular paradigm. *Alzheimers Dement*. 2022;19:1086-1098.

doi: 10.1002/alz.12789

105. Mortensen, MB, Jensen, JM, Sand, NPR, *et al*. Association of autoimmune diseases with coronary atherosclerosis severity and ischemic events. *J Am Coll Cardiol*. 2024;83(25):2643-2654.

doi: 10.1016/j.jacc.2024.04.030

106. Keyes E, Grinnell M, Jacoby D, *et al*. Assessment and management of the heightened risk for atherosclerotic cardiovascular events in patients with lupus erythematosus or dermatomyositis. *Int J Womens Dermatol*. 2021;7(5A):560-575.

doi: 10.1016/j.ijwd.2021.08.015

107. Popescu D, Rezus E, Badescu MC, *et al*. Cardiovascular risk assessment in rheumatoid arthritis: Accelerated atherosclerosis, new biomarkers, and the effects of biological therapy. *Life* (*Basel*). 2023;13(2):319.

doi: 10.3390/life13020319

108. Jin T, Huang W, Cao F, *et al*. Causal association between systemic lupus erythematosus and the risk of dementia: A mendelian randomization study. *Front Immunol*. 2022;13:1063110.

doi: 10.3389/fimmu.2022.1063110

109. Kodishala, C, Hulshizer, CA, Kronzer, VL, *et al*. Risk factors for dementia in patients with incident rheumatoid arthritis: A population-based cohort study. *J Rheumatol*. 2023;50(1):48-55.

doi: 10.3899/jrheum.220200

110. Song L, Wang Y, Zhang J, Song N, Xu X, Lu Y. The risks of cancer development in Systemic Lupus Erythematosus (SLE) patients: A systematic review and meta-analysis. *Arthritis Res Ther*. 2018;20:270.

doi: 10.1186/s13075-018-1760-3

111. Beydon M, Pinto S, De Rycke Y, *et al*. Risk of cancer for patients with rheumatoid arthritis versus general population: A national claims database cohort study. *Lancet Reg Health Eur*. 2023;35:100768.

doi: 10.1016/j.lanepe.2023.100768

112. Zamani M, Ebrahimtabar F, Alizadeh-Tabari S, *et al*. Risk of common neurological disorders in adult patients with inflammatory bowel disease: A systematic review and meta-analysis. *Inflamm Bowel Dis*. 2024;30:2195-2204.

doi: 10.1093/ibd/izae012

113. Bozza S, Fallarino F, Pitzurra L, *et al*. A crucial role for tryptophan catabolism at the host/*Candida albicans* interface. *J Immunol*. 2005;174(5):2910-2918.

doi: 10.4049/jimmunol.174.5.2910

114. Eroğlu İ, Eroğlu BÇ, Güven GS. Altered tryptophan absorption and metabolism could underlie long-term

symptoms in survivors of coronavirus disease 2019 (COVID-19). *Nutrition*. 2021;90:111308.

doi: 10.1016/j.nut.2021.111308

115. Kurgan Ş, Önder C, Balcı N, *et al*. Influence of periodontal inflammation on tryptophan-kynurenine metabolism: A cross-sectional study. *Clin Oral Investig*. 2022;26(9):5721-5732.

doi: 10.1007/s00784-022-04528-4

116. Harris DMM, Szymczak S, Schuchardt S, *et al*. Tryptophan degradation as a systems phenomenon in inflammation - an analysis across 13 chronic inflammatory diseases. *EBioMedicine*. 2024;102:105056.

doi: 10.1016/j.ebiom.2024.105056

117. Brown AJ, Brown GD, Netea MG, Gow NA. Metabolism impacts upon *Candida* immunogenicity and pathogenicity at multiple levels. *Trends Microbiol*. 2014;22(11):614-22.

doi: 10.1016/j.tim.2014.07.001

118. Modoux M, Rolhion N, Lefevre JH, *et al*. Butyrate acts through HDAC inhibition to enhance aryl hydrocarbon receptor activation by gut microbiota-derived ligands. *Gut Microbes*. 2022;14(1):2105637.

doi: 10.1080/19490976.2022.2105637

119. McCrory C, Lenardon M, Traven A. Bacteria-derived short-chain fatty acids as potential regulators of fungal commensalism and pathogenesis. *Trends Microbiol*. 2024;32:1106-1118.

doi: 10.1016/j.tim.2024.04.004

120. Badawy AA. Tryptophan metabolism and disposition in cancer biology and immunotherapy. *Biosci Rep*. 2022;42(11):BSR20221682.

doi: 10.1042/BSR20221682

121. Seo SK, Kwon B. Immune regulation through tryptophan metabolism. *Exp Mol Med*. 2023;55(7):1371-1379.

doi: 10.1038/s12276-023-01028-7

122. Savonije K, Weaver DF. The role of tryptophan metabolism in Alzheimer's disease. *Brain Sci*. 2023;13(2):292.

doi: 10.3390/brainsci13020292

123. Xie L, Wu Q, Li K, *et al*. Tryptophan metabolism in Alzheimer's disease with theinvolvement of microglia and astrocyte crosstalk and gut-brain axis. *Aging Dis*. 2024;15(5):2168-2190.

doi: 10.14336/AD.2024.0134

124. Xue C, Li G, Zheng Q, *et al*. Tryptophan metabolism in health and disease. *Cell Metab*. 2023;35(8):1304-1326.

doi: 10.1016/j.cmet.2023.06.004

125. Ojo ES, Tischkau SA. The role of AhR in the hallmarks of brain aging: Friend and foe. *Cells*. 2021;10(10):2729.

doi: 10.3390/cells10102729

126. Wang Z, Snyder M, Kenison JE, *et al*. How the AhR became important in cancer: The role of chronically active AhR in cancer aggression. *Int J Mol Sci*. 2020;22(1):387.

doi: 10.3390/ijms22010387

127. Zhu K, Meng Q, Zhang Z, *et al*. Aryl hydrocarbon receptor pathway: Role, regulation and intervention in atherosclerosis therapy (Review). *Mol Med Rep*. 2019;20(6):4763-4773.

doi: 10.3892/mmr.2019.10748

128. Zeng X, Feng M, Lu J, *et al*. Beyond transcription, aryl hydrocarbon receptor plays a protective role in periodontitis by interacting with CaMKII. *J Periodontol*. 2024.

doi: 10.1002/JPER.24-0021

129. Meissner WG, Remy P, Giordana C, *et al*. Trial of lixisenatide in early Parkinson's disease. *N Engl J Med*. 2024;390(13):1176-1185.

doi: 10.1056/NEJMoa2312323

130. Edison P. *GLP-1 Drug Liraglutide May Protect Against Dementia*. Philadelphia: Alzheimer's Association International Conference® (AAIC®); 2024, Available from: https://aaic.alz.org/downloads2024/aaic-2024-glp-1-ph2-trial.pdf [Last accessed on 2024 Dec 09].

131. Wang L, Xu R, Kaelber DC, Berger NA. Glucagon-like peptide 1 receptor agonists and 13 obesity-associated cancers in patients with type 2 diabetes. *JAMA Netw Open*. 2024;7(7):e2421305.

doi: 10.1001/jamanetworkopen.2024.21305

132. Kherad Z, Yazdanpanah S, Saadat F, Pakshir K, Zomorodian K. Vitamin D3: A promising antifungal and antibiofilm agent against *Candida* species. C*urr Med Mycol*. 2023;9(2):17-22.

doi: 10.18502/cmm.2023.345062.1416

133. Lei J, Xiao W, Zhang J, *et al*. Antifungal activity of vitamin D_3 against *Candida albicans in vitro* and *in vivo*. *Microbiol Res*. 2022;265:127200.

doi: 10.1016/j.micres.2022.127200

134. Zhang Y, Yan R, Zhou Q. ACE2, B0AT1, and SARS-CoV-2 spike protein: Structural and functional implications. *Curr Opin Struct Biol*. 2022;74:102388.

doi: 10.1016/j.sbi.2022.102388

135. Essex M, Millet Pascual-Leone B, Löber U, *et al*. Gut microbiota dysbiosis is associated with altered tryptophan metabolism and dysregulated inflammatory response in COVID-19. *NPJ Biofilms Microbiomes*. 2024;10:66.

doi: 10.1038/s41522-024-00538-0

136. Centers for Disease Control and Prevention. *MTHFR Gene Variant and Folic Acid Facts*. Available from: https://www.cdc.gov/folic-acid/data-research/mthfr/index.html [Last accessed on 2024 Dec 09].

137. Barak AJ, Beckenhauer HC, Tuma DJ. Methionine synthase. A possible prime site of the ethanolic lesion in liver. *Alcohol*. 2002;26(2):65-67.

doi: 10.1016/s0741-8329(01)00201-4

138. Ponti G, Pastorino L, Manfredini M, *et al*. COVID-19 spreading across world correlates with C677T allele of the methylenetetrahydrofolate reductase (MTHFR) gene prevalence. *J Clin Lab Anal*. 2021;35(7):e23798.

doi: 10.1002/jcla.23798

139. Meng LH, Awakawa T, Li XM, *et al*. Discovery of (±)-penindolenes reveals an unusual indole ring cleavage pathway catalyzed by P450 monooxygenase. *Angew Chem Int Ed Engl*. 2024;63(26):e202403963.

doi: 10.1002/anie.202403963

140. Mansmann HC Jr. Consider magnesium homeostasis: III: Cytochrome P450 enzymes and drug toxicity. *Appl Immunohistochem Mol Morphol*. 1994;8:7-28.

doi: 10.1089/pai.1994.8.7

141. Kong F, Wang J, Han R, *et al*. Antifungal activity of magnesium oxide nanoparticles: Effect on the growth and key virulence factors of *Candida albicans*. *Mycopathologia*. 2020;185:485-494.

doi: 10.1007/s11046-020-00446-9

142. Ashique S, Kumar S, Hussain A, *et al*. A narrative review on the role of magnesium in immune regulation, inflammation, infectious diseases, and cancer. *J Health Popul Nutr*. 2023;42(1):74.

doi: 10.1186/s41043-023-00423-0

143. Yang Z, Zhang Y, Gao J, Yang Q, Qu H, Shi J. Association between dietary magnesium and 10-year risk of a first hard atherosclerotic cardiovascular disease event. *Am J Med Sci*. 2024;68(4):355-360.

doi: 10.1016/j.amjms.2024.05.014

144. Rosanoff A, Dai Q, Shapses SA. Essential nutrient interactions: Does low or suboptimal magnesium status interact with vitamin D and/or calcium status? *Adv Nutr*. 2016;7(1):25-43.

doi: 10.3945/an.115.008631

145. Du K, Zheng X, Ma ZT, Lv JY, Jiang WJ, Liu MY. Association of circulating magnesium levels in patients with Alzheimer's disease from 1991 to 2021: A systematic review and meta-analysis. *Front Aging Neurosci*. 2022;13:799824.

doi: 10.3389/fnagi.2021.799824

146. Chen F, Wang J, Cheng Y, *et al*. Magnesium and cognitive health in adults: A systematic review and meta-analysis. *Adv Nutr*. 2024;15:100272.

doi: 10.1016/j.advnut.2024.100272

147. Garnaud C, Champleboux M, Maubon D, Cornet M, Govin J. Histone deacetylases and their inhibition in *Candida* species. *Front Microbiol*. 2016;7:1238.

doi: 10.3389/fmicb.2016.01238

148. Singh V, Lee G, Son H, *et al*. Butyrate producers, "The Sentinel of Gut": Their intestinal significance with and beyond butyrate, and prospective use as microbial therapeutics. *Front Microbiol*. 2023;13:1103836.

doi: 10.3389/fmicb.2022.1103836

149. Patman G. Gut microbiota: *Lactobacillus acidophilus* opens the door to butyrate. *Nat Rev Gastroenterol Hepatol*. 2015;12:552.

doi: 10.1038/nrgastro.2015.153

150. Spacova I, Allonsius CN, De Boeck I, *et al*. Multifactorial inhibition of *Candida albicans* by combinations of lactobacilli and probiotic *Saccharomyces cerevisiae* CNCM I-3856. *Sci Rep*. 2024;14:9365.

doi: 10.1038/s41598-024-59869-9

151. Davie JR. Inhibition of histone deacetylase activity by butyrate. *J Nutr*. 2003;133(7 Suppl):2485S-2493S.

doi: 10.1093/jn/133.7.2485S

152. Simonetti G, Passariello C, Rotili D, Mai A, Garaci E, Palamara AT. Histone deacetylase inhibitors may reduce pathogenicity and virulence in *Candida albicans*. *FEMS Yeast Res*. 2007;7(8):1371-1380.

doi: 10.1111/j.1567-1364.2007.00276.x

153. Yang C, Li G, Zhang Q, *et al*. Histone deacetylase Sir2 promotes the systemic *Candida albicans* infection by facilitating its immune escape via remodeling the cell wall and maintaining the metabolic activity. *mBio*. 2024;15:e00445.

doi: 10.1128/mbio.00445-24

154. Sanaei M, Kavoosi F. Histone deacetylases and histone deacetylase inhibitors: Molecular mechanisms of action in various cancers. *Adv Biomed Res*. 2019;8:63.

doi: 10.4103/abr.abr_142_19

155. Xu K, Dai XL, Huang HC, Jiang ZF. Targeting HDACs: A promising therapy for Alzheimer's disease. *Oxid Med Cell Longev*. 2011;2011:143269.

doi: 10.1155/2011/143269

156. Liaw A, Liu C, Bartold M, Ivanovski S, Han P. Salivary histone deacetylase in periodontal disease: A cross-sectional pilot study. *J Periodontal Res*. 2023;58(2):433-443.

doi: 10.1111/jre.13104

157. Jane Tseng C, McDougle CJ, Hooker JM, Zürcher NR. Epigenetics of autism spectrum disorder: Histone deacetylases. *Biol Psychiatry*. 2021;91:922-933.

doi: 10.1016/j.biopsych.2021.11.021

158. Siddiqui MT, Cresci GAM. The immunomodulatory functions of butyrate. *J Inflamm Res*. 2021;14:6025-6041.

doi: 10.2147/JIR.S300989

159. Ivashkiv LB. IFNγ: Signalling, epigenetics and roles in immunity, metabolism, disease and cancer immunotherapy. *Nat Rev Immunol*. 2018;18:545-558.

doi: 10.1038/s41577-018-0029-z

160. Liu S, Ren J, Ten Dijke P. Targeting TGFβ signal transduction for cancer therapy. *Sig Transduct Target Ther*. 2021;6:8.

doi: 10.1038/s41392-020-00436-9

161. Ku S, Haque MA, Jang MJ, *et al*. The role of *Bifidobacterium* in longevity and the future of probiotics. *Food Sci Biotechnol*. 2024;33:2097-2110.

doi: 10.1007/s10068-024-01631-y

162. Badal VD, Vaccariello ED, Murray ER, *et al*. The gut microbiome, aging, and longevity: A systematic review. *Nutrients*. 2020;12(12):3759.

doi: 10.3390/nu12123759

163. Yu R, Cao X, Sun L, *et al*. Inactivating histone deacetylase HDA promotes longevity by mobilizing trehalose metabolism. *Nat Commun*. 2021;12:1981.

doi: 10.1038/s41467-021-22257-2

164. Seitz HK, Stickel F. Acetaldehyde as an underestimated risk factor for cancer development: Role of genetics in ethanol metabolism. *Genes Nutr*. 2010;5(2):121-128.

doi: 10.1007/s12263-009-0154-1

165. Rehm J, Hasan OSM, Black SE, Shield KD, Schwarzinger M. Alcohol use and dementia: A systematic scoping review. *Alzheimers Res Ther*. 2019;11(1):1.

doi: 10.1186/s13195-018-0453-0

166. Gibson A, Woodside JV, Young IS, *et al*. Alcohol increases homocysteine and reduces B vitamin concentration in healthy male volunteers--a randomized, crossover intervention study. *QJM*. 2008;101(11):881-887.

doi: 10.1093/qjmed/hcn112

167. Hasan T, Arora R, Bansal AK, *et al*. Disturbed homocysteine metabolism is associated with cancer. *Exp Mol Med*. 2019;51:1-13.

doi: 10.1038/s12276-019-0216-4

168. Smith AD, Refsum H, Bottiglieri T, *et al*. Homocysteine and dementia: An international consensus statement. *J Alzheimers Dis*. 2018;62(2):561-570.

doi: 10.3233/JAD-171042

169. Hu X, Wang JB, Zhao Y, *et al*. Homocysteine as a trigger and potential therapeutic target for autoimmune diseases. *Autoimmun Rev*. 2023;22(9):103389.

doi: 10.1016/j.autrev.2023.103389

170. Peng J, Wu Z. MTHFR act as a potential cancer biomarker in immune checkpoints blockades, heterogeneity, tumor microenvironment and immune infiltration. *Discov Oncol*. 2023;14(1):112.

doi: 10.1007/s12672-023-00716-0

171. Reagan AM, Christensen KE, Haber A, *et al*. A common risk variant in the MTHFR gene contributes to age-related cerebrovascular dysfunction in VCID. *Alzheimers Dement*. 2020;16:e038657.

doi: 10.1002/alz.038657

172. Rodrigues RR, Gurung M, Li Z, *et al*. Transkingdom interactions between Lactobacilli and hepatic mitochondria attenuate western diet-induced diabetes. *Nat Commun*. 2021;12:101.

doi: 10.1038/s41467-020-20313-x

173. Li M, Chi X, Wang Y, Setrerrahmane S, Xie W, Xu H. Trends in insulin resistance: Insights into mechanisms and therapeutic strategy. *Sig Transduct Target Ther*. 2022;7:216.

doi: 10.1038/s41392-022-01073-0

174. Sohail MU, Yassine HM, Sohail A, Thani AAA. Impact of physical exercise on gut microbiome, inflammation, and the pathobiology of metabolic disorders. *Rev Diabet Stud*. 2019;15:35-48.

doi: 10.1900/RDS.2019.15.35

175. Hu D, Liu J, Yu W, *et al*. Tryptophan intake, not always the more the better. *Front Nutr*. 2023;10:1140054.

doi: 10.3389/fnut.2023.1140054

176. Nikolic DM, Dimitrijevic-Sreckovic V, Ranin LT, *et al*. Homeostatic microbiome disruption as a cause of insulin secretion disorders. *Candida albicans*, a new factor in pathogenesis of diabetes: A STROBE compliant cross-sectional study. *Medicine* (*Baltimore*). 2022;101(45):e31291.

doi: 10.1097/MD.0000000000031291

177. Vazquez-Munoz R, Dongari-Bagtzoglou A. Anticandidal activities by *Lactobacillus* Species: An update on mechanisms of action. *Front Oral Health*. 2021;2:689382.

doi: 10.3389/froh.2021.689382

178. Rastogi S, Singh A. Gut microbiome and human health: Exploring how the probiotic genus *Lactobacillus* modulate immune responses. *Front Pharmacol*. 2022;13:1042189.

doi: 10.3389/fphar.2022.1042189

179. Korkmaz H, Sirin FB, Torus B. Could there be a role of serum zonulin increase in the development of hypercalcemia in primary hyperparathyroidism. *Endocrine*. 2021;72:234-238.

doi: 10.1007/s12020-020-02504-0

180. Lischka J, Schanzer A, Baumgartner M, de Gier C, Greber-Platzer S, Zeyda M. Tryptophan metabolism is associated with bmi and adipose tissue mass and linked to metabolic

disease in pediatric obesity. *Nutrients*. 2022;14(2):286.

doi: 10.3390/nu14020286

181. Cussotto S, Delgado I, Anesi A, *et al*. Tryptophan metabolic pathways are altered in obesity and are associated with systemic inflammation. *Front Immunol*. 2020;11:557.

doi: 10.3389/fimmu.2020.00557

182. Mailing LJ, Allen JM, Buford TW, Fields CJ, Woods JA. Exercise and the Gut microbiome: A review of the evidence, potential mechanisms, and implications for human health. *Exerc Sport Sci Rev*. 2019;47(2):75-85.

doi: 10.1249/JES.0000000000000183

183. Rogiers O, Frising UC, Kucharíková S, *et al*. Candidalysin crucially contributes to Nlrp3 inflammasome activation by *Candida albicans* hyphae. *mBio*. 2019;10(1):e02221-18.

doi: 10.1128/mBio.02221-18

184. Gouasmi R, Ferraro-Peyret C, Nancey S, *et al*. The kynurenine pathway and cancer: Why keep it simple when you can make it complicated. *Cancers* (*Basel*). 2022;14(11):2793.

doi: 10.3390/cancers14112793

185. Fernandes BS, Inam ME, Enduru N, Quevedo J, Zhao Z. The kynurenine pathway in Alzheimer's disease: A meta-analysis of central and peripheral levels. *Braz J Psychiatry*. 2023;45(3):286-297.

doi: 10.47626/1516-4446-2022-2962

186. Pallotta MT, Rossini S, Suvieri C, *et al*. Indoleamine 2,3-dioxygenase 1 (IDO1): An up-to-date overview of an eclectic immunoregulatory enzyme. *FEBS J*. 2022;289(20):6099-6118.

doi: 10.1111/febs.16086

187. Aburto MR, Cryan JF. Gastrointestinal and brain barriers: Unlocking gates of communication across the microbiota-gut-brain axis. *Nat Rev Gastroenterol Hepatol*. 2024;21:222-247.

doi: 10.1038/s41575-023-00890-0

ACCSCIENCE PUBLISHING

Microbes & Immunity

CASE REPORT

Migraine-like headache due to frontal osteitis and meningitis in a delayed diagnosis of SAPHO syndrome: A case report and literature review

João Moura[1,2]*, Raquel Faria[2,3,4], and Ernestina Santos[1,2,3,4]

[1]Department of Neurology, Hospital de Santo António, Centro Hospitalar Universitário de Santo António, Porto, Portugal

[2]Unit of Multidisciplinary Research in Biomedicine, Instituto de Ciências Biomédicas Abel Salazar, University of Porto, Porto, Portugal

[3]Clinical Immunology Unit, Hospital de Santo António, Centro Hospitalar Universitário de Santo António, Porto, Portugal

[4]Laboratory for Integrative and Translational Research in Population Health, University of Porto, Porto, Portugal

Abstract

Synovitis, acne, pustulosis, hyperostosis, and osteomyelitis (SAPHO) syndrome is a rare polygenic autoinflammatory disorder that is associated with headaches of different etiological origins. Herein we report the case of a patient with SAPHO syndrome and provide a literature review. The patient was a 64-year-old female who complained of a recurrent headache, which had persisted for several years, and diffuse arthralgias. A computed tomography-angiogram demonstrated the narrowing of the left carotid canal. The patient had an erythrocyte sedimentation rate of 19 mm/s, and her cerebrospinal fluid contained 20 leukocytes/μL (13 mononuclear) and 0.43 g/L of proteins. Bone scintigraphy showed radiotracer uptake in the frontal bones and spine. The patient's son had previously been diagnosed with SAPHO syndrome; therefore, the possibility of a disorder in the same spectrum was considered. Corticotherapy followed by sulphasalazine resolved the symptoms. This case illustrates an atypical cranial and meningeal involvement of the SAPHO autoinflammatory process. Our findings underscore the importance of considering immune-mediated disorders in the differential diagnosis of headaches.

Keywords: Migraine; Headache; Frontal osteitis; SAPHO syndrome; Autoinflammatory syndrome

***Corresponding author:**
João Moura
(moura.neuro@chporto.min-saude.pt)

Citation: Moura J, Faria R, Santos E. Migraine-like headache due to frontal osteitis and meningitis in a delayed diagnosis of SAPHO syndrome: A case report and literature review. *Microbes & Immunity*. 2025;2(3):162-167. doi: 10.36922/mi.4667

Received: August 27, 2024

Revised: September 12, 2024

Accepted: October 18, 2024

Published online: November 28, 2024

1. Background

The distinction between primary and secondary headache disorders is pivotal in clinical practice. Several immune-mediated diseases occur with headache, particularly migraine.[1] Synovitis, acne, pustulosis, hyperostosis, and osteomyelitis (SAPHO) syndrome is a polygenic autoinflammatory disorder associated with conditions involving the central nervous system, including headache.[2]

This report presents the case of a patient with SAPHO syndrome, featuring headache as the predominant clinical feature, highlighting the multifaceted nature of headache

etiology. Besides, we review the existing evidence in the literature to corroborate this association.

2. Case presentation

A 64-year-old female presented to the neurology outpatient clinic in 2016 with complaints of headaches. She described a heavyweight sensation on the left hemicrania associated with periods of intense, sharp, frontal pain that sometimes lasted for days, often interrupting sleep. She had suffered from headaches during adolescence. Over-the-counter anti-inflammatory drugs were seldom effective in relieving her symptoms. Her past medical history showed epidermoid papilloma of the tongue, which was removed in 2014. Further inquiry of her past medical history revealed inflammatory polyarthralgia occurring in her hands, wrists, sternum, and lumbar spine. She also reported occasional vesicles appearing in the lower back.

The neurological examination was unremarkable, except for the discovery of allodynia in the left hemicrania. The patient reported no pain on the superficial temporal arteries. A computed tomography (CT)-angiogram (Figure 1) demonstrated absent filling in the left internal carotid artery with a small carotid canal opening giving rise to a narrow left internal carotid artery (shaped like a pencil tip) that was more distally occluded. The posterior and anterior communicating arteries granted collateral flow to its supraclinoid segment. Her erythrocyte sedimentation rate was 19 mm/s (normal level) and there were no other anomalies in the blood panel findings, including levels of autoantibodies. An attempt to control symptoms with escitalopram, amitriptyline, and alprazolam was found to be ineffective.

Over the years, the headache attacks have become more frequent and severe. In 2018, she reported daily severe and throbbing frontal headaches, which generally lasted several hours and impacted the left eye, with associated tearing and redness, a condition refractory to acetaminophen (1 gr tid) and prophylactic propranolol (80 mg/day). During the examination, there was intense allodynia in the left hemicrania. Given the atypical features of migraine and accompanying symptoms, a lumbar puncture was performed to obtain cerebrospinal fluid for analysis, which revealed 20 leukocytes/μL (13 mononuclear, normal: <5/μL), 44 erythrocytes/μL, 0.52 g/L glucose (normal: <0.45 g/L), and 0.43 g/L proteins (normal: <0.5 g/L). No oligoclonal bands were present. Results from brain CT and magnetic resonance imaging (MRI) were unremarkable (Figure 2). The patient refused to undergo a temporal artery biopsy. Bone scintigraphy with ^{99}mTC (Figure 3) showed slight hyperactivity in the frontal bones and peripheral joints, including the sternoclavicular and sacroiliac joints.

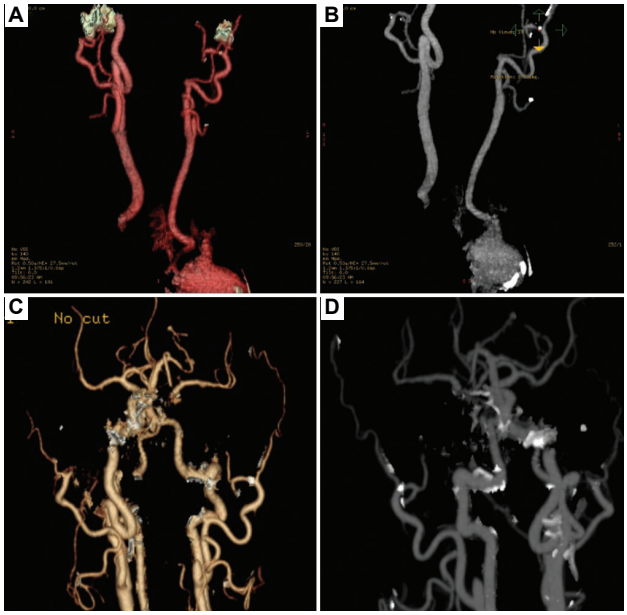

Figure 1. (A and B) Computed tomography-angiogram shows interruption in the C4–C5 segments of the left internal carotid artery, after the carotid bulb, featuring a "pencil-tip pattern." The left carotid canal is considerably narrower compared to the right one, due to hyperostosis of the walls. (C and D) Overall, the images suggest a hypoplasic and eventually dissected left internal carotid artery. The posterior and anterior communicating arteries granted collateral flow to its supraclinoid segment.

Classical X-ray showed cervical and dorsal syndesmophytes and calcified ischiatic and calcanean enthesitis. Human leukocyte antigen (HLA) analysis showed that the patient does not harbor a risk allele for spondyloarthopaties.

The patient's 45-year-old son developed sternocostoclavicular inflammatory hyperostosis in his forties, followed by palmo-plantar pustulosis and cystic acne. He had no history of headaches. His scintigraphy showed radiotracer uptake in the sternum and pubic symphysis. He was diagnosed with SAPHO syndrome and was on a treatment of interleukin-17 inhibitors, at the time of writing this report, which resulted in a favorable clinical outcome. Whole exome sequencing using a 34-gene panel for autoinflammatory diseases failed to detect any pathogenic variants.

The possibility that our patient also had SAPHO syndrome was considered. A trial of prednisolone 10 mg daily for 1 month led to an improvement of all the patient's symptoms, with almost complete resolution of the headache, and it promptly recurred when she stopped taking the medicine. Sulphasalazine and etoricoxib were initially enough to control the symptoms, but she further needed escalation to adalimumab 40 mg every other week, with almost complete remission.

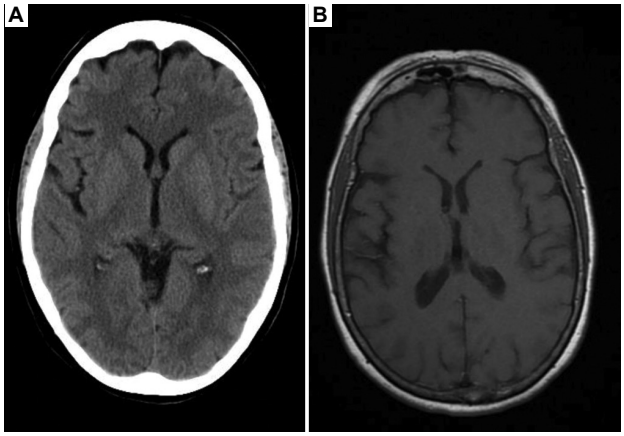

Figure 2. Brain (A) computer tomography and (B) magnetic resonance imaging in the axial plane with normal findings in the brain parenchyma, meninges, and bone.

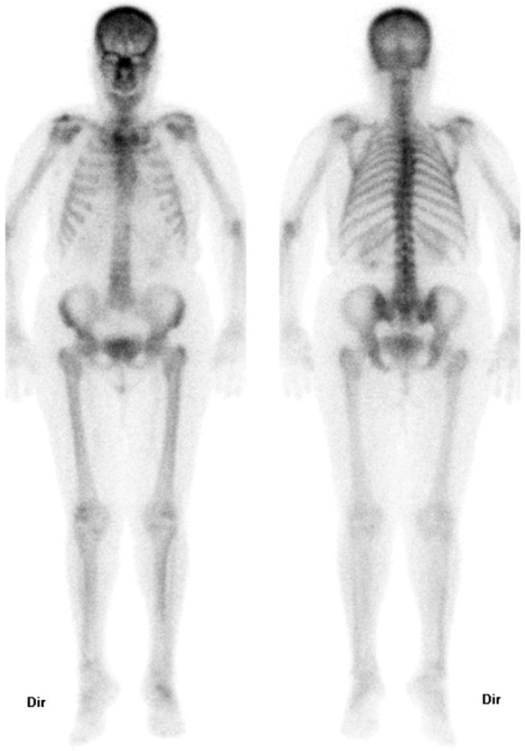

Figure 3. Technetium-99m-hydroxymethylene diphosphonate scintigram shows diffuse uptake in the frontal bones (left panel) and cervical/dorsal syndesmophytes (right panel).

3. Discussion

The current case revolves around a patient with a headache, which features an initial tension-type headache, followed by a migraine-like pattern. The advanced age of onset, inconsistent phenotype, and lack of response to several drugs prompted searching for a secondary cause. Besides the headache, this patient complained of inflammatory arthralgias affecting both axial and peripheral joints, consistent with the characteristics of spondyloarthropathy, further corroborating the possibility of an underlying systemic immune-mediated disorder. This possibility was brought to our attention by the fact that her son had been diagnosed with SAPHO syndrome.[3] In our patient, a psoriatic spondyloarthropathy diagnosis was also considered; however, findings of the cranial and sternum osteitis categorized it as SAPHO syndrome end of the spectrum, added by the fact of concurrent SAPHO syndrome diagnosis on her son.

SAPHO syndrome is classically characterized by a variety of osteoarticular disorders – synovitis, osteitis, hyperostosis, enthesitis – associated with acne or pustulosis (large fluid-filled blister-like areas). The diagnosis of SAPHO syndrome was conducted according to the diagnostic criteria proposed by Benhamou *et al.*:[4] (i) osteoarticular manifestations in severe acne; (ii) osteoarticular manifestations in palmoplantar pustulosis; (iii) hyperostosis with or without dermatosis; and (iv) recurrent multifocal chronic osteomyelitis involving the axial or peripheral skeleton, with or without dermatosis. However, the diagnosis of this entity remains controversial due to variability in clinical presentations.[5,6] Reports of patients with an incomplete constellation of the syndrome reflect these issues.[7,8] The most well-described neurological involvements in SAPHO syndrome occur in the form of hypertrophic pachymeningitis and/or headache, and, less commonly, aseptic meningitis.[9] Spinal lesions in the form of spondylodiscitis are also common but rarely lead to spinal compression.[9]

Familial clustering of SAPHO syndrome-like phenotypes has been previously acknowledged.[10] Familial transmission is associated with an autosomal-dominant neutrophil disorder characterized by impairment of internal oxidant production.[11] More recently, a study using array comparative genomic hybridization in a family comprising two SAPHO syndrome cases (mother and daughter) unveiled copy number variation in four genes (*CSF2RA*, *NOD2*, *MEGF6*, and *ADAM5*) that were validated in 360 case and control samples, establishing convincing evidence for a genetic component in this autoinflammatory disorder.[12]

In the literature, the occurrence of headaches with relation to skull vault involvement in SAPHO syndrome has been reported.[2,13-16] Some of these cases are summarized in Table 1. The headache is considered to be bone-related, even in cases with associated hypertrophic pachymeningitis, which may also occur in SAPHO syndrome.[17] The headache is typically unilateral, recurrent, and with prominent hypersensitivity of the overlying

Table 1. Clinical and imaging features of previously reported cases of SAPHO syndrome associated with headache

Case report	Headache type (age at presentation)	Associated symptoms	CSF composition	Radiotracer accumulation in bone scintigraphy	Gadolinium-enhancing lesions in MRI	Treatment	Response
DiMeco *et al.* (2000)[14]	Recurrent incapacitating headaches (34)	Allodynia, swelling	Normal	First left rib	Left parietal bone, extending to the scalp	Surgery	Moderate
Hiwatani *et al.* (2008)[15]	Severe headache (52)	Fever	Mild pleocytosis (101/mm^3, 98% lymphocytes, 2% polymorphs), slightly high protein (52 mg/dL)	Sternoclavicular joints	No	Meloxicam 10 mg daily	Complete
Uematsu *et al.* (2012)[16]	Chronic severe left temporal headache (50)	Allodynia	-	Left parietal bone, left sterno-costo-clavicular joint, right femoral head, and intervertebral joints	Left temporal muscle, left parietal bone, and dura mater	Intravenous methylprednisolone, methotrexate	Moderate
Tsugawa *et al.* (2014)[2]	Recurrent right frontal headache (57)	Allodynia, swelling	Normal	Right bone, temporal, sternum, and left medial clavicula	Frontotemporal muscle/fascia	Prednisolone 15 mg daily	Complete
Shiraishi *et al.* (2014)[17]	Severe forehead headache (40)	Swelling, fever	Normal	Frontoparietal bones, sternocostoclavicular joint and sternum	Right frontoparietal bone marrow and dura mater	Intravenous methylprednisolone, prednisolone 15 mg daily	Moderate
Present case	Recurrent left hemicrania headache (adolescence)	Arthralgias	20 leukocytes/μL, 44 erythrocytes/μL, 0.52 g/L glucose 0.43 g/L proteins	Frontal bones and peripheral joints, including the sternoclavicular and sacroiliac	No	Sulphasalazine and etoricoxib	Almost complete

Abbreviations: SAPHO: Synovitis, acne, pustulosis, hyperostosis, and osteomyelitis, CSF: Cerebrospinal fluid; MRI: Magnetic resonance imaging.

skin,[2] which is also present in this patient. The MRI typically shows a pattern of T1 gadolinium enhancement in the involved tissues and bone (Table 1), which was not demonstrated in this patient where no contrast agent was administered in the routine MRI initially ordered.[18] Considering the inflammatory cerebrospinal fluid, another possibility is aseptic meningitis, a condition also associated with SAPHO syndrome.[15] The absence of focal bone or tissue lesions in the MRI and bone scintigraphy could lend credence to this possibility. Despite the considerably long history of headaches in this patient, recurrent aseptic meningitis would have been associated with underlying inflammatory syndromes.[19] Bone scintigraphy typically shows areas of focal hyperactivity in the affected bone, but a pattern of diffuse enhancement on the frontal and temporal bones has previously been reported.[17]

The finding of a stenotic internal carotid artery due to the narrowing of the carotid canal opening on the skull base could potentially be explained by hyperostosis of the carotid canal. Narrowing of the proximal segments of the internal carotid artery has been previously reported in SAPHO syndrome cases.[20] The vascular narrowing is probably caused by focal hypertrophic pachymeningitis due to osteitis of the skull bone, potentially resulting in brain infarction[12] or even moyamoya disease.[21] While no signs of an active inflammatory process in the adjacent bone were present in brain imaging, we cannot preclude the possibility that this process had already occurred in the past, leading to the formation of stenotic vessels. The other possibility is that the internal carotid artery is constitutionally hypoplasic. Of note, hyperostosis in other segments (cervical) may lead to neurovascular lesions due to cervical spine compression.[22,23]

In agreement with the existing literature, our patient also showed an improvement of headache in response to immunosuppression (not only steroids but also sulphasalazine and adalimumab).[2]

We recognize that evident signs of osteomyelitis and pustulosis, core features of SAPHO syndrome, were lacking in this patient. However, the presence of focal hyperostosis accompanied by a predominantly axial arthropathy corroborates the diagnosis of SAPHO syndrome. Likewise, the occasional vesicles reported by the patient could correspond to acne and be associated with the syndrome, although no overt signs of palmoplantar pustulosis were present. Response to prednisolone, sulphasalazine, and

adalimumab further supports the possibility of a headache secondary to a systemic inflammatory process associated with the spectrum of SAPHO syndrome.

4. Conclusion

The current case report presents an atypical intracranial involvement tied to the inflammatory process inherent in SAPHO syndrome through a well documentation of the syndrome's distinctive imaging and analytical features. These findings underscore the importance of considering systemic inflammatory disorders in the differential diagnosis of headaches.

Acknowledgments

None.

Funding

None.

Conflict of interest

E. Santos is on the advisory board for Biogen, Genzyme, Bayer, Merck, Alexion, and Novartis, and has received a grant from Roche. The authors certify that there is no conflict of interest regarding the publication of this paper.

Author contributions

Conceptualization: All authors
Investigation: All authors
Methodology: All authors
Writing – original draft: João Moura
Writing – review & editing: All authors

Ethical approval and consent to participate

No ethical approval was required. Informed consent was taken from the patient before participation.

Consent for publication

Written informed consent for publishing was obtained by the patient.

Availability of data

Not applicable.

References

1. Biscetti L, Vanna DG, Cresta E, *et al.* Headache and immunological/autoimmune disorders: A comprehensive review of available epidemiological evidence with insights on potential underlying mechanisms. *J Neuroinflamm*. 2021;18:259.

   doi: 10.1186/s12974-021-02229-5

2. Tsugawa J, Ouma S, Fukae J, Tsuboi Y. Recurrent unilateral headache associated with SAPHO syndrome. *Intern Med*. 2014;53:1559-1562.

   doi: 10.2169/internalmedicine.53.2150

3. Dihlmann W, Dihlmann WS, Hering L. Acquired hyperostosis syndrome - AHYS - (sternocostoclavicular hyperostosis, pustulotic arthro-osteitis, SAPHO-syndrome): Bone scintigraphy of the anterior chest wall. *Clin Rheumatol.* 1997;16:13-24.

   doi: 10.1007/BF02238758

4. Benhamou CL, Enjolras O, Delrieu F, Prier A, Camus JP, Amor B. Pseudoseptic arthritis and bacterid of Andrews. *Rev Rhum Mal Osteoartic*. 1984;51:229-231.

5. Furer V, Kishimoto M, Tsuji S, *et al*. The diagnosis and treatment of adult patients with SAPHO syndrome: Controversies revealed in a multidisciplinary international survey of physicians. *Rheumatol Ther*. 2020;7:883-891.

   doi: 10.1007/s40744-020-00235-2

6. Yildirim DT, Sari İ. SAPHO syndrome: Current clinical, diagnostic and treatment approaches. *Rheumatol Int*. 2023;44:2301-2313.

   doi: 10.1007/s00296-023-05491-3

7. Dantas RLF, Dantas F, Mourão GDNTR, Mattos CB, Fonseca DTKV. Synovitis, acne, pustulosis, hyperostosis, osteitis (SAPHO) syndrome mimicking bone metastases in the spine: A presentation of two cases and literature review. *Cureus*. 2024;16:e64974.

   doi: 10.7759/cureus.64974

8. Duan N, Chen X, Liu Y, Wang J, Wang Z. Multimodal imaging findings of SAPHO syndrome with no skin lesions: A report of three cases and review of the literature. *Exp Ther Med*. 2016;12:2665-2670.

   doi: 10.3892/etm.2016.3689

9. Diprose KW, Jordan A, Anderson EN. Autoinflammatory syndromes in neurology: When our first line of defence misbehaves. *Pract Neurol*. 2022;22:145-153.

   doi: 10.1136/practneurol-2021-003031

10. Castillo DFJ, Caniego T, Hurtado-Nédélec M, *et al*. THU0466 unraveling the genetic basis of familial SAPHO syndrome with next-generation sequencing. *Ann Rheum Dis*. 2014;73:344.

11. Ferguson JP, Lokuta AM, El-Shanti IH, Muhle L, Bing X, Huttenlocher A. Neutrophil dysfunction in a family with a SAPHO syndrome-like phenotype. *Arthritis Rheum*. 2008;58:3264-3269.

    doi: 10.1002/art.23942

12. Guo C, Tian X, Han F, Liu L, Gao J, Ma X. Copy number variation of multiple genes in SAPHO syndrome. *J Rheumatol*. 2020;47:1323-1329.

doi: 10.3899/jrheum.181393

13. Seno A, Arata J, Matsuura Y, Suemitsu I. Palmoplantar pustulosis with pustulotic arthroosteitis involving temporal osteomyelitis and meningitis. *J Dermatol*. 2000;27:269-272.

    doi: 10.1111/j.1346-8138.2000.tb02163.x

14. Dimeco F, Clatterbuck ER, Li WK, Mccarthy FE, Olivi A. Synovitis, acne, pustulosis, hyperostosis, and osteitis syndrome presenting as a primary calvarial lesion. *J Neurosurg*. 2000;93:693-697.

    doi: 10.3171/jns.2000.93.4.0693

15. Hiwatani Y, Miwa H, Kondo T. Aseptic meningitis as a rare manifestation of SAPHO syndrome. *Neurology*. 2008;71:1645-1647.

    doi: 10.1212/01.wnl.0000334758.75290.d0

16. Uematsu M, Tobisawa S, Nagao M, Matsubara S, Mizutani T, Shibuya M. Headache as a manifestation of SAPHO syndrome with a lesion extending to the dura mater, parietal bone, and temporal muscle. *Rinsho Shinkeigaku*. 2012;52:106-110.

    doi: 10.1016/j.jns.2014.12.020

17. Shiraishi W, Hayashi S, Iwanaga Y, Murai H, Yamamoto A, Kira JI. A case of synovitis, acne, pustulosis, hyperostosis, and osteitis (SAPHO) syndrome presenting with hypertrophic pachymeningitis. *J Neurol Sci*. 2015;349:229-231.

    doi: 10.1016/j.jns.2014.12.020

18. Chen S, Wu Y, Li C. Synovitis, acne, pustulosis, hyperostosis, and osteitis syndrome: Is radiological imaging adequate for the diagnosis? *Int J Rheum Dis*. 2024;27:e15028.

    doi: 10.1111/1756-185X.15028

19. Lee HD, Lee JS. Recurrent aseptic meningitis as an initial clinical presentation of primary Sjögren's syndrome. *J Neurocrit Care*. 2019;12:46-50.

    doi: 10.1016/j.jstrokecerebrovasdis.2020.105522

20. Yazawa Y, Itabashi R. Hypertrophic pachymeningitis related brain infarction in synovitis-acne-pustulosis-hyperostosis osteomyelitis syndrome. *J Stroke Cerebrovasc Dis*. 2021;30:105522.

    doi: 10.11477/mf.1436203545

21. Horie N, Baba M, Kawada K, *et al*. A case of moyamoya disease associated with SAPHO syndrome. *Neurol Surg*. 2017;45:533-539.

    doi: 10.1016/j.jbspin.2014.02.002

22. Sanges S, Ducoulombier V, Sivery B, Delhaye N, Haffner C, Houvenagel E. Thrombosis of the left subclavian vein complicating SAPHO syndrome: A case report. *Joint Bone Spine*. 2014;81:460-461.

    doi: 10.1111/1756-185X.15238

23. Shen D, Chen N, Dong X, *et al*. Case report: Complications of SAPHO syndrome: Thoracic outlet syndrome. Int J Rheum Dis. 2024;27:e15238.

    doi: 10.1111/1756-185X.15238

ACCSCIENCE PUBLISHING

Microbes & Immunity

COMMUNICATION

Establishment of a highly sensitive and specific anti-EphB2 monoclonal antibody (Eb_2Mab-12) for flow cytometry

Rena Ubukata, Hiroyuki Suzuki, Miu Hirose, Hiroyuki Satofuka, Tomohiro Tanaka, Mika K. Kaneko, and Yukinari Kato*

Department of Antibody Drug Development, Tohoku University Graduate School of Medicine, Sendai, Miyagi, Japan

Abstract

Ephrin type-B receptor 2 (EphB2) is a member of the Eph family tyrosine kinase receptors. EphB2 binds to ephrin-B1, ephrin-B2, and ephrin-B3, which are critical regulators of vascular and neural development, influencing cell migration and axon guidance. EphB2 is overexpressed in several tumors, including glioma, breast cancer, hepatocellular carcinoma, and malignant mesothelioma, where it functions as a tumor promoter. Therefore, the development of monoclonal antibodies (mAbs) targeting EphB2 is essential for the diagnosis and treatment of EphB2-positive tumors. In this study, we developed novel mAbs for human EphB2 using the Cell-Based Immunization and Screening method. Among the established anti-EphB2 mAbs, Eb_2Mab-12 (mouse IgG_1, kappa) showed reactivity toward EphB2-overexpressed Chinese hamster ovary-K1 cells (CHO/EphB2) and an endogenously EphB2-expressing cancer cell line (LS174T), as confirmed by flow cytometry. The dissociation constant (K_D) values of Eb_2Mab-12 for CHO/EphB2 and LS174T were determined to be 1.7×10^{-9} M and 4.4×10^{-10} M, respectively, using flow cytometry. Furthermore, Eb_2Mab-12 exhibited no cross-reactivity with other members of the EphA and EphB receptors. These results indicate that Eb_2Mab-12 possesses high affinity and specificity in detecting EphB2, suggesting its potential application in tumor therapy.

Keywords: EphB2; Monoclonal antibody; Cell-Based Immunization and Screening; Flow cytometry

***Corresponding author:**
Yukinari Kato
(yukinari.kato.e6@tohoku.ac.jp)

Citation: Ubukata R, Suzuki H, Hirose M, *et al.* Establishment of a highly sensitive and specific anti-EphB2 monoclonal antibody (Eb2Mab-12) for flow cytometry. *Microbes & Immunity.* 2025;2(3):168-177. doi: 10.36922/mi.5728

Received: October 30, 2024

1st revised: December 6, 2024

2nd revised: December 21, 2024

Accepted: January 3, 2025

Published online: January 16, 2025

1. Introduction

The mammalian ephrin and Eph system comprises eight cell surface ephrin ligands (five ephrin-As and three ephrin-Bs) and 14 receptor tyrosine kinases (nine EphA and five EphB receptors).[1-6] The interaction between Eph receptors and ephrins occurs through dimerization or oligomerization, which leads to the tyrosine phosphorylation of Eph receptor and ephrin-B.[7] The phosphorylated tyrosine recruits cytoplasmic effectors containing Src-homology 2 domains, phosphotyrosine-binding domains, and PDZ domains.[8] Consequently, the Eph receptor-ephrin complexes activate bidirectional signaling – forward signaling from the Eph receptors and reverse signaling from the ephrins – which is essential for intercellular communication among similar or different

cell types.[2,6,9] Through this bidirectional signaling, the Eph system regulates tissue development, homeostasis, and regeneration; dysregulation of this system is implicated in various diseases, including cancer.[3,4,10-21] Hence, monoclonal antibody (mAb)-based tumor therapies have been developed for certain Eph receptors.[10,22-29]

Dysregulation of the Eph system is observed in both tumor cells and tumor microenvironment.[19] The Eph system plays distinct roles in tumor development, functioning as both tumor promoters and suppressors depending on the cellular context.[19] Ephrin type-B receptor 2 (EphB2) is overexpressed in several tumors, such as glioblastoma,[30] breast cancer,[31] hepatocellular carcinoma,[32] and malignant mesothelioma,[21] correlating with poor clinical outcomes. In these tumors, EphB2 promotes migration and invasion through forward signaling.[33,34]

In contrast, the expression of EphB2 is downregulated in certain tumors, such as colorectal cancer.[35] In the intestinal epithelium, EphB receptors facilitate the proliferation of stem and progenitor cells.[36] Notably, intestinal epithelial cell migration is impaired in mice lacking EphB2 and EphB3. Without EphB signaling, there is approximately a 50% reduction in the number of proliferating cells.[36] Furthermore, EphB receptor expression is elevated in intestinal adenomas,[37] but functions as a tumor suppressor by inhibiting invasive growth. EphB signaling promotes adherens junction formation in colorectal cancer cells, thereby suppressing cancer progression by inhibiting invasive growth.[38] Loss of EphB2 expression occurs during the progression to carcinoma and initiation of invasive growth.[39]

To evaluate the expression of EphB2 and target EphB2-positive cancer cells, the development of mAbs against EphB2 is essential. Previous studies have developed anti-receptor tyrosine kinase mAbs against the human epidermal growth factor receptor (EGFR) (clone EMab-17),[40] HER2 (H_2Mab-19),[41] and HER3 (H_3Mab-17)[42] using the Cell-Based Immunization and Screening (CBIS) method. The CBIS method involves immunizing antigen-overexpressed cells followed by high-throughput hybridoma screening using flow cytometry. This study reports the development of the novel anti-EphB2 mAbs using the CBIS method.

2. Materials and methods

2.1. Antibodies

OptiBuild™ RB545 mouse anti-human EphB2 mAb (clone 2H9; mouse IgG_1, kappa) was purchased from BD Bioscience (USA). Alexa Fluor 488-conjugated anti-mouse IgG was purchased from Cell Signaling Technology, Inc. (USA).

2.2. Preparation of cell lines

LS174T (human colorectal cancer), LN229 (human glioblastoma), Chinese hamster ovary (CHO)-K1, and P3X63Ag8U.1 (P3U1) cell lines were obtained from the American Type Culture Collection (USA).

pCMV6-myc-DDK vector with EphB2 (Catalog No.: RC223882, Accession No.: NM_004442) was purchased from OriGene Technologies, Inc. (USA). The EphB2 plasmids were transfected into CHO-K1 and LN229 cells using a Neon transfection system (Thermo Fisher Scientific Inc., USA). Stable transfectants were established through cell sorting using the 2H9 conjugated with RB545 and a cell sorter (SH800; Sony Corp., Japan), followed by cultivation in a medium containing 0.5 mg/mL of G418 (Nacalai Tesque, Inc., Japan).

Other Eph receptor cDNAs, including EphA1 (Catalog No.: RC213689, Accession No.: NM_005232), EphA4 (Catalog No.: RC211230, Accession No.: NM_004438), EphA5 (Catalog No.: RC213206, Accession No.: NM_004439), EphA6 (Catalog No.: RC223510, Accession No.: NM_001080448), EphA7 (Catalog No.: RC226293, Accession No.: NM_004440), EphA8 (Catalog No.: RC220352, Accession No.: NM_020526), EphA10 (Catalog No.: RC218374, Accession No.: NM_001099439), EphB1 (Catalog No.: RC214301, Accession No.: NM_004441), and EphB6 (Catalog No.: RC229404, Accession No.: NM_004445), were purchased from OriGene Technologies, Inc. (USA). EphA2 (Catalog No.: HGY095959, Accession No.: NM_004431), EphA3 (Catalog No.: HGY053437, Accession No.: NM_005233), and EphB3 (Catalog No.: HGX039581, Accession No.: NM_004443) cDNAs were purchased from RIKEN DNA Bank (Japan).

EphA2 and EphB3 cDNAs were cloned into a pCAGzeo vector (FUJIFILM Wako Pure Chemical Corporation, Japan), EphB6 cDNA was cloned into a pCMV6 vector, EphA1 cDNA was cloned into a pCAGzeo-ssnPA vector, while EphA3, EphA4, EphA5, EphA6, EphA7, EphA8, EphA10, and EphB1 cDNAs were cloned into a pCAGzeo_ssnPA16 vector.

The plasmids were transfected into CHO-K1 cells and stable transfectants were established through staining with mAbs: an anti-EphA2 mAb (clone SHM16; BioLegend, USA), an anti-EphB3 mAb (clone 647354; R&D Systems Inc., USA), an anti-EphB6 mAb (clone T49-25; BioLegend, USA), and an anti-PA tag mAb (clone NZ-1 for EphA2, EphA3, EphA4, EphA5, EphA6, EphA7, EphA8, EphA10, and EphB1), followed by sorting using SH800. After sorting, the cells were cultivated in a medium containing 0.5 mg/mL of Zeocin (InvivoGen, USA) or 0.5 mg/mL of

G418. This process resulted in the establishment of the Eph receptors-overexpressed CHO-K1 (e.g., CHO/EphB2) clones. In addition, the CHO/PA16-EphB4 cell line had been previously established.[43]

CHO-K1 cells, Eph receptors-overexpressed CHO-K1 cells, and P3U1 cells were cultured in a Roswell Park Memorial Institute (RPMI)-1640 medium (Nacalai Tesque, Inc., Japan), supplemented with 10% heat-inactivated fetal bovine serum (FBS; Thermo Fisher Scientific Inc., USA), 100 units/mL of penicillin, 100 μg/mL of streptomycin, and 0.25 μg/mL of amphotericin B (Nacalai Tesque, Inc., Japan). LS174T, LN229, and EphB2-overexpressed LN229 (LN229/EphB2) cells were cultured in Dulbecco's Modified Eagle Medium (Nacalai Tesque, Inc., Japan), supplemented with 10% FBS, 100 units/mL of penicillin, 100 μg/mL streptomycin, and 0.25 μg/mL amphotericin B. All cells were grown in a humidified incubator at 37°C with an atmosphere of 5% CO_2 and 95% air.

2.3. Development of hybridomas

The animals were housed under specific pathogen-free conditions. All animal experiments were approved by the Animal Care and Use Committee of Tohoku University (Permit number: 2022MdA-001).

Two 5-week-old BALB/cAJcl mice were purchased from CLEA Japan (Japan) to develop mAbs against EphB2. The immunization protocol involved intraperitoneal administration of LN229/EphB2 (1×10^8 cells) mixed with 2% Alhydrogel adjuvant (InvivoGen, USA). This initial immunization was followed by 3 additional weekly injections (1×10^8 cells/mouse), culminating in a final booster intraperitoneal injection (1×10^8 cells/mouse) 2 days before harvesting spleen cells. The harvested spleen cells were subsequently fused with P3U1 cells using PEG1500 (Roche Diagnostics, USA). Hybridomas were cultured in the RPMI-1640 medium with 10% FBS, 5% BriClone (NICB, Ireland), 100 units/mL of penicillin, 100 μg/mL of streptomycin, and 0.25 μg/mL of amphotericin B. For hybridoma selection, hypoxanthine, aminopterin, and thymidine (Thermo Fisher Scientific Inc., USA) were added to the medium. The supernatants were subsequently screened using flow cytometry with CHO/EphB2 and CHO-K1 cells.

The cultured supernatant of Eb_2Mab hybridomas was then applied to 1 mL of Ab-Capcher (ProteNova, Japan). After washing with phosphate-buffered saline (PBS), the antibodies were eluted with an IgG elution buffer (Thermo Fisher Scientific Inc., USA). Finally, the eluates were concentrated, and the elution buffer was replaced with PBS using Amicon Ultra (Merck KGaA, Germany).

2.4. Flow cytometric analysis

Cells were harvested following brief exposure to 0.25% trypsin and 1 mM ethylenediaminetetraacetic acid (Nacalai Tesque, Inc., Japan). After trypsinization, the cells were washed with 0.1% bovine serum albumin in PBS (blocking buffer) and treated with 0.01, 0.1, 1, and 10 μg/mL of primary mAbs for 30 min at 4°C. Subsequently, the cells were treated with Alexa Fluor 488-conjugated anti-mouse IgG (1:2,000). In addition, the cells were suspended in 0.01, 0.1, 1, and 10 μg/mL concentrations of the 2H9. Fluorescence data were collected using the SA3800 Cell Analyzer (Sony Corp). Cells were gated on the dot plot based on side scatter and forward scatter, and the fluorescence intensity was determined using FlowJo software (BD Biosciences, USA).

2.5. Determination of dissociation constant (K_D) by flow cytometry

CHO/EphB2 and LS174T cells were suspended in serially-diluted Eb_2Mabs for 30 min at 4°C. The cells were treated with Alexa Fluor 488-conjugated anti-mouse IgG (1:200). The cells were suspended in serially diluted 2H9 conjugated with RB545. Fluorescence data were collected using the BD FACSLyric (BD Biosciences, USA). The K_D was calculated by fitting saturation binding curves to the built-in one-site binding models in GraphPad PRISM 6 (GraphPad Software, USA).

3. Results

3.1. Development of anti-EphB2 mAbs using the CBIS method

Mice were immunized with LN229/EphB2 cells to develop anti-EphB2 mAb (Figure 1A). The spleen was excised, and splenocytes were fused with myeloma P3U1 cells (Figure 1B). The developed hybridomas were subsequently seeded into ten 96-well plates and cultivated for 6 days. The positive wells were screened by selecting CHO/EphB2-reactive and CHO-K1-non-reactive supernatants using flow cytometry (Figure 1C). A total of 133 positive wells (13.9%) out of 956 wells were obtained. After limiting the dilution of the positive wells and several additional screenings, 12 clones were finally established (Figure 1D).

3.2. Flow cytometric analysis using anti-EphB2 mAbs

Eight mouse IgG_1 clones (Eb_2Mab-1, 2, 3, 4, 7, 8, 10, and 12) were selected, and the mAbs were purified from the supernatants (Table 1). The specificity of Eb_2Mabs and 2H9 in 14 Eph receptor tyrosine kinases-expressed CHO-K1 was were investigated. 2H9 exhibited reactivity to not only CHO/EphB2 but also to CHO/EphA4, CHO/EphB1, and

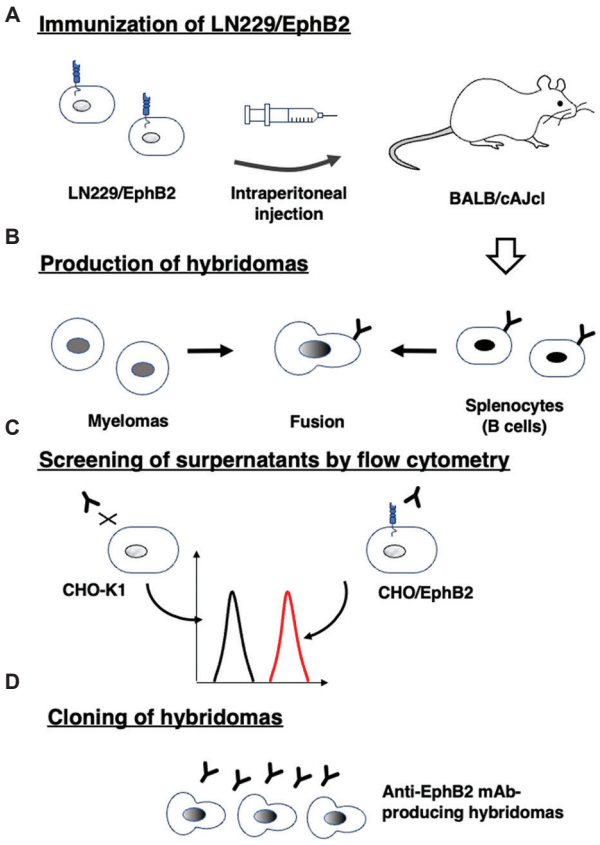

Figure 1. The production of anti-EphB2 monoclonal antibodies. (A) LN229/EphB2 cells were immunized into two BALB/cAJcl mice. (B) The spleen cells were fused with P3U1 cells. (C) The supernatant of hybridomas producing anti-EphB2 mAbs was screened through flow cytometry using CHO-K1 and CHO/EphB2 cells. (D) After limiting dilution, the anti-EphB2 mAbs were finally established.
Abbreviations: CHO/EphB2: EphB2-overexpressing Chinese hamster ovary-K1 cells; CHO: Chinese hamster ovary; mAbs: Monoclonal antibodies.

Table 1. Cross-reactivity and K_D values of Eb_2Mabs (IgG_1 isotype) in flow cytometry

Clones	Isotype	Cross-reactivity	K_D ($\times 10^{-9}$ M)
Eb_2Mab-1	IgG_1, kappa	–	5.9
Eb_2Mab-2	IgG_1, kappa	–	6.4
Eb_2Mab-3	IgG_1, kappa	EphA3, EphB1, EphB3	1.1
Eb_2Mab-4	IgG_1, kappa	–	3.3
Eb_2Mab-7	IgG_1, kappa	–	5.2
Eb_2Mab-8	IgG_1, kappa	EphB3	9.5
Eb_2Mab-10	IgG_1, kappa	EphB3	3.4
Eb_2Mab-12	IgG_1, kappa	–	1.7*

CHO/EphB2 was used to determine the KD. Cross-reactivity was determined by flow cytometry (Figures S2-S4). Eb_2Mab-5 is IgG3. Eb_2Mab-6, Eb2Mab-9, and Eb2Mab-11 are IgM. *The data are presented in Figure 4A.
Abbreviations: IgG: Immunoglobin G.

CHO/EphB3 at a concentration of 1 μg/mL (Figure S1). In contrast, Eb_2Mab-1, 2, 4, 7, and 12 were recognized as specific to CHO/EphB2, with no cross-reactivity observed even at 10 μg/mL. Conversely, Eb_2Mab-3 demonstrated cross-reactivity to EphA3, EphB1, and EphB3. In addition, Eb_2Mab-8 and 10 also showed cross-reactivity to EphB3 (Figures S2-4 and Table 1). Flow cytometry was subsequently conducted using the Eb_2Mabs and 2H9 against CHO/EphB2, CHO-K1, LN229/EphB2, and LN229 cells. Dose-dependent recognition of CHO/EphB2 cells was observed for the Eb_2Mabs at concentrations of 10, 1, 0.1, and 0.01 μg/mL (Figure S5). Among the EphB2-specific Eb_2Mabs (Eb_2Mab-1, 2, 4, 7, and 12), Eb_2Mab-12 showed the high reactivity (Figure 2A). Dose-dependent recognition of CHO/EphB2 cells was also noted for 2H9 at concentrations of 10, 1, 0.1, and 0.01 μg/mL; however, this was less effective compared to Eb_2Mab-12 (Figure 2A). Parental CHO-K1 cells were not recognized even at a concentration of 10 μg/mL for either Eb_2Mab-12 and 2H9 (Figure 2B). The superior reactivity of Eb_2Mab-12 compared to 2H9 was also observed in LN229/EphB2 and LN229 cells (Figure S6). Weak expression of endogenous EphB2 in LN229 had been previously confirmed through quantitative PCR and western blot analyses.[44]

The reactivity of Eb_2Mabs and 2H9 against an endogenous EphB2-expressing colorectal cancer cell line, LS174T, was investigated.[45] Eb_2Mabs recognized LS174T cells dose-dependently at concentrations of 10, 1, 0.1, and 0.01 μg/mL (Figure S7). Among the Eb_2Mabs, Eb_2Mab-12 showed the highest reactivity (Figure 3). In contrast, 2H9 was found to react with LS174T cells at concentrations greater than 0.1 μg/mL (Figure 3). These results suggest that Eb_2Mab-12 specifically recognizes EphB2 and is effective in detecting endogenous EphB2 through flow cytometry.

3.3. Determination of the binding affinity of EphB2 mAbs using flow cytometry

Flow cytometry was conducted, and the geometric mean of the fluorescence intensity was plotted against the concentration of mAbs to determine the K_D values of Eb_2Mabs and 2H9. The K_D values of Eb_2Mab-12 and 2H9 for CHO/EphB2 were determined as 1.7×10^{-9} M and 3.4×10^{-9} M, respectively (Figure 4A). While the K_D values for other Eb_2Mabs were also determined, Eb_2Mab-12 exhibited the highest affinity among the EphB2-specific clones (Table 1). Furthermore, the K_D values of Eb_2Mab-12 and 2H9 targeting LS174T were determined to be 4.4×10^{-10} M and 1.9×10^{-9} M, respectively (Figure 4B). These results indicate that Eb_2Mab-12 possesses a superior affinity for both CHO/EphB2 and LS174T compared to 2H9.

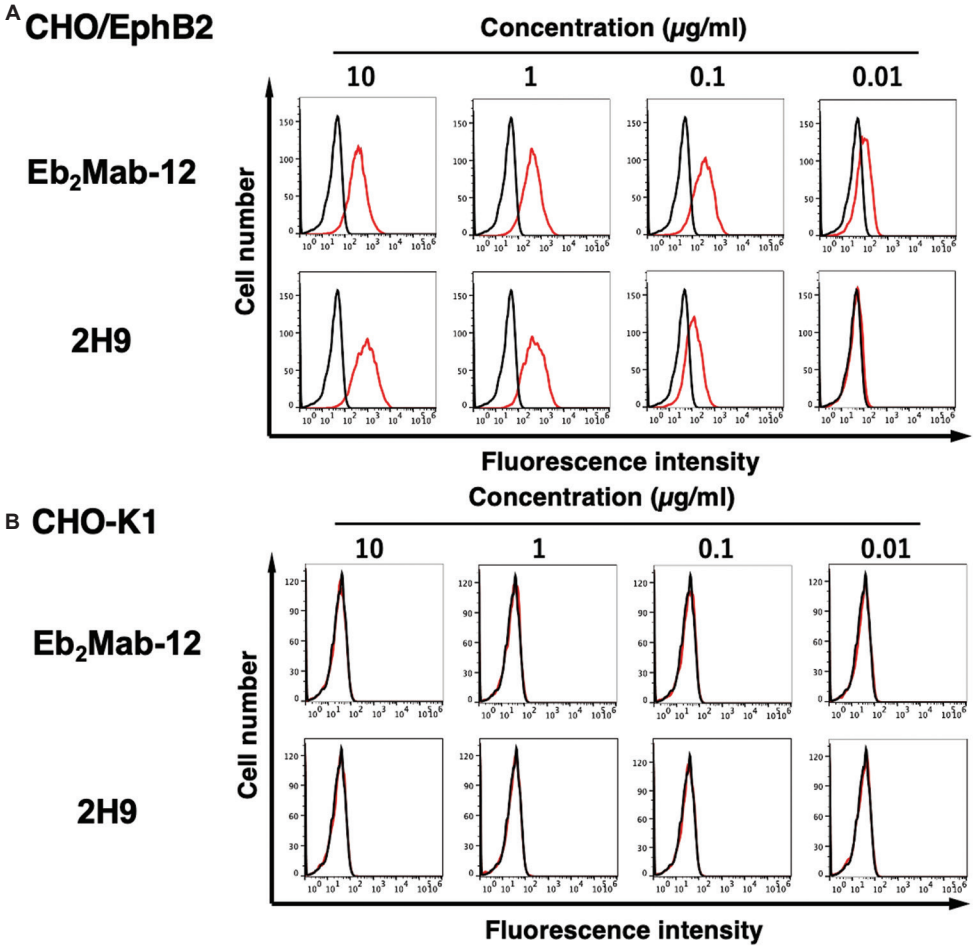

Figure 2. Flow cytometry of EphB2-expressed CHO-K1 cells using Eb_2Mab-12 and 2H9. CHO/EphB2 (A) and CHO-K1 (B) cells were treated with 0.01–10 μg/mL of Eb_2Mab-12 or 2H9 conjugated with RB545 (red line). The Eb_2Mab-12 treated cells were further incubated with anti-mouse IgG conjugated with Alexa Fluor 488. Fluorescence data were subsequently collected using the SA3800 Cell Analyzer. The black line represents the negative control (blocking buffer).

Abbreviations: CHO/EphB2: EphB2-overexpressing Chinese hamster ovary-K1 cells; CHO: Chinese hamster ovary; IgG: Immunoglobulin G; mAbs: Monoclonal antibodies.

4. Discussion

An anti-EphB2 mAb, clone 2H9, was extensively characterized and developed for tumor therapy as an antibody-drug conjugate.[46] The 2H9 was established through the immunization of mice with the EphB2 ectodomain produced by a baculovirus expression system.[46] However, 2H9 showed cross-reactivity to CHO/EphA4, CHO/EphB1, and CHO/EphB3 (Figure S1). This limitation highlights the need for more specific antibodies that can effectively target EphB2 without such cross-reactivity. In this study, anti-EphB2 mAbs were established using the CBIS method (Figure 1). Among the established mAbs, Eb_2Mab-12 exhibited superior reactivity compared to 2H9 in CHO/EphB2 (Figure 2), LN229/EphB2 (Figure S2), and LS174T (Figure 3) cells. Furthermore, Eb_2Mab-12 possesses a higher affinity toward CHO/EphB2 and LS174T compared to 2H9 (Figure 4). Importantly, no cross-reactivity was observed for Eb_2Mab-12 even at high concentrations (Figures S2-4 and Table 1). Therefore, Eb_2Mab-12 is recognized as a highly sensitive and specific anti-EphB2 mAb for flow cytometry.

The interaction of EphB2 with ligands was effectively blocked by 2H9, which also inhibited the autophosphorylation of EphB2.[46] However, 2H9 did not affect the proliferation of EphB2-positive tumor cells.[46] The identification of the epitope is essential to assess the properties of Eb_2Mab-12 and 2H9. Hence, the RIEDL insertion for epitope mapping (REMAP) and PA insertion for epitope mapping (PAMAP) methods was developed to determine the conformational epitopes of mAbs. The epitopes of anti-EGFR mAb (EMab-134)[47] and anti-CD44

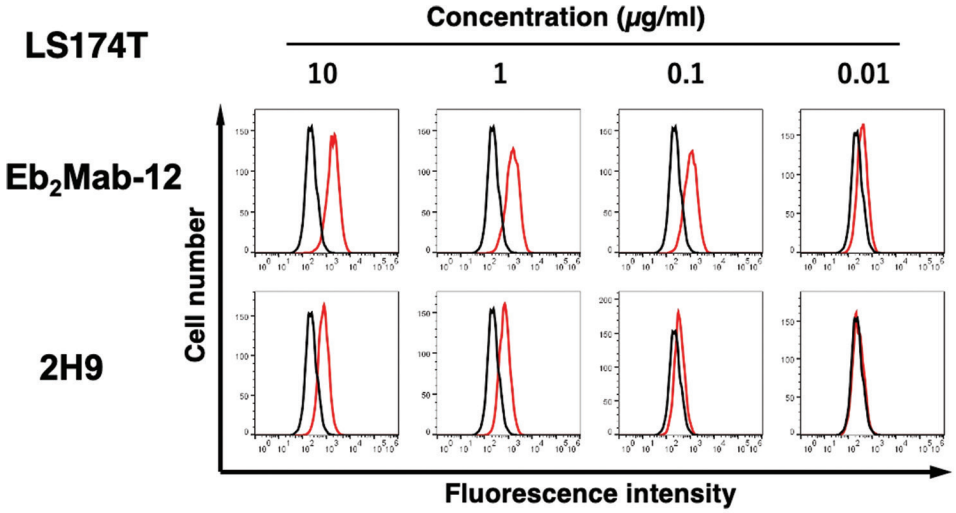

Figure 3. Flow cytometry of endogenous EphB2-expressing cells using Eb_2Mab-12 and 2H9. LS174T cells were treated with 0.01 – 10 μg/mL of Eb_2Mab-12 or 2H9 conjugated with RB545 (red line). The Eb_2Mab-12 treated cells were further incubated with anti-mouse IgG conjugated with Alexa Fluor 488. The fluorescence data were subsequently collected using the SA3800 Cell Analyzer. The black line represents the negative control (blocking buffer).
Abbreviation: IgG: Immunoglobulin G.

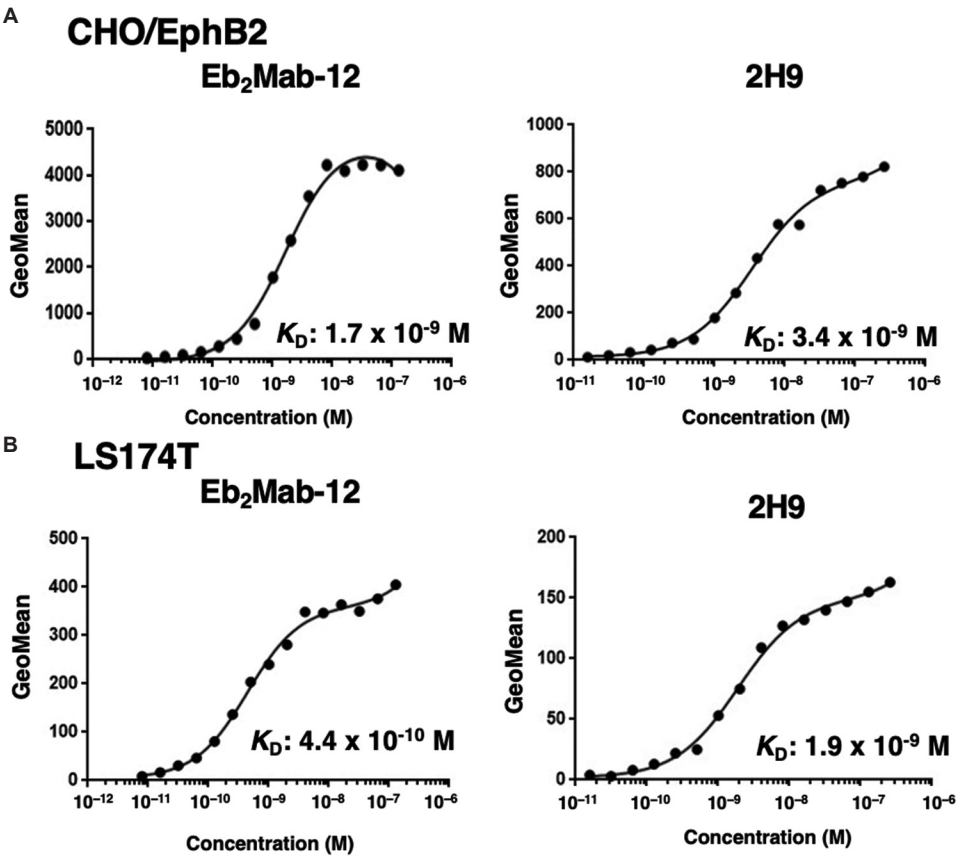

Figure 4. The binding affinity of Eb_2Mab-12 and 2H9. CHO/EphB2 (A) and LS174T (B) cells were suspended in serially diluted Eb_2Mab-12. The cells were treated with anti-mouse IgG conjugated with Alexa Fluor 488. The cells were also suspended in serially diluted 2H9 conjugated with RB545. The fluorescence data were subsequently collected using the BD FACSLyric, followed by the calculation of the K_D using GraphPad PRISM 6.
Abbreviation: IgG: Immunoglobulin G.

mAb (C_{44}Mab-46)[48] were successfully determined using the REMAP method. In addition, the epitopes of anti-mouse CD39 mAb (C_{39}Mab-1) were identified using both REMAP and PAMAP methods.[49] Therefore, further studies are required to elucidate the epitope and biological activities of Eb_2Mab-12.

The expression of EphB2 in more than 100 cell lines was investigated using flow cytometry, with LS174T exhibiting the highest expression (Figure 3). Since LS174T is a transplantable cancer cell line in BALB/c nude mice,[50] the *in vivo* anti-tumor effects of Eb_2Mab-12 can be evaluated. To achieve this, conversion of Eb_2Mab-12 (mouse IgG_1) to mouse IgG_{2a} subclass is essential for enhancing effector activation ability. Previously, recombinant mAbs were produced, converting them into the mouse IgG_{2a} subclass from mouse IgG_1. In addition, defucosylated IgG_{2a} mAbs were produced using fucosyltransferase 8-deficient CHO-K1 cells to enhance the antibody-dependent cellular cytotoxicity and *in vivo* anti-tumor effect in mouse xenograft models.[51] Therefore, a class-switched and defucosylated version of Eb_2Mab-12 could significantly contribute to the treatment of EphB2-positive tumors in pre-clinical studies. The properties of Eb_2Mabs (Eb_2Mab-3, 8, and 10), which showed cross-reactivity, were also determined (Table 1). Such mAbs may be useful when targeting multiple EphBs for mAb-based therapies.

Cancer-specific mAbs (CasMabs) have been developed against HER2 (H_2Mab-250),[52] podocalyxin (PcMab-6),[53] and podoplanin (LpMab-2),[54] demonstrating reactivity with cancer cells, but not normal cells in flow cytometry. The strategy used in this study is also applicable for selecting anti-EphB2 CasMabs from Eb_2Mabs (Table 1) or from clones derived from remaining positive wells. It has been confirmed that EphB2 is detectable in certain normal epithelial cells, prompting the screening of anti-EphB2 CasMabs. The unique properties of H_2Mab-250 could facilitate the development of HER2-targeting chimeric antigen receptor (CAR)-T-cells, which are currently undergoing a clinical phase I study in the US.[55] Therefore, the development of Eb_2Mabs for CAR-T applications is deemed necessary for treating EphB2-positive tumors.

5. Conclusion

An anti-EphB2 mAb, Eb_2Mab-12 exhibits high affinity and specificity to EphB2, suggesting its potential application in tumor diagnosis and therapy.

Acknowledgments

None.

Funding

This research was supported partially by the Japan Agency for Medical Research and Development (AMED) under grant numbers: JP24am0521010 (to Y.K.), JP24ama121008 (to Y.K.), JP24ama221339 (to Y.K.), JP23am0401013 (to Y.K.), JP24ama221339 (to Y.K.), JP24bm1123027 (to Y.K.), and JP24ck0106730 (to Y.K.), and by the Japan Society for the Promotion of Science (JSPS) Grants-in-Aid for Scientific Research (KAKENHI) grant numbers: 24K11652 (to H.Satofuka), 22K06995 (to H.Suzuki), 21K20789 (to T.T.), 21K07168 (to M.K.K.), and 22K07224 (to Y.K).

Conflict of interest

The authors have no conflicts of interest.

Authors contributions

Conceptualization: Mika K. Kaneko, Yukinari Kato
Formal analysis: Rena Ubukata
Investigation: Rena Ubukata, Miu Hirose, Hiroyuki Satofuka, Tomohiro Tanaka, Hiroyuki Suzuki
Methodology: Mika K. Kaneko
Writing – original draft: Rena Ubukata, Hiroyuki Suzuki
Writing – review & editing: Hiroyuki Suzuki, Yukinari Kato

Ethics approval and consent to participate

All animal experiments were approved by the Animal Care and Use Committee of Tohoku University (Permit number: 2022MdA-001).

Consent for publication

Not applicable.

Availability of data

The data presented in this study are available in the article.

Further disclosure

The paper has been uploaded to a preprint server (DOI: 10.20944/preprints202406.0704.v2).

References

1. Zhu Y, Su SA, Shen J, *et al*. Recent advances of the Ephrin and Eph family in cardiovascular development and pathologies. *iScience*. 2024;27(8):110556.
   doi: 10.1016/j.isci.2024.110556
2. Pasquale EB. Eph receptor signaling complexes in the plasma membrane. *Trends Biochem Sci*. 2024;49(12):1079-1096.
   doi: 10.1016/j.tibs.2024.10.002
3. Pasquale EB. Eph receptors and ephrins in cancer progression. *Nat Rev Cancer*. 2024;24(1):5-27.

doi: 10.1038/s41568-023-00634-x

4. Anderton M, Van der Meulen E, Blumenthal MJ, Schäfer G. The Role of the eph receptor family in tumorigenesis. *Cancers* (*Basel*). 2021;13(2):206.

   doi: 10.3390/cancers13020206

5. Liang LY, Patel O, Janes PW, Murphy JM, Lucet IS. Eph receptor signalling: From catalytic to non-catalytic functions. *Oncogene*. 2019;38(39):6567-6584.

   doi: 10.1038/s41388-019-0931-2

6. Pasquale EB. Eph receptors and ephrins in cancer: Bidirectional signalling and beyond. *Nat Rev Cancer*. 2010;10(3):165-180.

   doi: 10.1038/nrc2806

7. Pasquale EB. Eph receptor signalling casts a wide net on cell behaviour. *Nat Rev Mol Cell Biol*. 2005;6(6):462-475.

   doi: 10.1038/nrm1662

8. Arora S, Scott AM, Janes PW. Eph receptors in cancer. *Biomedicines*. 2023;11(2):315.

   doi: 10.3390/biomedicines11020315

9. Lau A, Le N, Nguyen C, Kandpal RP. Signals transduced by Eph receptors and ephrin ligands converge on MAP kinase and AKT pathways in human cancers. *Cell Signal*. 2023;104:110579.

   doi: 10.1016/j.cellsig.2022.110579

10. Toracchio L, Carrabotta M, Mancarella C, Morrione A, Scotlandi K. EphA2 in cancer: molecular complexity and therapeutic opportunities. *Int J Mol Sci*. 2024;25(22):12191.

    doi: 10.3390/ijms252212191

11. Scarini JF, Gonçalves MWA, De Lima-Souza RA, *et al*. Potential role of the Eph/ephrin system in colorectal cancer: Emerging druggable molecular targets. *Front Oncol*. 2024;14:1275330.

    doi: 10.3389/fonc.2024.1275330

12. Guo X, Yang Y, Tang J, Xiang J. Ephs in cancer progression: Complexity and context-dependent nature in signaling, angiogenesis and immunity. *Cell Commun Signal*. 2024;22(1):299.

    doi: 10.1186/s12964-024-01580-3

13. Stergiou IE, Papadakos SP, Karyda A, Tsitsilonis OE, Dimopoulos MA, Theocharis S. EPH/Ephrin signaling in normal hematopoiesis and hematologic malignancies: Deciphering their intricate role and unraveling possible new therapeutic targets. *Cancers (Basel)*. 2023;15(15):3963.

    doi: 10.3390/cancers15153963

14. Papadakos SP, Dedes N, Gkolemi N, Machairas N, Theocharis S. The EPH/Ephrin system in pancreatic ductal adenocarcinoma (PDAC): From pathogenesis to treatment. *Int J Mol Sci*. 2023;24(3):3015.

    doi: 10.3390/ijms24033015

15. Psilopatis I, Souferi-Chronopoulou E, Vrettou K, Troungos C, Theocharis S. EPH/Ephrin-targeting treatment in breast cancer: A new chapter in breast cancer therapy. *Int J Mol Sci*. 2022;23(23):15275.

    doi: 10.3390/ijms232315275

16. Psilopatis I, Pergaris A, Vrettou K, Tsourouflis G, Theocharis S. The EPH/Ephrin system in gynecological cancers: Focusing on the roots of carcinogenesis for better patient management. *Int J Mol Sci*. 2022;23(6):3249.

    doi: 10.3390/ijms23063249

17. Psilopatis I, Karniadakis I, Danos KS, *et al*. May EPH/ephrin targeting revolutionize lung cancer treatment? *Int J Mol Sci*. 2022;24(1):93.

    doi: 10.3390/ijms24010093

18. Papadakos SP, Petrogiannopoulos L, Pergaris A, Theocharis S. The EPH/ephrin system in colorectal cancer. *Int J Mol Sci*. 2022;23(5):2761.

    doi: 10.3390/ijms23052761

19. Liu W, Yu C, Li J, Fang J. The roles of EphB2 in cancer. *Front Cell Dev Biol*. 2022;10:788587.

    doi: 10.3389/fcell.2022.788587

20. Chen X, Yu D, Zhou H, *et al*. The role of EphA7 in different tumors. *Clin Transl Oncol*. 2022;24(7):1274-1289.

    doi: 10.1007/s12094-022-02783-1

21. Goparaju C, Donington JS, Hsu T, Harrington R, Hirsch N, Pass HI. Overexpression of EPH receptor B2 in malignant mesothelioma correlates with oncogenic behavior. *J Thorac Oncol*. Sep 2013;8(9):1203-1211.

    doi: 10.1097/JTO.0b013e31829ceb6a

22. Cha JH, Chan LC, Wang YN, *et al*. Ephrin receptor A10 monoclonal antibodies and the derived chimeric antigen receptor T cells exert an antitumor response in mouse models of triple-negative breast cancer. *J Biol Chem*. 2022;298(4):101817.

    doi: 10.1016/j.jbc.2022.101817

23. Xiao T, Xiao Y, Wang W, Tang YY, Xiao Z, Su M. Targeting EphA2 in cancer. *J Hematol Oncol*. 2020;13(1):114.

    doi: 10.1186/s13045-020-00944-9

24. Tang FHF, Davis D, Arap W, Pasqualini R, Staquicini FI. Eph receptors as cancer targets for antibody-based therapy. *Adv Cancer Res*. 2020;147:303-317.

    doi: 10.1016/bs.acr.2020.04.007

25. London M, Gallo E. Critical role of EphA3 in cancer and current state of EphA3 drug therapeutics. *Mol Biol Rep*. 2020;47(7):5523-5533.

    doi: 10.1007/s11033-020-05571-8

26. Janes PW, Vail ME, Gan HK, Scott AM. Antibody targeting of eph receptors in cancer. *Pharmaceuticals (Basel)*. 2020;13(5):88.

    doi: 10.3390/ph13050088

27. Buckens OJ, El Hassouni B, Giovannetti E, Peters GJ. The role of Eph receptors in cancer and how to target them: Novel approaches in cancer treatment. *Expert Opin Investig Drugs*. 2020;29(6):567-582.

    doi: 10.1080/13543784.2020.1762566

28. Saha N, Robev D, Mason EO, Himanen JP, Nikolov DB. Therapeutic potential of targeting the Eph/ephrin signaling complex. *Int J Biochem Cell Biol*. 2018;105:123-133.

    doi: 10.1016/j.biocel.2018.10.006

29. Taki S, Kamada H, Inoue M, *et al*. A novel bispecific antibody against human CD3 and ephrin receptor A10 for breast cancer therapy. *PLoS One*. 2015;10(12):e0144712.

    doi: 10.1371/journal.pone.0144712

30. Zhou F, Wang B, Wang H, *et al*. circMELK promotes glioblastoma multiforme cell tumorigenesis through the miR-593/EphB2 axis. *Mol Ther Nucleic Acids*. 2021;25:25-36.

    doi: 10.1016/j.omtn.2021.05.002

31. Lam S, Wiercinska E, Teunisse AF, Lodder K, Ten Dijke P, Jochemsen AG. Wild-type p53 inhibits pro-invasive properties of TGF-β3 in breast cancer, in part through regulation of EPHB2, a new TGF-β target gene. *Breast Cancer Res Treat*. 2014;148(1):7-18.

    doi: 10.1007/s10549-014-3147-8

32. Leung HW, Leung CON, Lau EY, *et al*. EPHB2 Activates β-catenin to enhance cancer stem cell properties and drive sorafenib resistance in hepatocellular carcinoma. *Cancer Res*. 2021;81(12):3229-3240.

    doi: 10.1158/0008-5472.Can-21-0184

33. Nakada M, Niska JA, Miyamori H, *et al*. The phosphorylation of EphB2 receptor regulates migration and invasion of human glioma cells. *Cancer Res*. 2004;64(9):3179-3185.

    doi: 10.1158/0008-5472.can-03-3667

34. Nakada M, Niska JA, Tran NL, McDonough WS, Berens ME. EphB2/R-Ras signaling regulates glioma cell adhesion, growth, and invasion. *Am J Pathol*. 2005;167(2):565-576.

    doi: 10.1016/s0002-9440(10)62998-7

35. Xi HQ, Wu XS, Wei B, Chen L. Eph receptors and ephrins as targets for cancer therapy. J Cell Mol Med. 2012;16:2894-2909.

    doi: 10.1111/j.1582-4934.2012.01612.x

36. Holmberg J, Genander M, Halford MM, *et al*. EphB receptors coordinate migration and proliferation in the intestinal stem cell niche. *Cell*. 2006;125(6):1151-1163.

    doi: 10.1016/j.cell.2006.04.030

37. Batlle E, Henderson JT, Beghtel H, *et al*. Beta-catenin and TCF mediate cell positioning in the intestinal epithelium by controlling the expression of EphB/ephrinB. *Cell*. 2002;111(2):251-263.

    doi: 10.1016/s0092-8674(02)01015-2

38. Cortina C, Palomo-Ponce S, Iglesias M, *et al*. EphB-ephrin-B interactions suppress colorectal cancer progression by compartmentalizing tumor cells. *Nat Genet*. 2007;39(11):1376-1383.

    doi: 10.1038/ng.2007.11

39. Jubb AM, Zhong F, Bheddah S, *et al*. EphB2 is a prognostic factor in colorectal cancer. *Clin Cancer Res*. 2005;11(14):5181-5187.

    doi: 10.1158/1078-0432.Ccr-05-0143

40. Takei J, Kaneko MK, Ohishi T, Kawada M, Harada H, Kato Y. A novel anti-EGFR monoclonal antibody (EMab-17) exerts antitumor activity against oral squamous cell carcinomas via antibody-dependent cellular cytotoxicity and complement-dependent cytotoxicity. *Oncol Lett*. 2020;19(4):2809-2816.

    doi: 10.3892/ol.2020.11384

41. Kato Y, Ohishi T, Sano M, *et al*. H(2)Mab-19 anti-human epidermal growth factor receptor 2 monoclonal antibody therapy exerts antitumor activity in pancreatic cancer xenograft models. *Monoclon Antib Immunodiagn Immunother*. 2020;39(3):61-65.

    doi: 10.1089/mab.2020.0011

42. Asano T, Ohishi T, Takei J, *et al*. AntiHER3 monoclonal antibody exerts antitumor activity in a mouse model of colorectal adenocarcinoma. *Oncol Rep*. 2021;46(2):173.

    doi: 10.3892/or.2021.8124

43. Nanamiya R, Suzuki H, Kaneko MK, Kato Y. Development of an Anti-EphB4 monoclonal antibody for multiple applications against breast cancers. *Monoclon Antib Immunodiagn Immunother*. 2023;42(5):166-177.

    doi: 10.1089/mab.2023.0015

44. Qiu W, Song S, Chen W, Zhang J, Yang H, Chen Y. Hypoxia-induced EPHB2 promotes invasive potential of glioblastoma. *Int J Clin Exp Pathol*. 2019;12(2):539-548.

45. Genander M, Halford MM, Xu NJ, *et al*. Dissociation of EphB2 signaling pathways mediating progenitor cell proliferation and tumor suppression. *Cell*. 2009;139(4):679-692.

    doi: 10.1016/j.cell.2009.08.048

46. Mao W, Luis E, Ross S, *et al*. EphB2 as a therapeutic antibody drug target for the treatment of colorectal cancer. *Cancer Res*. 2004;64(3):781-788.

    doi: 10.1158/0008-5472.can-03-1047

47. Sano M, Kaneko MK, Aasano T, Kato Y. Epitope mapping of an antihuman EGFR monoclonal antibody (EMab-134)

using the REMAP method. *Monoclon Antib Immunodiagn Immunother*. 2021;40(4):191-195.

doi: 10.1089/mab.2021.0014

48. Asano T, Kaneko MK, Takei J, Tateyama N, Kato Y. Epitope mapping of the Anti-CD44 monoclonal antibody ($C(_{44})$ Mab-46) using the REMAP method. *Monoclon Antib Immunodiagn Immunother*. 2021;40(4):156-161.

doi: 10.1089/mab.2021.0012

49. Okada Y, Suzuki H, Tanaka T, Kaneko MK, Kato Y. Epitope mapping of an Anti-Mouse CD39 monoclonal antibody using PA scanning and RIEDL scanning. *Monoclon Antib Immunodiagn Immunother*. 2024;43(2):44-52.

doi: 10.1089/mab.2023.0029

50. Sharkey RM, Govindan SV, Cardillo TM, *et al*. Selective and concentrated accretion of SN-38 with a CEACAM5-targeting antibody-drug conjugate (ADC), labetuzumab govitecan (IMMU-130). *Mol Cancer Ther*. 2018;17(1):196-203.

doi: 10.1158/1535-7163.Mct-17-0442

51. Li G, Suzuki H, Ohishi T, *et al*. Antitumor activities of a defucosylated antiEpCAM monoclonal antibody in colorectal carcinoma xenograft models. *Int J Mol Med*. 2023;51(2):18.

doi: 10.3892/ijmm.2023.5221

52. Kaneko MK, Suzuki H, Kato Y. Establishment of a novel cancer-specific Anti-HER2 monoclonal antibody H(2) Mab-250/H(2)Casmab-2 for breast cancers. *Monoclon Antib Immunodiagn Immunother*. 2024;43(2):35-43.

doi: 10.1089/mab.2023.0033

53. Suzuki H, Ohishi T, Tanaka T, Kaneko MK, Kato Y. A cancer-specific monoclonal antibody against podocalyxin exerted antitumor activities in pancreatic cancer xenografts. *Int J Mol Sci*. 2023;25(1):161.

doi: 10.3390/ijms25010161

54. Kato Y, Kaneko MK. A cancer-specific monoclonal antibody recognizes the aberrantly glycosylated podoplanin. *Sci Rep.* 2014;4:5924.

doi: 10.1038/srep05924

55. Hosking M, Shirinbak S, Omilusik K, *et al*. 268 Development of FT825/ONO-8250: An off-the-shelf CAR-T cell with preferential HER2 targeting and engineered to enable multi-antigen targeting, improve trafficking, and overcome immunosuppression. *J Immunother Cancer*. 2023;11(Suppl 1):A307.

doi: 10.1136/jitc-2023-SITC2023.0268

Our Journals

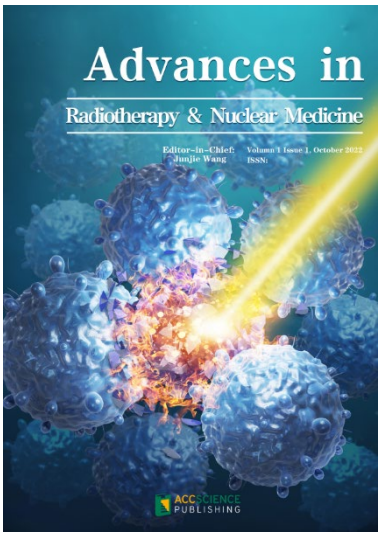

Advances in Radiotherapy & Nuclear Medicine (ARNM) is a peer-reviewed and open-access journal that aims to publish and disseminate novel research in the breadth of neurology and neuroscience. *ARNM* covers subject areas, including but not limited to the following:

- Conventional Radiotherapy (CR)
- Stereotactic Body Radiation Therapy (SBRT)
- Brachytherapy (BT)
- Boron Neutron Capture Therapy (BNCT)
- Particle Therapy (proton and heavy ions) (PT)
- Targeted and Immunotherapy (TI)
- Combined Modality Therapy (Heat therapy, electric field therapy, nursing, technology) (CMT)
- Radiation Biology (RB)
- Radiation Physics (RP)
- Innovative Radiation Technology (IRT)
- Positron Emission Tomography (PET)
- Radiopharmaceuticals and Radio-tracer (RR)
- Molecular Imaging and Radionuclide Therapy (MI & RT)
- Single-photon Emission Computed Tomography (SPETCT)

Artificial Intelligence in Health is an online open-access, multidisciplinary journal dedicated to publishing high-quality peer-reviewed research in all areas of Artificial Intelligence in health and medicine science. By publishing high-quality research papers, reviews, and case studies, the journal seeks to contribute to the scientific community's understanding of the potential, challenges, and impact of AI and its applications on health delivery, patient outcomes, and population health. *Artificial Intelligence in Health* covers topics, including but not limited to the following: AI-based medical diagnosis and prognosis, AI clinical decision support systems, AI-driven drug discovery and development, AI-enabled healthcare operations and management, and the research and application in telemedicine, AI-assisted electronic health records and clinical informatics, AI-based research and application of wearable devices for diagnosis and treatment and social implications of AI in health.

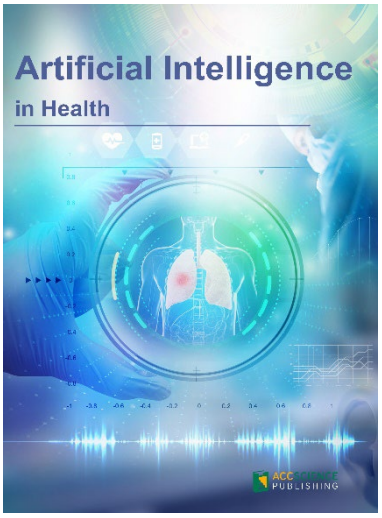

Start a new journal

Write to us via email if you are interested to start a new journal with AccScience Publishing. Please attach your CV, professional profile page and a brief pitch proposal in your email. We shall inform you of our decision whether we are interested to collaborate in starting a new journal.

Contact: info@accscience.com

https://accscience.com/journal/MI

Contact
www.accscience.com
9 Raffles Place, Republic Plaza 1 #06-00 Singapore 048619
Email: editorial@accscience.com
Phone: +65 8182 1586